Author:
Najjar, Haneen F Y

Title:
Cardiac Remodelling and Vulnerability to Ischaemia/Reperfusion Injury with Ageing and High-Fat Diet

Cardiac Remodelling and Vulnerability to Ischaemia/Reperfusion Injury with Ageing and High-Fat Diet

By

Haneen Najjar

Supervisors: Prof. Saadeh Suleiman & Prof. Sarah George

A Dissertation submitted to The University of Bristol in accordance with the requirements for award of the degree of Doctor of Philosophy in The Faculty of Health Sciences

The Bristol Medical School (THS)

March 2020

Word Count: 59,568

Abstract

Background: Ageing and high-fat diet (HFD) are both associated with metabolic, cellular, structural, and functional remodelling of the heart. There are conflicting reports regarding the vulnerability of the ageing heart to cardiac insults including ischaemia and reperfusion (I/R), and similarly, the vulnerability of the heart after HFD. Very few studies have been done on the effects of HFD in the ageing heart. In this work, we first investigated the effects of ageing on cardiac remodelling and vulnerability to I/R compared to adults. We then investigated the effects of HFD in the ageing heart compared to normal diet (ND) aged matched controls. We hypothesized that both ageing and HFD increase the vulnerability of the heart to I/R injury.

Methods: C57BL/6 adult (8 weeks) and ageing (80 weeks) male mice were used in this work. Ageing mice were fed a standard ND or HFD for a period of 24 weeks. Animal body weights, heart weights, and epidydimal fat pads were all measured. Plasma glucose and lipid metabolites were also measured using nuclear magnetic resonance (NMR). Hearts were extracted and processed for measuring cardiac energy metabolites and amino acids (AA) using high performance liquid chromatography (HPLC). Additionally, they were used for protein and phospho-protein quantification using liquid chromatography tandem mass spectrometry (LC-MS/MS). Histological examination of cardiac tissue included using light microscopy and electron microscopy for ultrastructural examination. Finally, vulnerability of the heart to I/R injury was tested using the Langendorff perfusion system.

Results: Ageing animals had significant increase in body weight, epidydimal fat pads, cardiac hypertrophy, with decreased plasma glucose levels. Remodelling of the ageing heart included metabolic changes such as changes in cardiac energy metabolites with decreased phosphorylation potential, and a decrease in total protein amino acid pool as well as taurine. Additionally, cellular remodelling was observed as cardiac protein groups were mainly upregulated during aging including mitochondrial proteins, ionic channel proteins, antioxidant enzymes, apoptosis-related proteins, structural (collagen) proteins, and lipid and carbohydrate metabolism. Phospho-proteins (ionic transport related proteins, cardiac signalling and apoptosis, metabolism and energy production, and structural proteins) were also mainly upregulated with ageing. Finally, ageing was associated with structural change including increased lipid deposits in the heart and an increase in capillary/myocyte ratio. There was an increase in total size and lumen size of coronary arteries with decrease in arterial wall/total artery and lumen size ratios, and there were changes in mitochondrial morphometry (mitochondria became smaller in size and elongated) but not mitochondrial distribution.

Feeding aging mice HFD was associated with marked obesity, increased body fat, and significantly higher plasma VLDL and LDL, but lower glucose and lactate levels. HFD was also associated with atherosclerosis, smaller coronary arteries with smaller lumen sizes, and a higher artery wall/artery size and lumen size ratios. Additionally, HFD reduced capillary/myocyte ratio and increased fibrosis in ageing hearts. Metabolically, HFD reduced total energy rich phosphates and this was associated with altered mitochondrial morphometry as they became larger in size and more rounded, with more densely distributed PN and SSL mitochondria. Finally, majority of proteins that changed after HFD in ageing were downregulated. These included mitochondrial proteins and carbohydrates metabolism. Proteins that increased with HFD included structural (collagen) proteins, apoptotic, and lipid metabolism. Antioxidant enzymes and ionic transport related proteins changed in both directions (up and downregulation). Phosphorylated proteins were also mainly downregulated with HFD in the ageing heart (ionic transport, cardiac signalling and apoptosis, carbohydrate metabolism, transport, structural proteins, and enzymes).

No significant changes were found in the function and vulnerability of the ageing hearts compared to their adult controls, nor in the ageing hearts after HFD compared to their ND controls to I/R injury.

Conclusion: Ageing and HFD (in the ageing heart) are associated with cardiac metabolic, cellular, and structural remodelling. However, these alterations do not alter the heart's vulnerability to I/R injury.

Dedication

I would like to dedicate this thesis to my family, who have always been there for me, for their constant love, care, support, and encouragement. I would not be here without you.

Acknowledgments

Author's Declaration:

I declare that the work in this dissertation was carried out in accordance with the requirements of the University's Regulations and Code of Practice for Research Degree Programmes and that it has not been submitted for any other academic award. Except where indicated by specific reference in the text, the work is the candidate's own work. Work done in collaboration with, or with the assistance of, others, is indicated as such. Any views expressed in the dissertation are those of the author.

SIGNED: *Haneen Najjar*   DATE: *20/3/2020*

List of Publications and Presentations

Oral Presentations:

➢ 5the International Congress on Analytical Proteomics, Caparica, Portugal (July 2017). "Proteomic Remodelling in Ageing Mouse Heart".

Poster Presentations:

➢ 5the International Congress on Analytical Proteomics, Caparica, Portugal (July 2017). "Proteomic Remodelling in Ageing Mouse Heart".

➢ 3rd European Section Meeting of the International Academy of Cardiovascular Sciences, Marseille, France (October 2016). "Fibrosis and collagen types in aging mouse hearts"

➢ Physiology 2016, A Joint Meeting of the American Physiological Society and The Physiological society, Dublin, Ireland (July 2016). "Proteomic remodelling of mitochondria in ageing mouse hearts".

Published Abstracts:

➢ Najjar H, Lin H, Williams H, Heesom K, George SJ, Suleiman MS. "Proteomic Remodelling in Ageing Mouse Heart". JIOMICS 2017; 7:23-46.

➢ Najjar H, Lin H, Williams H, Heesom K, George SJ, Suleiman MS. "Fibrosis and collagen types in aging mouse hearts". Curr Res Cardiol Vol 3 No 3, 2016.

➢ Najjar H, Lin H, Williams H, Heesom K, George SJ, Suleiman MS. "Proteomic remodelling of mitochondria in ageing mouse hearts". Proc Physiol Soc 36 (2016).

Table of Contents

List of Tables:

List of Figures:

Chapter 5:

Abbreviations

A band – Anisotropic band

ACC – Acetyl coenzyme A carboxylase

ADP – Adenosine diphosphate

Akt – Protein kinase B

AMP – Adenosine monophosphate

AMPK – Adenosine monophosphate-activated protein kinase

ANOVA – Analysis of variance

ANT – Adenine nucleotide translocase

ATP – Adenosine triphosphate

BAX – B-cell lymphoma 2-associated X protein

Bcl-2 – B-cell lymphoma 2

BSA – Albumin from bovine serum

Ca^{2+} – Calcium ion

$CaCl_2$ – Calcium chloride

CACT – Carnitine-acylcarnitine translocase

CaMKII – Ca^{2+}/calmodulin-dependent protein kinase II

cAMP – Cyclic adenosine monophosphate

CAT – Catalase

CK – Creatine kinase

Cl^- – Chloride ion

CO_2 – Carbon dioxide

CoA – Coenzyme A

CoASH – Coenzyme A

CPT – Carnitine palmitoyltransferase

CS – Citrate synthase

Cyt c – Cytochrome c

DDSA – Dodecenyl succinic anhydride

DMSO – Dimethyl sulphoxide

DNA – Deoxyribonucleic acid

DRP1 – Dynamin-1-like protein

e- – Electron

ECL – Enhanced chemiluminescence

EDTA – Ethylenediaminetetraacetic acid

EGTA – Ethylene glycol-bis(2-aminoethylether)-N,N,N',N'-tetraacetic acid

ERK1/2 – Extracellular signal-regulated protein kinases 1 and 2

ETC – Electron transport chain

FA – Fatty acid

FACS – Fatty acyl coenzyme A synthetase

FAD^+ – Flavin adenine dinucleotide, oxidised

$FADH_2$ – Flavin adenine dinucleotide, reduced

FAO – Fatty acid oxidation

FAT/CD36 – Fatty acid translocase/Cluster of Differentiation 36

FIS1 – Mitochondrial fission 1 protein

g – Acceleration due to gravity

G6P-DH – Glucose-6-phosphate dehydrogenase

GAPDH – Glyceraldehyde 3-phosphate dehydrogenase

GDP – Guanosine diphosphate

GLUT4 – Glucose transporter type 4

GMP – Guanosine monophosphate

GPx – Glutathione peroxidase

GTP – Guanosine triphosphate

H^+ – Hydrogen ion/proton

H_2O – Water

H_2O_2 – Hydrogen peroxide

HEPES – 4-(2-Hydroxyethyl)piperazin-1-ylethanesulphonic acid

HF – High-fat diet group

HO- – Hydroxyl ion

HPLC – High-performance liquid chromatography

I band – Isotropic band

IMM – Inner mitochondrial membrane

IMP – Inosine monophosphate

I/R – Ischaemia/reperfusion

K^+ – Potassium ion

K_2CO_3 – Potassium carbonate anhydrous

KH_2PO_4 – Potassium dihydrogen phosphate

KOH – Potassium hydroxide

LDH – Lactate dehydrogenase

LV – Left ventricle

MCD – Malonyl coenzyme A decarboxylase

Mfn-1 – Mitofusin 1

Mfn-2 – Mitofusin 2

Mg – Magnesium

$MgSO_4 \cdot 7H_2O$ – Magnesium sulphate

MPC – Mitochondrial pyruvate carrier

mPTP – Mitochondrial permeability transition pore

mRNA – Messenger ribonucleic acid

Na^+ – Sodium ion

Na_2HPO_4 – Di-sodium hydrogen phosphate

NaCl – Sodium chloride

NAD^+ – Nicotinamide adenine dinucleotide, oxidised

NADH – Nicotinamide adenine dinucleotide, reduced

$NADP^+$ – Nicotinamide adenine dinucleotide phosphate, oxidised

NAD(P)H – Nicotinamide adenine dinucleotide phosphate, reduced

$NaH_2PO_4 \cdot 2H_2O$ – Sodium dihydrogen phosphate

$NaHCO_3$ – Sodium hydrogen carbonate

NH_2 – Amine group

NO^- – Nitric oxide ion

O_2 – Oxygen

$O_2^{-\bullet}$ – Superoxide

$\bullet OH$ – Hydroxyl radical

$ONOO^-$ – Peroxynitrite

OPA1 – Optic atrophy 1

P-Akt – Phosphorylated protein kinase B

PBS – Phosphate buffered saline

Pi – Inorganic phosphate

PKA – Protein kinase A

PLN – Phospholamban

PPAR – Peroxisome proliferator-activated receptor

RIPA – Radio-immunoprecipitation assay

ROS – Reactive oxygen species

rpm – Revolutions per minute

SDS – Sodium dodecyl sulphate

SEM – Standard error of the mean

Ser – Serine

SERCA – Sarco/endoplasmic reticulum Ca^{2+}-ATPase

SOD – Superoxide dismutase

SOD-1 – Superoxide dismutase 1

SR – Sarcoplasmic reticulum

TCA – Tricarboxylic acid

TMT – Tandem mass tag

TTC – 2, 3, 5-triphenyl-tetrazolium chloride

UCP3 – Uncoupling protein 3

v/v – volume/volume

w/v – weight/volume

w/w – weight/weight

Z line – Zwischenscheibe line

1. Introduction

1.1   Cardiovascular Diseases

Cardiovascular diseases (CVD) are the number one cause of death worldwide. In 2016, 17.9 million people died from CVD, with 85 % of those deaths being from heart attack and stroke [World Health Organisation (WHO)]. In the UK, 170,000 people die from CVD each year, which accounts for 28 % of deaths yearly [British Heart Foundation (BHF)]. Coronary heart disease (CHD) (also known as ischaemic heart disease) is the most common type of CVD and is characterised by the gradual build-up of fatty material (plaques) within the coronary arteries (atherosclerosis) causing the obstruction of blood flow to the heart and leading to heart attack (BHF).

1.2   Overall View of the Cardiovascular System

The cardiovascular system (circulatory system) is made up of the heart and the blood vessels. The heart contains four chambers, two upper atria, and two lower ventricles. Major blood vessels carry the blood from and back to the heart, and branch to smaller vessels and capillaries that circulate the whole body. Oxygenated blood is delivered to the left atrium of the heart via the pulmonary veins, then passes into the left ventricle through the left atrioventricular valve (bicuspid or mitral valve), and then it is pumped from the left ventricle via the aorta to the whole body. The aortic valve (semilunar valve) prevents blood from flowing backwards. Coronary arteries branch from the aorta to supply the outer cardiac muscle tissue with blood. Veins return deoxygenated blood from the body into the right atrium of the heart via the superior and inferior venae cava, which then passes through the right atrioventricular valve (tricuspid valve) to the right ventricle, and from there it is pumped to the lungs via the pulmonary arteries. Regulation of the cardiovascular system is maintained through three homeostatic mechanisms; neural, endocrine, and autoregulatory mechanisms [16].

The heart consists of three layers, the epicardium (outer lining), the myocardium (the middle layer made up of myocytes), and the endocardium (the inner layer). These three layers are surrounded by the pericardium that protects the heart.

Blood vessels also consist of three layers (tunics); outer tunica externa, a middle tunica media, and an inner tunica intima. The outer tunica externa is made up of connective tissue (collagen and elastic) that help support and facilitate stretching of the vessels. The middle tunica media is made up of smooth muscle cells that regulate blood flow by vasodilation or vasoconstriction. Finally, the inner tunica intima is made up of endothelial cells. Unlike arteries and veins, capillaries only consist of one layer, the tunica intima [17].

1.3   Cardiac Metabolism

There are two main substrates used for energy production in the heart: carbohydrates and fatty acids (FAs). In normal conditions, these substrates contribute 30 % and 70 % of the energy for the heart from carbohydrates (and a small amount of ketone bodies and amino acids) and FAs, respectively. The mitochondria generates 90-95 % of that energy through oxidative phosphorylation, while the remaining 5-10 % of energy comes from glycolysis and the tricarboxylic acid (TCA) cycle [15, 18]. The majority of cardiac energy (60-70 %) is used for contractility, and the remainder (30-40 %) is used for sarcoplasmic reticulum calcium ATPase (SERCA) and other ion pumps [19]. The heart is a metabolically flexible organ as the ratio of energy from its different substrates shifts under different conditions in accordance with energy demands, oxygen availability, and subcellular changes [20]. The energy pool in the heart consists of adenosine triphosphate (ATP) and phosphocreatine (PCr); which acts as a transporter and buffer system for ATP [21]. A simplified schematic pathway of metabolism in the heart is shown in figure 1.1 [15].
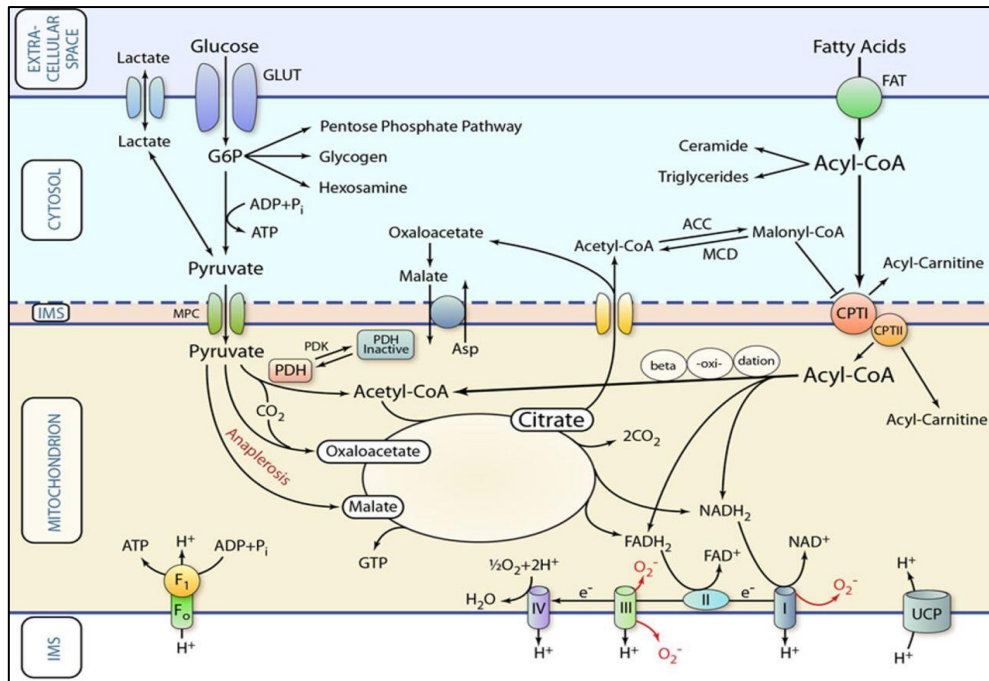
Figure 1.1: Metabolism and energy production in the heart [15]. More details are provided in the text above.

1.3.1   Glucose Metabolism

Glucose is transported into the cytosol of the cell via glucose transporters (GLUTs) such as GLUT1; which is the major transporter in foetal hearts, and GLUT4; the dominant transporter in adult hearts [22, 23]. Then, glucose is phosphorylated inside the cell into glucose-6-phosphate (G6P) which is used for glycogen synthesis, the pentose phosphate pathway (PPP), or the main glycolytic pathway yielding pyruvate, nicotinamide adenine dinucleotide (NADH), and a small amount of ATP [24, 25]. The pyruvate then is either converted into lactate or enters the mitochondria to be oxidized into acetyl-CoA by the enzyme pyruvate dehydrogenase (PDH). Additionally, it can be carbonylated into oxaloacetate or malate (anaplerotic pathway) [5]. The heart stores glucose as glycogen to be used as a substrate for energy production under conditions of increased energy demands because glucose is 20-30 % more metabolically efficient in producing ATP per mole of oxygen (O_2) compared to FAs [26].

Glucose oxidation is mainly regulated by the enzyme PDH, which is inhibited by acetyl-CoA and NADH (product inhibition), phosphorylation in the E1 subunit by PDH kinase (PDK) and activated by dephosphorylation by PDH phosphatase.

High circulating FAs are considered an inhibitor of glucose metabolism because they enhance the expression of PDK4; the main form of PDK in the heart, via peroxisome proliferator activated receptor-α (PPARα), resulting in phosphorylation of PDH and inhibition of the oxidation of pyruvate from glycolysis and lactate [27, 28]. The enzyme PDH phosphatase activates PDH by dephosphorylation and is increased by calcium (Ca^{2+}) and magnesium (Mg^{2+}). This is what happens in β-adrenergic receptor stimulation of the heart, as cytosolic Ca^{2+} transient increases and mitochondrial Ca^{2+} concentrations rise, leading to the activation of PDH phosphatase and increased oxidation of pyruvate [29-31]. Figure 1.2 shows the regulation of glucose oxidation in the heart [5].
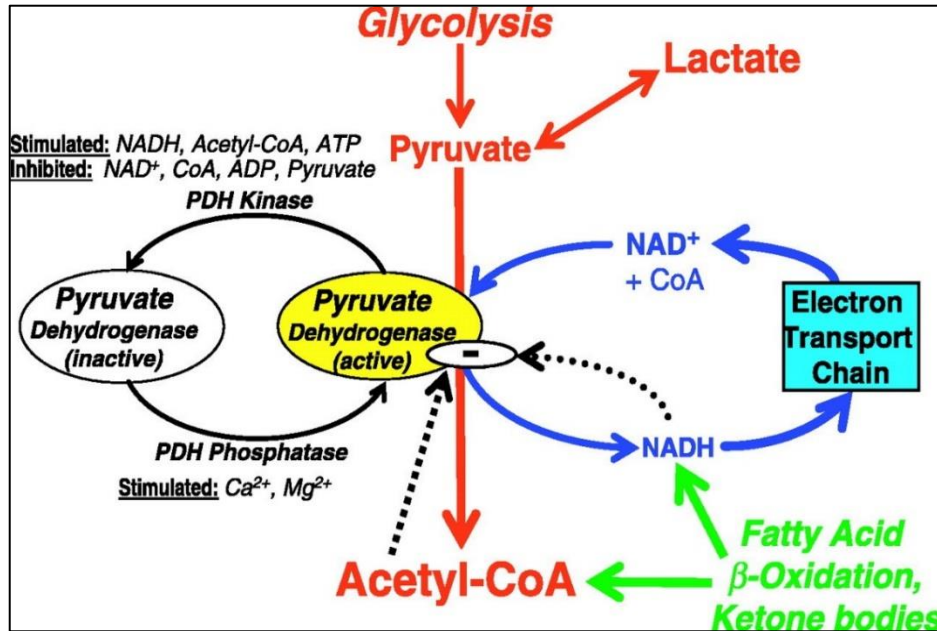
Figure 1.2: Regulation of carbohydrate oxidation in the heart [5].
Details are mentioned in the text above.

1.3.2   Fatty Acid Metabolism

For FAs to enter the cell they either enter by passive diffusion or they need a transporter protein called FA translocase and the membrane FA binding protein [32, 33]. CD36 is the most abundant FA translocase in the heart and it regulates the rates of FA uptake in the heart [32, 34, 35]. In the cytosol, FAs are esterified into fatty acyl-coenzyme A (CoA) which is then either esterified into triglycerides by glycerol phosphate acyltransferase or converted into long-chain acylcarnitine to enter the mitochondria [36]. This is done by the enzyme carnitine palmitoyltransferase I (CPT I), and is an essential regulatory step in the oxidation of FAs [36]. In the healthy heart, 70-90 % of fatty acyl-CoA is converted into acylcarnitine, and the remaining 30-10 % is esterified into triglycerides [37, 38]. The cardiac triglycerides pool is important for energy production during reperfusion of ischaemic hearts [39]. The long chain acylcarnitine then enters the mitochondrial matrix by carnitine acyltranslocase and is converted back into acyl-CoA by CPT II. Acyl-CoA is then oxidised (β-oxidation) to give acetyl-CoA, NADH, and reduced flavin adenine dinucleotide ($FADH_2$) [20].

CPT I is regulated by malonyl-CoA and other mechanisms that inhibit FA oxidation [40-42]. Malonyl-CoA is a product of carboxylation of extra-mitochondrial acetyl-CoA by acetyl-CoA carboxylase (ACC) [43] [44, 45]. ACC is inhibited by phosphorylation by adenosine $5'$ monophosphate-activated protein kinase (AMPK), which in turn accelerates FA oxidation [46]. Malonyl-CaA is converted back into acetyl-CoA and carbon dioxide (CO_2) by the enzyme malonyl-CoA decarboxylase [47] [48]. Figure 1.3 shows the regulation of FA metabolism in the heart [5].
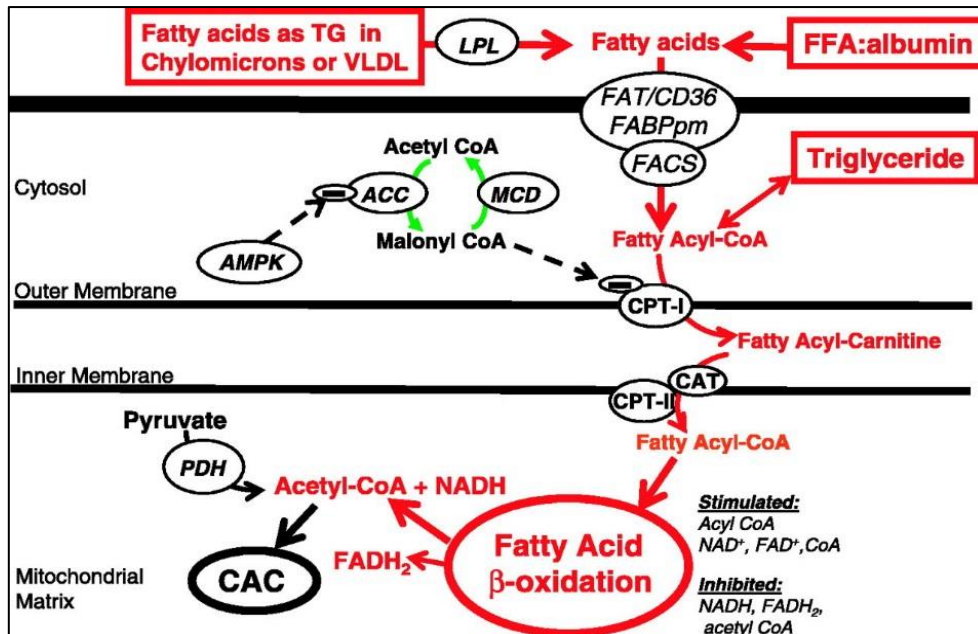
Figure 1.3: Process of fatty acid oxidation in the heart [5]. Details are provided in the text above.

1.3.3   Tricarboxylic Acid Cycle (Krebs Cycle)

Acetyl-CoA from glucose and FA oxidation enters the TCA cycle to generate ATP, CO_2, and $NADH_2$. The acetyl-CoA joins with oxaloacetate to form citrate via the enzyme citrate synthase. The citrate then goes into a series of reactions ending in the formation of oxaloacetate, which joins with acetyl-CoA once again starting a new cycle (figure1.4 [11]).

Intermediates in the TCA cycle are consistently used for other pathways such as amino acid and nucleic acid synthesis, and thus they need to be replenished from sources other than acetyl-CoA (e.g. carboxylation of pyruvate into malate) [49]. This process is called anaplerosis and is crucial in the heart as impairment causes cardiac dysfunction and disease [49-51]. One TCA cycle yields 3 NADH, 1 $FADH_2$, and only 1 ATP molecule. NADH and $FADH_2$ from the TCA cycle then enter the electron transport chain (ETC) located in the inner mitochondrial membrane for oxidative phosphorylation generating reactive oxygen species (ROS) mainly from complexes I and III [52].
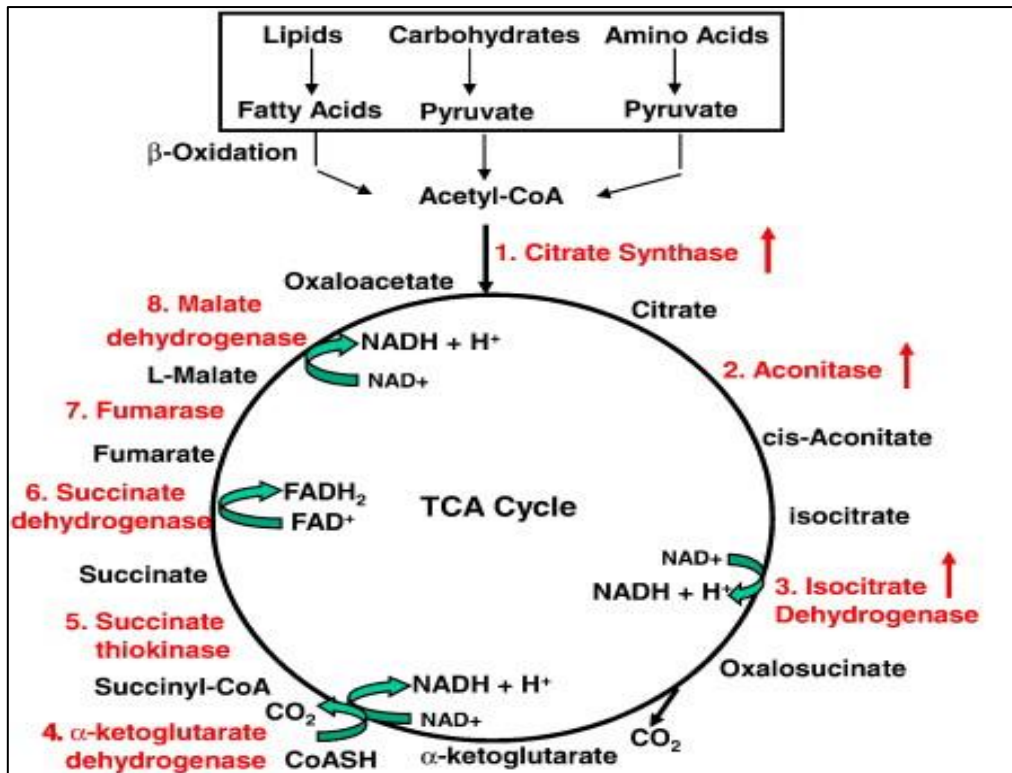
Figure 1.4: Illustration of the TCA (Krebs) cycle [11]. Details are provided in the text above.

1.3.4   Oxidative Phosphorylation

The ETC consists of four complexes, complex I (NADH-quinone oxidoreductase), complex II (succinate dehydrogenase), complex III (ubiquinol-cytochrome c oxidoreductase), and complex IV (cytochrome c oxidase).

As described in [3], NADH donates two electrons to complex I which uses them to transfer 4 hydrogen ions (H^+) into the inter-membrane space. The two electrons are then transferred to complex III via coenzyme Q, which results in 4 more H^+ being transferred into the inter-membrane space from this complex. Cytochrome C carries the two electrons into complex IV. In complex IV, the two electrons react with O_2 yielding H_2O and resulting in two H^+ being transferred into the inter-membrane space. So, the total number of protons from NADH becomes 10.

33

FADH$_2$ enters complex II of the ETC and is then carried by coenzyme Q into complex III (resulting in 4 H$^+$ being transferred into the inter-membrane space), and then into complex IV via cytochrome C resulting in two more H$^+$ being transferred into the inter-membrane space. Making the total number of protons 6 from FADH$_2$.

ATP synthase then uses this proton gradient to make energy and synthesise ATP from adenosine diphosphate (ADP) and inorganic phosphate (Pi). Four protons are used to make one molecule of ATP, meaning NADH and FADH$_2$ can generate 2.5 and 1.5 ATP molecules, respectively. Figure 1.5 shows a schematic representation of the ETC complexes and the oxidative phosphorylation process [3].
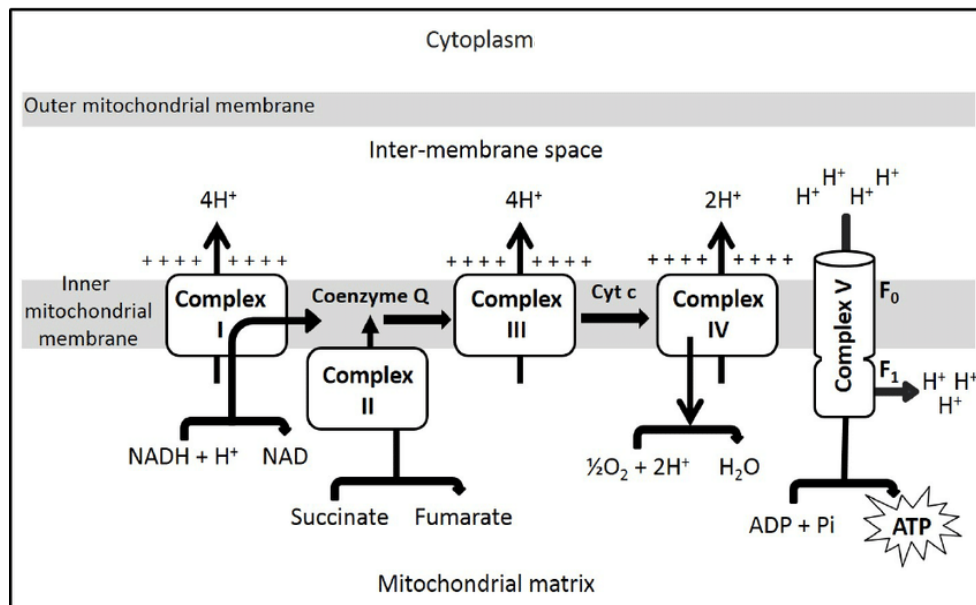
Figure 1.5: Representation of the mitochondrial ETC complexes and the oxidative phosphorylation process [3] Details are provided in the text above.

1.3.5 Ketone Bodies Metabolism

Ketone bodies (β-hydroxybutyrate and acetoacetate) are made from FAs in the liver, and in normal conditions their contribution to cardiac energy is relatively small. However, in situations like starvation or uncontrolled diabetes, levels of ketone bodies in the plasma are elevated and they become a major source of energy for the heart [43]. Metabolism of ketone

bodies inhibits the oxidation of glucose and lactate, as well as the uptake and oxidation of FAs [53-56].

1.4 Excitation-Contraction Coupling

1.4.1 Excitation (Action Potential)

Excitation-contraction (EC) coupling is the process of generating an energy dependant electrical signal that leads to the contraction of the heart. Pacemaker cells in the sinoatrial (SA) node in the right atrium generate this electrical signal, which then passes through the myocytes of the atria via gap junctions and into the ventricles via the atrioventricular (AV) node [57].

The action potential in the SA node differs than that in the AV node by having no actual resting phase. There are three phases in the SA node action potential. Phase 4 is the spontaneous depolarisation phase that triggers the action potential when membrane potential reaches between – 40 and – 30 mV. This is followed by phase 0 which is the depolarisation phase. And finally, phase 3 which is repolarisation of the membrane, when membrane potential reaches about – 60 mV. The depolarisation in the SA node mainly depends on slow Ca^{2+} currents instead of fast Na^+ current, which leads to a slower action potential referred to as slow response action potential [433].

The action potential has five phases of depolarisation and repolarisation (phase 0–4). As described in [9], phase 4 is called the resting phase, where the myocyte membranes have a negative potential of around -90 mV due to the movement of potassium ions (K^+) across the membrane via the inward rectifying potassium channels. When the electrical signal flows from the SA node it leads to rapid depolarisation of the resting membrane (phase 0). Depolarisation happens due to the opening of the voltage gated sodium channels and entry of sodium ions (Na^+) into the myocytes. This is followed by the early repolarisation phase (phase 1), where the sodium channels are inactivated and chloride (Cl^-) and (K^+) are moved out of the cell, causing the membrane potential to become positive. Phase 2 of the action potential occurs when

the balance between influx of Ca^{2+}, through L-type Ca^{2+} channels (which open at a potential greater than -40 mV), and efflux of (K^+), through delayed rectifier potassium channels, becomes balanced and the potential plateaus. Finally, when membrane potential drops below -40 mV, the delayed rectifier potassium channels remain open, and the L-type calcium channels close, causing rapid repolarisation (phase 3), until the membrane reaches a potential of -90 mV returning to its resting (phase 4) state. This is shown in figure 1.6 below.
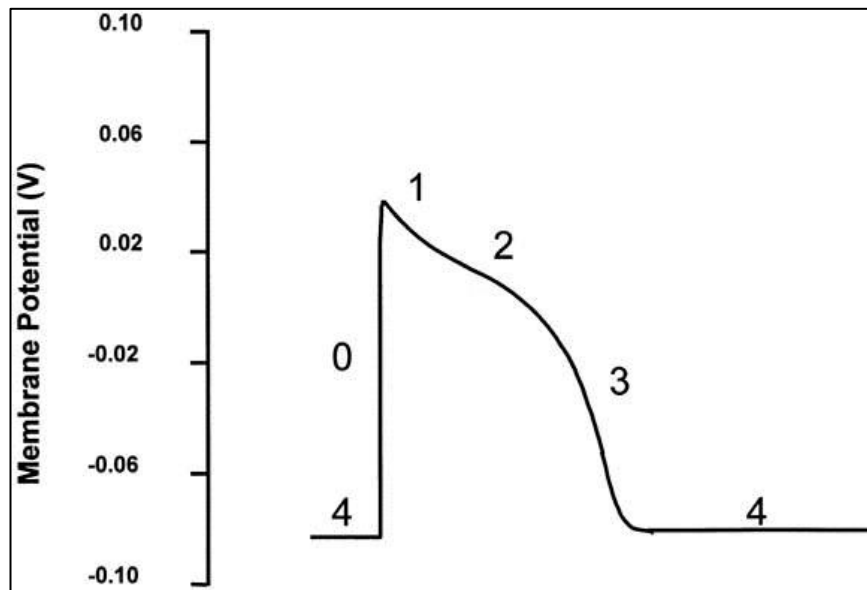
Figure 1.6: Schematic representation of the cardiac action potential [9].

1.4.2 Contraction

There are two types of filaments: thin (actin) filament, and thick (myosin) filament. The actin filament is a helix made up of two chains of polymerised actin molecules, and the myosin filament consists of a long tail with two heads at one end of the tail [58]. These two filaments make up the contraction unit in the heart called the sarcomere. The sarcomere has two bands depending on the arrangement of the filaments; the isotropic band (I band) which is made up of thin actin filaments, and the anisotropic band (A band) which is made up of both actin and myosin filaments. These two bands are contained between Zwischenscheibe lines (Z lines) [59]. The thin actin filament has the troponin complex which consists of troponin I (the

inhibitor of the actin-myosin interaction), troponin C (the calcium binding site), and troponin T (which binds to tropomyosin).

For the contraction to occur, intracellular Ca^{2+} needs to bind to the thin actin myofilament through troponin C. During phase 3 in the action potential when L-type calcium channels open and Ca^{2+} enter the cell, this causes the release of more Ca^{2+} from the sarcoplasmic reticulum (SR); regulated by ryanodine receptor (RyR), increasing the intracellular Ca^{2+} concentration from 0.1 μM to 1 μM in adult cardiomyocytes [6]. This process is known as calcium-induced calcium release (CICR). Intracellular Ca^{2+} then binds to actin causing conformation changes that unblock the myosin binding site on the actin molecule [60]. The two filaments bind together (The Cross-Bridge Cycle), and this process utilises energy by hydrolysing ATP, releasing phosphate, and leading to contraction with the shortening of the I bands and the moving of the Z lines closer (the sliding filament theory) [59].

1.4.3 Relaxation

During relaxation, a number of proteins lower the concentration of cytosolic Ca^{2+}. Calsequestrin is a calcium binding protein in the SR that acts on the RyR when cytosolic Ca^{2+} concentrations are high, and the SR calcium content is low. Calsequestrin inhibits RyR stopping the release of more Ca^{2+} from the SR and allowing the SR to refill [6]. Additionally, SERCA regulates the uptake of Ca^{2+} into the SR to facilitate relaxation [61]. The sodium/calcium exchanger (NCX) is the major pathway by which calcium is extruded from the cell [62]. When cytosolic Ca^{2+} concentrations fall, the calcium-troponin C complex dissociates allowing relaxation.

Additional proteins that are involved in the homeostasis of cellular calcium include cyclic adenosine monophosphate (cAMP), which activates protein kinase A (PKA). Activated PKA phosphorylates phospholamban (PLN) (a protein that inhibits the action of SERCA), which

inhibits its activity leading to the activation of SERCA [63]. Figure 1.7 shows the EC coupling and regulation of intracellular calcium concentration [6].
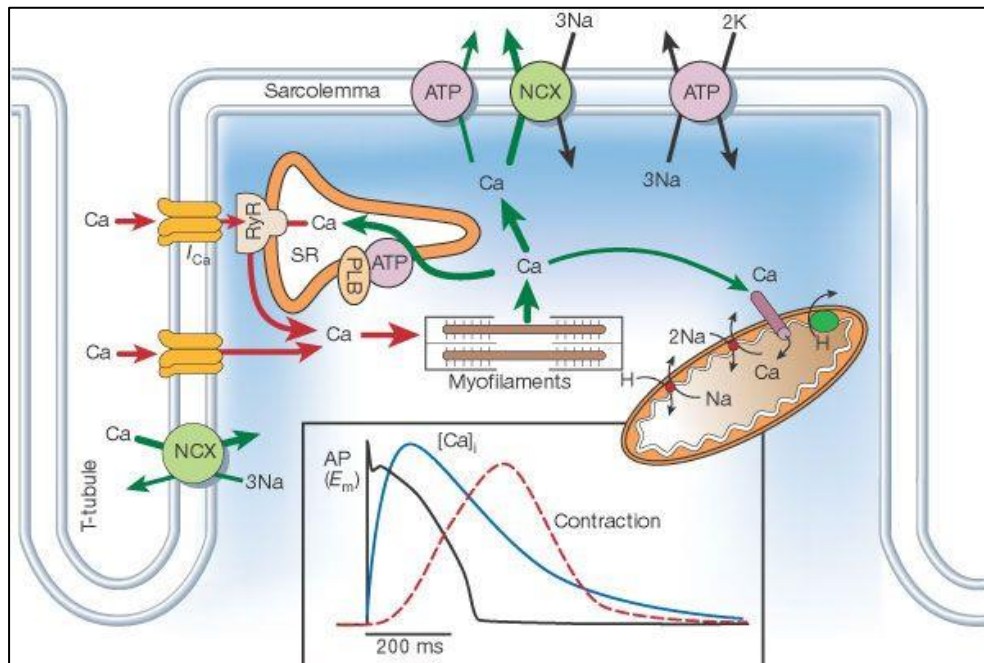
Figure 1.7: Excitation-contraction (EC) coupling in the heart and intracellular calcium regulation [6]. Details are provided in the text above.

1.5   Ischaemia/Reperfusion Injury

1.5.1   Overview

Cessation or reduction of blood flow to the heart (ischaemia) predisposes the myocytes to reperfusion injury when blood flow is reintroduced to the heart (reperfusion) [64]. The main alterations in I/R causing injury to the heart are generation of ROS, ionic disturbances leading to cellular Ca^{2+} overload, change in cellular pH, inflammation, and the opening of the mitochondrial permeability transition pore (mPTP). In ischaemia, the absence of oxygen results in the cell switching to anaerobic metabolism, which results in lactate accumulating in the myocyte leading to a drop in pH (< 7.0). The decrease in pH and accumulation of protons in the cell activates the sodium/hydrogen ion exchanger (Na+/H+ exchanger) which extrudes the excess H^+ in an attempt to neutralize the pH of the cell, which leads to the efflux of protons in

exchange for Na^+ entering the myocyte. Due to the lack of ATP during ischaemia, the sodium/potassium ATPase activity is stopped, which leads to the accumulation of Na^+ inside the cell. In order to extrude Na^+ from the cell, the NCX is activated, and this leads to the accumulation of Ca^{2+} (calcium overload) in the myocyte (figure 1.8).
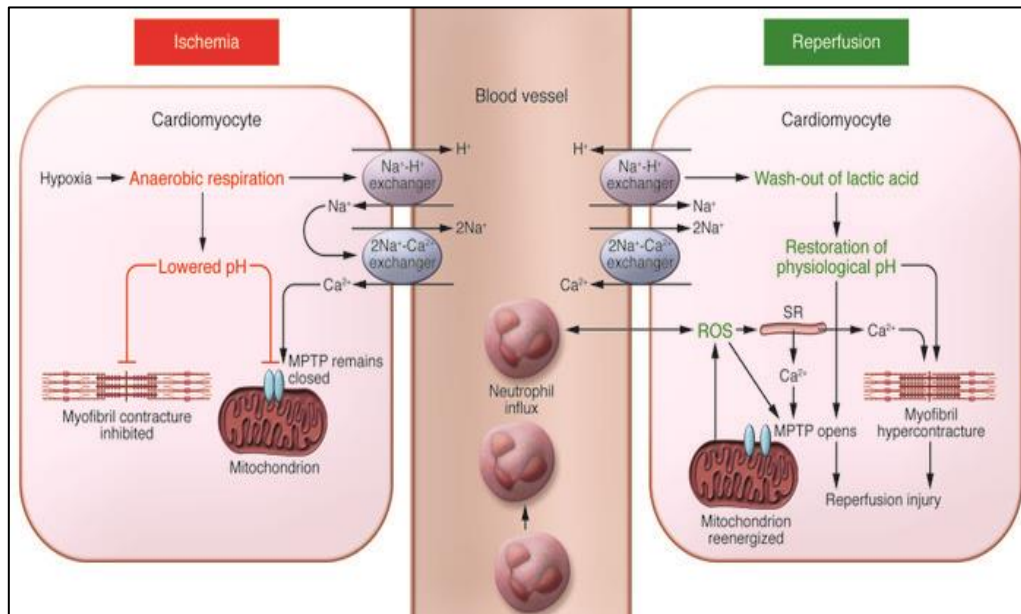
Figure 1.8: Components of myocardial I/R injury [13].

During reperfusion, oxygen and metabolites are restored for aerobic metabolism, oxidative phosphorylation, and ATP production, however, reperfusion is associated with additional tissue injury as evident by the fact that intervention during reperfusion have shown to reduce infarct size by 50 % [64]. Factors mentioned earlier (oxidative stress, the rapid restoration of cellular pH, and the opening of the mPTP) mostly happen during reperfusion.

Reperfusion injury can trigger reversible injury including arrythmias and cardiac stunning (contractile dysfunction), irreversible microvascular obstruction, and lethal myocardial reperfusion injury (death of cardiomyocytes that were viable before reperfusion) [13]. Microvascular obstruction is characterised by capillary damage and sluggish blood flow that hinders the reperfusion of an ischaemic area [65]. This dysfunction in capillaries can be caused

by a number of reasons such as impairment in vasodilation, compression by swelling myocytes, and neutrophil plugging, and it is associated with worsened clinical outcomes such as larger MI size, LV remodelling, and lower ejection fraction [66-69].

1.5.1.1 The Role of pH

The role of pH in I/R injury has been studied and is called the pH paradox [70]. Manipulations to delay the normalisation of cellular pH during reperfusion confirmed its protective role against I/R. Reperfusion with an acidic buffer to slow the normalisation of pH in the cell has been shown to reduce cell loss in rat hepatocytes [71]. Blocking the Na^+/H^+ exchanger in an attempt to delay cellular pH restoration, helped in reducing loss of myocytes. This effect is independent of intracellular Ca^{2+} concentration, as it did not reduce Ca^{2+} concentration in the cell [70]. Additionally, blocking the NCX reduced intracellular calcium but not cell death [70]. The mechanism proposed here by the author is that during ischaemia there is a release of hydrolytic enzymes (phospholipases and proteases) that are activated once pH is normalised during early reperfusion. Additionally, the normalisation of pH increases the mitochondrial permeability and activates myofibrillar ATPase, which increases the ATP demands in the cell.

1.5.1.2 The Role of Cellular Calcium Overload

Intracellular calcium overload starts during ischaemia when the sodium/calcium exchanger is activated. This is exacerbated when reperfusion starts because of disruption of plasma membrane, damage of SR from ROS, and the re-energisation of the cell [13]. In addition to calcium overloading inside the cell, it enters the mitochondria through the calcium uniporter, and this induces the opening of the mPTP [72].

1.5.1.3 The Role of The Calpain System

Calpains are Ca^{2+}-dependent nonlysosomal cystein proteases localized in the cytosol of the cell when in their inactive form [73]. The calpain family consists of more than 25 calpains or calpain-like proteins. Calpains can either be ubiquitous proteins found in almost all cells, or

tissue-specific proteins such as calpain 3 found in skeletal muscle. There are two main isoforms of calpains, μ-calpain (calpain 1) and m-calpain (calpain 2). The micro/milli-molar indicates the Ca^{2+} concentrations required for the activation of each type [74].

Under normal physiological conditions, calpain proteins are found in the cytosol of the cell in their inactive form, bound to their inhibitor calpastatin [75]. When intracellular Ca^{2+} concentrations increase, calpains are translocated into the cellular membrane for activation, but activation only happens upon reperfusion when pH levels in the cell are normalised [76].

Activated calpains in turn activate a number of growth factor receptors, cytoskeletal proteins, microtubules associated proteins, and mitochondrial proteins, which all play a role in cellular processes such as differentiation and apoptosis [77]. More importantly, because calpains are part of the integrated proteolytic system, once activated they target cardiac structural proteins that are required for cardiac structural integrity. Both myofibrillar and regulatory proteins of the contractile apparatus (important for sarcomere) are affected by calpains activation [78]. Additionally, T-tubules junctophilin are also proteolyzed by calpains [79, 80]. The dysfunction or loss of organisation of sarcomere and T-tubules are both associated with numerous
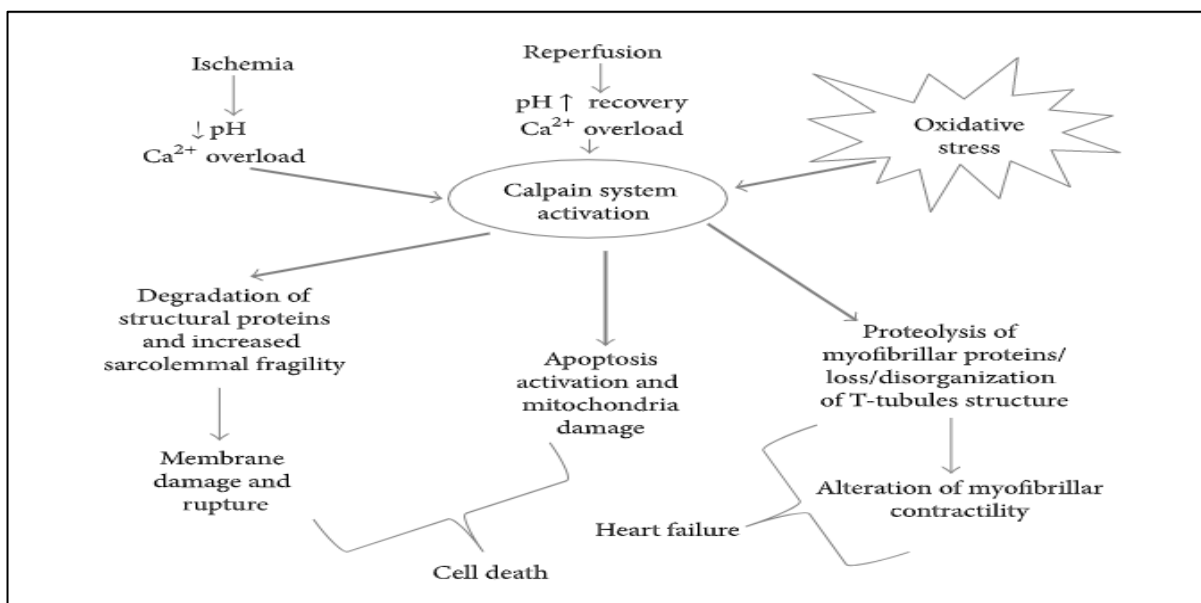
Figure 1.9: Calpain system activation in I/R injury [7].

cardiovascular diseases including I/R injury and heart failure [81-83] figure 1.9 shows the activation of calpain proteins [7].

1.5.1.4 The Role of Mitochondrial Permeability Transition Pore

The mPTP was first described in the late 1970s by Haworth and Hunter [84]. Its role in I/R injury was first described in 1987 [85]. The mPTP remains closed throughout ischaemia and only opens when reperfusion of the heart starts [86]. During ischaemia, the acidosis of the cell helps in maintain the mPTP closed, but as reperfusion starts, there is an increase in Ca^{2+} concentration, oxidative stress and rapid normalisation of the cellular pH which all contribute to the opening of the mPTP [86-88].

The opening of the mPTP causes the influx of water and solutes into the mitochondria leading to its swelling. The inner mitochondrial membrane can accommodate for this increase, however the outer mitochondrial membrane ruptures releasing the contents of the inter-membrane space, which include pro-apoptotic and apoptosis-inducing factors (e.g. cytochrome C) [89].

This explains the reported apoptosis in most of the studies investigating ischaemia followed by reperfusion rather than in ischaemia on its own [90-92].

1.5.1.5 The Role of Oxidative Stress

ROS are highly reactive molecules that have an unpaired electron in their outer shell. They include hydrogen peroxide (H_2O_2), the superoxide radical anion ($O_2^{\bullet-}$), and the hydroxyl radical ($OH^{\bullet}$) [93]. Oxidative stress occurs when the generation of ROS is higher than their neutralisation by antioxidant defences in the body. ROS lead to DNA oxidation, lipid peroxidation, damage to proteins and membranes, ultimately affecting permeability, structure, and function [94].

Reperfusion increases ROS through mitochondrial reenergisation and activation of a number of enzymes such as NADPH oxidases (NOX). NOX uses NADPH as the electron donor to

reduce O_2 and generate $O_2^{\bullet-}$ [95]. Studies have shown that the absence of this enzyme (using NOX knock-out mice) reduced reperfusion injury and infarct size by up to 50 % [96].

Another enzyme activated during reperfusion is xanthine oxidase. This enzyme is present in the vascular endothelium and produces ROS (specially $O_2^{\bullet-}$), which activates neutrophils and their adherence to endothelial cells, leading to the production of more xanthine oxidase and thus more superoxide radicals [97]. Additionally, during ischaemia, xanthine dehydrogenase can be further converted into xanthine oxidase [98].

Another enzyme involved in ROS-reperfusion injury is the endothelial nitric oxide (NO) synthase (eNOS), which is involved in the regulation of vascular function. With the disruptions that occur during I/R, eNOS can become uncoupled and starts producing $O_2^{\bullet-}$ instead of NO [99].

In addition to ROS, reactive nitrogen species (RNS), mainly peroxynitrite anion (ONOO-), contribute to reperfusion injury [98]. ONOO- is produced by the reaction between $O_2^{\bullet-}$ and NO, and its production leads to the uncoupling of eNOS and the other NOS isoform (iNOS), increasing the production of $O_2^{\bullet-}$ [100].

1.5.1.6   The Role of Inflammation

It is not clear whether inflammation is a result of I/R injury or a contributing factor to the injury. Some studies looking at the effects of using anti-inflammatory substances in I/R showed that targeting the inflammation reduced I/R injury significantly. A study in felines targeted the neutrophil-endothelial cells interaction by administering P-selectin glycoprotein ligand-1 prior to reperfusion, which caused a significant reduction in injury caused by I/R [101]. Another study using a monoclonal antibody against the intercellular adhesion molecule-1 in endothelial cells to prevent the neutrophil-endothelial interaction in rabbits, also showed an improvement in I/R outcome and reduction in infarct size [102]. Additionally, another study using inhibition of the complement activation in rats showed that targeting C5 complement resulted in a

reduction in apoptosis and necrosis, and neutrophil infiltration after I/R [103]. However, other trials using the same approaches showed negative results [104, 105].

1.6 Ageing and Cardiovascular Disease

Ageing is considered a risk factor for CVD and heart failure (HF), mainly because of its effects on the structural, functional, molecular, and cellular remodelling of the cardiovascular system that causes heart dysfunction [8]. Hypertension, CHD, stroke, and heart failure are all forms of CVD that are prevalent in the elderly population (> 65 years) and are estimated to increase by 10 % in the next 20 years [106]. The leading cause of death in Europe and the United States is CHD, which associates strongly with ageing [107-109].

1.6.1 Cardiovascular Structural and Functional Changes with Ageing

Structurally, some of the most common changes that occur with ageing in the heart include hypertrophy. Even though with ageing there is a loss of cardiomyocyte numbers; 45 million myocytes are lost in the left ventricle each year, there is an increase in their size as a compensatory mechanism and this contributes to the cardiac hypertrophy and increased myocardial thickness seen in the ageing heart [110, 111]. In addition, the heart also changes from an elliptical to spheroidal shape with an increase in the thickness of the interventricular septum (IVS) [112]. Due to increased workload and decreased cardiac reserve capacity in the ageing heart, compensatory mechanisms and functional changes occur in the heart and these include changes in heart rate, end systolic and diastolic volumes, contractility, and sympathetic signalling, which eventually contribute to CVD. Increased left ventricular wall thickness and size leads to a decrease in early diastolic cardiac filling, which in turn increases the cardiac filling pressure, the prevalence of atrial fibrillations and other arrythmias, and the likelihood of HF [12]. Suggested mechanisms for these dysfunctions include alterations in calcium handling,

growth factor regulation, and collagen deposition. Figures 1.10 and 1.11 illustrate some of the

structural and functional changes in the ageing cardiovascular system [8].
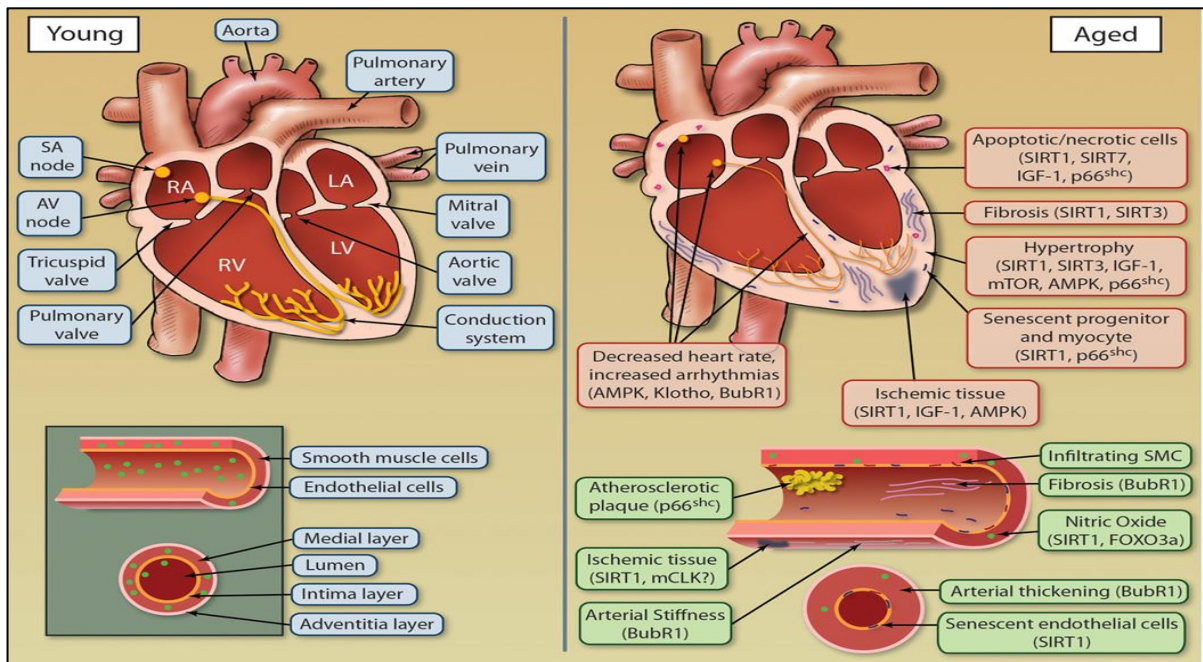
Figure 1.10: Age-related changes in cardiovascular tissues [8].
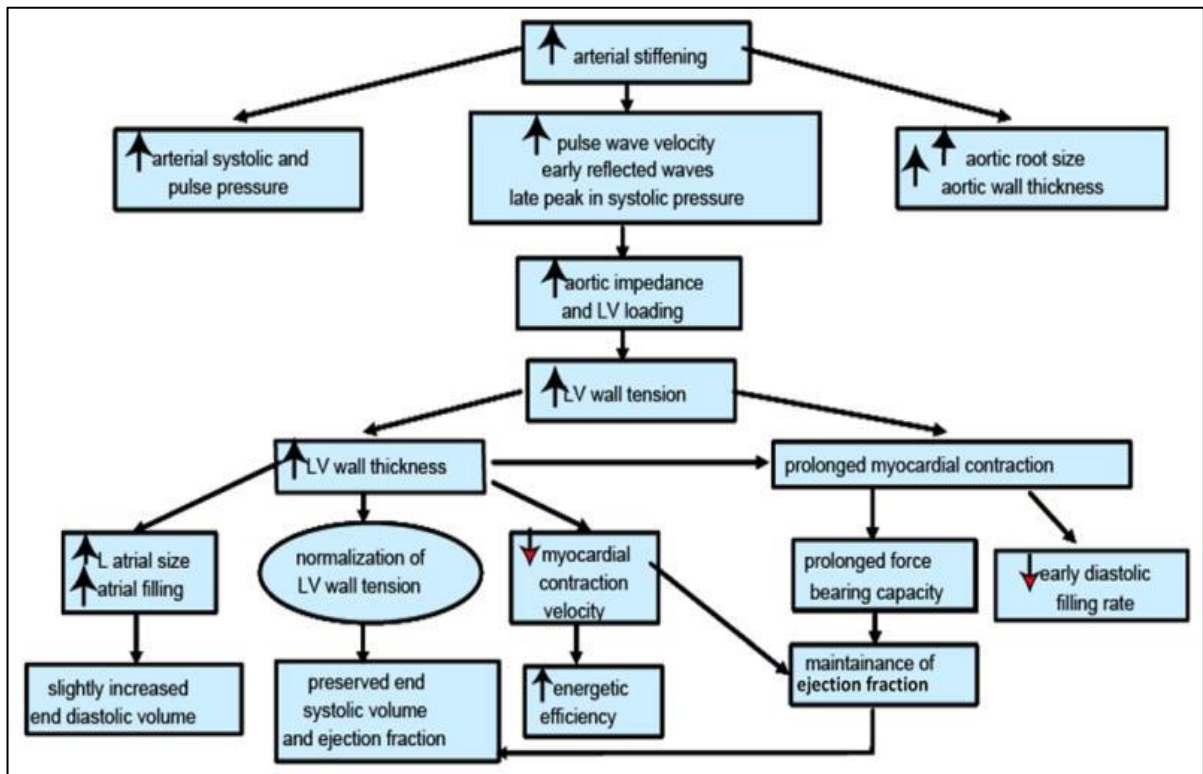
Figure 1.11: Age-related cardiac and arterial changes in healthy humans [12]

In addition to age-related cardiac changes, ageing also affects the vascular system. Common changes include thickening of large arteries, and loss of vascular elasticity [113]. Furthermore, the arterial wall media undergoes hypertrophy, accumulation of extracellular matrix, calcium deposits, and a decrease in vasodilators release and increase synthesis of vasoconstrictors in the vascular endothelium; which contributes to the vascular stiffness [114, 115]. Endothelial vasodilation reduction in ageing is thought to be secondary to a reduction in NO bioavailability, which is reduced due to a decrease in nitric oxide synthase (eNOS) [116-118].

Another common structural change seen with ageing is fibrosis. Collagen content and non-enzymatic collagen cross-linking increases with ageing, alongside fragmentation of elastic fibrils, which contributes further to the stiffening and loss of elasticity in the aged vessels [116]. These vascular changes in ageing contribute to hypertension, stroke, and the development of atherosclerosis.

Additional changes that occur with ageing also include the deposition of fat around the sinoatrial (SA) node, calcification of the left side of the cardiac skeleton, and a decline in number of pacemaker cells. These factors affect the cardiac conduction system and contractility, leading to arrhythmias such as atrial fibrillation, paroxysmal supraventricular tachycardia, and ventricular arrhythmias [12]. Despite all the changes that happen in the cardiovascular system with ageing, left ventricular ejection fraction (LVEF) and resting systolic function do not change [119].

These changes make the heart more prone to injury and stress, and with the accumulation of other conditions associated with ageing such as obesity, dyslipidaemia, and metabolic syndrome, the injury threshold of the ageing heart becomes lower [12].

1.6.2 Cardiac Metabolism in Ageing

Ageing affects the metabolism of the heart independent of disease. The major shift in metabolism with ageing is a decrease in the uptake and oxidation of FAs, with no change in

glucose oxidation, despite a decrease in GLUT4 expression in the ageing heart [120, 121]. PDH complex is a key enzyme that regulates the competition between mitochondrial glucose and FA oxidation. The phosphorylation of this enzyme by PDK in ageing is decreased favouring glucose oxidation [122]. Other changes observed in the ageing heart regarding metabolism include a decrease in the activity of CPT I and carnitine exchange in old rat hearts [123]. Additionally, the suppression of glucose oxidation by FAs was not evident in the ageing heart [123]. Furthermore, a reduction in the expression of PPARα; which regulates genes of FA metabolic enzymes, and the activity of cytochrome oxidase, citrate synthase, and 3-hydroxylacyl-CoA dehydrogenase (which are PPARα target enzymes) were all observed in the ageing heart, and were prevented by swim training [124]. The metabolic changes associated with ageing are similar to those seen in HF [125].

The energy pool in the heart consists of ATP and PCr; which acts as a transporter and buffer system for ATP, and this is an important determinant of cardiac function and performance [21]. It was found that the PCr:ATP ratio is significantly correlated with diastolic function, peak cardiac power output, and peak oxygen consumption, and that is decreased significantly with ageing, as well as being inversely correlated with heart rate [126]

Depletion of cardiac energy reserves has been associated with heart failure and left ventricular dysfunction, and a number of trials aimed at preserving this energy and counteracting the depletion using drugs; such as Angiotensin-converting enzyme (ACE) inhibitors, CPT inhibitors, and β-blockers have all shown to improve cardiac function and performance [127-129].

1.6.3 Calcium Homeostasis and Excitation-Contraction Coupling in the Ageing Heart

With ageing, contraction is prolonged, and relaxation is incomplete [130]. A number of factors lead to this change in EC coupling and change in contractility including a change in

myofilament proteins where they shift from α-myosin heavy chains to β-myosin heavy chains, which in turn decreases the myosin ATPase activity [131]. In addition to myofilament proteins, other proteins involved in calcium handling are altered with ageing and contribute to the change in EC coupling. L-type calcium channels have shown to increase in number and activity in the ageing heart with a decrease in their inactivation, all which prolongs the action potential [12]. Additionally, proteins of the SR controlling calcium release and reuptake are altered with ageing. Calsequestrin; the major SR calcium binding protein that stops the action of RyR2, showed no change in the ageing heart compared to the adult heart [132]. On the other hand, RyR2 showed a reduction in the ageing heart [133, 134]. The regulation of RyR2 by phosphorylation by Ca^{2+}/calmodulin-dependent kinase II (CaM kinase II) was also reduced in ageing which may affect calcium release from the SR as well [135]. All of these changes indicate slower calcium release from the SR in the ageing heart.

Another important protein is SERCA2a, which is affected in the ageing heart in activity and regulation [136, 137]. Decreased expression of SERCA2a; which helps in the SR reuptake of calcium, may cause the prolongation of contraction seen in the ageing heart, and also its regulation by PLB; an endogenous inhibitor that increases in ageing myocytes, contributes furthermore to the slowing of calcium reuptake [132]. Furthermore, phosphorylation of PLB by PKA increases the activity of SERCA2a and thus speeds relaxation, but this phosphorylation is decreased with ageing, which also prolongs contraction [135]. Additionally, CaM kinase II; which phosphorylates SERCA2a increasing its activity, is reduced in the ageing heart [135].

Finally, another component of interest in the EC coupling is NCX, which functions in removing calcium from the myocyte during relaxation. Studies on NCX activity in the ageing heart show contradictory findings where it is either decreased or remains unchanged with ageing [138, 139]. However, a recent study showed an increase in NCX activity in ageing ventricular

myocytes, which may aid in removing calcium from the myocytes during relaxation and compensate for the decrease in SERCA2a activity [140].

All of these changes are expected to slow SR calcium reuptake, reduce SR calcium content, and prolong the calcium transient, which subsequently leads to the contractile dysfunction seen in the ageing heart. Figure 1.12 shows changes in EC coupling and calcium homeostasis in the ageing heart.
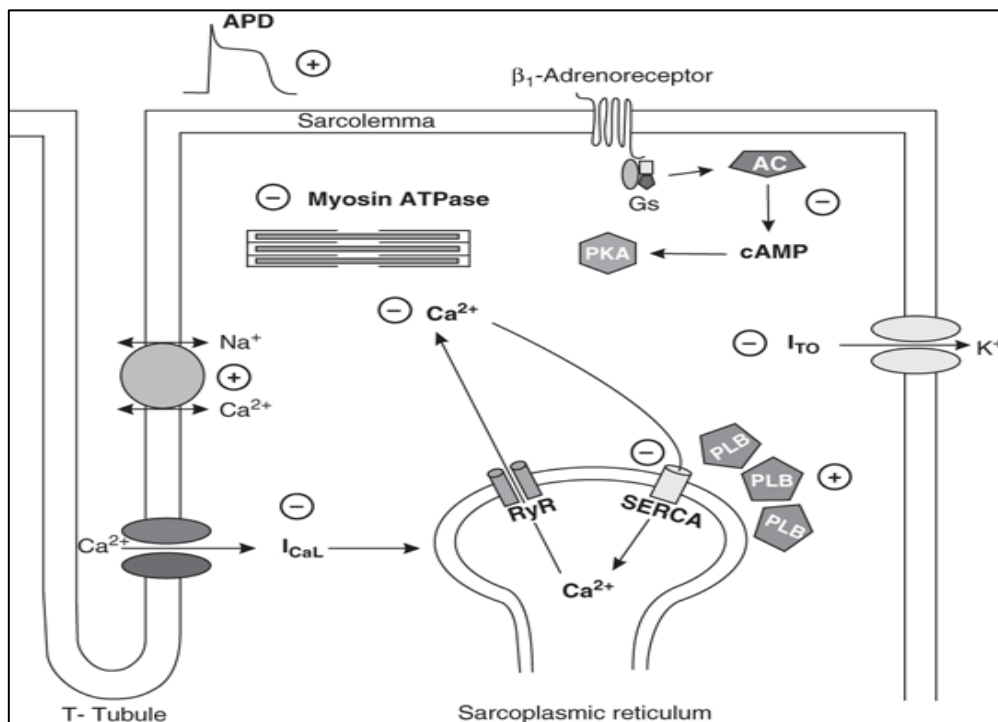
Figure 1.12: Age-related alterations in EC coupling in the heart [4].

1.6.4 Mitochondria in the Ageing Heart

1.6.4.1   Mitochondrial Morphology

Numerous studies have looked at the effects of ageing on mitochondrial function and morphology, with regards to their different subpopulations (interfibrillar (IF), Subsarcolemmal (SSL), and perinuclear (PN)). Some of the age-related changes reported include a decrease in mitochondrial number, oxidative phosphorylation, and cytochrome oxidase enzyme activity in rats [141]. However, these changes were only seen in IF mitochondria and not in SSL ones.

Another study in Fischer 344 rats described the variations in mitochondrial subpopulation cristae. SSL mitochondria mainly had lamelliform cristae (in situ) and after isolation, whereas IF mitochondria mainly had tubular or a mixture of tubular and lamelliform cristae (in situ) and mainly a mixture of both with the more lamelliform cristae after isolation. This showed that unlike SSL mitochondria, IF mitochondria tend to change after isolation [142]. Even though there was no change in cristae with ageing; suggesting their lack of involvement in the mitochondrial defect seen in ageing, the inner mitochondrial membrane per unit volume of mitochondria decreased significantly in aged rats of both Wistar and OXYS strains [143, 144]. Changes in mitochondria showing only in IF subpopulation were also observed in conditions other than ageing such as diabetes mellitus and cardiomyopathy [145, 146]

1.6.4.2 Mitochondrial Electron Transport Chain and Oxidative Phosphorylation

Oxidative phosphorylation in the mitochondria is changed with ageing mainly due to changes in ETC complex activity, protein levels, and inner mitochondrial membrane phospholipids [147]. SSL mitochondria have been found to maintain respiratory capacity in the ageing heart in rodents, however IF mitochondria appeared to consume less oxygen [141, 148-150]. This decline in oxygen consumption associated with a defect in ETC complex III and IV [151].

Additionally, the mitochondrial biogenesis and biogenesis regulatory proteins such as peroxisome proliferator-activated receptor-gamma coactivator-1alpha (PGC-1alpha) are decreased in the ageing heart [152-155].

Cardiolipin is a phospholipid in the inner mitochondrial membrane which is important for regulating ETC complex proteins and is found to be decreased with ageing, making it a target of intervention for preventing age-induced mitochondrial dysfunction [156].

Complex IV (cytochrome oxidase) defect with ageing is mainly due a defect in its inner membrane environment and a defect in its subunits. There is a 25 % decrease in the complex

IV subunit VIIa in the ageing heart, only in IF mitochondrial [157]. A possible decrease in cardiolipin content in the immediate complex environment may affect its organisation into supercomplexes and thus affecting its enzyme activity [158]. These defects decrease energy production, increase ROS production, and increase cell stress responses.

1.6.4.3 Reactive Oxygen Species

ROS can be generated in the cytosol by xanthine oxidases, the plasma membrane by NADPH oxidases, and most importantly in the mitochondria [147]. In the mitochondria, ROS are generated from complex I, II, and III, and from monoamine oxidases (MAO) that transfer electrons from amine groups to oxygen generating hydrogen peroxide and p66[Shc] [159, 160]. Due to the defects in the ETC mentioned earlier, electrons leak from the ETC and react with oxygen generating superoxide anions which in turn can be reduced to hydroxyl radicals and hydrogen peroxide [147].

Reports on ROS production in ageing heart are controversial, as some studies report increase production while others report no change in ROS production [161-164]. Hydrogen peroxide production was reported to increase with ageing in both SSL and IF mitochondria. Some studies report higher hydrogen peroxide production in SSL mitochondria, while others report higher production in in IF mitochondria [151, 165]. On the other hand, other studies report no difference in the ROS production in ageing between the two mitochondrial subpopulations [160]. Additionally, MAO-A and MAO-B were reported to be elevated in aged rat hearts and mice hearts respectively [166]. Also, mitochondrial p66[Shc] was reported to increase with ageing in SSL mitochondria [167].

Increased ROS formation has been linked to reduced life expectancy; however, this has not always been proven. When it comes to the antioxidant catalase, mice overexpressing catalase were reported to have better lifespan compared to their wild type counterparts [168]. This was

not the case with antioxidant manganese superoxide dismutase-2, as overexpression or reductions in the antioxidant did not affect lifespan or cell death in mice [169, 170].

1.6.4.4 Mitochondrial Permeability Transition Pore

The mPTP under normal non-stressed conditions remains closed and is opened by ROS, increased calcium concentration, mitochondrial membrane depolarisation. Once opened, it leads to mitochondrial swelling, rupture of the mitochondrial outer membrane, and the release of pro-apoptotic factors into the cell and eventually cell death (as mentioned earlier in the introduction – page 37).

The opening of the mPTP is affected by ageing. The calcium retention capacity of the mPTP was not found to be different between adult and aged rat hearts in SSL mitochondria [171]. However, it was reduced in IF mitochondria in aged rat hearts [172].

Additionally, cyclosporin-A is an mPTP inhibitor which was found to be effective in delaying ROS-induced mPTP opening in young but not aged rat hearts [173].

1.6.5 Ischaemia/Reperfusion Injury in the Ageing Heart

Ageing has been associated with increased vulnerability to I/R injury. It has been reported that the ageing heart has reduced oxidative phosphorylation as well as a decrease in complexes III and IV activity of the mitochondria, which contributes to this increased intolerance to ischaemia in the ageing heart [174]. Additionally, a study in Fischer 344 aged rats (24 months old) reported increased vulnerability of the isolated perfused heart to I/R compared to young (6 months of age) hearts. This was demonstrated by decreased functional recovery, increased tissue damage and CK release as well as LDH release [175]. Also, in another rat study using F344 BN rats (19 months vs. 4 months), ageing hearts were shown to be more vulnerable to myocardial I/R and this was associated with increased apoptosis characterised by increased expression of BAX to Bcl-2 ratio [176]. The ischaemic tolerance was shown to decrease in middle age (50 weeks of age) in Fischer 344 rats and progressed with increasing age, and was

suggested to be related to higher levels of intracellular sodium pre-ischaemia in middle aged and aged hearts, which led to a higher increase in sodium levels in the cell at the end of ischaemia [177]. Similarly, female Wistar rats aged 8-10 months and 24-28 months were used for comparing cardiac vulnerability, and increased vulnerability of the ageing heart to I/R injury was associated with Ca^{2+} homeostasis (increased sarcolemmal permeability for Ca^{2+} and decreased Ca^{2+} accumulating capacity of SR) [178]. In addition to studies using rats, mice were also studied for examining the vulnerability to I/R with ageing. C57BL/6 mice (6-8 months vs. 22-24 months) were used for I/R experimentation, and ageing hearts had larger infarction, myofiber tears, DNA fragmentation, and mitochondrial disruption [179]. Authors in the study suggested a decrease in coronary circulation and collateral flow as factors associated with this increased vulnerability in the ageing heart. Increased susceptibility to I/R injury was also reported to start during middle age in mice (12 months) with impaired ventricular contractility [180]. Authors in the study used 5 age groups (2-4 months, 8 months, 12 months, 18 months, and 24-28 months) and reported that diastolic dysfunction and impairments in functional recovery after I/R appeared since adulthood. LDH release from the heart during reperfusion showed a different pattern where it increased until middle age and then fell with further ageing to a level similar to that found in young adult hearts (2-4 months). Additionally, another study reported increased vulnerability of the ageing heart to I/R injury and associated this to the protein sestrin2 [181]. Sestrin2 is a stress-inducible protein that is important for AMPK activation. In this study, C57BL/6 mice were used (3-4 months vs. 10-12 months vs. 24-26 months) and ageing hearts had decreased tolerance to I/R as they had larger infarction, and this was associated with a decrease in sestrin2 levels. Also, hearts from 18 months old wild type mice compared to 7 months old hearts were shown to be more vulnerable to I/R injury, and this was exacerbated by decreased activity of SIRT3 (Silent information regulator of transcription 3) [182].

In contrast to previous studies, 13 months old C57BL/6 mice showed no difference in vulnerability to I/R injury measured by infarct size compared to 3 months old controls [183]. The difference seen was after ischaemic preconditioning when aged mice did not respond as adult mice did, and this was attributed to decreased levels of Connexin 43.

Conflicting results were also reported in human myocardium with regards to vulnerability to I/R in ageing, however, ischaemic preconditioning was not affected in the ageing heart as it was in mice [184, 185].

A number of studies have been looking at interventions to increase the ageing heart's tolerance to I/R injury. Caloric restriction was shown to reduce the ageing heart's vulnerability to I/R in mice and was associated with the AMPK-SIRT1 signalling pathway [186]. Additionally, elevated intracellular creatine levels in CrT-OE aged mice hearts (78 ± 5 weeks of age) showed better tolerance to ischaemia compared to their wild type littermates [187].

1.7   High-Fat Diet and Cardiovascular Health

It is well established that high fat diets contribute to obesity and the development of chronic diseases such as diabetes, metabolic syndrome, various types of cancer [188-190]. High fat diets are also linked to the development of cardiovascular diseases, and this is related more to the type of fat in the diet rather than the percentage of fat intake from total energy [191]. The way dietary fats affect cardiovascular health is not only confined to raising serum levels of cholesterol, but through different mechanisms including hypertension, insulin resistance, and inflammation [192]. HFDs typically comprise of 32-60 % calories from fat, and even though it is unlikely for a human diet to contain 60 % calories from fat, this is used in experiments to reduce the experimental time course [193]. These diets can either be obesogenic or atherogenic. Obesogenic diets are accompanied by weight gain and a development of a diabetic phenotype, while atherogenic HFDs are not [194].

1.7.1 High-Fat Diet and Cardiovascular Remodelling

HFD is known to affect the heart structurally and functionally. These diets are associated with changes in adiposity, glucose tolerance, insulin resistance, and hyperleptinemia [195]. It has been shown that a diet high in fat leads to cardiomyocyte hypertrophy and increased myocardial interstitial fibrosis, and unlike metabolic changes associated with HFD (e.g. hyperglycaemia); these structural changes occur even in the absence of obesity [196]. In a study using Wistar-Kyoto rats, HFD was associated with increase in body weight, metabolic changes, increase in systolic blood pressure, cardiac hypertrophy with no change in cardiomyocyte size, increased interstitial fibrosis, and a shift from α to β myosin heavy chain (MHC) expression [197]. Again, these structural cardiac changes were directly related to the fat intake independent of obesity. Martins et al. (2015) reported that Wistar rats fed HFD for 20 weeks showed significantly higher levels of glucose, larger left atrium diameter, larger myocyte cross sectional areas, and increased interstitial collagen fraction compared to their ND controls [196]. Additionally, another study using Dahl salt sensitive rats fed either a low fat or high fat diet for 12 weeks reported that increased dietary lipid intake is associated with cardiac growth, remodelling of the left ventricle, contractile dysfunction, and alterations in gene expression, but this effect was diminished in the presence of hypertension [198].

HFD cardiac remodelling was also studied in mice and showed similar findings. Calligaris et al. (2013) studied the effects of HFD on C57BL/6 mice for a period of 16 months [199]. The HFD fed mice were characterised by increases in weight, hyperglycaemia, insulin resistance, hyperinsulinemia, and hypercholesterolemia starting from the 8th month of feeding. By 16 months of feeding, they showed vasoconstriction, contractility dysfunction, increased heart mass, cardiomyocyte hypertrophy, fibrosis, and cardiac metabolic compensation compared to their ND controls [199]. Additionally, a study in rabbits reported that high fat feeding for 18 weeks induced a type II diabetes phenotype, which was associated with cardiac changes such

as LV hypertrophy, abnormalities in repolarization and arrhythmias during hyperkalaemia [200].

Additional structural remodelling of the heart with HFD includes collagen deposits, intercellular spaces, disorganisation of cardiomyocytes, deposition of fat under the pericardium as well as around vessels and between cardiomyocytes, and a thicker vascular wall with reoriented nuclei [201]. The same previously mentioned study, which was done on rabbits, found ultrastructural remodelling of the heart with HFD manifested in a decrease of myofibrils that became degenerated, sarcomere disorganization, larger intracellular junctions, decreased mitochondria distribution, damaged junctional complexes, and multiple vacuolization. The damage in the mitochondria resulted in them swelling, becoming elongated, with variations in size and cristae organisation.

The consumption of HFD has adverse effects on the heart even in the case of short periods of exposure [202]. In this study, the researchers used C57BL/6 male mice and fed them a ND or HFD for 9 days, and then performed a transverse aortic constriction (TAC) before continuing the feeding for another 28 days. HFD feeding for a short duration induced insulin resistance alongside increased LV remodelling and dysfunction after TAC.

Cardiac remodelling associated with HFD has been attributed to a number of cellular/molecular changes. Prolonged exposure to HFD has been associated with a reduction in collagen type I expression with no change in collagen type III [203]. However, other studies report upregulation of the expression of collagen I and III and TGF-β1 (transforming growth factor β1) with HFD [204]. Additionally, HFDs affect the calcium handling proteins expression and upregulates them in the SR [205]. In rats fed HFD for 15 weeks, obesity was associated with increased plasma insulin, glucose, and leptin concentrations. In addition, SERCA2a, RyR2 and PLB mRNA were all increased, but no changes were found in Cacna1c (α-1C subunit of the voltage-gated L-type Ca^{2+} channel) and NCX. However, another study in rats showed that HFD

and obesity do not alter the expression of PLB or its phosphorylation [206]. Also, SERCA2 activation was reduced via calmodulin kinase in HFD-induced obesity, which was related to the cardiac dysfunction seen in obesity [207].

HFD associated cardiac remodelling and dysfunction was also related to SIRT3 [208]. In this study, the role of SIRT3 was assessed by using WT and SIRT3 knockout mice. These mice were fed either a normal diet or a HFD for a period of 16 weeks. Mice on the HFD showed a significant decrease in SIRT3 expression in the heart, as well as an increase in ROS formation, impairment in HIF (hypoxia inducible factor) signalling, and a decrease in capillary density in the heart. KO mice on HFD in this study also showed increased ROS production and further reduction in cardiac function compared to their ND controls.

Wang et al. (2015) suggested that cardiac hypertrophy and fibrosis caused by prolonged feeding with a HFD is mediated by GSK-3β (Glycogen synthase kinase 3 beta) inhibition [209]. This study used 7-week-old CD1 male mice, either given a ND or HFD for a period of 11 months. Additionally, Roberts et al. (2015) reported that metabolic adaptation favouring lipid metabolism and downregulation of glucose metabolism (noted by a reduction in pAMPK, GLUT4, and hexokinase2), which offered protection to the heart from obesity related cardiomyopathy (hypertrophy, cardiomyocyte lipid droplets, and metabolic alterations) in C57BL/6 mice fed HFD [210]. Also, Duda et al. (2007) reported that a low carbohydrate/high-fat diet in rats for 2 months in addition to abdominal aortic binding (AAB) attenuates pressure overload-induced LV hypertrophy and dysfunction compared with high-carbohydrate diets [211]. This was also accompanied by lower levels of insulin and leptin which suggests they may contribute to this LV remodelling.

Another factor associated with HFD cardiac remodelling and dysfunction is toll-like receptor 4 (TLR4). A study by Hu and Zhang (2017) reported several cardiac changes due to 12 weeks of HFD feeding in WT mice. These changes included decreased fractional shortening and

cardiomyocyte contractility, alterations in intracellular Ca^{2+} release and clearance, and elevated ROS generation and oxidative stress [212]. These effects were all attenuated when TLR4 knockout mice were used, and authors suggested this could have been done through a NF-κB/JNK-dependent activation of autophagy. Additionally, Birse et al. (2010) concluded that HFD induces cardiac dysfunction by deregulation of the insulin-TOR signalling pathway. This study was conducted in Drosophila flies and exhibited similar cardiac changes to mammalians fed HFD. These flies showed increased triglycerides, alterations in insulin/glucose homeostasis, cardiac lipid accumulation, reduced cardiac contractility, and severe structural pathologies. Once the insulin-TOR signalling pathway was inhibited, these effects no longer existed [213]. Ouwens et al. (2005) also suggested that HFD induced cardiac dysfunction is related to myocardial insulin signalling. In their study, rats were fed either a ND or HFD for 7 weeks. HFD rats had higher levels of glucose, cardiac structural changes, and triglycerides accumulation. HFD altered several enzymes involved in the insulin signalling including insulin-stimulated IRS1-associated phosphatidylinositol 3′-kinase, protein kinase B, glycogen synthase kinase-3β, endothelial nitric oxide synthase, and forkhead transcription factors. Additionally, HFD reduced the insulin mediated phosphorylation of phospholamban, which is essential in cardiac contractility [214].

1.7.2 High-Fat Diet and Cardiovascular Remodelling in Ageing

In addition to studying the effects of HFD on the heart, a few researchers have compared this effect in young and aged hearts. Young and aged (3 and 18 months) C57BL/6 mice were fed a normal diet, a low-fat diet, and a high fat diet for 16 weeks. Results of this study showed that the aged heart is less able to adapt to a high fatty acid load, and this led to more predominant structural alterations and accumulation of lipid intermediates in the cardiomyocytes [155]. Another study by Shiou et al. (2017) looked at the effects of HFD in ageing rat hearts with hypertensive disease. 44 week old spontaneously hypertensive rates and Wistar Kyoto rats were

given either ND or HFD for 27 weeks [215]. Results of this study showed that HFD aggravates hypertensive heart disease associated with ageing, worsened atrial and ventricular remodelling, and led to impairment of left ventricular systolic function.

1.7.3 High-Fat Diet and Mitochondria

HFD has been associated with cardiac remodelling and dysfunction. Part of the underlying cause is how the diet affects the mitochondria, which play an important role in heart performance. Numerous studies report the effect of HFD on mitochondrial oxidative functions in the presence of obesity and/or insulin resistance [216-220]. A study on rats fed HFD for 28 weeks showed alterations in the mitochondrial biogenesis, dynamics, morphology and function [221]. Authors reported changes in gene expressions involved in mitochondrial dynamics, a decrease in mitochondrial DNA, a reduction in the activities of complex I-III and citrate synthase; which led to a decrease in mitochondrial respiration, and morphological alteration (disappearance of the z line, lower mitochondrial density, decrease in size, disruption of the cristae). Additionally, mitochondrial fusion genes mfn1, mfn2, and opa1 and the mitochondrial fission genes drp1 and fis1 were all downregulated after HFD. Another study in C57BL/6J mice reported that HFD causes impairment in mitochondrial oxidative phosphorylation characterised by a reduction in complexes 1 and 3 activity [222]. However, the authors concluded that this impairment was associated with the high calorie content of the diet rather than the high fat, as they observed similar dysfunction in another group of mice fed with high calorie low fat diet. The composition of HFD and duration of feeding are important determinants of the diet's effect on mitochondrial function [223].

1.7.4 High-Fat Diet and Vulnerability of the Heart to Ischaemia/Reperfusion Injury

Similar to ageing, HFD effects on cardiac vulnerability and tolerance to I/R injury are contradictory. Even though obesity is a risk factor for cardiac disease and failure, it has been associated with lower mortality risk as well (the obesity paradox) [224]. A study on B6D2F1

mice fed HFD for 6 months reported a decrease in infarct size and improved overall left ventricular function in the absence of hyperglycaemia and hypertension [225]. Another study using three different strains of mice fed HFD for 16 weeks also found that HFD is effective against I/R injury as it delays the normalisation of pH during the start of reperfusion [226]. However, this beneficial effect was seen in two of the three strains used, indicating the role of genetics in the dietary effect.

High fat diet has been shown to be cardioprotective against I/R injury when consumed acutely for a period of 24 hours to 2 weeks prior to ischaemia [227]. The authors found that with acute HF feeding there is a decrease in injury (infarct size) by more than 50% and this was associated with an increase in autophagy and reduction in apoptosis. Additionally, in a study where rats were fed either HFD, HSD (high-sucrose diet), or a normal diet for a period of 16 weeks, and were subjected to regional ischaemia for 35 mins followed by one hour of reperfusion, showed that the two special obesogenic diets had cardioprotective effects with reducing infarct size compared to the control group [228]. However, pre-conditioning of these hearts; measured by functional recovery and improvements in infarct size, was not as effective as it was in the control hearts. Authors of this study suggested that insulin resistance and elevated insulin levels might have been the reason for the cardio protection seen in the diet-induced obese hearts, as insulin is known to activate the RISK pathways [64]. Similarly, a study in mice fed HFD for 8 weeks showed a reduction in the intolerance to I/R after 30 mins of ischaemia, associated with a decrease in transcriptional factor of activated mitochondria (Tfam) [229]. Another study in rats reported cardioprotective effects of HFD for 16 weeks, associated with an improvement in mitochondrial oxidative phosphorylation (measured by glutamate, malate and palmitoyl-carnitine) and a reduction in mitophagy (measured by PINK1 (PTEN-induced kinase 1) and p^{62} expression) [230].

In contrast to the previous studies, rats fed a HFD for 32 weeks showed decreased tolerance to I/R after 40 mins of ischaemia followed by 120 mins of reperfusion, with larger infarct sizes and lower functional recovery compared to their controls [231]. Decreased tolerance was associated with a decrease in the total and phosphorylated Akt, GSK-3β, and eNOS expression. Similarly, mice fed HFD for 12 weeks showed reduced tolerance to I/R which was associated with overexpression of NOD-like receptor pyrin domain containing 3 (Nlrp3) inflammasome (a protein that induces interleukin 18 and interleukin-1β), reduction in hypoxia inducible factor 2α, and components of the pro-survival signalling pathway (RISK) [232]. Additionally, HF feeding for 90 days increased susceptibility to I/R injury in Guinea pigs and was associated with increased inflammatory markers (tumor necrosis factor-α (TNF-α) and interleukin-6 (IL-6)) after reperfusion [233]. Also, HFD was associated with increased susceptibility to I/R in HGI (hypertensive glucose intolerant) rats, which significantly increased infarct size compared to their controls and was associated with increased levels of plasma triglycerides and lipotoxicity [234]. Similarly, HF fed rats for 12 weeks developed ischaemic intolerance and demonstrated larger infarct size and mitochondrial dysfunction compared to their controls [235]. In addition, Littlejohns et al. (2014) reported increased vulnerability of the heart to I/R injury in C57BL/6J male mice that were fed HFD for 20-21 weeks. These hearts showed lower functional recovery, increased CK release and an infarct size compared to their controls [236]. In another study by Liu et al (2014), a high fat low carbohydrate diet fed to 12 week-old adult male Sprague-Dawley rats (for as little as 2 weeks) increased their vulnerability to I/R injury and increased incidences of fatality by ventricular arrhythmias and cardiac failure. This was done using an in vivo I/R model where the rats were stabilized for 20 mins, followed by a 30 min occlusion of the LAD (left anterior descending) artery, and 120 mins of reperfusion [237]. The same authors studied the effects of high fat low carbohydrate diet again in an in vitro model in 2016, where isolated hearts of the Adult male Sprague Dawley rats were subjected to low

flow ischaemia for 60 mins (0.3 ml/min) followed by 60 mins of reperfusion. Similarly, findings of this study reported an impaired recovery in the function of the hearts fed HFD due to the effect of the diet on the myocardial properties [238].

Few studies have explored the combined effects of HFD and ageing on the vulnerability of the heart and the results show conflicting findings. One study on female mice looked at the effects of AMPK alpha-2-subunit deletion with high fat diet on the aged heart. WT and KO adult and aged mice were used (6 and 18 months old respectively). Generally, ageing seemed to have a positive effect on ischaemic tolerance, but this was lost with 6 months of HFD feeding [239]. Another study on Wistar rats reported that HFD induced obesity did not affect the hearts vulnerability to regional ischaemia with ageing, but it improved it in young hearts [240].

1.8   Summary

It is evident that age and HFD can alter vulnerability to ischaemia and reperfusion. The underlying mechanisms are not presently known especially in aging hearts with the added cardiovascular burden of HFD. Understanding cardiac remodelling at the molecular, metabolic, and structural level during aging and in response to HFD will enable better design of therapeutic interventions to protect hearts form cardiac insults during ageing and obesity.

1.9   Hypothesis & Aims

1.9.1 Hypothesis

1. Ageing-related cellular, molecular, structural, and functional remodelling of the heart increases its vulnerability to ischaemia/reperfusion injury.

2. HFD-related cellular, molecular, structural, and functional remodelling of the ageing heart increases its vulnerability to ischaemia/reperfusion injury.

1.9.2 Aims

1. To study the effects of ageing on cardiac metabolic remodelling, proteomics/phosphoproteomics with emphasis on mitochondrial, metabolism,

structural, ionic transport, antioxidant, and apoptosis proteins. And to study the effects of ageing on myocardial structure including myocytes, vasculature, tissue fibrosis, and subcellular organelles such as mitochondria.

2. To study the effect of HFD in ageing on cardiac metabolic remodelling, proteomics/phosphoproteomics with emphasis on mitochondrial, metabolism, structural, ionic transport, antioxidant, and apoptosis proteins. And to study the effect of HFD in ageing on myocardial structure including myocytes, vasculature, tissue fibrosis, and subcellular organelles such as mitochondria.

3. Finally, to investigate the effects of ageing and HFD on cardiac function (coronary flow) and tolerance to I/R injury.

2.   Materials and Methods

2.1 Materials

2.1.1 Reagents Used

Experimental reagents used and their companies of origin are listed below:

Agar Scientific (Essex, UK)

Glutaraldehyde solution (25 %)

Bio-Rad (Hertfordshire, UK)

Precision Plus Protein™ All Blue Standards

Quick Start™ Bradford 1 x Dye Reagent

BOC Healthcare (Surrey, UK)

95 % oxygen/5 % carbon dioxide medical gas mixture

BOC Industrial Gases (Surrey, UK)

Liquid nitrogen

Fisher Scientific UK Ltd (Leicestershire, UK)

D-glucose anhydrous

Magnesium sulphate ($MgSO_4 \cdot 7H_2O$)

Sodium chloride (NaCl) 68

Sodium dodecyl sulphate (SDS)

Merck (New Jersey, USA)

Magnesium chloride ($MgCl_2$)

Randox (County Antrim, UK)

CK-NAC assay (CK113)

CK-NAC assay (CK522)

Roche (Sussex, UK)

cOmplete, EDTA-free protease inhibitor cocktail tablets

PhosSTOP phosphatase inhibitor cocktail tablets

Sigma-Aldrich™ (Dorset, UK)

2, 3, 5-triphenyl-tetrazolium chloride (TTC)

2-mercaptoethanol

Albumin from bovine serum (BSA)

Calcium chloride solution (1 M) (CaCl2) 69

Chelerythrine Chloride

Dimethyl sulphoxide (DMSO)

Ethylene glycol-bis(2-aminoethylether)-N,N,N',N'-tetraacetic acid (EGTA)

Folin and Ciocalteu's phenol reagent

Formaldehyde solution (36.5-38 %)

Glycine

Methanol

Lowry reagent

Nonidet™ P 40 substitute solution

Phosphate buffered saline (PBS) tablets

Sodium deoxycholate

Sodium hydroxide (NaOH)

Tocris Bioscience (Bristol, UK)

TWS 119

Dorsomorphin Dihydrochloride

VWR International Ltd (Leicestershire, UK)

4-(2-Hydroxyethyl) piperazin-1-ylethanesulphonic acid (HEPES)

Di-sodium hydrogen phosphate (Na_2HPO_4)

Hydrochloric acid fuming (37 %) (HCl)

Potassium chloride (KCl)

Potassium dihydrogen phosphate (KH_2PO_4)

Sodium hydrogen carbonate ($NaHCO_3$)

2.2   Animals

C57BL/6 male mice aged either 8 or 80 weeks were purchased from Charles River (Margate, UK). The animals were housed at the University of Bristol animal unit, allowed to recover from transit and then used when required. The aged mice were fed either a ND or HFD (described in section 2.3). All mice were given *ad libitum* access to food and water and maintained on a 12-hr light/dark cycle. All animals were treated in accordance with the United Kingdom Home Office regulations, Animals (Scientific Procedures) Act of 1986.

The animals were humanely killed using Schedule 1 procedure; stunning followed by cervical dislocation or euthanized by an intraperitoneal injection of 20 mg of pentobarbital sodium (which were provided by fellow researcher Dr. Helen Williams and used to prepare histological samples). Hearts were excised right away and used for various experiments, and the animals and their epididymal fat pads were weighed after sacrifice.

2.3   Diet

Adult mice were only fed a normal standard murine chow diet (Special Diets Services, UK, code: 801900). This diet consists of 22 %, 13 %, and 65 % of calories from protein, fats, and carbohydrates respectively (appendix 7.1). Ageing mice were either fed a ND or a HFD (Special Diets Services, UK, code: 821424). The HFD group were purchased around 50-60 weeks old and were switched to the HFD for 20-24 weeks before they were used.

 The HFD composition was 45 %, 18 %, and 37 % calories from fat, carbohydrates, and proteins respectively (appendix 7.1). The energy content of the diets was 16.26 mJ/kg and 19.67 mJ/kg for ND and HFD, respectively. Figure 2.1 shows the mice feeding regime.
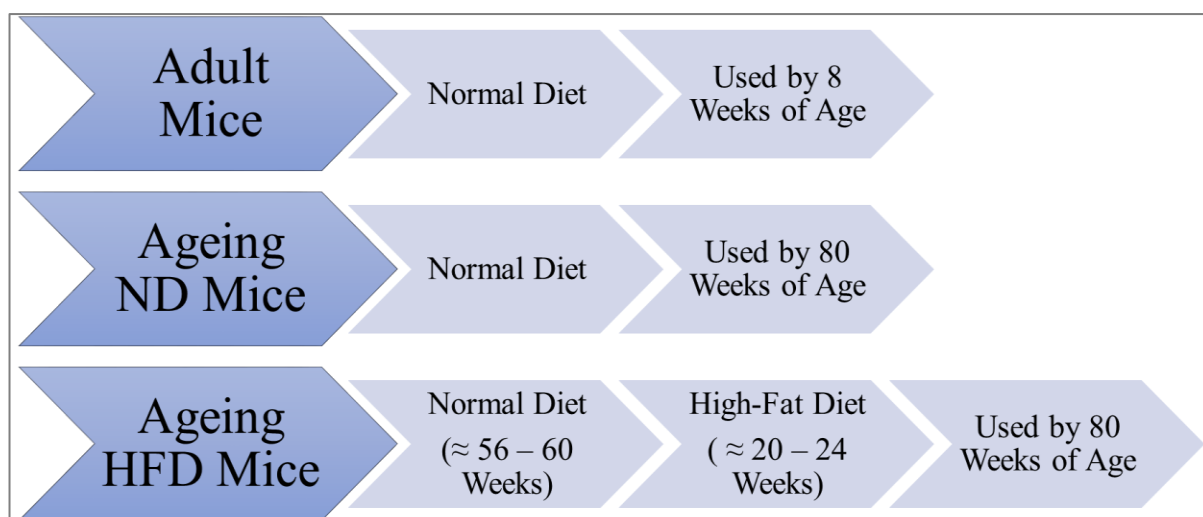
Figure 2.1: Age of experimental animals and their feeding regime.

2.4 Methods

2.4.1 High Performance-Liquid Chromatography

2.4.1.1 Cardiac Tissue Extraction

Hearts were collected from freshly sacrificed mice, snap frozen immediately in liquid nitrogen, and stored at - 80° C until extraction. The apex was used for the extraction to measure amino acids and energy metabolites.

LP3 tubes were prepared and labelled with accordance to samples being processed. 500 µL of perchloric acid (PCA) (4.8 % PCA, prepared with 8 mL of 60 % PCA and made up to 100 mL with distilled water) was added to the tubes, which were kept in an ice box throughout the whole experiment. Tubes were weighed twice, making sure the difference between the two weighing is less than 0.001 gm, and the average was calculated. Samples were kept and processed in liquid nitrogen throughout the whole experiment. The tissue was first crushed into fine powder using a pestle and mortar, added to the labelled tubes, and vortexed (Rotamixer 7871, Hook & Tucker Instruments). Samples were then centrifuged at 4000 rpm for 10 min at 4° C (Allegra X-22R, Beckman Coulter). Tubes were weighed again as they were the first time to determine the weight of the tissue added. The supernatant was collected (400 µL) into

another LP3 tube, 400 mL of K_2CO_3 (0.44 M potassium carbonate, prepared with 6.08 gm K_2CO_3 and made up to 100 mL with distilled water) was added to neutralise the extract, and the tubes were vortexed twice with a 2 min interval between. Samples were centrifuged once more as they were the first time to remove the insoluble potassium perchlorate, and the supernatant was collected into two different Eppendorf tubes. In the first tube, 100 µL of supernatant was added with 100 µL of hydrochloric acid (HCL), vortexed and then dried in a savant (AS160 Automatic Speed Vac) to a pressure less than 400 U, and finally stored at - 20° C until used for amino acid analysis. The rest of the supernatant (400-500 µL) was collected into a bigger Eppendorf tube and stored at - 20° C until used for energy metabolite analysis.

2.4.1.2 HPLC

The HPLC instrumentation consists of four main components which are the pump (Beckman System Gold 125 Solvent Module Pump), the autosampler (Beckman System Gold 507e Autosampler, Beckman Coulter Ltd, UK), the separation column (changeable depending on the measured components), and the detector (Beckman System Gold 166 Detector, Beckman Coulter Ltd, UK).

There are two phases in the HPLC analysis: the stationary phase, and the mobile phase. The stationary phase is when the sample is injected and binds to the separation column, and the mobile phase is when the pump forces the HPLC eluent solution through the separation column. The elution time of the measured compound depends on the solubility of that compound in the stationary phase, and then it is measured by absorbance. Figure 2.2 demonstrates the principle of HPLC in a simplified way.
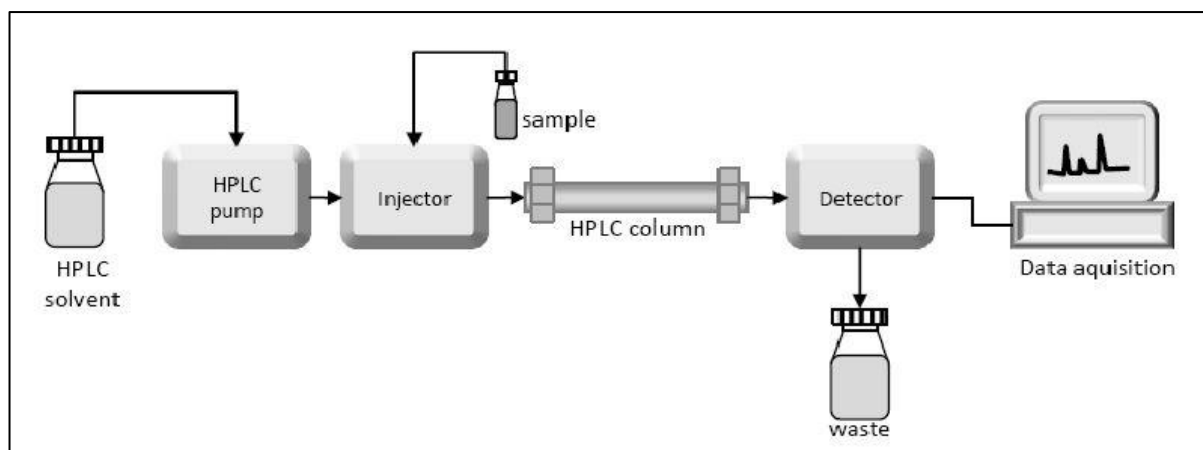
Figure 2.2: A schematic diagram of the high-performance liquid chromatography components. (laboratoryinfo.com).

2.4.1.3   Metabolites Analysis

The separation column used was a 3 μm octadecyl silane Hypersil column (150 mm x 4.6 mm) (Thermo Scientific, UK). The composition of the mobile phase is important for the elution of metabolites. Two eluents were used in the mobile phase, eluent A (150 mM KH_2PO_4 and 150 mM KCl, set at pH 6.0 with KOH) and eluent B (eluent A with 15 % (v/v) HPLC grade acetonitrile added). The composition of the mobile phase was controlled using a low-pressure gradient mixing device. Eluent B changed linearly during sample analysis between the time points (table 2.1). Temperature was constant (in the range 17-19° C) for the analytical column, and absorption was measured at 254 nm.

Table 2.1: Composition of the mobile phase over time of metabolite analysis.

Time (min)	Flow speed (mL · min-1)	Eluent A (%)	Eluent B (%)
0	0.9	100	0
0.1	0.9	97	3
3.0	0.9	91	9
7.0	0.9	0	100
8.5	0.9	100	0

The metabolites measured were ATP, ADP, AMP, GTP, GDP, GMP, IMP, xanthine, hypoxanthine, β-NAD, inosine and adenosine. 10 µL of standard samples (prepared as described previously in Ally and Park 1992) or 20 µL of the extracted samples were injected into the system which then bound to the column. Depending on the composition of the mobile phase as mentioned previously, the metabolites were eluted at different time points. The area under the peak for each metabolite was determined, compared to the standard sample and then corrected for weight. Figure 2.3 shows an example for a standard and a sample chromatograph.
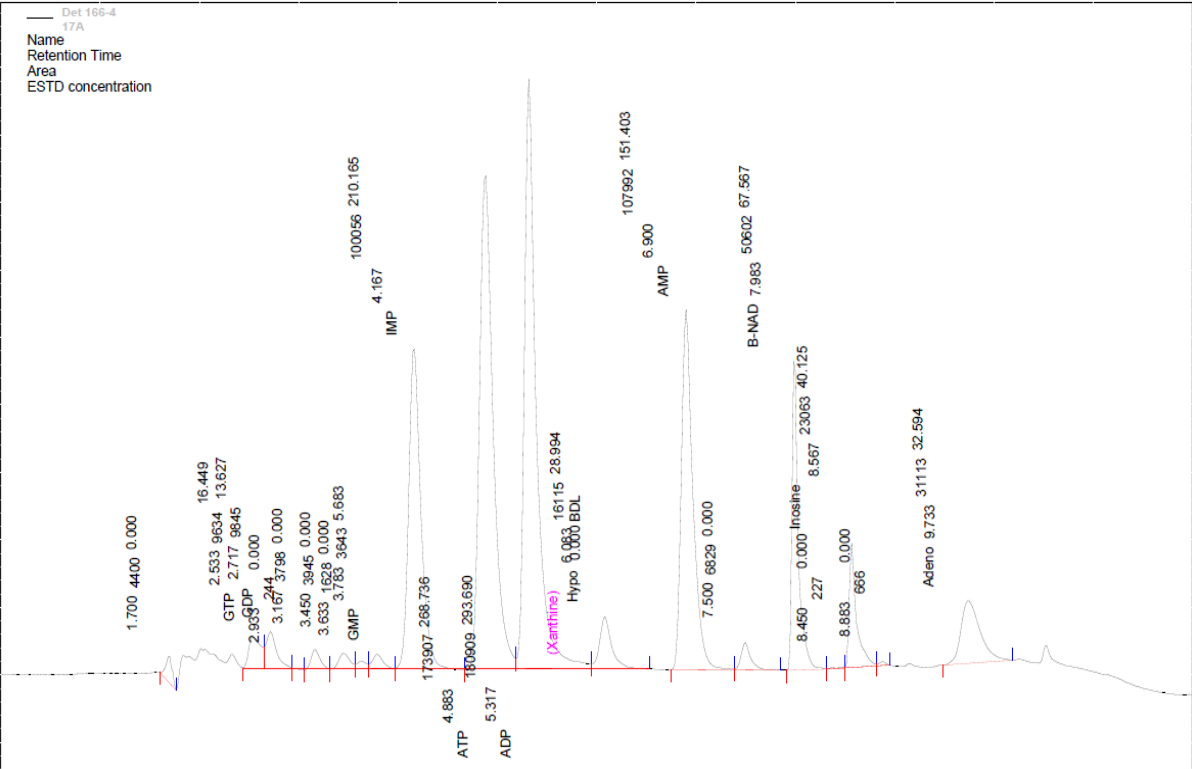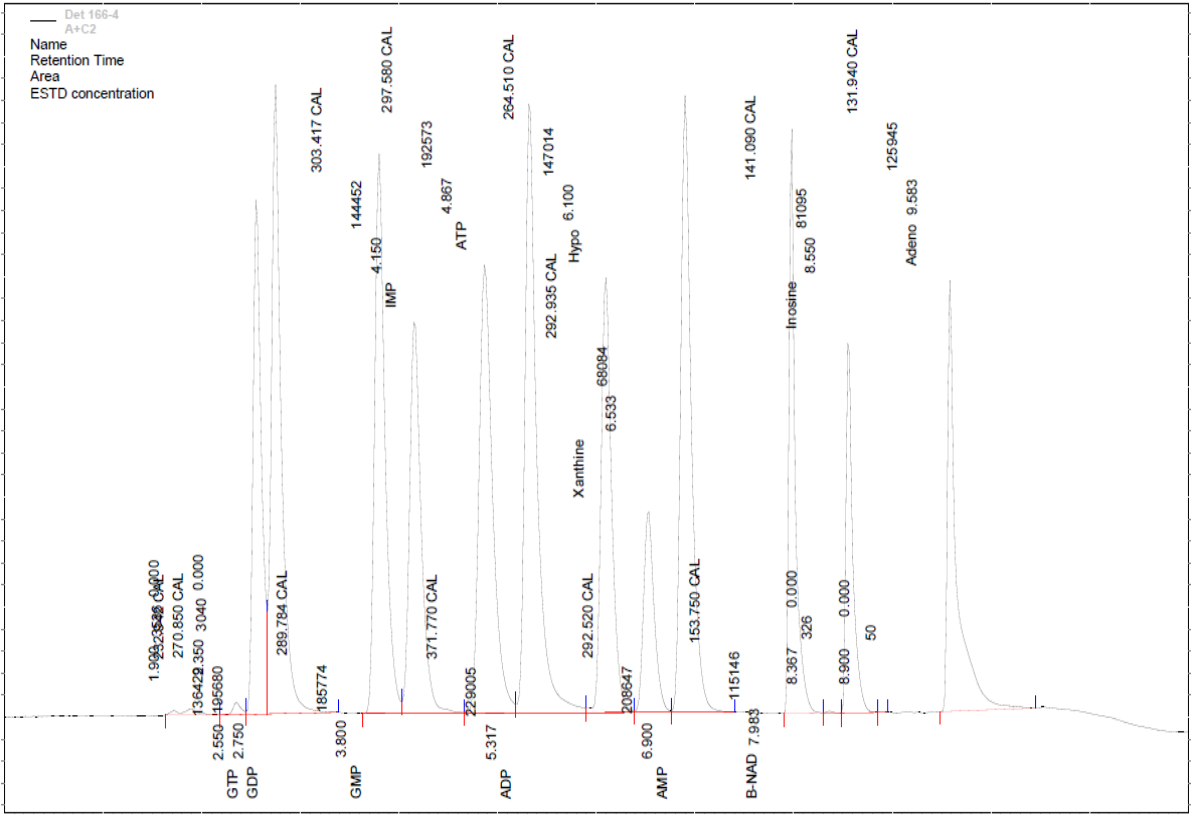
Figure 2.3: High-performance liquid chromatographs of measured metabolites from a standard (top) and a sample (bottom). (Credit: Ben Littlejohns).

2.4.2 Nuclear Magnetic Resonance Spectroscopy

2.4.2.1   Sample Collection

Blood samples were collected from mice of different age groups (adults, aged, aged HFD), by scooping or pipetting blood from the thoracic cavity after heart extraction for other experiments into ethylenediaminetetraacetic acid (EDTA)-coated Eppendorfs. Eppendorfs were kept in ice until samples were centrifuged for 10 mins at 10000 RPM in 4º C. Plasma samples were stored at -80º C until they were sent to the NMR facility at The University of Bristol Chemistry School.

2.4.2.2   NMR Spectroscopy

NMR principle revolves around the mechanical properties (spinning and electrical charge) of the nucleus of the atom, using an external magnetic field that is exposed towards the nuclei of the biomolecule which leads to energy transfer when this field is removed. This magnetic field is exposed towards hydrogen nuclei In the 1H-NMR. [241]. This occurs at a wavelength which is recorded and interpreted based on the properties of the molecule (the type and number of hydrogen nuclei and their interactions within the molecule) [242].

Samples were analysed in the School of Chemistry at The University of Bristol, using model (700 MHz Bruker AVANCE HD, Bruker BioSpin GmbH, Germany) NMR spectroscope. Once defrosted, plasma was transferred into 1.7mm CryoProbe and dissolved with NMR buffer (1 PBS tablet, 0.16 g Trimethylsilylpropanoic acid (TSP), 0.2 g sodium azide NaN_3 in 170 ml type I water and 20 ml deuterium oxide (D_2O), adjusted to pH 7.4) and kept at 4˚C during the process of NMR.

The NMR spectroscope consists of liquid handling robots, a sample holder, and a radiofrequency (RF) pulse transmitter and receiver. A signal is obtained from the RF receiver, amplified, and strengthened by a recorder that transforms the spectrum for analysis. The spectra are transformed using Bruker TopSpin software (Bruker, Germany) into 1D-1H Carr–Purcell–

Meiboom–Gill (CPMG) pulse sequence which is used for analysis. Figure 2.4 shows a schematic diagram for the NMR spectroscope principle.
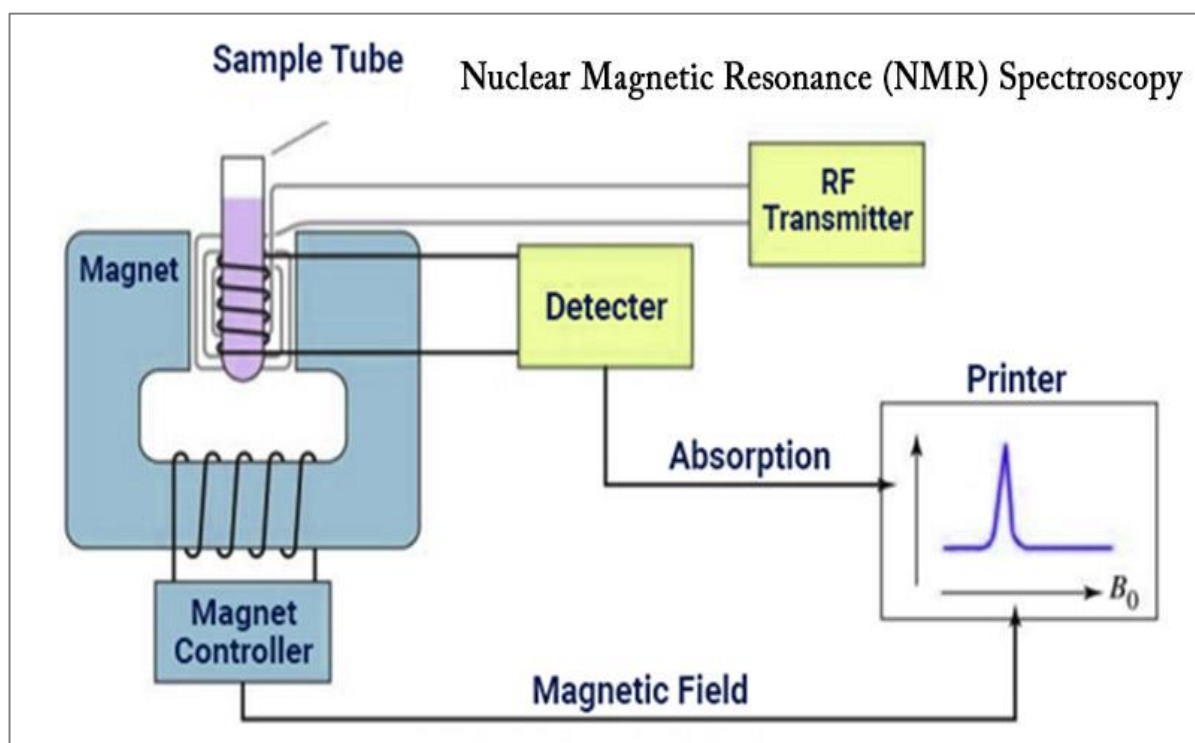
Figure 2.4: Schematic diagram showing NMR spectroscopy principle.
https://byjus.com/chemistry/nmr-spectroscopy/

2.4.2.3   Metabolite and Data Analysis

Data obtained from NMR samples were analysed using the software MestReNova (Mnova, MestReNova Research SL, Spain). A reference of Trimethylsilylpropanoic acid (TSP) was used for the samples, at a concentration of 4.6 mM. Metabolites analysed included lipid and carbohydrate metabolites, which were compared between the various age or diet groups by choosing the peak area annotated to each metabolite from Mnova (peaks referenced to available literature, figure 2.5 [10]) and then comparing their averages.
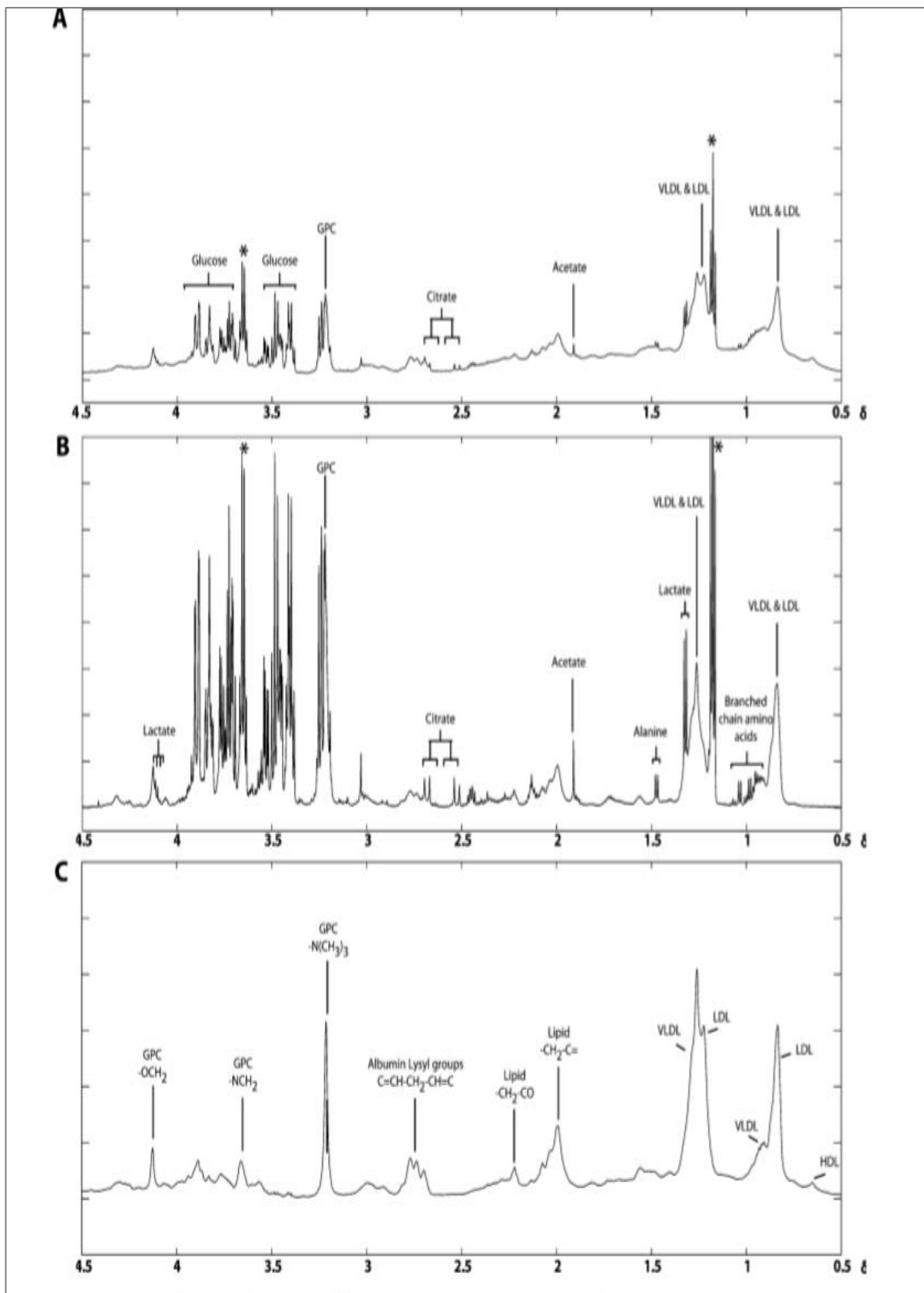
Figure 2.5: 1H NMR plasma spectra. Acquired using (A) standard 1D pulse sequence (B) the Carr−Purcell−Meiboom−Gill sequence (C) a diffusion edited pulse sequence *Ethanol contaminant. [10]

2.4.3 Liquid Chromatography Tandem Mass Spectrometry

2.4.3.1   Sample Collection

Left ventricles were used for protein extraction and analysis. Samples were collected from freshly sacrificed mice and snap frozen in liquid nitrogen until they were used for protein extraction.

2.4.3.2   Protein Extraction

50 mg of tissue was weighed (cut into small pieces) into 1 ml universal tubes with 50 beads, and 10 µL/mg of RIPA buffer (1 PBS tablet, 1 % Nonidet p-40, 0.5 % Sodium deoxycholate, 0.1% SDS, pH 7.4) was added to each tube, with 1 tablet of each Protease inhibitor cocktail (Roche 04693159001) and Phosphatase inhibitor cocktail (Roche 04906845001). The tissue was then homogenised 4 times; 10 seconds each, using Minilys tissue homogenizer (Bertin technologies, France) at 25000 rpm, and left to rock on a shaker (Labnet International Inc., USA) while in the ice box for 30 min at 4° C. Samples were then pipetted out of the tubes into regular Eppendorf tubes, and centrifuged at 13.000 x g for 10 min at 4° C. The supernatant was removed and split into 3 tubes (100 µL each). One of the three tubes was used for the protein quantification of the samples, while the other two were stored in the -80° C freezer.

2.4.3.3   Protein Quantification

The total protein content of the samples was determined using the Bradford assay (Bradford 1976).

Using a 5mg/mL standard BSA solution to plot the standard curve, 5 LP4 tubes were prepared (in duplicates), and 1, 2, 3, 4, and 5 µL of the solution was pipetted into them. A blank tube with no added solution was used for zeroing of the spectrophotometer. Then, 3 mL of the Bradford reagent was added to each LP4 tube, vortexed, and left for 15 min before reading the absorbance. The samples were prepared in a similar way after being diluted with water (1:3 dilution), with 5 µL of each sample added into an LP4 tube (in duplicate), and 5 µL of RIPA buffer used as blank. 3 mL of the Bradford reagent was added to all of the tubes, vortexed, and

left for 15 min before readings were taken. Absorbance was read using the spectrophotometer (Bibby Scientific Limited, UK) after setting the temperature to 20ºC, and at 595 nm wavelength. Microsoft Excel was used to plot the standard curve and calculate protein concentrations in the samples (figure 2.6).

From the curve, the amount of protein in the samples was calculated using the equation ($y = 0.0216x + 0.0124$). This was divided by 5 (the volume of sample used) to obtain the concentration of each sample proteins, then multiplied by 3 to correct for dilution. Protein quantification and identification was determined using Proteomics.
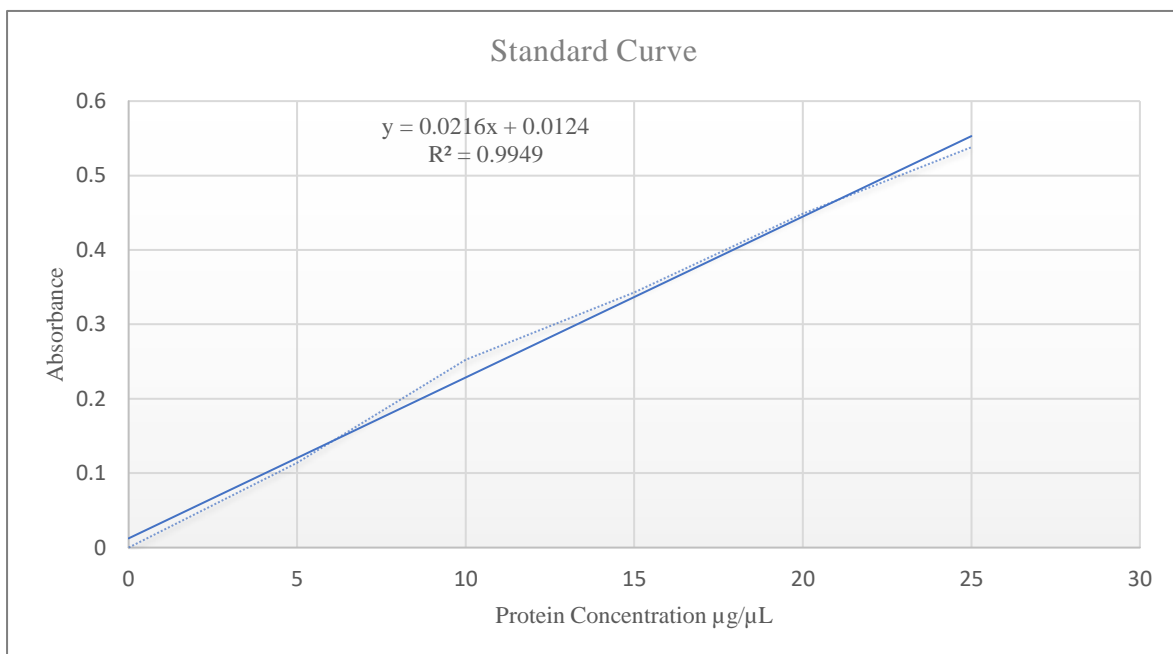
Figure 2.6: Standard curve for protein quantification showing protein concentration (μg/μL) plotted against absorbance at 595 nm.

2.4.3.4　LC-MS/MS

2.4.3.4.1　Total Proteins

For the proteomics analysis, we needed to send 60 µl of sample at a concentration of 2 µg/µl.

samples were prepared according to these calculations and made up to 60 µl with distilled

water. They were stored in the -80° C freezer until they were sent off for analysis at the Medical

School. Analysis of proteins in ventricular tissue samples was performed by the University of

Bristol Proteomics Facility using tandem mass tags (TMTs) (Thermo Fisher Scientific, UK).

The samples were first digested with trypsin (Promega, UK), and the resultant peptides in each

sample were tagged with a unique TMT. Each TMT consists of a mass reporter, a mass

normaliser, and a NH_2 reactive group (figure 2.7).
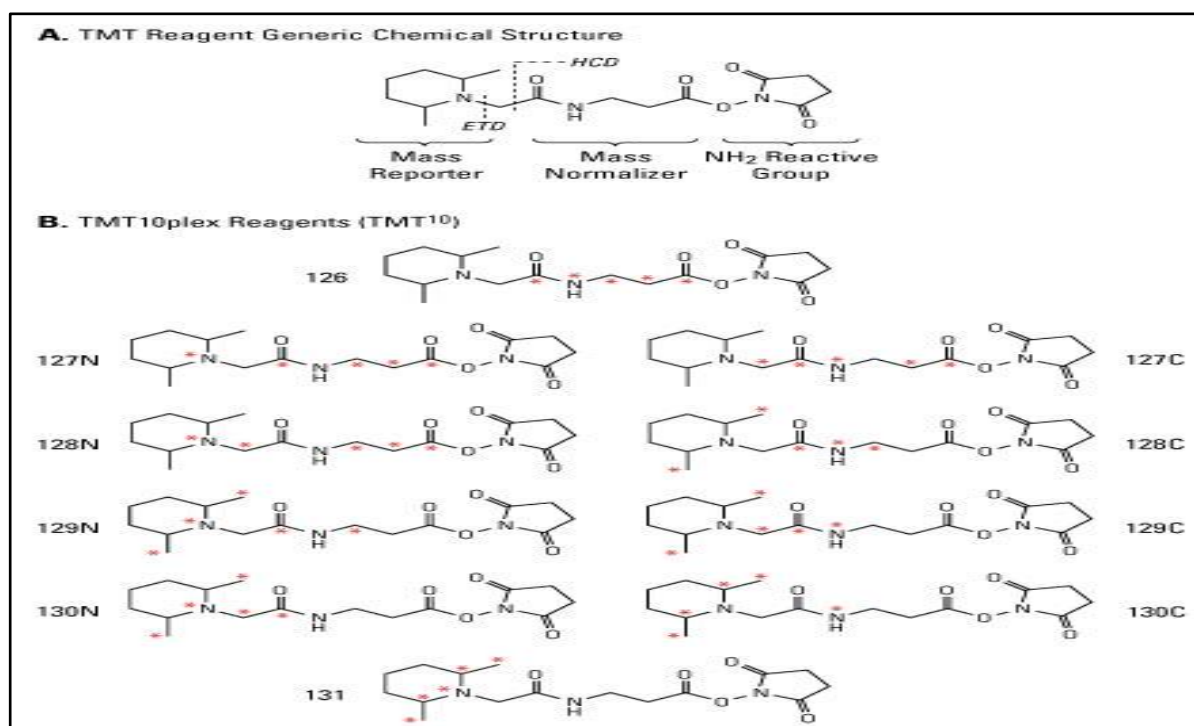
Figure 2.7: A: Structure of the amine-reactive TMT Reagents. B: TMT10plex reagent structures with 13C and 15N heavy isotope positions (red asterisks). (https://www.thermofisher.com/order/catalog/product/90110)

Each mass reporter (there are 10 mass reporters, figure 2.6B) has a unique mass and binds to a

specific sample (to label each individual sample). The mass normaliser normalises the mass

reporter to ensure all tags have a constant mass. And the NH_2 reactive group allows for amine-specific binding to the peptides.

In the first run, 4 adult samples were tagged (126, 127N, 127C, and 128N), 5 aged samples (128C, 129N, 129C, 130N, and 130C), and a pooled sample was created from all the previous samples (131). In the second run, 5 aged ND samples and 5 aged HFD samples were run without a pool.

During LC-MS/MS, the mass reporter is cleaved by collision induced dissociation (CID), which allows the cluster and detection of these reporters at the low mass end of the MS/MS spectra, where each reporter indicates the abundance of peptides in each sample (tagged by that reporter) (figure 2.8).
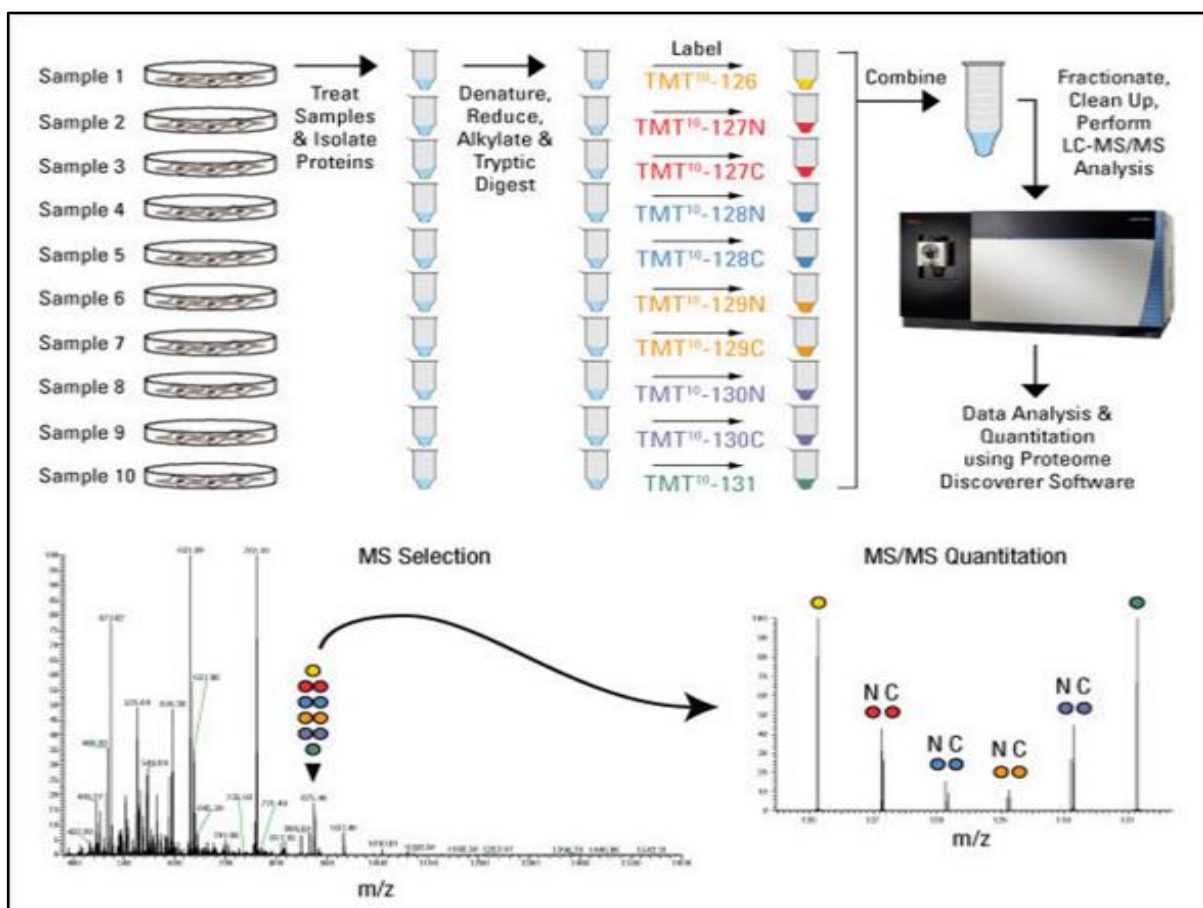
Figure 2.8: Scheme for MS experiment. Explained in detail in the text above. (https://www.thermofisher.com/order/catalog/product/90110)

2.4.3.4.2   Phospho-proteins

For the analysis of phospho-proteins, a phosphorylation enrichment step is added to the previously described technique. After pooling the samples, they are passed through a titanium dioxide column, where phospho-peptides bind to the column and the non-phosphorylated peptides elute. The phospho-peptides are eluted afterwards and analysed using the LC-MS/MS. The peptides identified were searched against UniProt/SwissProt Mouse database using the SEQUEST (Ver. 28 Rev. 13) algorithm to determine which protein they came from. Proteins and peptides were analysed using Thermo Proteome Discoverer 1.2.0.208 software (Thermo Scientific, UK).

2.4.4   Histology

2.4.4.1   Light Microscopy

2.4.4.1.1   Tissue Fixation

Hearts were excised from freshly sacrificed mice and put in cold Krebs-Henseleit buffer (120 mM NaCl, 25 mM NaHCO$_3$, 11 mM D-glucose anhydrous, 1.2 mM KH$_2$PO$_4$, 1.2 mM MgSO$_4$.7H$_2$O, 4.8 mM KCl and 2 mM CaCl$_2$). The hearts were then cannulated and perfused with the same buffer for 10 mins, and then cut horizontally into 3 pieces, and placed in a small tube with fixative solution (10 % paraformaldehyde in PBS). The hearts were left in fixative overnight (24 hours) before processing and embedding. Adult and aged ND hearts were processed by Dr. Hellen Williams.

2.4.4.1.2   Tissue Processing and Embedding

After fixation, heart sections were placed in a cassette and kept in PBS for processing. The processing was done using ThermoFisher Scientific ExcelsiorTM AS Tissue Processor, which dehydrates the tissue by using ethanol to remove water from the sections and allow the paraffin wax to infiltrate it during embedding.

Embedding was done using Thermo Scientific™ HistoStar™ Embedding Workstation. Specific metal moulds were used to pour paraffin wax into before placing the tissue in them

(orienting it in the desired position), then allowing the wax to solidify by placing the metal mould onto an ice block. Finally, a cassette with the tissue label was placed on the block, and more wax was added on top to attach the two parts together. This was left to solidify and cool before removing the block from the metal mould.

2.4.4.1.3   Cutting the Blocks and Preparing the Slides

The blocks were cooled prior to cutting by placing them on the ice block. They were then sectioned into 5 μm sections with the Thermo Scientific™ Shandon™ Finesse™ 325 Manual Microtome. After cutting a section, it was placed in the water bath and picked up using a slide and labelled with the sample name, date, and thickness of section. The slides were then placed in the oven at 37°C to dry overnight before staining.

2.4.4.1.4   Staining the Slides

A. H&E Staining

Eosin is an acidic dye which stains basic components of the cell such as proteins and cytoplasmic structures. These are called acidophilic or eosinophilic and when stained appear pink in colour. Haematoxylin is a basic dye which stains acidic components of the cell such as nucleic acid (DNA and RNA). These structures are called basophilic and are stained in a blue purplish colour. This staining provides a detailed view of the tissue and allows examination of the organisation or disorganisation of the cells, and any abnormalities such as nuclear changes. The slides were first prepared by rinsing them in clearene to dissolve the wax, and then different preparations of alcohol to remove the clearene. They were then rinsed and hydrated with water so that the dyes can penetrate the tissue properly. Haematoxylin dye was used to stain the nuclei and other component, and it initially stained them a reddish-purple colour. Then a weak alkaline solution was added to make the dye a dark blue colour. After that, the second Eosin dye was added to stain the rest of the cellular component in different shades of pink. Finally, the slides were rinsed, dehydrated with alcohol, and cleared with clearene. Once all of this was

done, the slides were covered with mounting media (DPX) and a cover slip and left to dry under the fume hood overnight.

This staining was not used to measure anything specific, but rather to show a representation of how the cardiomyocytes appear in longitudinal and cross-sectional areas in each age and diet group.

B. EVG Staining

This stain is used to identify elastic fibres. The iron-haematoxylin compound in the dye attaches to elastin, then a counterstain (most likely Van Gieson's stain) is used to contrast the principle stain. Elastic fibres and nuclei are stained black, collagen fibres are stained red, and the rest of the cell components are stained yellow. This stain is commonly used to examine blood vessels and skin.

The slides were first prepared by rinsing them in clearene to dissolve the wax, and then different preparations of alcohol to remove the clearene. They were then rinsed and hydrated with water so that the dyes could penetrate the tissue. Then, they were decolourised with 1% oxalic acid, and rinsed with water. These steps are called the Mallory bleach sequence. The slides were then rinsed in 70% industrial methylated spirits (IMS) and stained with Miller's stain for around 1 hr. Slides were then washed with 70% IMS, rinsed with water, and stained with Van Gieson's counterstain. Finally, the slides were rinsed, dehydrated with alcohol, and cleared with clearene. Once all of this was done, they were covered with mounting media (DPX) and a cover slip and left to dry under the fume hood overnight.

This staining was used to examine arteries and how they compare or change with ageing and then with HFD. Measurements were done using ImageJ software and included total artery size (micrometers^2), lumen size (micrometers^2), and then the thickness of the arterial wall was calculated from the previous two measurements and expressed as a ratio to total artery and lumen size.

C. The Auto-Stainer (Thermo Scientific™ Varistain™ 24-4 Automatic Slide Stainer)

H&E and EVG staining were done using the auto-stainer. The first staining took around 51 min, and the second one took around 2 hours and 3 min. The auto-stainer contains 24 compartments, 14 of which were used in the H&E staining, and 18 were used in the EVG staining. Slides were arranged in a metal rack and placed in the first compartment of the machine. The machine was switched on, and set on 1 for H&E or 2 for EVG. After around 20 mins in the first setting, tap water was run and checked regularly to avoid overflow. With the second staining, this step occured after 1 hour and 42 min. After the staining, the slides were covered in mounting media and a cover slip and left to dry under the fume hood overnight.

D. Masson's Trichrome Staining

This staining is used to detect the collagen fibres in the tissue such as the skin and heart. The fibres are stained blue, the nuclei are black, and the remaining cellular components are stained red.

The slides were placed in the oven for 20 mins prior to staining. They were then rinsed in clearene for 15 mins, and in 100 %, 95 %, and 70 % IMS for 3 mins, 3mins, and 10 mins respectively, and finally rinsed in distilled water. This is to deparaffinise and hydrate the tissue. The staining process started by staining in Mayer's hematoxylin for 1 min, and then washing the slides in running warm water for 10 min before rinsing them with distilled water. After that, the slides were soaked in Biebrich scarlet-acid fuchsin solution (3 ml glacial acetic acid, 2.4 gm of biebrish scarlet, 0.3 gm of acid fuchsin, and 300 ml distilled water) for 15 mins, and rinsed in distilled water again. They were then differentiated in phosphomolybdic-phosphotungstic acid solution (25 gm of 5 % phosphomolybdic acid, 25 gm of 5 % phosphotungstic acid, and 1000 ml distilled water) for 15 min, and stained with aniline blue afterwards (2.5 gm aniline blue, 1 ml glacial acetic acid, and 100 ml distilled water) for 1-2 min and differentiated in 1 % acetic acid solution for 5 min. Slides were rinsed for the final time in distilled water.

Finally, the slides were soaked in 90 % or 95 % IMS and 100 % IMS (20 seconds each) and soaked again in clearene. The slides were ready after this to mount with resinous medium and covered and left under the fume hood to dry overnight.

This staining was used to measure fibrous tissue expressed as a percentage. Using ImageJ software, the threshold of the image was altered so that the blue colour (fibrous tissue) was highlighted then measured as an area, divided then by the total tissue area in the image and expressed as a percentage. Four images from four random areas were measured per heart.

E. Immunohistochemistry Staining (Isolectin Biotin 4)

Isolectin biotin 4 (IB4) staining was done. Slides were deparaffinised by placing them in cleareane (3 times for 5 mins each), and then in graduated alcohol (100 %, 90 %, and 70 % IMS) for 5 mins each. After that, they were rinsed in distilled water, and placed in 10 mM citrate buffer (2.1 g/1 L dist.H_2O) for 6 mins in the microwave for heating (this is done for antigen retrieval). The citrate buffer was then topped up with distilled water and the slides were heated in the microwave again for 6 mins. After that, the slides were left to cool at room temperature for 30 mins before rinsing them in PBS buffer (3 times). Bloxall solution was added on the tissue sections on the slides for 10 mins in order to inhibit endogenous peroxidase activity, and then rinsed again in PBS for 3 times. Then, 10 % goat serum was pipetted onto the tissue sections to block the non-specific Antigens and was left to incubate at room temperature for 30 mins. 50 µl of The IB4 antibody (primary antibody) was pipetted onto the tissue sections (diluted in PBS, 1:400) and left to incubate overnight at 4° C.

The following day, slides were washed in PBS (3 times). Then, 50 µl of PBS (instead of secondary antibody) was pipetted onto the sections and incubated at room temperature for 30 mins. This is because the primary antibody used here is conjugated with biotin, and thus does not need a secondary antibody. Sections were then washed once again in PBS (3 Times) and 50 µl of Extravidin-horseradish peroxidase (diluted 1:200 in PBS) was pipetted onto them and

incubated at room temperature for 30 min. Slides were then washed in PBS, and DAB (3, 3-diaminobenzidine) solution was pipetted onto them for 10 mins at room temperature. Slides wer washed in tap water after that, counter stained with Myors hematoxylin for 3 mins, and washed again in tap water for 5 mins. Finally, they were dehydrated in graduated alcohol and then clearene (to remove the alcohol) and mounted with DPX.

With this staining, capillaries are stained with a brown/black colour, and the cardiomyocytes appear light blue with the nuclei stained with a dark blue colour. This staining was used to count capillaries, which were expressed as a ratio to cardiomyocyte number. 3-4 different images from the LV were used per heart for the counting.

2.4.4.2 Electron Microscopy

2.4.4.2.1 Tissue Fixation

The hearts were extracted from freshly sacrificed animals and put into ice cold cardioplegic solution. The composition of the Krebs cardioplegic solution was (120 mM NaCl, 25 mM NaHCO$_3$, 11 mM glucose anhydrous, 0.22 gm Na pyruvate, 1.2 mM KH$_2$PO$_4$, 1.2 mM MgSO$_4$.7H$_2$O, 4.8 ml KCL, 1.2 mM CaCl$_2$, + 20 mM KCl). The hearts were then cannulated through the aorta and perfused with the cardioplegic solution at a rate of 1 ml/min, till the blood was washed out. After that, the hearts were perfused with a fixative solution at the same rate for 2-3 mins. The fixative solution (100 ml) was prepared as follows using 0.1 M phosphate buffer + 1 % glutaraldehyde + 1 % paraformaldehyde + 0.5 mM CaCl$_2$ and 1.7 mM D-glucose anhydrous. The phosphate buffer was prepared as follows: 76.76 gm HNa$_2$O$_4$P, 22.5 gm NaH$_2$PO$_4$.2H$_2$O, and 100 ml distilled water; pH = 7.4. 25 % glutaraldehyde and 4 % paraformaldehyde were used. Finally, hearts were kept in the fixative solution for at least an hour before they were washed with phosphate buffer and cut into small cubes so that they could be processed into blocks. The processing of these blocks was done by the Bioimaging facility in the Biomedical School, University of Bristol.

2.4.4.2.2 Tissue Processing

Processing and staining of the tissues were done by the Bioimaging facility in the Biomedical School, University of Bristol. The hearts were post-fixed in 1 % (w/v) OsO_4 in phosphate buffer for 90 min. They were then washed in phosphate buffer (3 times for 10 mins each), followed by washing with distilled water. The tissues were then stained in the dark in 3 % (w/v) uranyl acetate in distilled water for 30 min. This was followed by rinsing in distilled water again for 10 mins, dehydration in 70 %, 80 %, and 90 % ethanol (10 mins each). Afterwards, tissue was rinsed with propylene oxide (3 times for 10 mins each) and stored overnight in a sealed container. Finally, tissue was stored in EPON epoxy resin for 24 hours before embedding in EPON epoxy resin and polymerised at 60º C for 48-72 hours.

The tissue was cut and stained with uranyl acetate and lead citrate (94 mM lead nitrate, 140 mM sodium citrate and 0.19 mM NaOH), and was ready for imaging.

2.4.4.2.3 Imaging and Analysis

Electron micrographs were taken using a Tecnai 12 bioTWIN transmission electron microscope (FEI, Netherlands) in the Wolfson Bioimaging Facility at the University of Bristol. Three different areas from each heart/sample were imaged, with various magnifications.

Images were used to measure sarcomere length, mitochondria density (for the three subpopulations: perinuclear, interfibrillar, and subsarcolemmal), mitochondrial morphometry (including length, width, area/size, and calculating roundness and aspect ratio (length:width)), and counting lipid droplets. All these measurements were done using the software ImageJ.

2.4.5 Langendorff Perfusion

2.4.5.1   Pressure & Flow Rate Calibration

For pressure calibration, the pressure was measured through channel 3 in chart 5. It was first zeroed, then the Sphygmomanometer was attached to the transducer, and the readings (in mV) were recorded at 20, 40, 60, 80, 100, and 140 mmHg. This was repeated 2 or 3 times. These readings were then plotted against the pressure points in excel, where two points are chosen, and their values are calculated from the equation (y = 0.0362x - 0.0278). They were then used to calibrate the pressure in chart 5 and the scale was set to -50 and 140 mmHg. Figure 2.9.
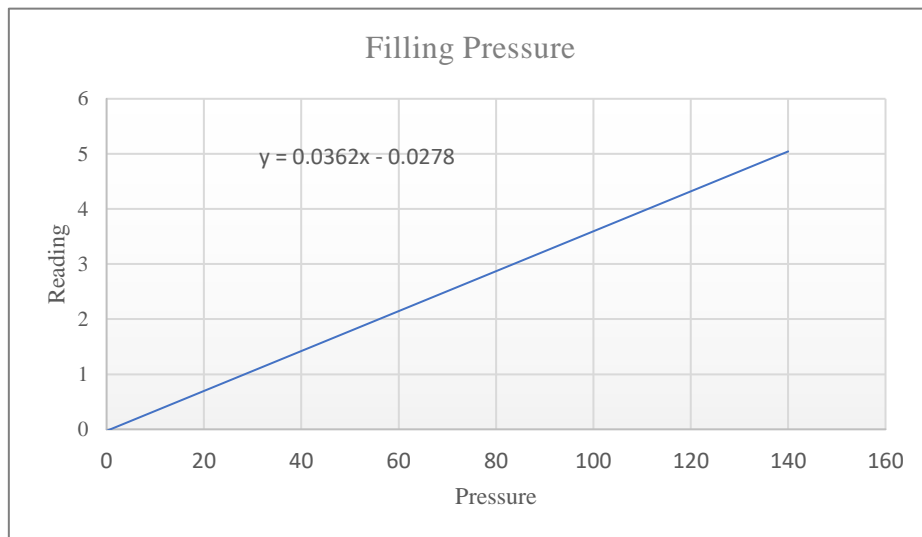
Figure 2.9: Standard curve for calibrating filling pressure.

Flow rate was calibrated in a similar way. The pump flow rate was zeroed (channel 4) when the pump was switched off. After that, the pump was switched on, and the rate was set at 0.5, then effluent was collected for a minute and measured. This was done at different flow rates (1.0, 1.5, and 2.0) in duplicates. These readings were plotted in excel again, and two points were chosen and calculated using the equation (y = 3.99x + 0.2) to use for the calibration in chart 5. Finally, the scales were set to -5 to 20 ml/mn. Figure 2.10.
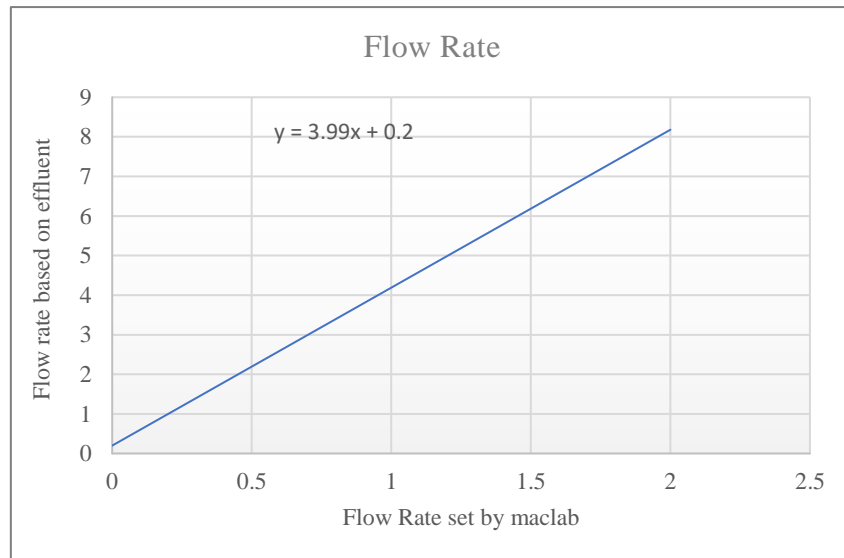
Figure 2.10: Standard curve for calibrating flow rate.

2.4.5.2 Ischemia/Reperfusion Injury

The Langendorff setup was prepared by switching on the temperature, the oxygen, and the MacLab. Krebs solution was added into the first compartment and run through the setup until it reached the needle without any bubbles. The pump was switched off for the pressure to be set, once that was done, the pump was switched back on and the rate was set at 1.0 ml/min. The heart was excised from a freshly sacrificed animal and immersed in ice-cold Krebs-Henseleit solution (in mM: 120 NaCl, 25 NaHCO$_3$, 11 D-Glucose anhydrous, Na pyruvate, 1.2 KH$_2$PO$_4$, 1.2 MgSO$_4$, 4.8 KCl, 1.2 CaCl$_2$). The heart was then cannulated through the aorta and retrogradely perfused with 37° C Krebs solution, gassed with 95 % O$_2$ and 5 % CO$_2$. The filling pressure (60 mmHg) was detected by a transducer, which sent a signal that was amplified by a MacLab Quad bridge amplifier and detected by a MacLab/4s. This was kept constant through a negative feedback control between the MacLab/4s controller and the peristaltic pump (Ismatec, Germany), regulated by a STH Pump Controller. This was continued for a 20 min stabilising period, followed by 35 min of global ischaemia, and 60 min reperfusion.

The heart effluent was collected 1 min before ischemia, and then during reperfusion at 1, 5, 10, 20, 30, and 60 mins. This was collected and kept in an ice box to be used for creatine kinase measurement afterward. Figure 2.11 shows the Langendorff perfusion setup.
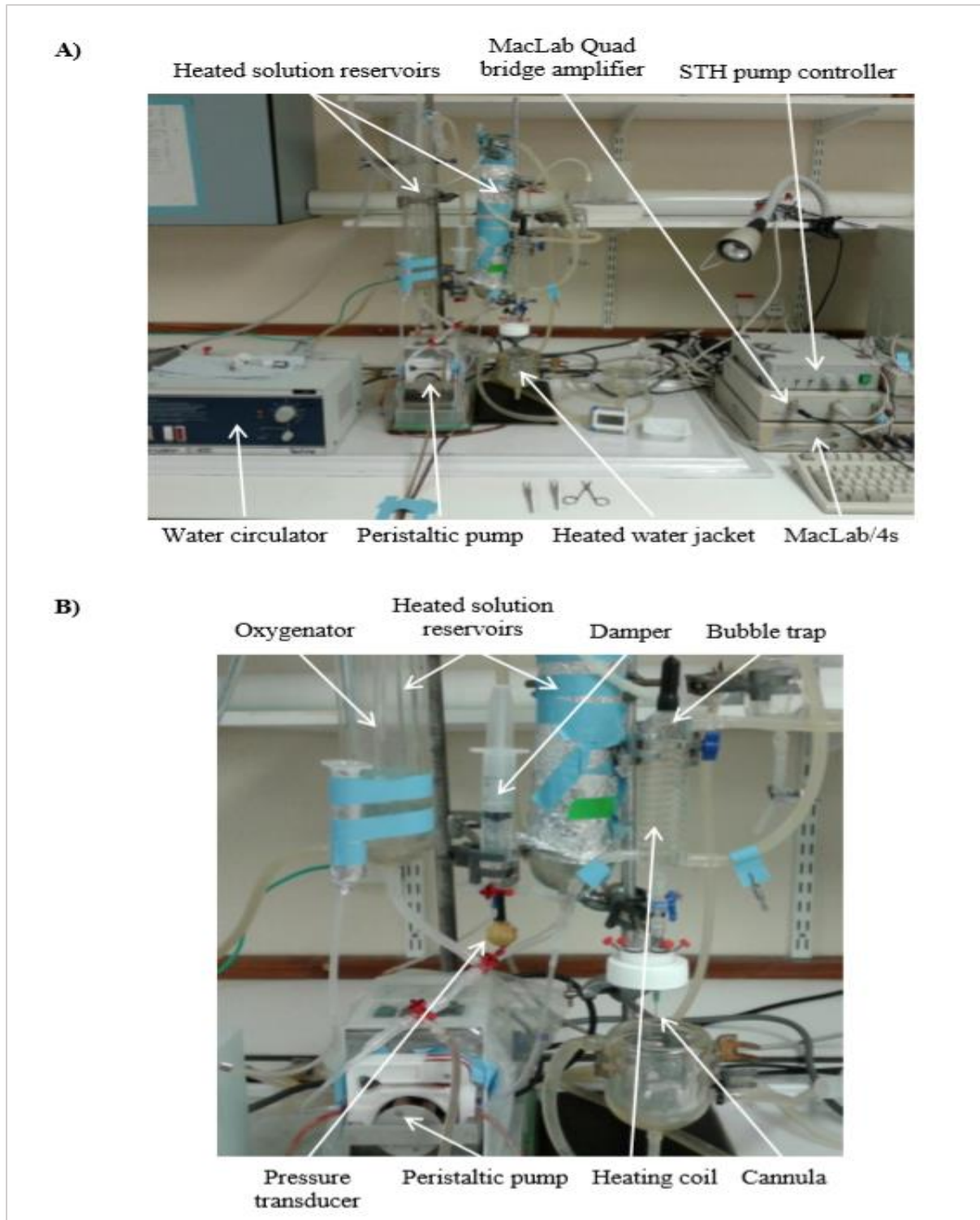
Figure 2.11: Langendorff Perfusion System. (Credit: Ben Littlejohns).

2.4.5.3 Triphenyl Tetrazolium Chloride Staining

At the end of reperfusion, hearts were frozen for 1 hour, then cut transversely into 4 slices (~2-mm-thick), immersed in 1 % (W/V) triphenyltetrazolium chloride (TTC) PBS solution, and incubated at 37° C for 20 min. the slices were then preserved in 4 % (V/V) formaldehyde PBS solution at 4° C overnight. Finally, they were rinsed in PBS, and imaged using a scanner (Epson, UK). Infarct size was calculated using ImagePro® Plus Version 6.2.0.424 software (Media Cybernetics, USA). The total area of each slice was measured (in pixels), followed by measuring the white infarcted area, and the pale pink area separately. Both of these areas were calculated as a percentage of total. This was done for each slice on both sides, and then averaged to get the final infarct size. Figure 2.12 shows an example of a mouse heart sliced and stained with TTC.
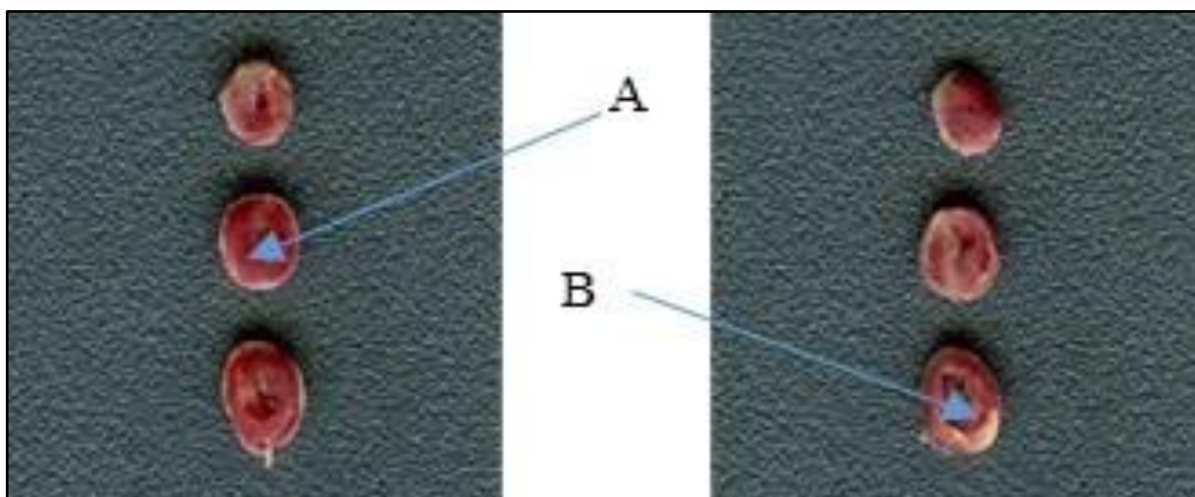
Figure 2.12: TTC staining of representative cross-sections of mouse hearts. A: Viable myocardium stained red. B: Infarct tissues appearing pale white.

2.4.5.4 Measuring of Cardiac Enzyme (Creatine Kinase) Release in Effluent

To measure CK, a commercially available kit from Randox, UK (CK113) was used. The substrate solution was prepared by adding 30 ml of solution into one vial of substrate. Then, 40 µL of effluent was added into 37° C incubated (5 min) 1 mL of solution and allowed to mix

for 2 min. Creatine kinase was then measured by measuring absorbance using the spectrophotometer (Bibby Scientific Limited, UK) at 340 nm, 37° C, and for 4 min. The reaction of this CK assay is shown in figure 2.13.

Mean difference in absorbance was then calculated and multiplied by 4047.5 to give the creatine kinase in international unit per L.
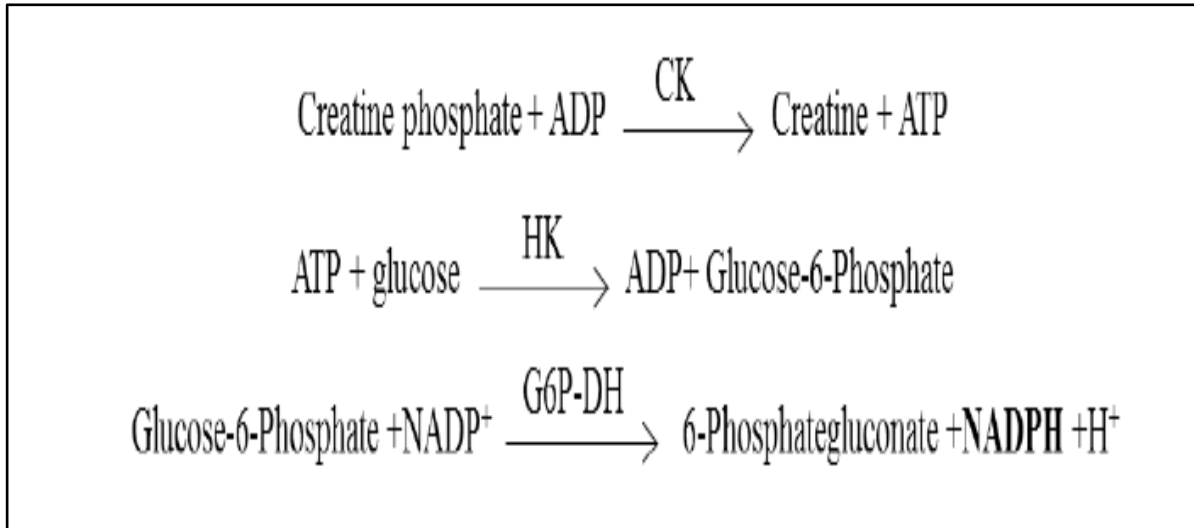
Figure 2.13: The reactions for the creatine kinase assay. CK = creatine kinase, HK = hexokinase and G6P-DH = glucose-6-phosphate dehydrogenase.

2.5 Statistical Analysis of the Data

Data were analysed using Microsoft Excel and IBM SPSS software (version 26) and were presented as mean ± SEM where appropriate. Proteomic data were presented as fold change between HFD and ND ageing hearts, and plasma metabolites as well as coronary artery sizes were presented as quartiles (showing the minimum, maximum, and 3 percentiles in between – 25th, 50th and 75th). Quartiles were used because plasma metabolites were calculated as area under the curve which caused large variations in the data. Similarly, coronary arteries measured ranged in size which would have been mispresented if mean ± SEM was used.

For the statistical tests used, the variance was first tested using the F-test followed by the Student's t-test, with Welch's correction if the data had unequal variance.

When comparing the three subpopulations of mitochondria within one age group, one-way ANOVA was used followed by Bonferroni post-hoc test, or Games-Howell post-hoc test if the data did not have equal variance. Finally, repeated measures ANOVA was used when comparing flow rate and CK release at different time points of ischaemia/reperfusion. All tests were performed as two-tailed tests and a P-value less than 0.05 was assumed to be significantly different.

3. Cardiac Remodelling with Ageing

3.1 Introduction

3.1.1 Overall Effect of Ageing on the Myocardium

Ageing is the most important risk factor for CVD; the leading cause of death in the population aged 65 years and older [8]. Ageing is associated with changes in the myocardium that eventually render the heart more vulnerable to insults. In the mouse, ageing is associated with a decrease in stroke volume and cardiac output [243]. The information below is focused on key aspects that are relevant to work presented in this thesis.

3.1.2 Age-Related Cardiac Structural and Functional Changes

Important myocardial changes include apoptotic and necrotic cardiomyocyte death, fibrosis, and hypertrophy [12]. Fibrosis is also seen in arteries which become stiff and thicker. Additionally, the presence of atherosclerosis with ageing makes the heart and blood vessels ischemic leading to an increase in the rate of apoptosis and necrosis [8]. Cardiac changes also affect heart rate which is decreased and can increase arrhythmias [12]. These changes are general changes that occur with ageing in all mammals, but the extent of these changes can be different.

3.1.3 Calcium Handling and Excitation-Contraction Coupling in the Ageing Heart

EC coupling describes how electrical activity (action potential) causes an increase in intracellular Ca^{2+} and contraction. EC coupling changes with ageing due to many reasons (Reviewed in [4]). The decrease in Ca^{2+} influx, Ca^{2+} release, and expression and activity of certain proteins involved in this phenomenon lead to prolongation of the action potential duration, contraction duration, and Ca^{2+} decay. Protein changes include the shift from α-myosin heavy chain to β-myosin heavy chain resulting in a decrease in myosin ATPase activity. Reduced expression of SERCA2 or reduced its activity - by increased PLB and/or its phosphorylation by PKA - leads to slowing in Ca^{2+} reuptake and prolonged contraction.

Additionally, the decrease in cAMP production leads a decrease in β-adrenergic stimulation. All of these changes contribute to the age-related decline in cardiac contractility.

3.1.4 Cardiomyocyte Metabolism in Ageing

The myocardium requires a consistent and sufficient supply of metabolites as it is constantly contracting. In the adult disease-free heart, glucose and FFAs comprise the main cardiac metabolic substrates to generate ATP; with FFAs accounting for 50-75 % of this energy supply via mitochondrial β-oxidation [109]. The ageing heart is associated with metabolic remodeling; where there is a decrease in FFAs oxidation and thus an increase in glucose utilization to total metabolic substrate [120]. This change was observed in human hearts as well as mouse and rat hearts [123]. The decrease in FFA oxidation is due to an impairment of FFA transport in aged hearts, as well as alterations in various metabolic proteins such as PDK, CPT1 and PPAR-α. [243] Another possible reason for this shift in metabolism is an increase in glucose uptake evident by increased myocardial GLUT-4 expression [244]. However, the opposite of this increase in expression was reported in other studies [120, 121].

3.1.5 Mitochondrial Function and Oxidative Phosphorylation in the Ageing Heart

Mitochondria possess many important functions; including metabolic and signaling pathways in the cell, but the primary function is production of ATP via a process called oxidative phosphorylation. With ageing, the mitochondria undergo morphological alterations that lead to functional decline. Mitochondria in aged tissue appear to be rounder, decrease in number, decrease in respiratory chain (RC) complex capacity [245]. Additionally, with ageing there is increase in Mitochondrial DNA (mtDNA) mutation, increase production of ROS, and thus increase oxidative damage in the tissues [246].

3.1.6 Reactive Oxygen Species and Antioxidant Defense Mechanisms in The Ageing Heart

ROS (e.g superoxide anion (O^{2-})) are generated in the cell as by-products of anabolic and catabolic processes, and in response to external stimuli such as ionizing radiation, chemical toxins, and transition metals [247]. They are mainly generated in the mitochondria from the ETC [163]. ROS react with macromolecules like lipids, proteins, and nucleic acids and cause damage to them [248]. They are neutralized in the body by antioxidants such as catalase, glutathione peroxidase, thioredoxin peroxidase, and superoxide dismutase. Denham Harman proposed a theory more than fifty years ago on ROS and ageing, stating that ageing is caused by ROS damage in the tissue, and the ability of the body to cope with this damage determines the lifespan [249]. In ageing, changes occurring in the mitochondria include increased production of ROS and impairment in antioxidant defense mechanisms [250, 251]. A few studies investigating antioxidant enzyme levels reported contradictory finding. One study noted an increase in glutathione peroxidase activity in the aged rat heart [252]. The same enzyme was investigated in aged women and showed that for every 1-year increase in age there was 2.9 micromol/min/L decrease in activity [253]. Another study investigating antioxidant enzymes in cultured hepatocytes reported a reduction in both superoxide dismutase expression by 60 %, and catalase expression by 50 % in cells from senescent animals [254], however whether these changes also occur in myocytes is not presently known.

3.2   Methods

Several techniques have been used to obtain the results in this chapter. These techniques are described in detail in chapter 2, page 59 (Materials & Methods).

3.2.1 High Performance Liquid Chromatography

HPLC was used for analysis of cardiac ventricular tissue to measure cardiac energy metabolites and AA content in the heart. Five samples for each age group were used. Details on this are found in chapter 2 under this method's section (page 64).

3.2.2 Nuclear Magnetic Resonance Spectroscopy

NMR was used to analyse plasma samples for blood lipid and glucose profile. Four adult and four ageing samples were used. For details on this technique and analysis see chapter 2 under this method's section (page 68).

3.2.3 Liquid Chromatography Tandem Mass Spectrometry

LC-MS/MS was used to detect proteins and phospho-protein levels in cardiac tissue. Five samples for each age group were sent for analysis, but only 4 adult samples were used because a pool sample was created and added to the run (10plex). This was done in case of the need to compare these samples with other samples from different runs. For details on this technique and analysis see chapter 2 under this method's section (page 71).

3.2.4 Light Microscopy

Hearts from adults and ageing mice were collected, fixed, processed, embedded, cut, and stained with four different stains (H&E, EVG, Masson's trichrome, and IHC-IB4) to examine cardiovascular structure and how it remodels with ageing. For details on techniques, imaging, and analysis see chapter 2 under this method's section (page 75).

3.2.5 Electron Microscopy

Hearts from adults and ageing mice (4 for each group) were collected, fixed, processed, embedded, cut, and stained to examine cardiac ultrastructure and how it remodels with ageing.

For details on techniques, imaging, and analysis see chapter 2 under this method's section (page 80).

3.3   Results

3.3.1 General Characteristics of Animals

3.3.1.1   Changes in Body and Heart Weights of Mice with Ageing

Animal weights significantly increased ($P < 0.001$) with ageing, with an approximate 38%

increase in ageing mice weights. (Table 3.1). Epididymal fat pads also showed a significant

increase (213% increase) with ageing ($P < 0.001$), with their percentage of total body weights

increasing significantly in the ageing animals as well ($P = 0.001$).

Table 3.1: Characteristics of the adult and ageing mice. Data are presented as mean ± SEM. Data were analysed using the unpaired t-test. * = $P < 0.05$, ** = $P < 0.001$ vs. adult

Measurement	Adult (8 Weeks) (n=6)	Ageing (80 Weeks) (n=10)
Body weight (gm)	23.79 ± 0.41	32.74 ± 0.83 **
Epididymal fat pad weight (gm)	0.29 ± 0.02	0.91 ± 0.11 *
Epididymal fat pads % of total body weight	1.22 ± 0.09	2.73 ± 0.28 *
Heart Wet Weight (gm)	0.15 ± 0.01	0.19 ± 0.01 *
Heart wet weight % of total body weight	0.62 ± 0.31	0.59 ± 0.03
Heart Dry Weight (gm)	0.03 ± 0.001	0.04 ± 0.001 *
Heart dry weight % of total body weight	0.11 ± 0.004	0.109 ± 0.01

Wet and dry hearts weights also increased with ageing. Heart weights increased significantly

with ageing, with a 25% (1.2 folds) increase in wet weight ($P = 0.009$), and a similar 25% (1.3

folds) increase in dry weight ($P = 0.002$). Despite this significant increase in heart weights,

their percentages of total body weights were not different between the two age groups due to

the simultaneous increase in body weights of the animals seen with ageing.

3.3.1.2   Changes in Plasma Metabolites with Ageing

Several carbohydrate and lipid metabolites were measured in the plasma using NMR analysis

(figure 3.1). These metabolites have been measured and expressed as area under the curve

(AUC). Lipid metabolites in the plasma increased with ageing, and so did lactate, but none of

these changes were significant. Additionally, pyruvate and glucose were decreased with

ageing, with glucose reducing significantly ($P = 0.002$) compared to adult mice. Figure 3.2

shows an example of the adult and aged samples NMR spectra.
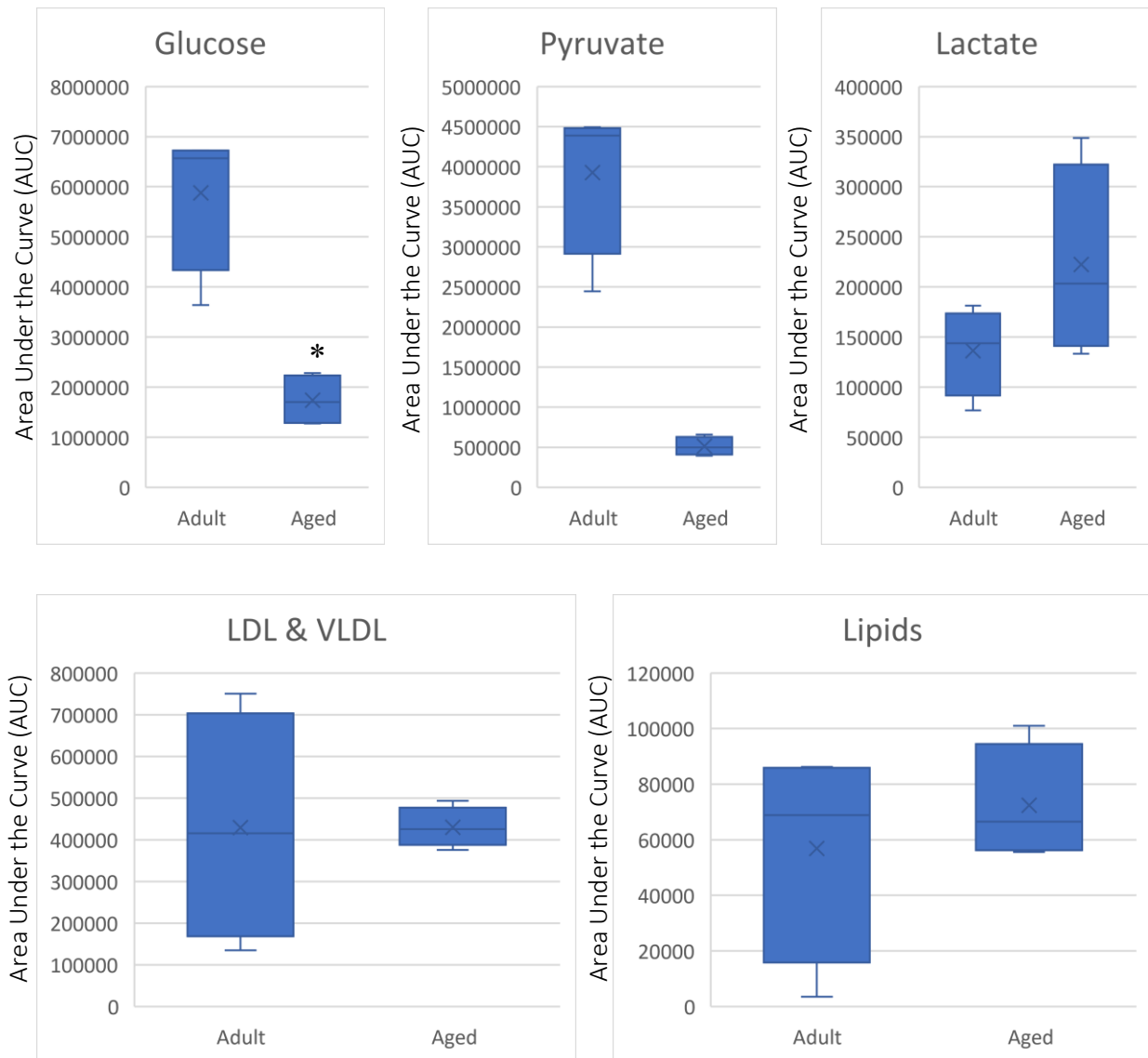
Figure 3.1: Plasma lipid and carbohydrate metabolites in adult and ageing mice.
Data are presented as box plots showing minimum value, 25th, 50th, and 75th percentiles,
and maximum value. Data were analysed using the unpaired t-test.
* = $P < 0.05$ vs. adult. N = 4 for each age group.
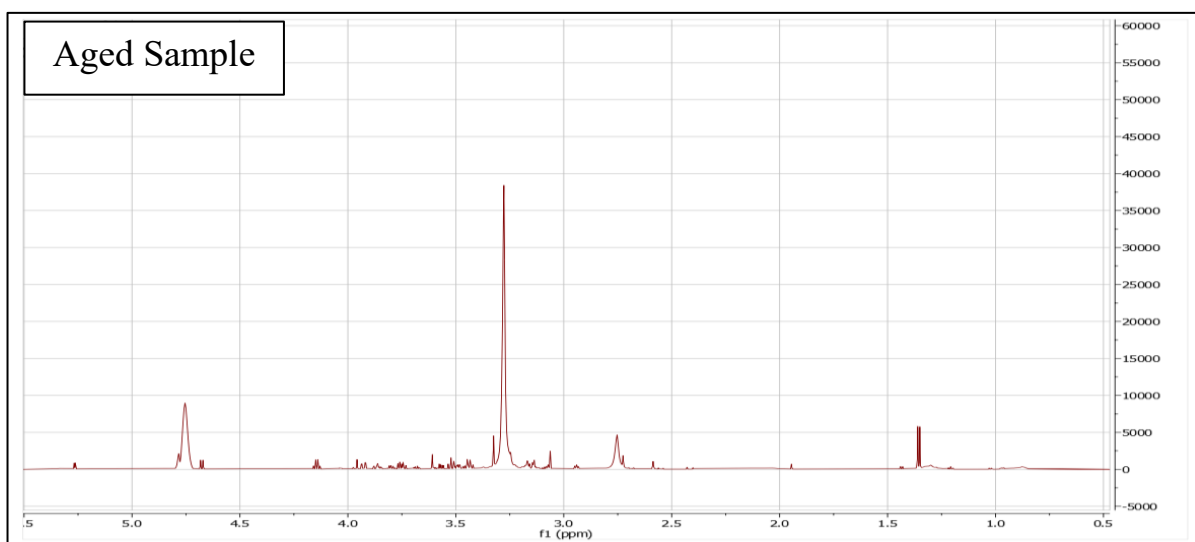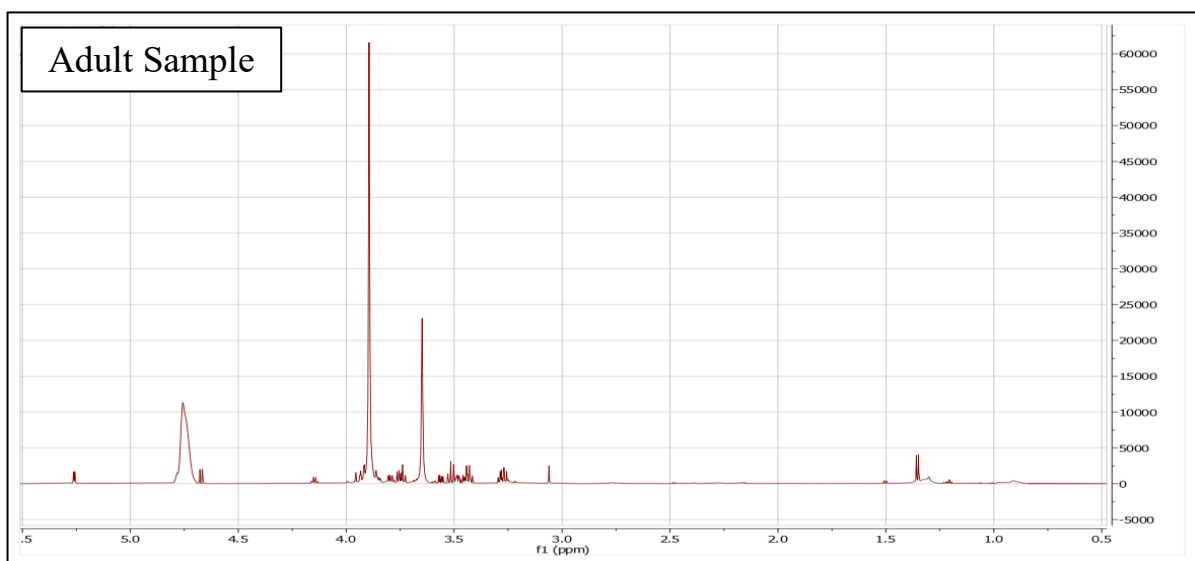
Figure 3.2: Example of adult sample (top) and ageing sample (bottom) NMR spectra.

3.3.2 Metabolic Changes

3.3.2.1　　　Changes in Cardiac Energy Metabolites with Ageing

Table 3.2 shows values for different energy metabolites in adult and ageing hearts. Some of these metabolites increase while others decrease. The only metabolites that changed significantly with ageing were guanosine monophosphate (GMP), inosine, and hypoxanthine. The first two increased in the aged heart and the last one was decreased.

Table 3.2: Cardiac energy metabolites in adult and ageing mice hearts.
Data are presented as mean ± SEM. Data were analysed using the unpaired t-test.
$* = P < 0.05$, $** = P < 0.001$. N = 5 for each age group.

Metabolite	Adult Hearts (µmole/gm tissue)	Ageing Hearts (µmole/gm tissue)	*P*-Value
GTP	0.16 ± 0.02	0.13 ± 0.01	0.20
GDP	0.08 ± 0.01	0.09 ± 0.01	0.64
GMP	0.03 ± 0.001	0.04 ± 0.002	0.009 *
IMP	0.18 ±0.05	0.13 ± 0.07	0.60
ATP	2.24 ± 0.25	1.98 ± 0.33	0.55
ADP	1.62 ± 0.14	1.77 ± 0.15	0.50
Hypoxanthine	0.21 ± 0.02	0.10 ± 0.01	0.0008 **
AMP	0.56 ± 0.06	1.02 ± 0.25	0.14
β-NAD	0.47 ± 0.04	0.55 ± 0.07	0.33
Inosine	0.15 ± 0.02	0.27 ± 0.03	0.009 *
Adenosine	0.10 ± 0.01	0.10 ± 0.01	0.82

Phosphorylation ratios (phosphorylation potential) for adenosine and guanosine energy metabolites were calculated and they were generally lower in the aged heart compared to the adult heart. However, only guanosine ratios were significantly reduced in the aged hearts, with a reduction from 2.01 ± 0.2 to 1.5 ± 0.08 for GTP/GDP ratio, and from 5.97 ± 0.87 to 3.53 ± 0.37 for GTP/GMP ratio. Cardiac energy charge [EC = (0.5 * ADP + ATP)/ (ATP + ADP + AMP)] was also calculated for both age groups and was lower in the aged heart compared to

the adult heart, but this reduction was not significant. Additionally, adenosine metabolites pool (ATP + ADP + AMP) was calculated and showed an increase in the aged heart compared to the adult heart but also not significantly (figure 3.3).
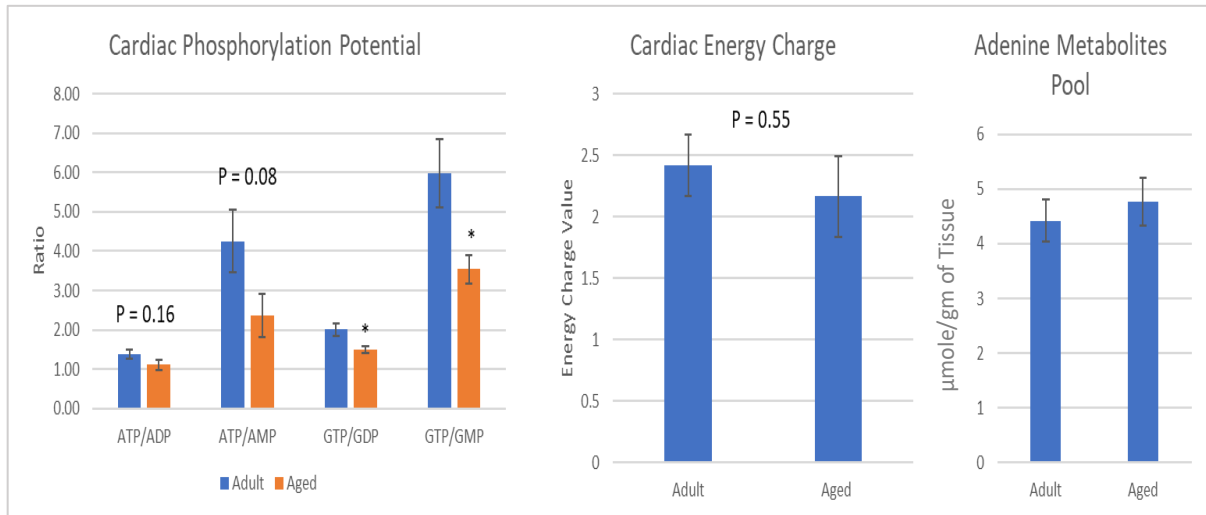
Figure 3.3: Cardiac phosphorylation potential, energy charge, and adenosine metabolites pool in adult and ageing hearts. Data are presented as mean ± SEM and were analysed using unpaired t-test.
* = $P < 0.05$ vs. adults. N = 5 for each age group.

3.3.2.2 Changes in Cardiac Amino Acids with Ageing

As seen in figure 3.4, 12 amino acids were detected, mostly non-essential ones except for the AAs histidine and threonine. Total AA pool decreased significantly with ageing ($P = 0.003$) from an average of 43.3 ± 1.1 nmole/mg in adult hearts to 37.1 ± 0.5 nmole/mg in aged hearts. Taurine contributes to more than half of the AA pool in both age groups (61% and 63% in adult and aged hearts respectively), and even though the percent of taurine from total AA pool was not significantly different with ageing; the amount of taurine was significantly reduced ($P = 0.008$) in the aged hearts from an average of 26.3 ± 0.6 nmole/mg to 23.3 ± 0.6 nmole/mg. All other AAs were also found in lower amounts in the aged heart compared to the adult heart, with significant changes ($P < 0.05$) in arginine, asparagine, histidine, serine, threonine, and alanine. Values of these significant AAs can be found in table 3.3.
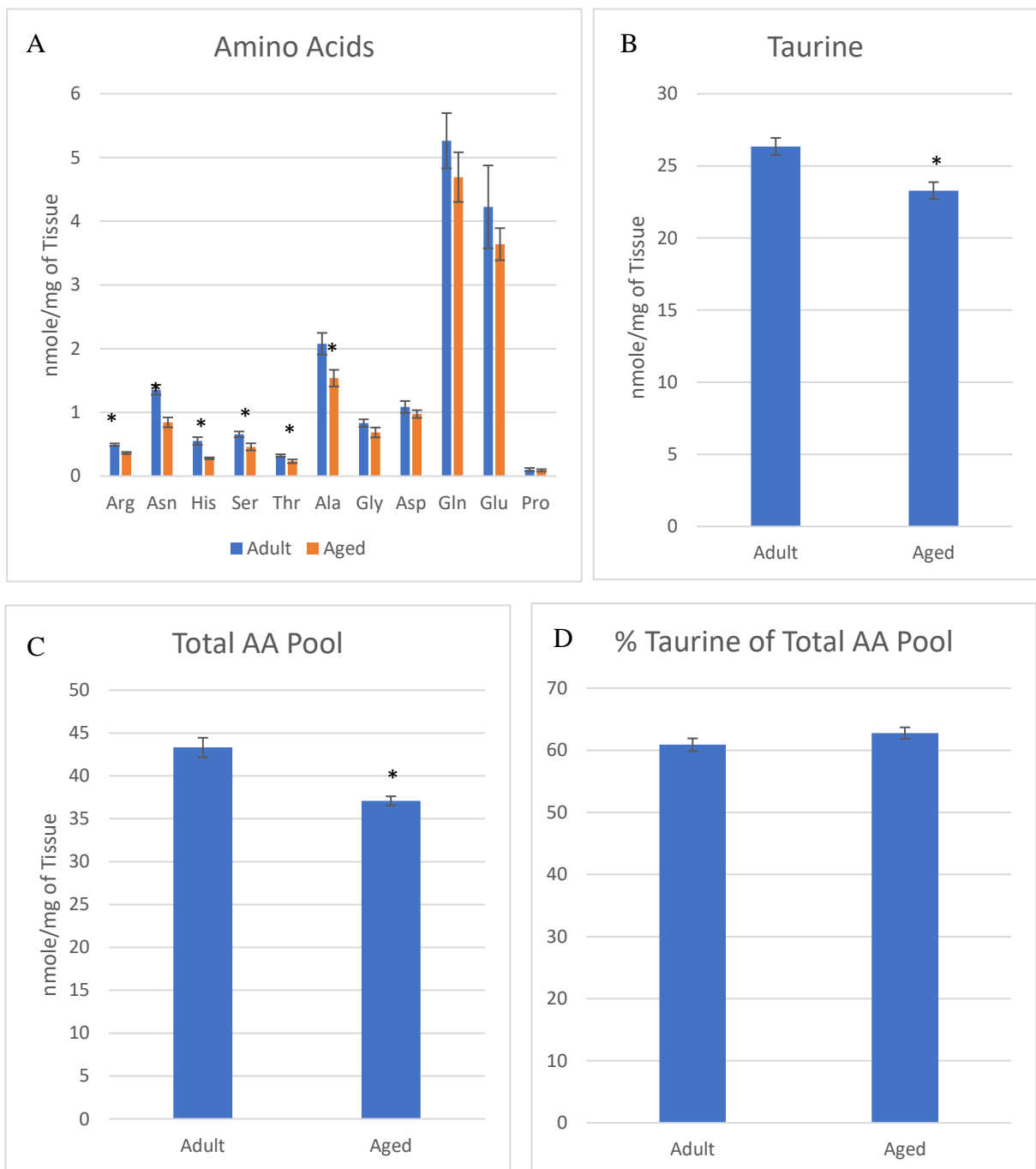
Figure 3.4: A) Amino acids in adult and ageing mice hearts. B) Taurine in adult and ageing mice hearts. C) Total amino acids pool. D) Taurine percent of total amino acids pool. Data are presented as mean ± SEM. Data were analysed using unpaired t-test. * = $P < 0.05$ vs. adult. N = 4 and 5 for adult and ageing hearts, respectively.

Table 3.3: Significantly different amino acids between adult and aged hearts. Data are presented as mean ± SEM. Data were analysed using the unpaired t-test. * = P < 0.05 vs. adult

Amino Acid	Adult Hearts (n = 5)	Aged Hearts (n = 4)
Arginine	0.49 ± 0.02	0.36 ± 0.02 *
Asparagine	1.36 ± 0.08	0.84 ± 0.08 *
Histidine	0.55 ± 0.06	0.28 ± 0.01 *
Serine	0.66 ± 0.04	0.46 ± 0.06 *
Threonine	0.32 ± 0.02	0.23 ± 0.03 *
Alanine	2.08 ± 0.17	1.54 ± 0.13 *

3.3.3 Myocardial Proteome/Phosphoproteome Changes

3.3.3.1 Changes in Cardiac Proteome Profile with Ageing

As demonstrated in figure 3.5, proteomics analysis for adult and aged hearts yielded a total of 6022 proteins. Of those, 1678 proteins were significantly different with ageing; with 98 being downregulated in the aged heart (6 %) and the remaining 1580 proteins being upregulated (94 %). In order to avoid false positive results, proteins with fold change smaller than 0.8 and greater than 1.3 were selected. 720 significant proteins fell within the selected fold change, and these were further categorised using the PANTHER classification system according to molecular function and biological processes (figure 3.6). the majority of these proteins are involved in binding and catalytic activity (based on molecular function), and cellular and metabolic processes (based on biological processes). Significant proteins within selected folds were further grouped into mitochondrial proteins, carbohydrate and lipid metabolism and transport proteins, ionic transport related proteins, antioxidant proteins, apoptosis related proteins, and structural proteins (collagen).
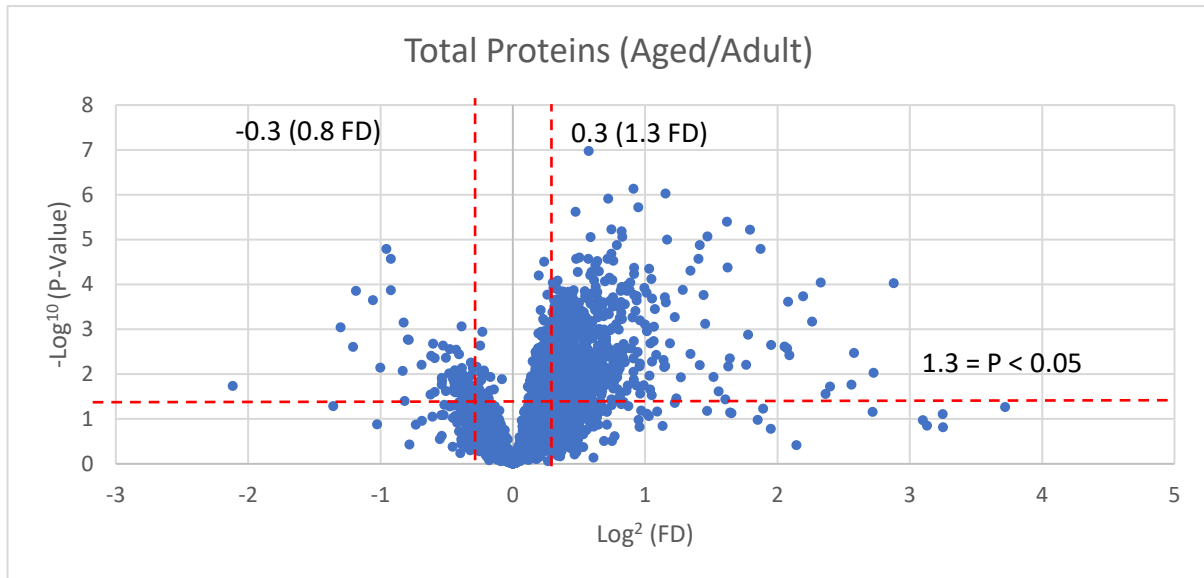
Figure 3.5: Volcano plot showing changes in proteins of ageing/adult mice hearts. X axis represents $\log^2$ of the FD (aged/adult) and Y axis represents $-\log^{10}$ of the P-value. Proteins above the horizontal red line are significantly different between the two age groups. Proteins on the right of the Y axis are upregulated with ageing (with the ones on the right of the vertical red line having a FD > 1.3), and proteins on the left side of the Y axis are downregulated with ageing (with the ones on the left of the second vertical red line having a FD < 0.8). Data were analysed using the unpaired t-test. N= 4 and 5 for adult and aged hearts, respectively.
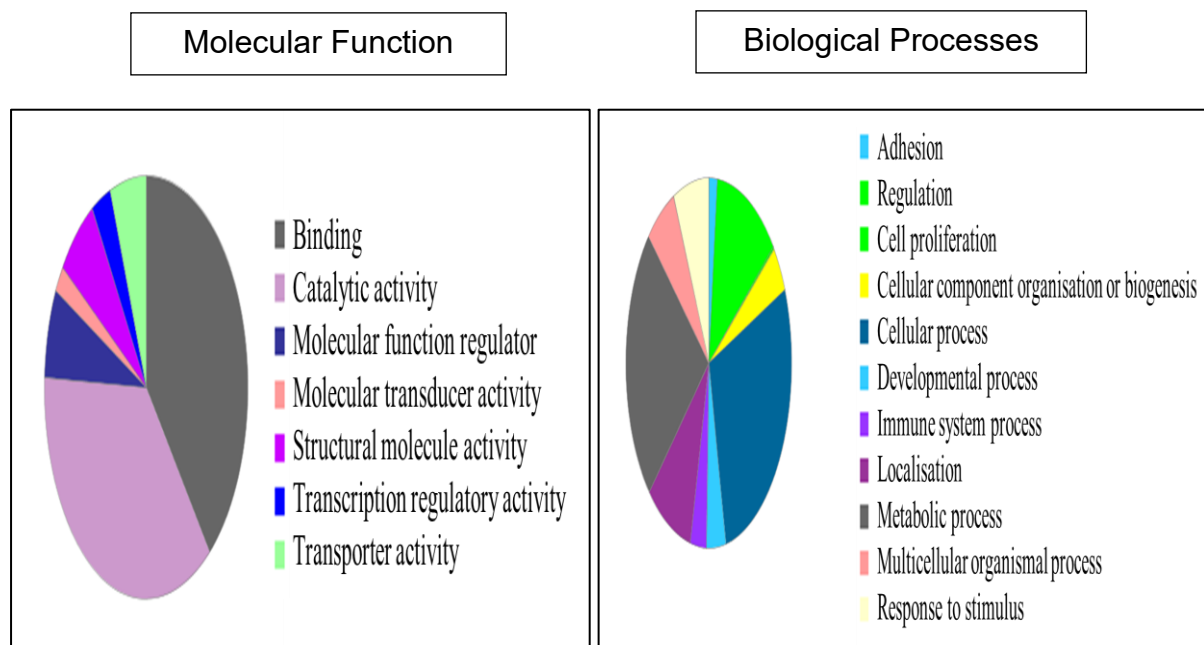
Figure 3.6: Classification of significantly different proteins within selected fold change (< 0.8 and > 1.3) between adult and ageing hearts using the PANTHER classification system. Proteins are classified according to molecular function and biological processes.

3.3.3.1.1 Mitochondrial Proteins

26 mitochondrial proteins changed significantly in the aged heart compared to the adult heart. All proteins were upregulated with ageing with the exception of aldehyde dehydrogenase X, 10-formyltetrahydrofolate dehydrogenase, and trimethyllysine dioxygenase. These proteins are involved in detoxification from alcohol-derived acetaldehyde, folate metabolism, and AA lysine metabolism respectively. Mitochondrial proteins were further categorised into lipid metabolism, AA metabolism, transport, and energy production (figure 3.7). Lipid metabolism proteins include acyl-coenzyme A synthetase ACSM5, enoyl-CoA hydratase domain-containing protein 2, and sterol 26-hydroxylase, mitochondrial, and were all upregulated in old age. AA metabolism proteins include 4-aminobutyrate aminotransferase, and serine beta-lactamase-like protein LACTB, mitochondrial, which were also upregulated in the aged heart. Mitochondrial transport proteins include mitochondrial import inner membrane translocase subunit Tim17-A, and mitochondrial dicarboxylate carrier. Finally, energy production proteins include ATP synthase subunit e, and succinyl-CoA ligase [GDP-forming] subunit beta. (For full list of protein names see appendix 7.2).
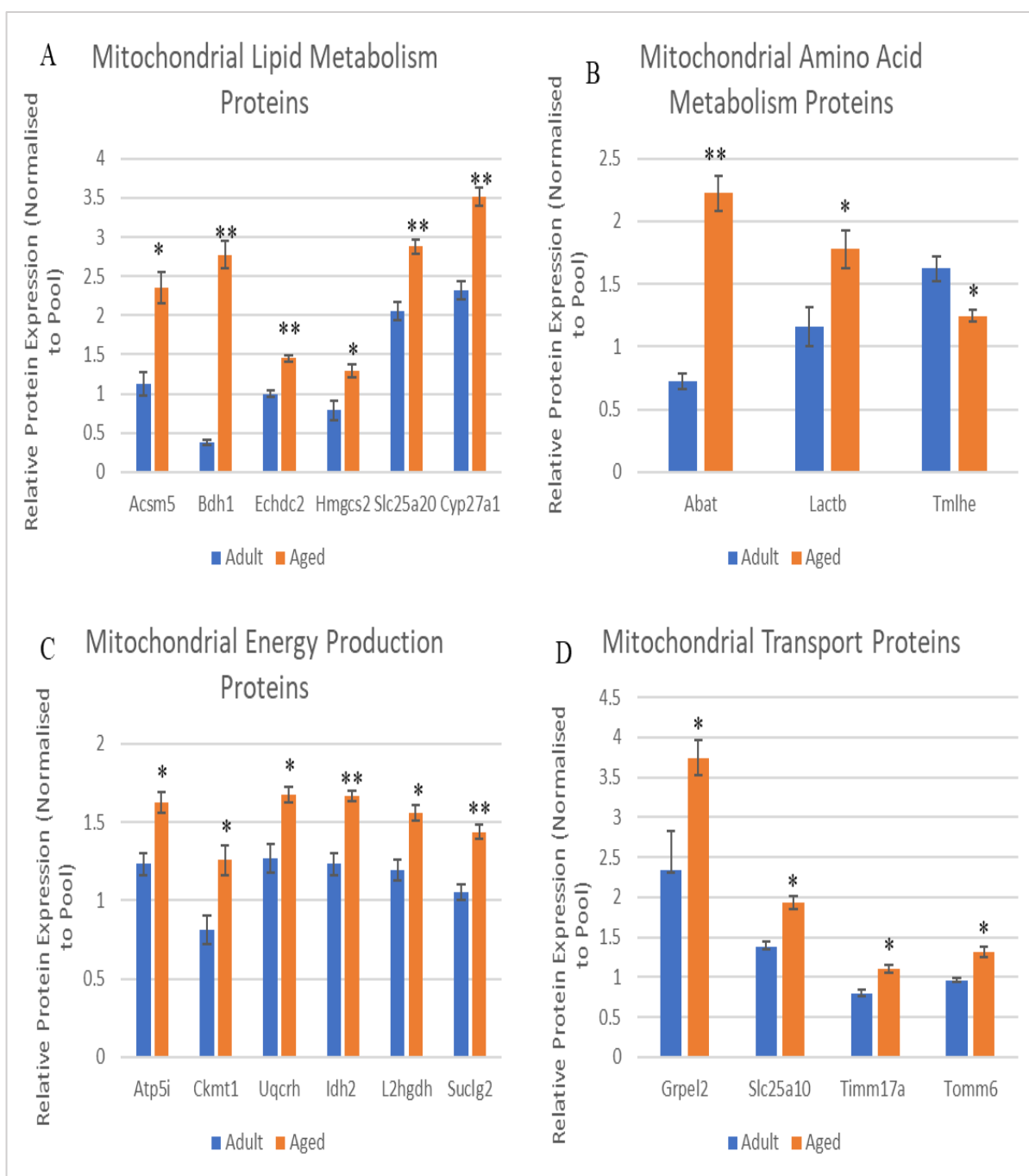
Figure 3.7: Significant mitochondrial proteins in adult and ageing mice hearts. A) Mitochondrial lipid metabolism proteins. B) mitochondrial amino acid metabolism proteins. C) mitochondrial energy production proteins. D) mitochondrial transport proteins. Data are expressed as mean ± SEM (of the relative protein expression normalised to a pool sample). Data were analysed using the unpaired t-test. All proteins selected fall within a FD < 0.8 and > 1.3. * = $P < 0.05$, ** = $P < 0.001$ vs. adult. n = 4 and 5 for adult and ageing hearts, respectively.

3.3.3.1.2 Ionic Transport-Related Proteins

Ionic transport related proteins include proteins involved in the ionic transport into and out of the cell such as Na^+, Ca^{2+}, Cl^-, and K^+ transport proteins (channels, pumps & exchangers). All proteins were upregulated in the aged heart compared to the adult heart (figure 3.8). Three sodium-related proteins increased with ageing including Sodium channel subunit beta-2, Sodium channel subunit beta-4, and Electrogenic sodium bicarbonate cotransporter NBCe1 variant D. Potassium-related proteins that were upregulated with ageing included Inward rectifier potassium channel 13 and Voltage-gated potassium channel Kv1.7. Finally, Sodium/calcium exchanger and Ryanodine receptor 2 were also upregulated with ageing and are involved in calcium homeostasis.
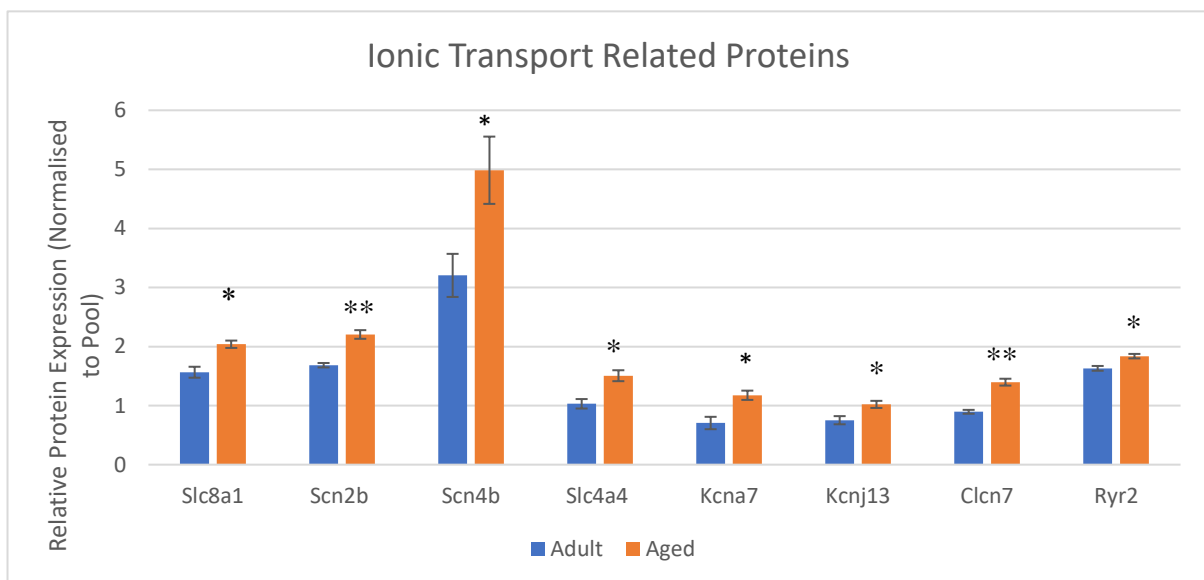
Figure 3.8: Significant ionic transport related proteins (calcium, sodium, and potassium) in adult and ageing mice hearts. Data are expressed as mean ± SEM (of the relative protein expression normalised to a pool sample). Data were analysed using the unpaired t-test. All proteins selected fall within a FD < 0.8 and > 1.3. * = $P < 0.05$, ** = $P < 0.001$ vs. adult. n = 4 and 5 for adult and ageing hearts, respectively.

3.3.3.1.3   Antioxidant Proteins

Extracellular superoxide dismutase, and glutathione peroxidase I and III are all proteins with antioxidant activity and are all upregulated in expression with ageing. Additionally, a group of 6 glutathione proteins involved in the defence against ROS were also upregulated with ageing (figure 3.9).
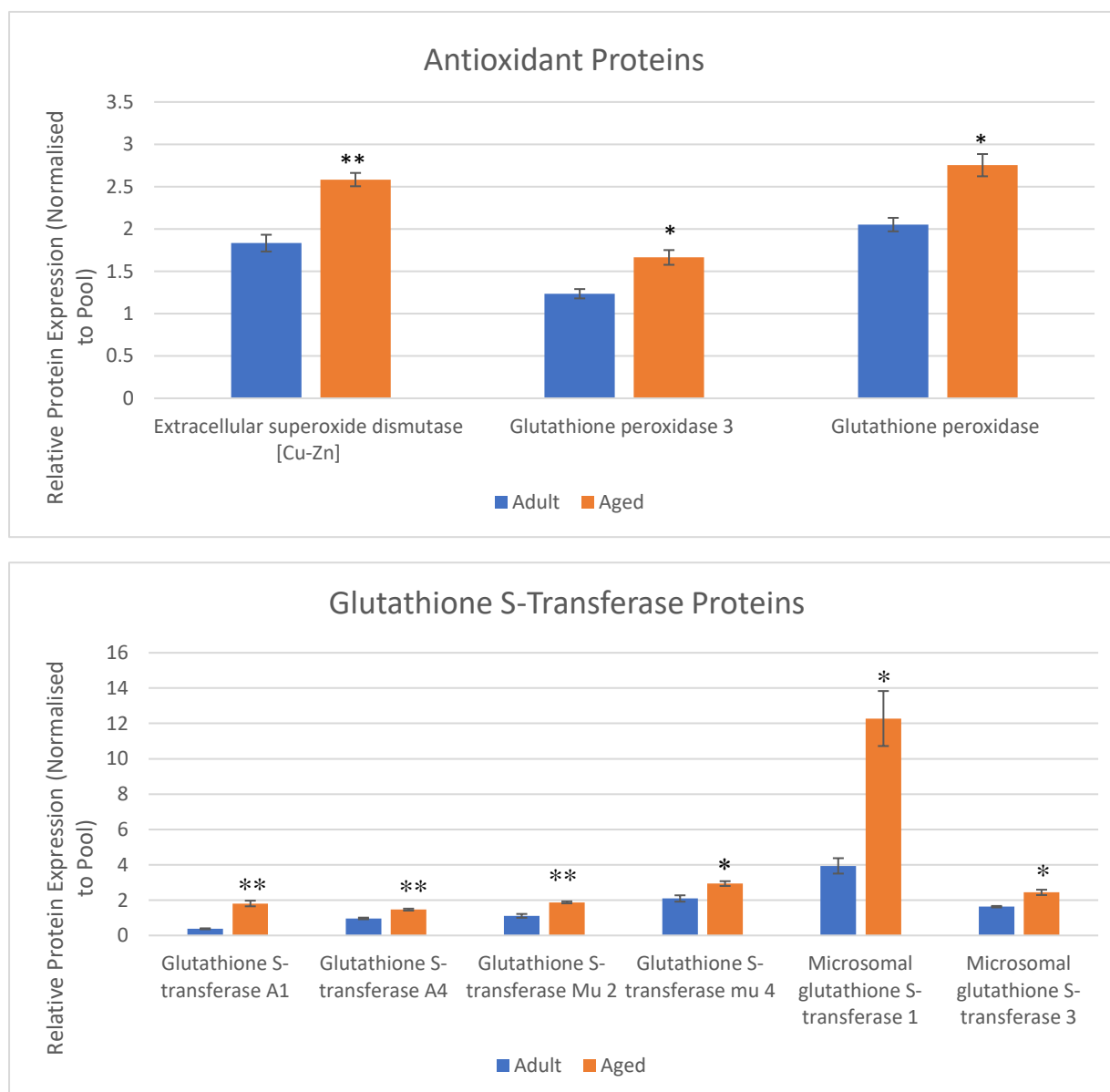
Figure 3.9: Significant antioxidants and defence related proteins in adult and ageing mice hearts. Data are expressed as mean ± SEM (of the relative protein expression normalised to a pool sample). Data were analysed using the unpaired t-test. All proteins selected fall within a FD < 0.8 and > 1.3. * = $P < 0.05$, ** = $P < 0.001$ vs. adult. n = 4 and 5 for adult and ageing hearts, respectively.

3.3.3.1.4 Apoptosis Related Proteins

Three apoptosis related proteins were identified and were all upregulated in the aged heart.

Two of these proteins are pro-apoptotic and one is anti-apoptotic (BCL2-associated athanogene

3). (figure 3.10).
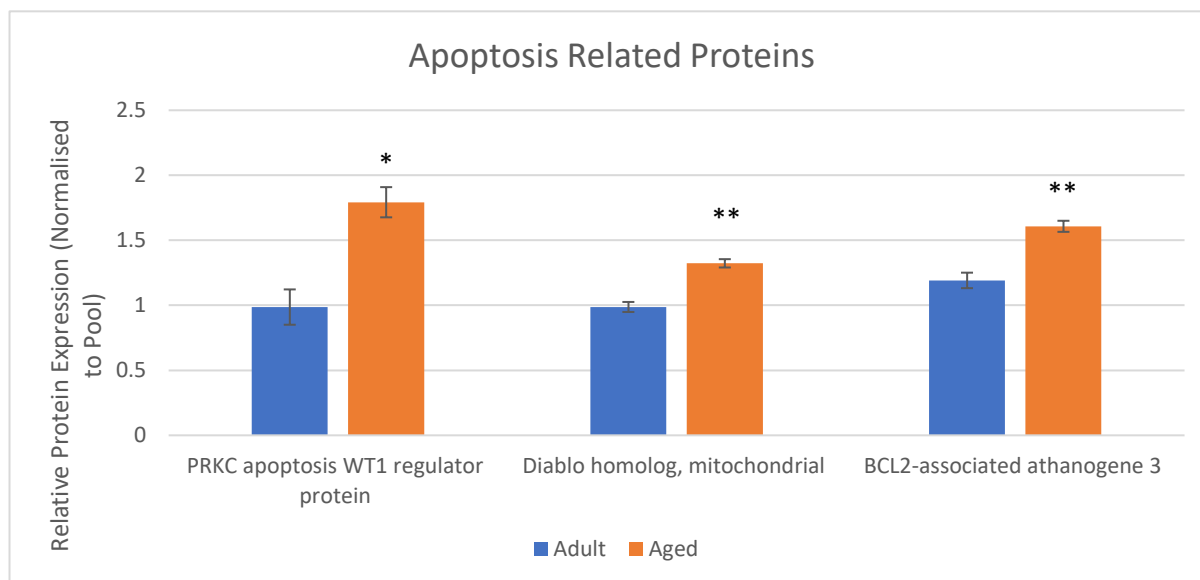
Figure 3.10: Significant apoptosis related proteins in adult and ageing mice hearts.
Data are expressed as mean ± SEM (of the relative protein expression normalised to a
pool sample). Data were analysed using the unpaired t-test. All proteins selected fall
within a FD < 0.8 and > 1.3. * = $P < 0.05$, ** = $P < 0.001$ vs. adult. n = 4 and 5 for adult
and ageing hearts, respectively.

3.3.3.1.5 Structural Proteins (Collagen)

Collagen proteins from the proteomics analysis showed a significant increase in expression

with ageing, with one protein decreasing in expression (collagen alpha-1 XIV chain) (figure

3.11). Five different chains from collagen I, VI, and XVIII were all upregulated in the aged
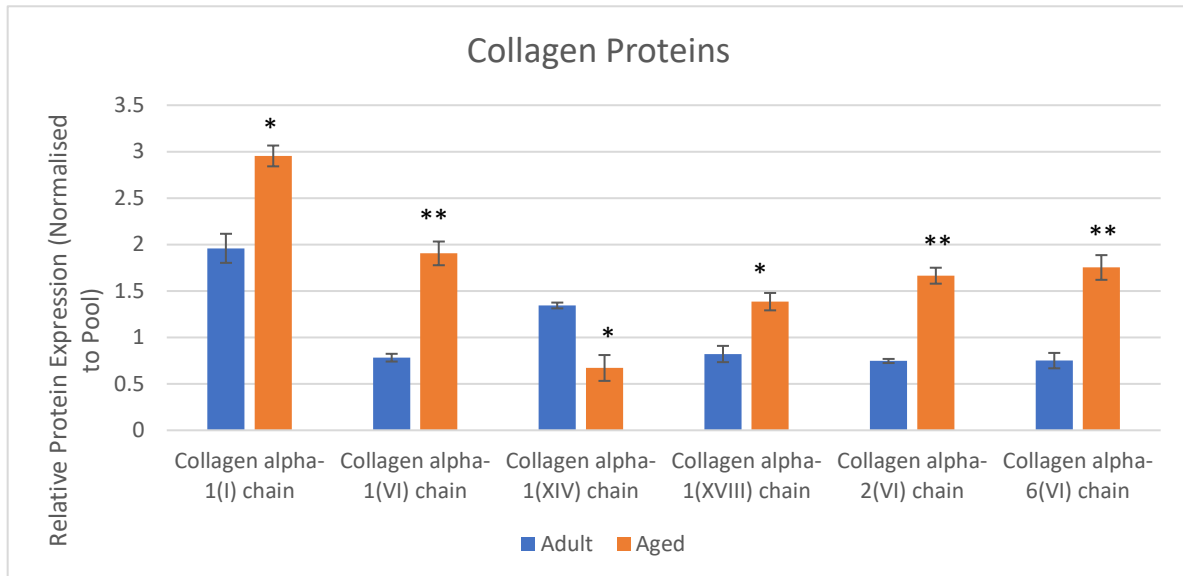
heart.

Figure 3.11: Significant collagen proteins in adult and ageing mice hearts. Data are expressed as mean ± SEM (of the relative protein expression normalised to a pool sample). Data were analysed using the unpaired t-test. All proteins selected fall within a FD < 0.8 and > 1.3. * = $P < 0.05$, ** = $P < 0.001$ vs. adult. n = 4 and 5 for adult and ageing hearts, respectively.

3.3.3.1.6 Lipid and Carbohydrate Metabolism and Related Transport Proteins

Lipid metabolism and related transport proteins were all upregulated in expression in the aged heart (figure 3.12A). Proteins included long-chain acyl-CoA synthetase, acyl-CoA dehydrogenase family member 11, and mitochondrial proteins (mentioned earlier) such as acyl-coenzyme A synthetase ACSM5. Carbohydrate-related proteins also followed a similar pattern of upregulation with ageing with the exception of the protein gamma-enolase that was downregulated in the aged heart (figure 3.12B). Gamma-enolase is involved in the pyruvate synthesis pathway from D-glyceraldehyde 3-phosphate. (For full list of protein names see appendix 7.2).
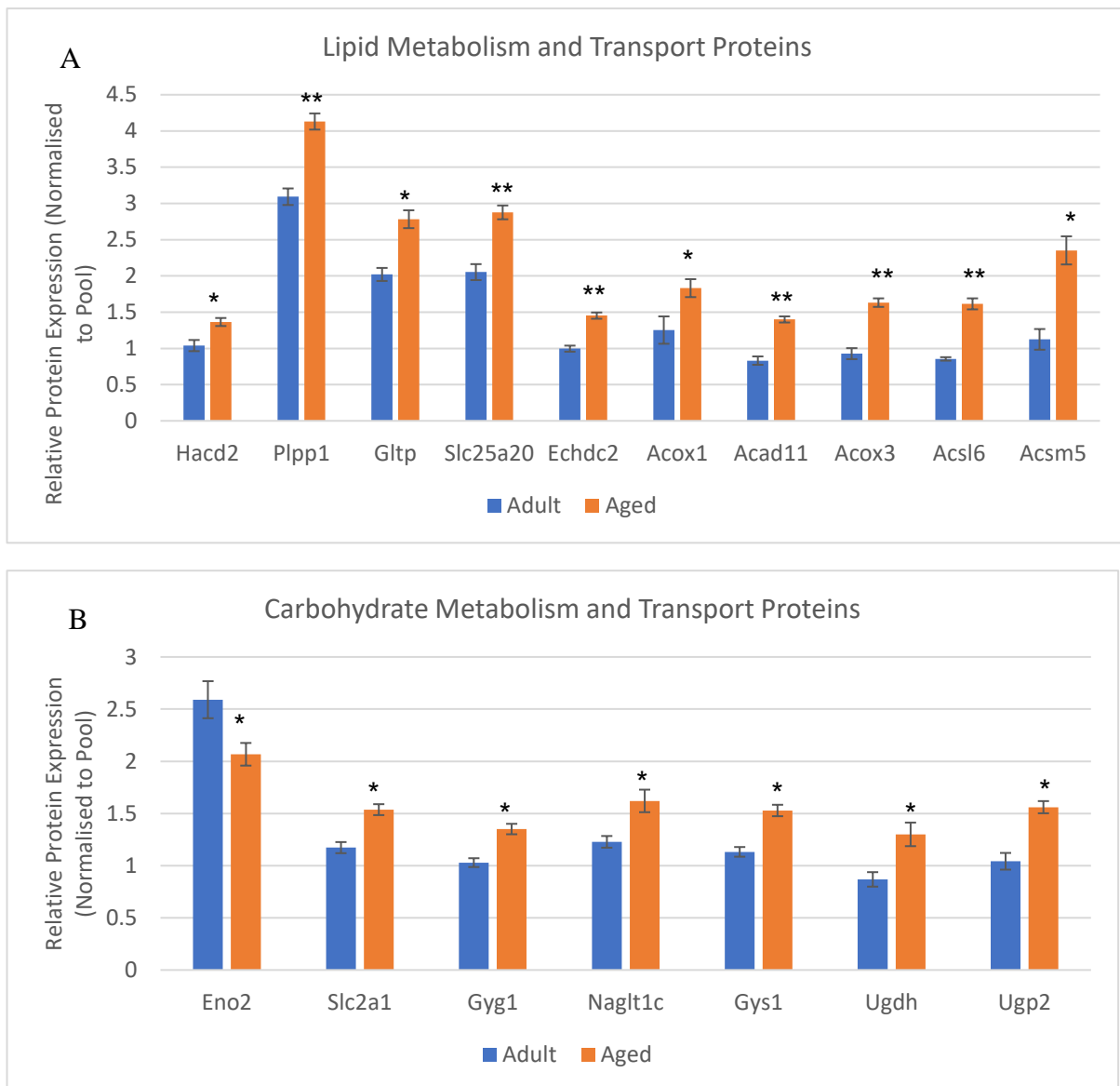
Figure 3.12: Significant lipid and carbohydrate metabolism and transport proteins in adult and ageing mice hearts. Data are expressed as mean ± SEM (of the relative protein expression normalised to a pool sample). Data were analysed using the unpaired t-test. All proteins selected fall within a FD < 0.8 and > 1.3. * = $P < 0.05$, ** = $P < 0.001$ vs. adult. n = 4 and 5 for adult and ageing hearts, respectively.

3.3.3.2 Changes in Cardiac Protein Phosphorylation with Ageing

Phospho-proteomics analysis yielded 2243 peptides with various modifications. Of these peptides we selected the phosphorylated ones and 71 phosphorylated peptides were found to be significantly different with ageing. Within selected fold change, 3 of these peptides were downregulated in phosphorylation, and the remaining were upregulated in the aged heart (33 peptides) as shown in figure 3.13.

These peptides were used to identify their relative proteins which were then further classified according to function (table 3.4).
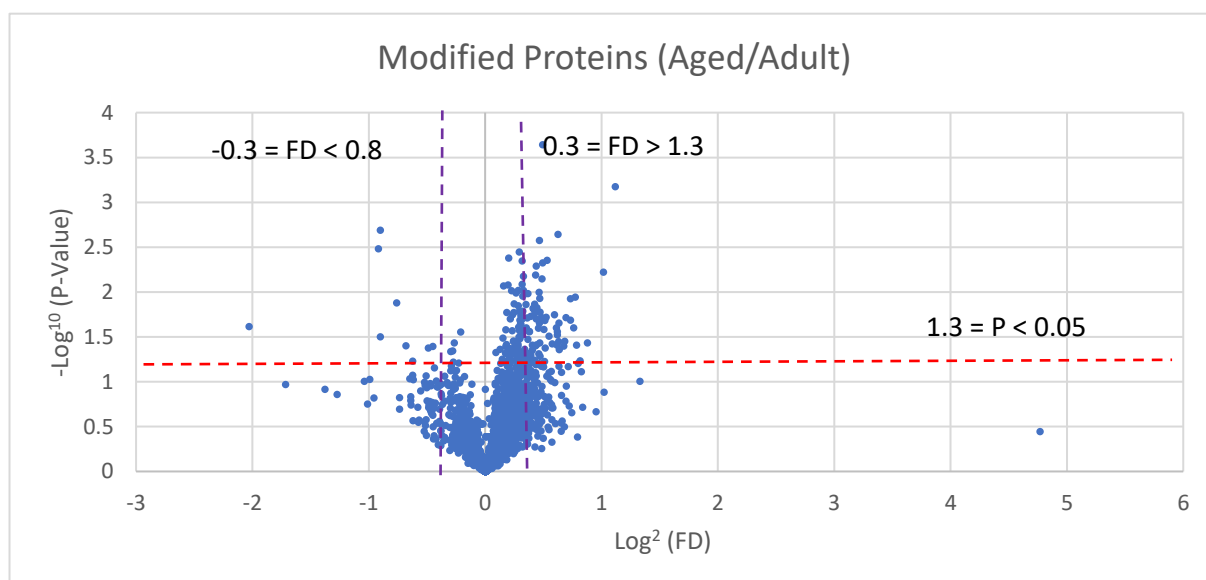
Figure 3.13: Volcano plot showing changes in protein modification of ageing/adult mice hearts. Proteins above the horizontal red line are significantly different between the two age groups. Proteins on the right of the Y axis are upregulated with ageing (with the ones on the right of the vertical purple line having a FD > 1.3), and proteins on the left side of the Y axis are downregulated with ageing (with the ones on the left of the second vertical purple line having a FD < 0.8). Data were analysed using the unpaired t-test. N= 4 and 5 for adult and aged hearts, respectively.

Table 3.4: Selected phospho-proteins that change significantly with ageing. Table shows proteins with their accession number, phosphorylation site, fold change (aged/adult), and P-value. Data were analysed using the unpaired t-test. * = P < 0.05, ** = P < 0.001 vs. adult.

Protein	Accession Number	Phospho-site	FD (Aged/Adult)	P-Value
Downregulated phospho-proteins with ageing				
Sodium channel protein type 5 subunit alpha GN=Scn5a	Q9JJV9	S460	0.71	0.042 *
Upregulated phospho-proteins with ageing				
Signal recognition particle receptor subunit alpha GN=Srpr	Q9DBG7	S295, S296, S297	1.38	0.049 *
Ionic transport				
Sodium-calcium exchanger (Fragment) GN=Slc8a1	Q91ZJ7	S282	1.31	0.047 *
Histidine rich calcium binding protein, isoform CRA_a GN=Hrc	G5E8J6	S421	1.36	0.039 *
Cardiac signalling and apoptosis				
Bcl-2-like protein 13 GN=Bcl2l13	P59017	S387	1.38	0.022 *
BCL2-associated athanogene 3 GN=Bag3	A6H663	S360	1.55	0.022 *
Heat shock protein HSP 90-beta GN=Hsp90ab1	P11499	S255	1.39	0.017 *
Heat shock protein beta-6 GN=Hspb6	Q5EBG6	S16	2.1	0.003 *
Sequestosome-1 GN=Sqstm1	Q64337	S368	1.55	0.043 *

Cysteine and glycine-rich protein 3 GN=Csrp3	P50462	S95	1.61	0.035 *
Metabolism and energy production				
Dihydrolipoyl dehydrogenase, mitochondrial GN=Dld	O08749	S297	1.32	0.044 *
Long-chain-fatty-acid--CoA ligase 1 GN=Acsl1	D3Z041	S230	1.42	0.026 *
Succinyl-CoA ligase [ADP-forming] subunit beta, mitochondrial GN=Sucla2	Q9Z2I9	S176	1.53	0.025 *
Structural				
Reticulon-4 GN=Rtn4	Q99P72	S165	1.59	0.039 *
Dystonin GN=Dst	Q91ZU6	S2148	1.43	0.020 *
Small muscular protein GN=Smpx	Q9DC77	S36	1.54	0.029 *
SRSF protein kinase 3 GN=Srpk3	Q9Z0G2	S49	1.66	0.012 *

One protein relating to ionic transport was downregulated in phosphorylation in the aged heart (Sodium channel protein type 5 subunit alpha) at Ser-460. The remaining phosphorylated proteins were all upregulated in the aged heart and were further categorised into several groups including ionic transport, cardiac signalling and apoptosis, metabolism and energy production, and structural proteins. These proteins are all mentioned in table 3.4 with their phosphorylation site and fold change between the two age groups. The biggest change with ageing is seen in the

phosphorylation of heat shock protein beta-6 at Ser-16, which is doubled in the ageing heart compared to the adult heart.

3.3.4 The Effects of Ageing on Cardiac Histology

3.3.4.1 Changes in Cardiac Structure with Ageing
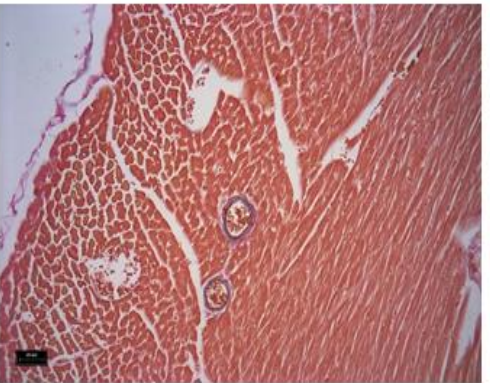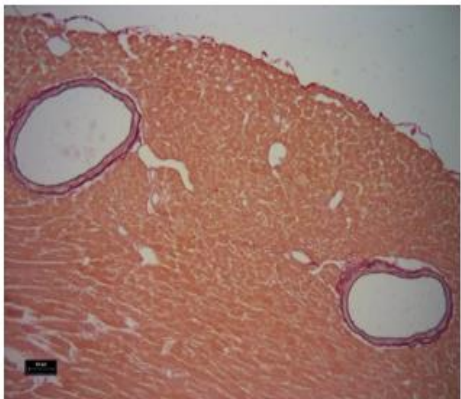
H&E staining is a basic stain used here only to provide a comprehensive picture of the heart sections from both age groups as shown in figure 3.14.

Age Group	Left Ventricle	Longitudinal Section of Cardiomyocytes	Cross-Section of Cardiomyocytes
Adult			
Aged			
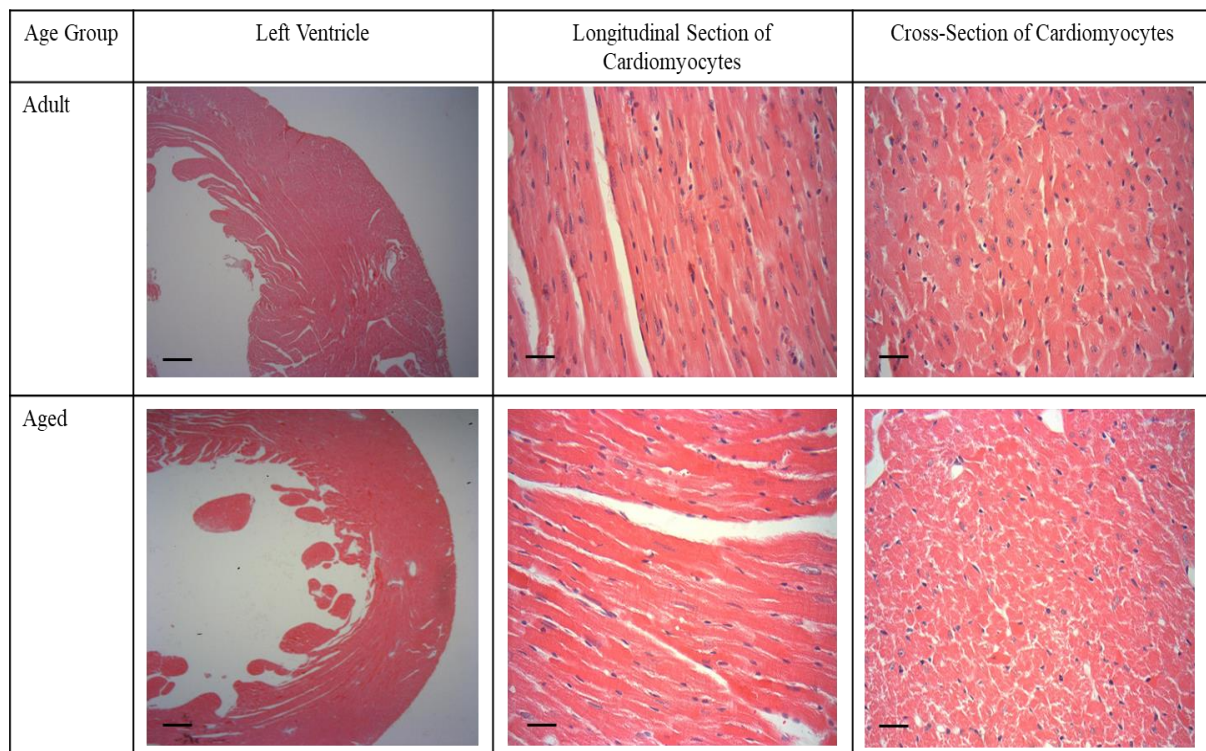
Figure 3.14: Haematoxylin and eosin staining of adult and ageing mice heart sections. Images show the left ventricle (objective lens magnification x4), and longitudinal and cross-sectional cardiomyocytes from the LV (objective lens magnification x40). Dark blue-purple dots in the images represent the nuclei. Scale bar is 20 microns.

3.3.4.2 Changes in Coronary Arteries with Ageing

EVG staining was used to highlight the arteries and show the elastin (stained in black) around them. Figure 3.15 shows representative images of large coronary arteries and some of the smaller arteries in both age groups and how they compare.

Age Group	Larger Arteries	Smaller Arteries
Adult		
Aged		

Figure 3.15: Verhoeff-van Gieson Staining of adult and ageing mice heart sections. Images show different size arteries (objective lens magnification x20). Black colour around the arteries in the images represents elastic fibres. Scale bar is 20 microns.

Using EVG stained sections, measurements of total artery size, artery lumen size, artery wall thickness, and arterial wall/total artery and lumen size ratios were taken. Figures 3.16 and 3.17 show the comparison between the two age groups.
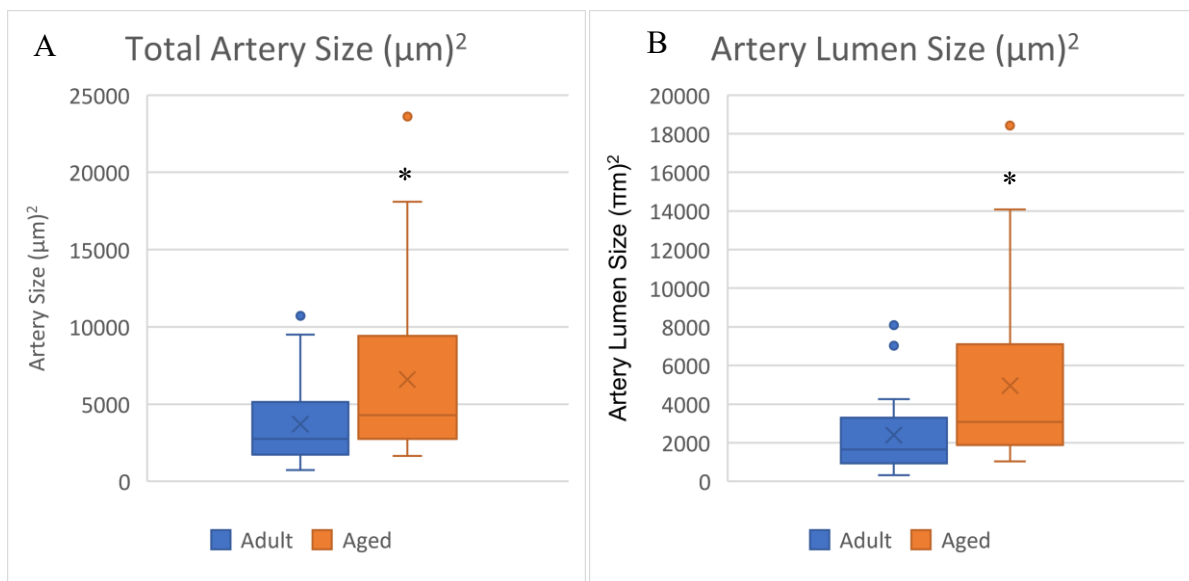
Figure 3.16: A) Total artery size (μm)^2 and B) Artery lumen size (μm)^2 in adult and ageing mice hearts. Data are presented as quartiles showing the minimum value, 25th percentile, 50th percentile, 75th percentile, maximum value, and the outliers. Data were analysed using the unpaired t-test.
* = $P < 0.05$ vs. adult. N= 8 and 5 for adult and ageing hearts, respectively.

Arteries of various sizes in the stained sections have been measured for their total size and lumen size, and quartiles (minimum value, 25th, 50th, 75th, and maximum value) have been calculated (excluding the outlier values). These values for both age group are presented in table 3.5. with ageing there is a significant increase in total artery size ($P = 0.011$) and lumen size ($P = 0.001$) compared to adults.

Quartile values shown in table 3.5 show a trend of increase in the aged group that goes up to 200% in some of the values. Values for total artery size change by 2.3, 1.5, 1.6, 1.9, and 1.7 folds respectively. Values for lumen size change by 3.1, 2.2, 1.9, 2.1, and 2 folds respectively with ageing.

Table 3.5: Quartile values of total artery size and artery lumen size in adult and ageing mice hearts. Values include the minimum value, 25th percentile, 50th percentile, 75th percentile, maximum value, and the outliers. N= 8 and 5 for adult and aged hearts respectively.

Quartiles	Total Artery Size in Adult Hearts $(\mu m)^2$ N = 8	Total Artery Size in Ageing Hearts $(\mu m)^2$ N = 5	Artery Lumen Size in Adult Hearts $(\mu m)^2$ N = 8	Artery Lumen Size in Ageing Hearts $(\mu m)^2$ N = 5
Min Value	734	1650	328	1026
25 Percentile	1807	2772	927	1995
50 Percentile	2713	4214	1550	3026
75 Percentile	4651	8608	3104	6429
Max Value	10717	18096	7025	14074
Outlier	11178	23605	8092 8187	18425

regarding arterial wall, four different sides of the artery wall were measured then averaged to express the wall thickness. These measurements showed no change with ageing. However, when expressing arterial wall area/total artery size, this ratio was significantly reduced in the aged heart ($P < 0.001$) from an average of 0.38 ± 0.02 in adults to an average of 0.28 ± 0.01 in aged hearts. Similarly, arterial wall area/lumen size ratio was also reduced significantly with ageing ($P < 0.001$) from an average of 0.7 ± 0.1 in adult hearts to 0.4 ± 0.03 in aged hearts. (figure 3.17).
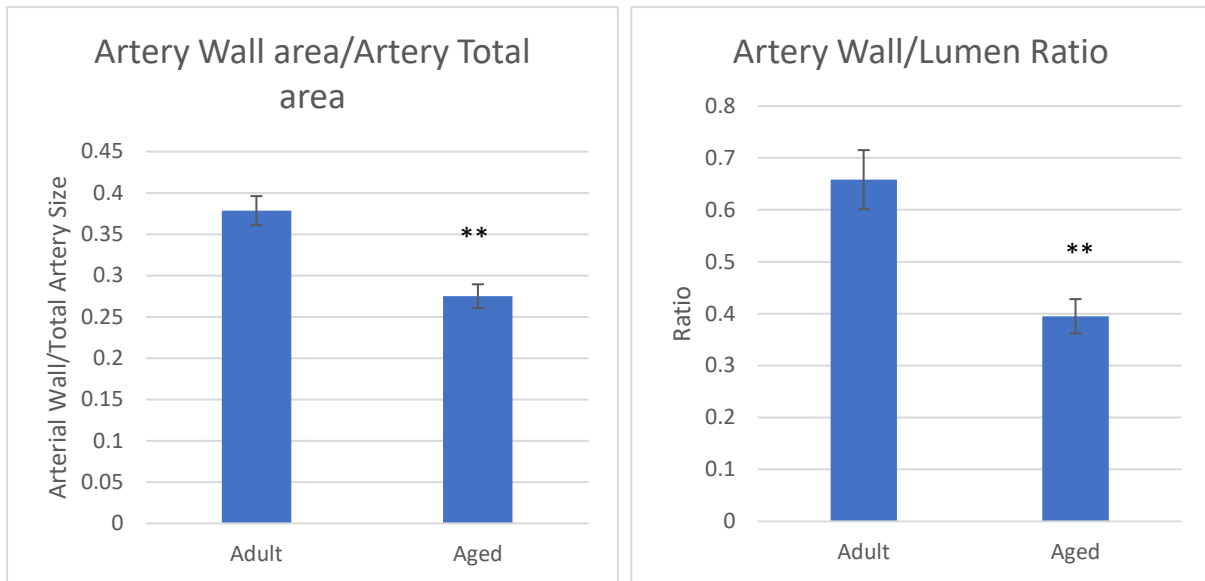
Figure 3.17: Ratios of arterial wall/total artery size and lumen size in adult and ageing mice hearts. Data are presented as mean ± SEM. Data were analysed using the unpaired t-test.
** = $P < 0.001$ vs. adult. N= 8 and 5 for adult and ageing hearts, respectively.

3.3.4.3 Changes in Fibrous Tissue with Ageing

When measuring fibrous tissue using histological sections stained with Masson's Trichrome stain, adult hearts had a low percentage of fibrous tissue in heart sections (1.5 ± 0.3 %), which was slightly increased with ageing (1.8 ± 0.3 %). However, this change was not statistically significant (figure 3.18).
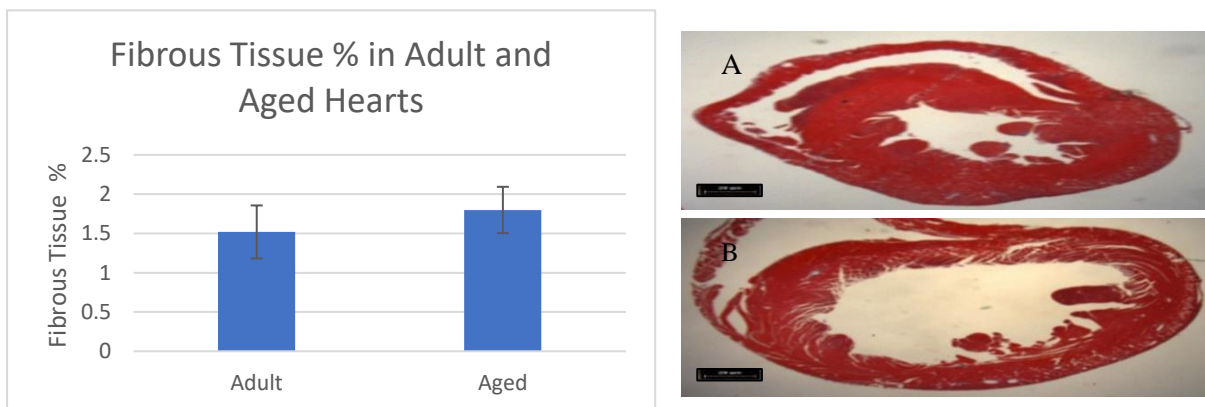
Figure 3.18: Fibrous tissue % in adult and ageing mice hearts. Quantification was done using Masson's Trichrome stained heart sections. Data are presented as mean ± SEM. Data were analysed using the unpaired t-test. N= 6 and 5 for adult and ageing hearts respectively. A) Example of adult heart. B) Example of aged heart. Images taken using objective lens magnification x1.25. Scale bar is 20 microns

3.3.4.4 Changes in Capillary/Myocyte Ratio with Ageing

Immunohisochemistry staining Isolectin biotin 4 (IB4) was used to stain capillaries with a brown colour. Images taken from the left ventricle of the hearts were used to measure capillary/cardiomyocyte ratio, and this ratio was significantly increased ($P < 0.001$) from an average of 1.5 ± 0.06 to 2.3 ± 0.03 in aged hearts (figure 3.19).
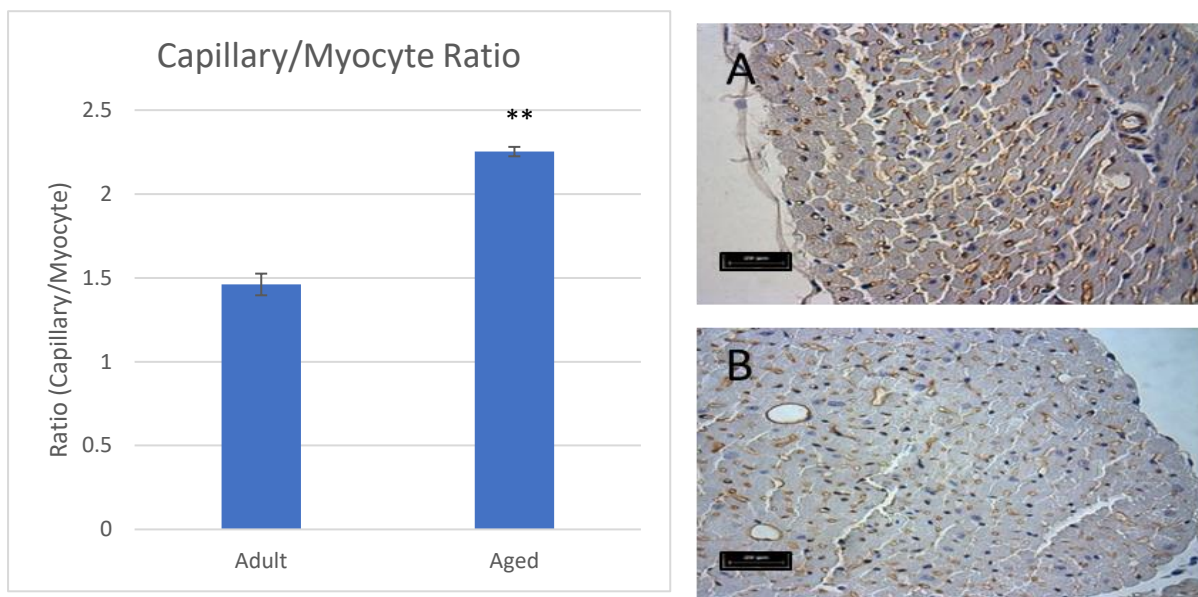
Figure 3.19: Capillary/myocyte ratio in adult and ageing mice hearts. Quantification was done using Isolectin biotin 4 (IB4) stained heart sections. Data are presented as mean ± SEM. Data were analysed using the unpaired t-test.
** = $P < 0.001$ vs. adult. N= 5 and 5 for adult and ageing hearts respectively. 3-4 images from the LV from each heart were used for the analysis.
A) Example of adult heart. B) Example of ageing heart. Images taken using objective lens magnification x40. Scale bar is 20 microns.

3.3.5 Ultra-Structural Changes

3.3.5.1   Changes in Diastolic Sarcomere Length with Ageing

Diastolic sarcomere length increased with ageing from an average of 1.99 ± 0.05 μm in the

adult heart to an average of 2.02 ± 0.1 μm in the aged heart, however this change was not

significant (figure 3.20).
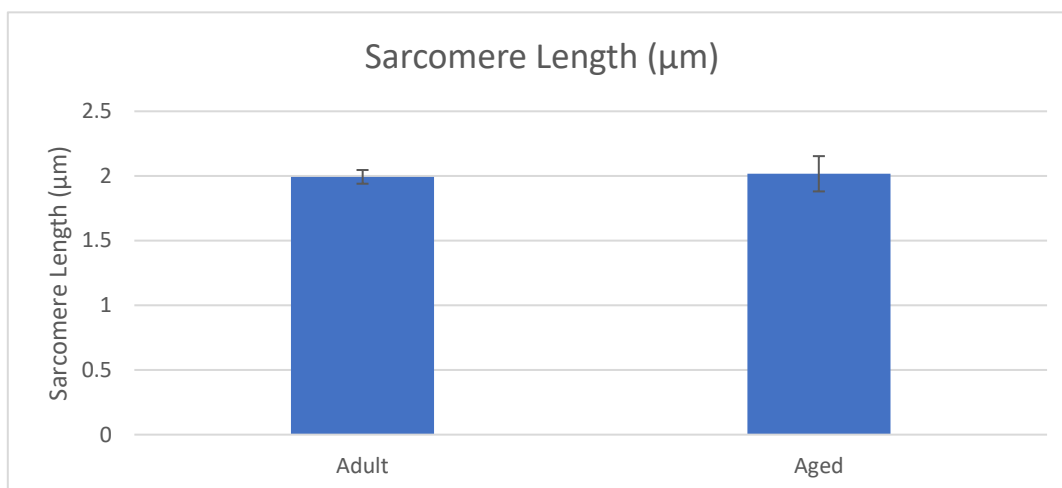
Figure 3.20: Diastolic sarcomere length in adult and ageing mice hearts.
Lengths were measured in electron micrographs using ImageJ. Data are
presented as mean ± SEM. Data were analysed using the unpaired t-test. N= 4
for adult and ageing hearts each, and ≈ 300 sarcomeres from each heart.

3.3.5.2   Changes in Mitochondrial Sub-Population Distribution
with Ageing

The distribution or density of mitochondria and their individual subpopulations was measured

in both age groups. In the adult heart, mitochondria covered 36 % of total myocyte area. The

majority of mitochondrial area comprised of interfibrillar mitochondria (IF) covering 26 %,

followed by subsarcolemmal (SSL) mitochondria (9 %), and finally the perinuclear (PN)

mitochondria covering only 1 % of total myocyte area. With ageing, the total mitochondrial

area was reduced to 32 %, with the IF comprising 25 % of total myocyte area, followed by the

SSL mitochondria comprising 6 % of this area, and finally the PN mitochondria covering only

1 % (figure 3.21).
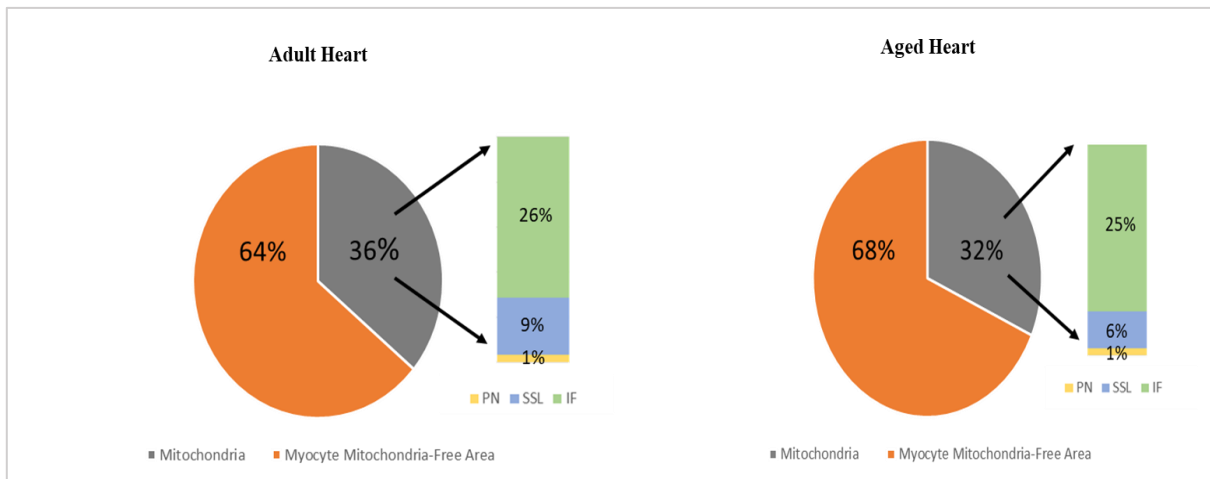
Figure 3.21: Mitochondrial sub-population distribution in adult and ageing mice hearts. Figure shows the percentage of myocyte covered by mitochondria, and the percent of each mitochondrial sub-population in both age groups.
N= 4 for adult and ageing hearts each. 3-4 fields from each heart were analysed.

Comparing these figures to understand the effects of ageing on the mitochondrial density, no significant change was found between the percent of myocyte area covered by total mitochondria nor the distribution of each mitochondrial subpopulation between the two age groups despite the reduction seen with ageing (figure 3.22).
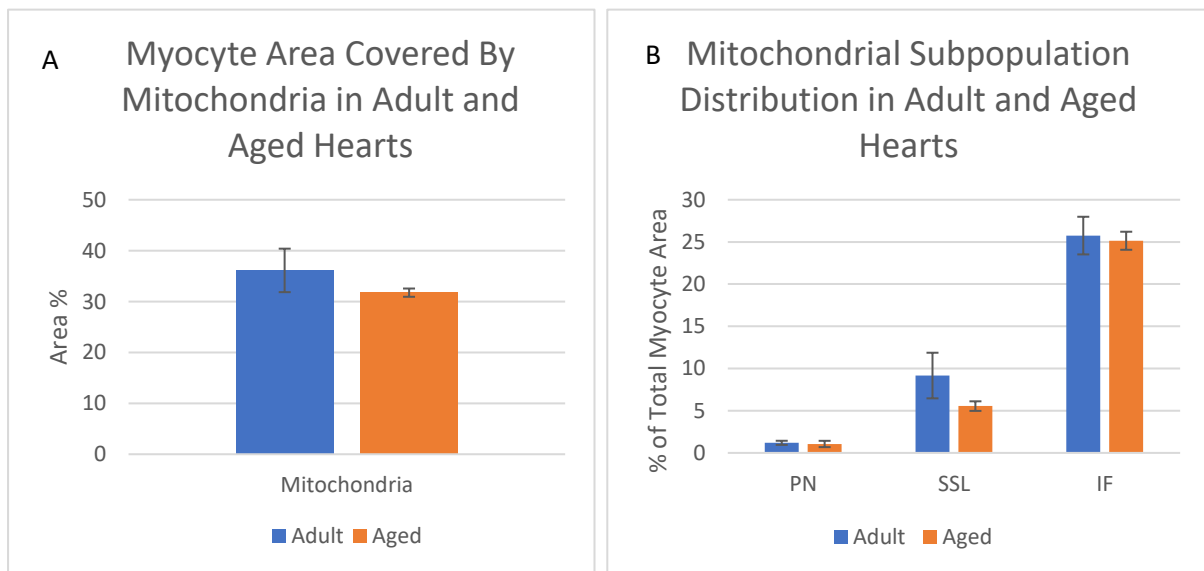
Figure 3.22: Mitochondrial distribution in adult and ageing mice hearts. A) Mitochondrial distribution as a percentage of total myocyte area. B) Mitochondrial distribution by sub-population as percentage of total myocyte area. Data are presented as mean ± SEM. Data were analysed using the unpaired t-test.
N= 4 for adult and ageing hearts each. 3-4 fields from each heart were analysed.

3.3.5.3 Changes in Mitochondrial Sub-Population Morphometry with Ageing

Before comparing the mitochondrial subpopulation morphometry between the two age groups, we compared the different subpopulations with one another within one age group.

3.3.5.3.1 Mitochondrial Sub-Population Morphometry in Adult Hearts

Several mitochondrial measurements were taken including length, width, size of the mitochondria, aspect ratio (length/width) and the roundness. When comparing the three subpopulations of mitochondria in the adult heart, the PN mitochondria appeared to be smaller in size and shorter in length and width, plus they were more rounded in shape compared to the other two subpopulations (figure 3.23). Additionally, SSL mitochondria seemed to be the biggest in size. However, the only significant difference was in the length ($P = 0.028$ vs. IF and $P = 0.42$ vs. SSL). PN mitochondria length averaged 0.82 ± 0.01 μm compared to 0.95 ± 0.03 μm and 0.94 ± 0.03 μm for IF and SSL mitochondria, respectively.
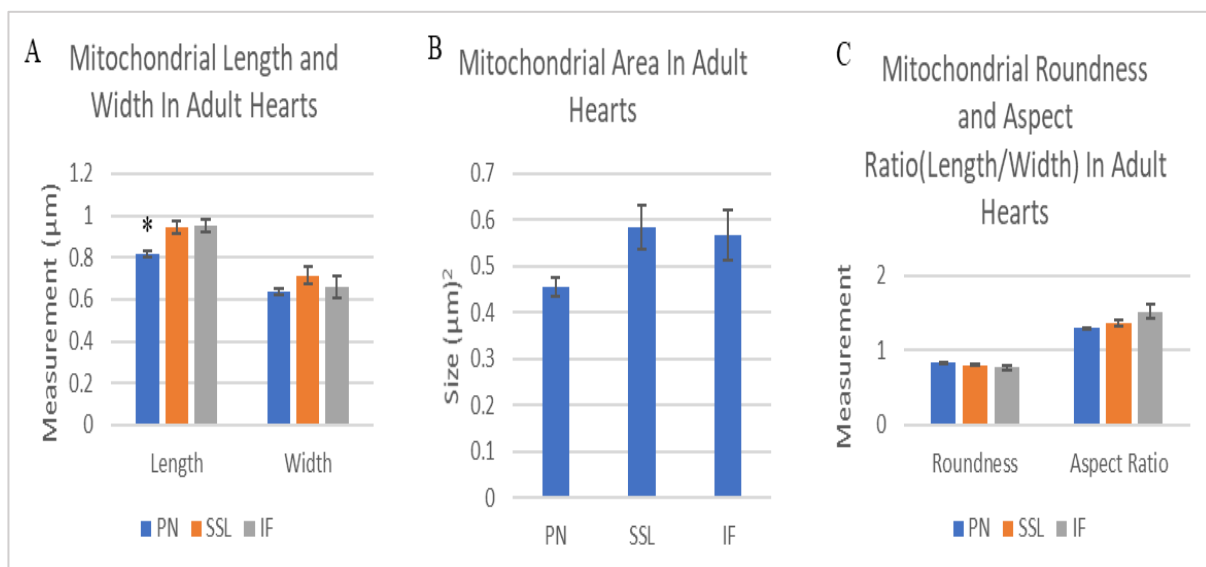
Figure 3.23: Mitochondrial sub-population morphometry in adult hearts. A) Mitochondrial length and width. B) Mitochondrial size. C) Mitochondrial roundness and aspect (L/W) ratio. Data are presented as mean ± SEM. Data were analysed using one-way ANOVA followed by the Bonferroni and Games-Howell post-hoc tests. * = P < 0.05 vs. SSL and IF mitochondria.
N= 4 hearts, and ≈ 300 mitochondria for each subpopulation.

3.3.5.3.2 Mitochondrial Sub-Population Morphometry in Ageing Hearts

In the ageing heart, the IF mitochondria were larger in size compared to the two other subtypes (figure 3.24). IF mitochondria average size was 0.46 ± 0.01 μm^2 compared to 0.25 ± 0.02 and 0.37 ± 0.02 μm^2 for PN and SSL mitochondria, respectively. Also, there was a significant difference in size between the PN and SSL mitochondria ($P = 0.006$).

Additionally, a similar difference was noted in the width of the mitochondria. The PN mitochondria had a width of 0.42 ± 0.01 μm, which was smaller compared to the other two subtypes that averaged 0.51 ± 0.01 μm for SSL and 0.57 ± 0.002 μm for IF mitochondria ($P = 0.002$ vs SSL and $P < 0.001$ vs. IF), and the SSL mitochondria was also shorter in width compared to the IF mitochondria ($P = 0.009$). Finally, PN mitochondria were also shorter in length with an average of 0.67 ± 0.04 μm compared to 0.9 ± 0.02 μm ($P = 0.007$) for IF mitochondria.
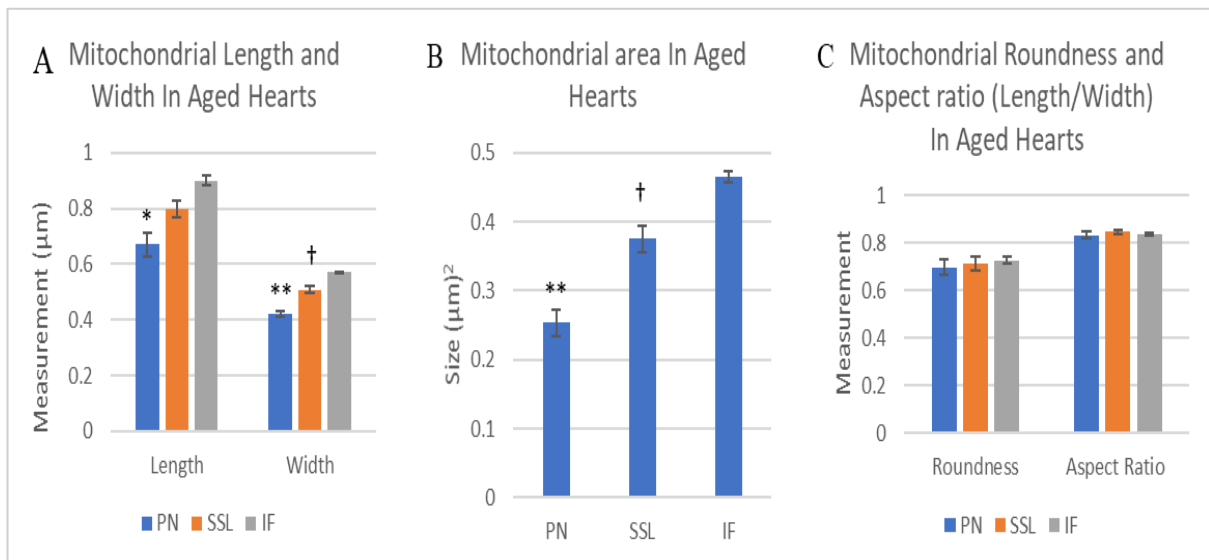
Figure 3.24: Mitochondrial sub-population morphometry in ageing hearts. A) Mitochondrial length and width. B) Mitochondrial size. C) Mitochondrial roundness and aspect (L/W) ratio. Data are presented as mean ± SEM. Data were analysed using one-way ANOVA followed by the Bonferroni and Games-Howell post-hoc tests. * = $P < 0.05$ vs. IF, ** = $P < 0.05$ vs SSL and IF, † = $P < 0.05$ vs IF mitochondria.
N= 4 hearts, and ≈ 300 mitochondria for each subpopulation.

3.3.5.3.3 Differences in Mitochondrial Sub-Population Morphometry Between Adult and Ageing Heart

I. *Perinuclear Mitochondria*

With ageing, PN mitochondria became significantly smaller with a decrease in both length and width and became less rounded in shape (figure 3.25). Length of aged PN mitochondria averaged at 0.67 ± 0.04 μm compared to 0.82 ± 0.01 μm in adult hearts ($P = 0.028$). Width of PN mitochondria decreased from an average of 0.64 ± 0.01 μm in adult hearts to 0.42 ± 0.01 μm in ageing hearts ($P < 0.001$). PN mitochondrial size also decreased from 0.46 ± 0.02 μm^2 to 0.25 ± 0.02 μm^2 in adult and ageing hearts respectively ($P = 0.002$). Finally, the aspect ratio of the PN mitochondria was increased from 1.3 ± 0.01 in adult hearts to 1.7 ± 0.1 in ageing hearts ($P = 0.019$), indicating less roundness in ageing mitochondria (the closer the aspect ratio to 1 the more rounded the mitochondria are), and this was also confirmed by the roundness measurement which decreased in the ageing group from 0.83 ± 0.01 in adults to 0.7 ± 0.03 ($P = 0.023$).
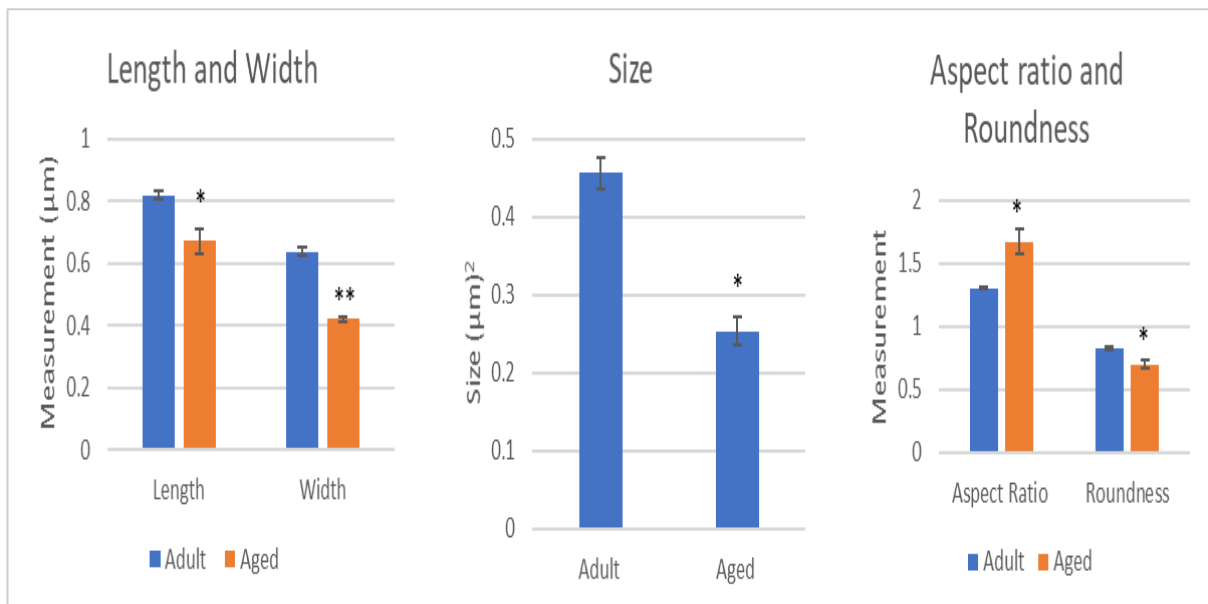
Figure 3.25: PN mitochondria morphometry in adult and ageing hearts. A) Mitochondrial length and width. B) Mitochondrial size. C) Mitochondrial roundness and aspect (L/W) ratio. Data are presented as mean ± SEM. Data were analysed using unpaired t-test.
* = $P < 0.05$ vs. adult, ** = $P < 0.001$ vs adult. N= 4 for adult and aged hearts each, and ≈ 300 mitochondria for each age group.

II. *Subsarcolemmal Mitochondria*

Similar to PN mitochondria, SSL mitochondria also became significantly smaller with a decrease in both length and width and became less rounded in shape with ageing (figure 3.26). Length of ageing SSL mitochondria averaged at 0.8 ± 0.03 µm compared to 0.94 ± 0.03 µm in adult hearts ($P = 0.03$). Width of SSL mitochondria decreased from an average of 0.72 ± 0.04 µm in adult hearts to 0.51 ± 0.01 µm in ageing hearts ($P = 0.009$). SSL mitochondrial size also decreased from 0.59 ± 0.05 µm^2 to 0.37 ± 0.02 µm^2 in adult and ageing hearts respectively ($P = 0.015$). Finally, the aspect ratio of the SSL mitochondria was increased from 1.4 ± 0.04 in adult hearts to 1.6 ± 0.5 in ageing hearts ($P = 0.015$), indicating less roundness in ageing mitochondria (the closer the aspect ratio to 1 the more rounded the mitochondria are), and this was also confirmed by the roundness measurement which decreased in the ageing group from 0.8 ± 0.01 in adults to 0.7 ± 0.02 ($P = 0.044$).
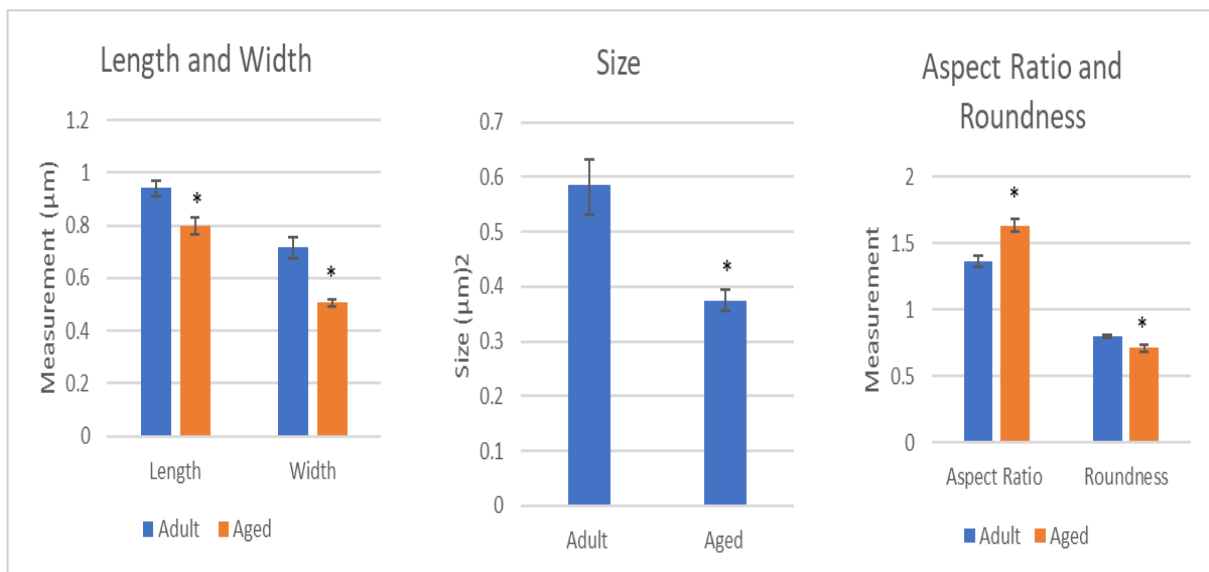
Figure 3.26: SSL mitochondria morphometry in adult and ageing hearts. A) Mitochondrial length and width. B) Mitochondrial size. C) Mitochondrial roundness and aspect (L/W) ratio. Data are presented as mean ± SEM. Data were analysed using unpaired t-test.
* = $P < 0.05$ vs. adult. N= 4 for adult and aged hearts each, and ≈ 300 mitochondria for each age group.

III. *Interfibrillar mitochondria*

IF mitochondria morphometry also showed a similar pattern to that observed in the two previous subpopulations, where in ageing hearts the mitochondria became smaller with a decrease in both length and width and became less rounded in shape (figure 3.27). However, none of the differences in measurements between the two age groups were statistically significant in this type of mitochondria.
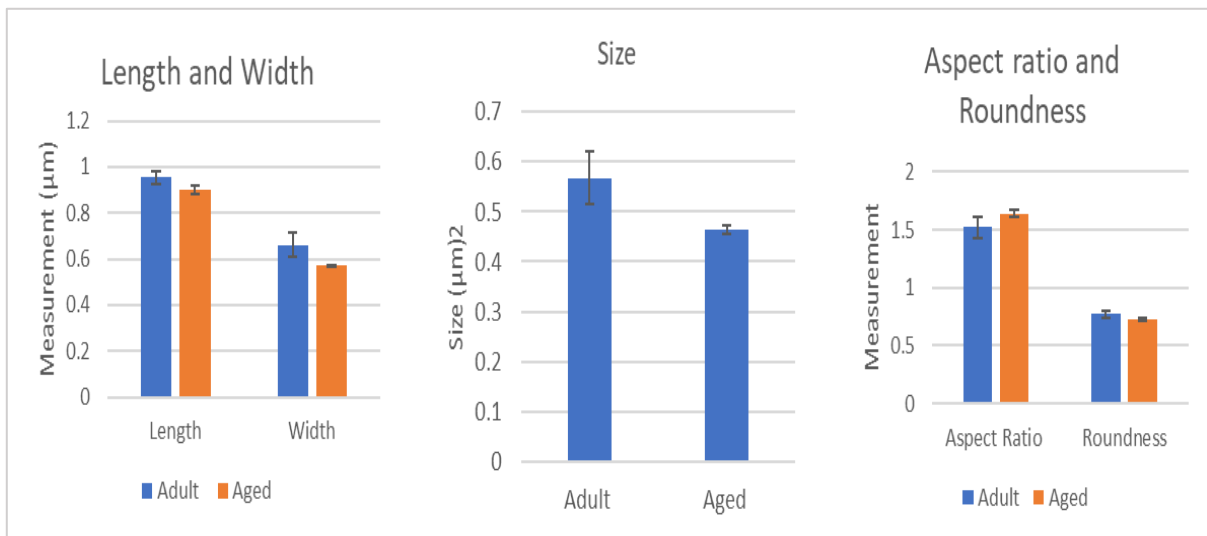
Figure 3.27: IF mitochondria morphometry in adult and ageing hearts. A) Mitochondrial length and width. B) Mitochondrial size. C) Mitochondrial roundness and aspect (L/W) ratio. Data are presented as mean ± SEM. Data were analysed using unpaired t-test.
N= 4 for adult and ageing hearts each, and ≈ 300 mitochondria for each age group.

3.3.5.4 Mitochondrial Fission and Fusion Proteins

Generally, mitochondria in the ageing heart appeared to become less rounded (more elongated), and this goes accordingly with the significant increase in mitochondrial fusion proteins Opa1 and Mfn2 in ageing hearts compared to adults (figure 3.28). Fission proteins Mff and Fis1 were also increased in the ageing heart but not significantly.
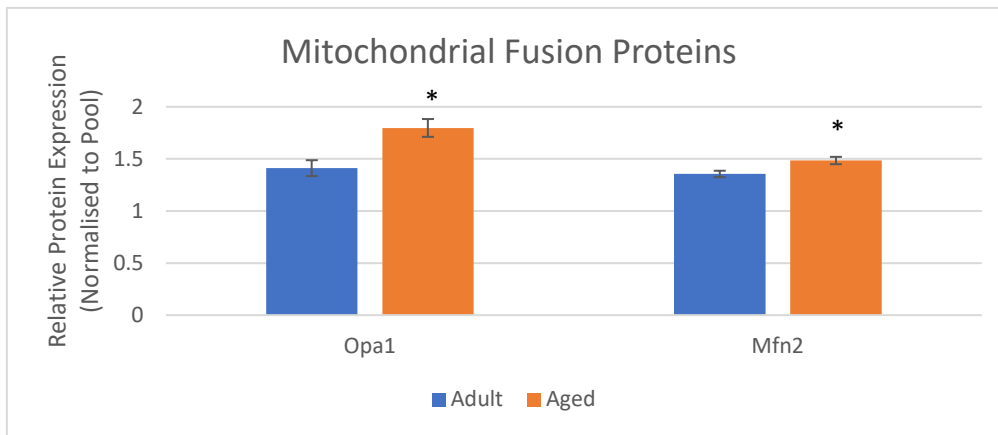
Figure 3.28: Significant mitochondrial fusion proteins in adult and ageing mice hearts. Data are expressed as mean ± SEM (of the relative protein expression normalised to a pool sample). Data were analysed using the unpaired t-test. All proteins selected fall within a FD < 0.8 and > 1.3.
* = $P < 0.05$. n = 4 and 5 for adult and ageing hearts, respectively. Opa1 (Dynamin-type G domain-containing protein), Mfn2 (Mitofusin-2).

3.3.5.5 Changes in Lipid Content (Lipid Droplet Count) with Ageing

Lipid content (droplet count) accumulation in the myocyte was determined by the number of lipid droplets/μm^2. With ageing, there was a significant increase in lipid droplets from an average of 0.01 ± 0.005 in adult hearts to 0.05 ± 0.01 in aged hearts ($P = 0.002$) (figure 3.29).
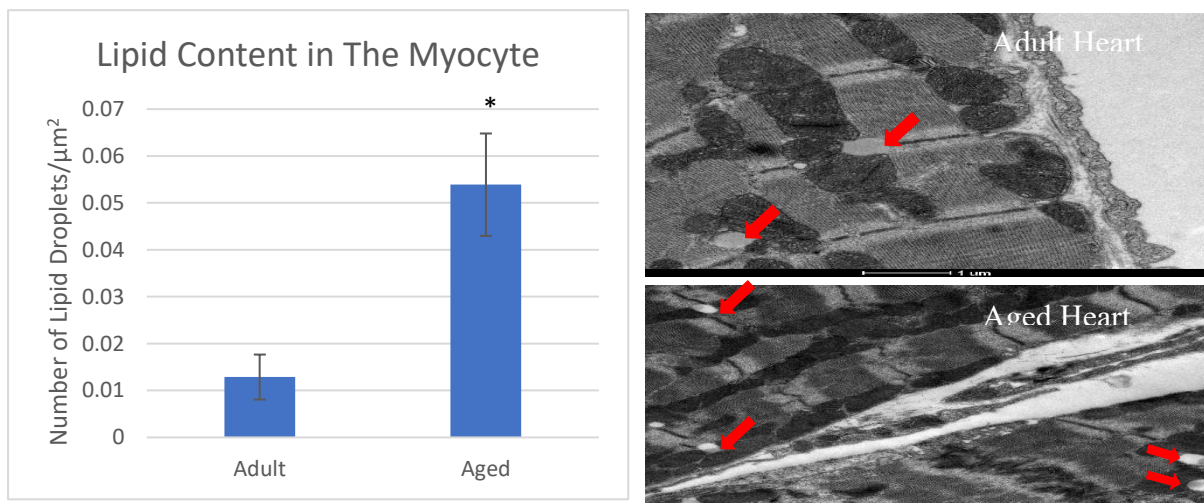
Figure 3.29: Lipid content (lipid droplet count) in adult and ageing hearts. Data are presented as mean ± SEM. Data were analysed using unpaired t-test.
* = $P < 0.05$ vs. adult. N= 4 for adult and ageing hearts each. 3-4 fields from each heart were analysed. Image shows electron micrographs of examples of lipid droplets (red arrows) in adult (top) and ageing hearts (bottom).

3.4 Discussion

3.4.1 Key Findings

A significant increase in body weight, epidydimal fat pads, and cardiac hypertrophy were seen with aging. There was also an increase in lipid deposits in the heart and an increase in capillary/myocyte ratio. There was an increase in total size and lumen size of coronary arteries, with decreased artery wall/total artery size and lumen size ratios. There were also changes in mitochondrial morphometry (mitochondria became smaller in size and more elongated) but not mitochondrial distribution.

Ageing was associated with changes in cardiac energy metabolites and a decrease in total protein amino acids pool as well as taurine. Most of the cardiac protein groups were upregulated during aging. These include mitochondrial proteins, ionic channel proteins, antioxidant enzymes, apoptosis-related proteins, structural (collagen) proteins, and proteins involved in lipid and carbohydrate metabolism. Phospho-proteins were also mainly upregulated with ageing. Ageing was associated with decreased plasma glucose levels. Ageing was not associated with a change in cardiac fibrosis or cardiomyocyte sarcomere length.

3.4.2 Ageing was Associated with Increase in Body Weight, Epidydimal Fat Pads, and Cardiac Hypertrophy

The first finding in this work is that mice had a significant increase in body weight (38% increase) with ageing, with a 213% increase in epidydimal fat pads compared to adult mice. This increase in total body weight in aged mice indicates obesity compared to their adult counterparts, but not within their age group as this is normal weight gain in C57BL/6 mice (figure 3.30).
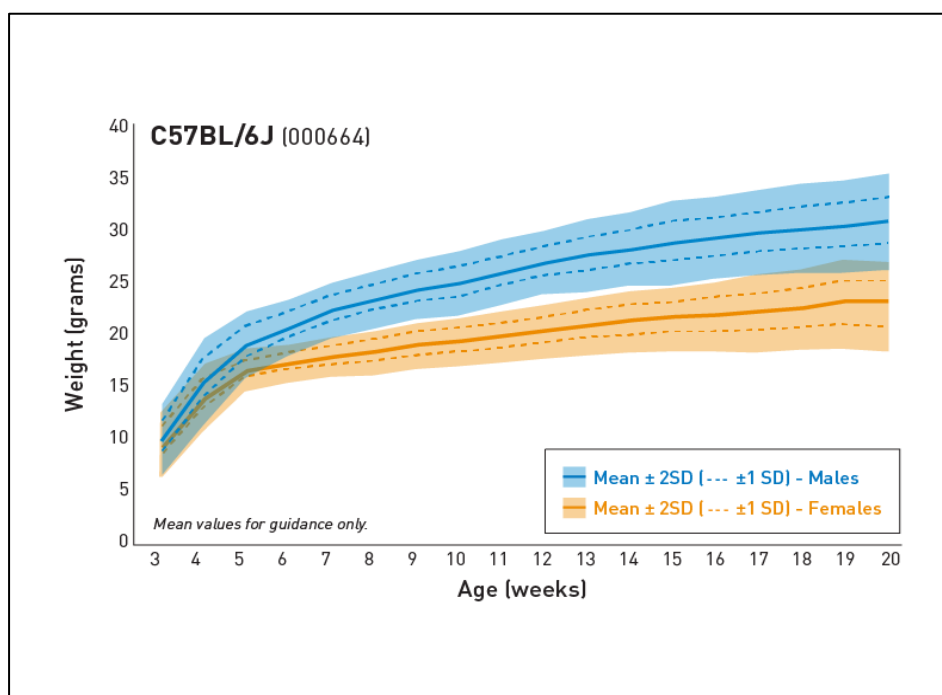
Figure 3.30: Body weight information for C57BL/6J mice. (https://www.jax.org/jax-mice-and-services/strain-data-sheet-pages/body-weight-chart-000664).

This change in body weight with ageing in C57BL/6 mice was also reported in a study by Lessard-Beaudoin et al. 2015, who showed that body weight in C57BL/6 mice increases until the age of 12 months (48 weeks) and then it plateaus [255]. Similarly, studies on different mice strains and different species also reported body weight changes with ageing [256-260]. The increase in fat pads observed in our work has also been reported by others with ageing, where they showed that body fat percentage in C57BL/6 mice remains constant until 6 months of age

and then increases between 6-12 months [259]. The reasons for total body weight and fat percentage increase with ageing are the various physiological changes that accompany ageing such as decreased metabolic rate, decreased activity level, loss of muscle mass, changes in adipose function and hormone secretion [261, 262]. Even though caloric intake was not measured in these two age groups so there is no way of knowing if the aged mice consumed more calories that contributed to their significant weight gain, however, Lipman and Grinker, 1996 reported that caloric intake was not the sole variable controlling weight gain when looking at weight changes in middle-aged female C57BL/6J mice [263].

Another finding in this work is the significant increase in heart weight in ageing mice compared to their adult controls. This is consistent with what others reported as heart weights of C57BL/6 mice increase until plateauing between 23-28 months of age [255]. This increase in heart weight is most likely due to the hypertrophy of the heart as with ageing several structural changes occur in the heart such as increase in cardiomyocyte size and increase in fibrosis. And even though the fibrosis was not present in these ageing hearts as seen from the results, cardiomyocytes did appear larger in size in the histological examination compared to the adult hearts.

3.4.3 Ageing was Associated with Decreased Plasma Glucose Levels

Ageing mice in our study had significantly lower plasma glucose levels compared to adult mice. This is consistent with what Leiter et al. 1988 reported when comparing adult (4-5 months) with aged (21-25 months) C57BL/6J male mice. The decrease in plasma glucose happened due to the increase in pancreatic β-cells size (with no fibrosis) accompanied with increased insulin secretion which resulted in increasing glucose uptake from the blood as well as improvement in glucose clearance when administered orally or interperitoneally, as authors in the study explained [264]. Gregg et al. 2016, also reported enhanced insulin secretion with ageing in mice which helps preserve glucose tolerance [265].

3.4.4 Ageing was Associated with Changes in Cardiac Energy Metabolites

Ageing hearts had significantly higher levels of GMP and inosine, and significantly lower levels of hypoxanthine and guanosine phosphorylation ratios.

A possible explanation for the increase in inosine levels and decrease in hypoxanthine levels is that both of these metabolites are purine by-products of ATP catabolism (figure 3.31 shows the metabolic pathway of ATP) [14].
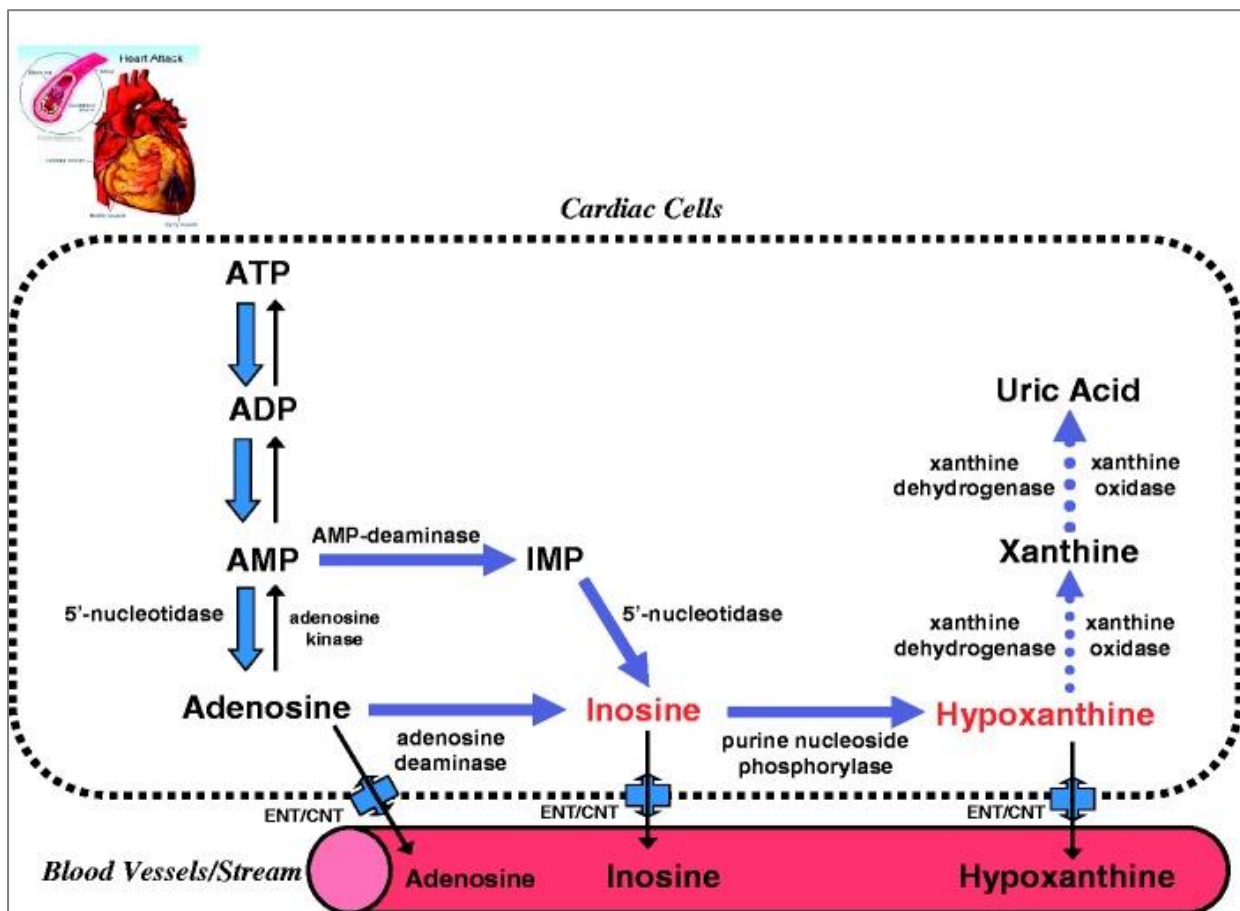
Figure 3.31: Cardiac ATP catabolic pathways during ischaemia. Abbreviations: ATP: adenosine triphosphate; ADP: adenosine diphosphate; AMP: adenosine monophosphate; IMP: inosine monophosphate; ENT: equilibrative nucleoside transporters; CNT: concentrative nucleoside transporters. [14].

Because hypoxanthine serves as a reserve for salvaging purine levels in high-energy demand tissues such as the heart and provides a reserve for about 95% of the body's recycled nucleotides; it is possible that its low levels in the ageing hearts is caused by its incorporation

into making ATP [266-268]. The fact that inosine levels are higher in the ageing heart could indicate an impairment or lower ability of the ageing heart to produce ATP, which was lower but not significantly compared to the adult heart. Additionally, decreased phosphorylation potential seen in our ageing hearts is another sign of this impairment in energy production associated with ageing [269].

3.4.5 Ageing was Associated with Decreased Total Amino Acid Pool and Taurine

Total amino acid pool in the heart decreased with ageing, with a decrease in taurine, arginine, asparagine, histidine, serine, threonine, and alanine.

Concentrations of AAs in cardiac tissue have been shown to change with various diseases and insults, however there are no studies that looked at the change in AAs concentrations with ageing in the heart [270]. The importance of this relates to the changes in cardiac metabolites or ionic state that occur during I/R, so investigating the metabolic state of the heart and how that changes with ageing would aid in explaining any changes in the hearts tolerance to I/R. The relationship between amino acids and CVD has become a topic of interest in recent years, with contradictory reports on their role in preventing or contributing to heart disease [271].

A decrease in AA pool in the ageing heart could indicate an increase in the hearts vulnerability as AAs have been used to assess metabolic status of the myocytes [272]. Additionally, they play an important role in the heart as they modulate metabolic enzymes; specially for glucose metabolism, improve the oxidative state by acting as precursors for some anti-oxidants, regulate gene expression and hormonal activity in the cells, and more importantly; serve as a primary source of fuel for energy production in conditions of energy starvation and metabolic remodelling such as ischaemia and heart failure [273]. Furthermore, taurine (which is decreased in the ageing heart) is the main osmolyte in the heart and has many important functions in the cardiomyocytes. It is essential for normal contractile function via the

modulation of Ca^{2+} transporters, as well as an osmoregulator in some species as it controls Na^+ movement [270]. In addition, taurine is implicated in the regulation of oxidative stress, modulation of kinases and phosphatases, and stabilisation of membranes through interacting with phospholipids [274].

Even though a number of the AAs associated with increased risk of CVD were found to be lower in ageing hearts in our work, reports on their association to CVD are contradictory. For example, glutamate, tyrosine, glutamine, and methionine (mainly through its metabolite homocysteine) were all reported to be associated with higher risk of heart disease [275-278]. These studies show that the contribution of these AAs to CVD is through mechanism involved in plaque formation, impairment of antioxidant activity, lipid peroxidation, and formation of macrophage foam cells. However, a study in postmenopausal women reported the opposite of this, where after adjustment for traditional CHD risk factors; glutamine was associated with decreased risk of CHD while glutamate levels were still a risk factor for CHD [279]. Also, other AAs have been found to have a protective role against CVD such as glycine and arginine [280]. Both of these AAs were involved in decreasing homocysteine levels and improving endothelial function [280]. A contradictory study associated arginine levels with atherosclerotic plaques [281]. So, we cannot conclude whether this decrease in AA pool in the ageing heart is protective or renders it more vulnerable to insults.

3.4.6 Proteins in the Ageing Heart were Mainly Upregulated

Ageing hearts showed a change in proteome profile compared to adult hearts, with 1678 proteins changing significantly. The majority of the proteins were upregulated with ageing, while only 6 % were downregulated. Not many studies have looked at the change in proteome profile with ageing. In aged female rats, cardiac mitochondrial proteomic analysis revealed a change in 67 proteins mainly related to cellular metabolism and energy production, oxidative stress, cell death, and muscle contraction [282]. in this study, ageing was associated with

decreased expression of mitochondrial ATP production, and increased expression of heat shock proteins as well as the antioxidant superoxide dismutase [282]. Changes in proteomics were also studied in humans and revealed a change of 217 plasma proteins with ageing [283]. Altered proteins were mainly involved in blood coagulation, chemokine and inflammatory pathways, axon guidance, peptidase activity, and apoptosis. Another study of the ageing heart proteome profile in A.BY/SnJ mice showed a significant change in lipid metabolism and fatty acid transport. Lipid metabolism and transport were higher in ageing, and ATP synthase was decreased [284]. Mitochondrial function and metabolism proteins are some of the main proteins altered with ageing, and can be preserved by inhibiting the mTOR signalling pathway [285].

3.4.6.1 Mitochondrial Proteins were Mainly Upregulated with Ageing

With ageing, there was an upregulation in mitochondrial proteins with the exception of a few that were downregulated. Proteins were involved in lipid metabolism, AA metabolism, energy production, and mitochondrial transport. Keeping in mind that the changes we have shown do not reflect protein activity but rather its expression in cardiac tissue, so an upregulation in expression in mitochondrial proteins could indicate a compensation mechanism for the decrease in mitochondrial efficiency in the aged heart compared to the adult heart.

A change in cardiac mitochondrial proteins with ageing has been reported in other studies. One study in aged mice (23-25 months of age) revealed a change in 24 mitochondrial proteins [147]. some of the proteins were upregulated such as energy production proteins, ketone body metabolism, and ETC proteins, while others were downregulated with ageing such as stress resistance proteins. Another study in aged female rats (24 months of age) found 35 mitochondrial proteins that changed with ageing, mainly involved in energy production [282]. There was a downregulation in ETC complex proteins and the antioxidant catalase. Upregulated proteins included cell stress resistance and cell death proteins. Additionally, a

study in aged mice (24 months of age) found that the majority of mitochondrial proteins are downregulated with ageing and only a few are upregulated [286]. Other studies on mitochondrial proteomics report contradicting findings, but that could be due to the variations in methods used, species, and genders [287-289].

3.4.6.2 Ionic Transport Related Proteins were Upregulated with Ageing

Eight ionic channel-related proteins were upregulated with ageing. Three sodium channel proteins were upregulated including the sodium channel subunit beta-2 which is important for regulating the activity and function of sodium ion channels. The sodium channel subunit beta-4 which modulates and regulates the activity and activation of certain sodium alpha channels. The electrogenic sodium bicarbonate cotransporter NBCe1 variant D which regulates intracellular pH by regulating the influx/efflux of bicarbonate ions across the cell membrane. Additionally, two potassium channel proteins were upregulated, the inward rectifier potassium channel 13 which allows potassium to enter the cell depending on the extracellular potassium concentration, and the voltage-gated potassium channel Kv1.7 which regulates voltage-dependant potassium permeability into the cells. Also, the chloride channel protein was upregulated in the ageing heart. This protein mediates the exchange of chloride ions for protons. And finally, the sodium/calcium exchanger 1 which regulates intracellular calcium by exchanging calcium ions for sodium ions across the cell membrane, and the ryanodine receptor 2 which mediates the release of calcium from the SR into the cytosol of the cell. These two calcium regulating proteins could be upregulated in the ageing heart as a compensation for the dysregulation and delays in calcium release and clearance from the cell that occur with ageing during EC coupling.

With ageing, the known changes reported in ion channel proteins include voltage-Ca2+-activated K+ channels in coronary smooth muscle, which decreased with ageing [290].

Additionally, long-lasting L-type Ca^{2+} voltage dependent channels and high-conductance BKCa channels, which also decreased with ageing [291]. Sodium channel subunit beta-2 has been increased in expression in dilated cardiomyopathy in humans, however, this increase was seen in gene expression and not in protein level [292].

None of the ion channel proteins that changed in this work with ageing were indicated in any age-related diseases [293].

3.4.6.3   Antioxidant Enzymes were Upregulated with Ageing

Antioxidant enzymes were upregulated in the ageing heart. As mentioned in the introduction (page 38), ageing is associated with increased oxidative stress. It has been shown that changes in antioxidants and oxidative level in ageing is tissue-specific [294]. Some studies report a decrease in antioxidant enzyme expression and/or activity with ageing, contributing to the age-related decline and dysfunction [295, 296]. Other studies report no change in antioxidants with ageing [297, 298]. On the other hand, some studies report an upregulation in antioxidant levels and activity with ageing. A study of oxidative stress and antioxidant levels in aged rats revealed an increase in both ROS and antioxidant enzymes (SOD and catalase) in kidneys, with no change in markers of damage or dysfunction [299]. This was also seen in the soleus muscle of aged rats where expression and activity of antioxidants (SOD, catalase, and glutathione peroxidase) were all upregulated [300]. Similarly, increased expression of antioxidants was also reported in aged rat hearts in response to an increase in ROS production by the mitochondria [165]. The increased expression in our work does not reflect activity of these enzymes but could indicate a protective mechanism associated with the increased ROS production known to be associated with ageing.

3.4.6.4   Apoptosis-Related Proteins were Upregulated with Ageing

In the ageing heart, the expression of three apoptotic proteins increased, two were pro-apoptotic and one was anti-apoptotic. PRKC apoptosis WT1 regulator protein is a pro-apoptotic protein

inducing apoptosis in cancer cells. Mitochondrial diablo homolog promotes apoptosis by activation of caspases and inhibition of the inhibitor of apoptosis protein (IAP). BCL2-associated athanogene 3 is an anti-apoptotic protein that acts as co-chaperone to HSP70 and HSC70.

Several studies have investigated apoptosis with ageing in various tissues and different species[301-309]. These studies have looked at several apoptosis related proteins including the expression of anti-apoptotic protein BCL-2, pro-apoptotic proteins Bax, cleaved caspase-3, caspase-9, and Bak, and results showed contradictory findings with ageing.

A possible explanation for the increase in pro-apoptotic proteins in the ageing hearts is the increase apoptosis in old age as mentioned earlier. The increased anti-apoptotic protein BCL2-associated athanogene 3 can be a compensatory mechanism to the increase in pro-apoptotic proteins.

3.4.6.5 Structural (Collagen) Proteins were Upregulated with Ageing

Collagen proteins were mainly upregulated in the ageing heart in this work. In the literature, collagen expression and synthesis in normal disease-free ageing has been shown to either decrease or remain unchanged in the heart in rats and sheep, especially collagen 1 and 3 [310-312]. The fibrosis seen in ageing was suggested to be attributed to post-synthetic or degradative processes [313]. Additionally, another study in rats reported that collagen synthesis was decreased by 10 folds in aged hearts [314]. Also, collagen 1 expression was reduced in middle aged and senescent mice hearts, but remained unchanged in old mice hearts compared to the young controls [315]. In this study, there was no difference in collagen expression between the young and old mice (same age as the mice used in our work). However, the young mice used in the study mentioned were older (6-9 months) than adult mice used in our work (2 months), which could explain the difference reported in the change of collagen expression.

Even though elevated levels of collagen expression have been reported in animals and humans when cardiovascular disease was present [316, 317], this does not mean that the elevation in collagen expression with ageing in our work reflects disease or vulnerability of the ageing heart, especially due to the fact that there was no significant change or increase in fibrosis as seen in the histological examination of cardiac sections.

3.4.6.6 Lipid and Carbohydrate Metabolism Proteins were upregulated with Ageing

Lipid and carbohydrate metabolism proteins were upregulated in the ageing heart in our work. Regarding the upregulation of carbohydrate enzymes, as mentioned earlier in the introduction (cardiac metabolism in ageing, page 42), there is a shift from FA utilisation to glucose utilisation in the aged heart. Glucose utilisation is enhanced as seen by the increased content of GLUT-4 (the glucose transporter) [318, 319]. Additionally, energy production from glycolysis was reported to be enhanced with ageing, and PFK activity (which determines glycolysis activity) is not affected by ageing [320]. In human hearts, the utilisation of glucose as a source of energy for the heart did not increase, but when comparing it as a percentage of total energy metabolite it was increased as FA utilisation decreases [321]. So, the increase in carbohydrate metabolism enzymes could be justified.

Regarding FA metabolism, cardiac FA oxidation is known to decrease with ageing, evident by the increased serum concentration of NEFA (non-esterified fatty acids), decreased CPT-1 activity (rate limiting enzyme for LCFA uptake), and decreased mitochondria oxidative phosphorylation [322]. The increase we see in our results in the expression of FA metabolism enzymes (which does not reflect their activity) could be a compensatory mechanism of the cells for the decrease in the utilisation of FAs.

3.4.7 Phospho-Proteins were Mainly Upregulated with Ageing

Most of the phosphorylated proteins that changed in the ageing heart compared to the adult heart were upregulated. These proteins were categorised into several groups including ionic

transport-related proteins, cardiac signalling and apoptosis, metabolism and energy production, and structural proteins. Many of the proteins detected have no or little information available in the literature on their phosphorylation sites. Ionic transport-related proteins included sodium-calcium exchanger, which is a protein responsible for regulating cytoplasmic calcium levels as it mediates the exchange of calcium and sodium ions across cell membrane [323]. Another calcium regulator is the histidine rich calcium-binding protein which is important for cardiac function and contraction [324]. Apoptotic proteins included pro-apoptotic protein Bcl-2-like protein 13, and anti-apoptotic protein BCL2-associated athanogene 3, which were both upregulated in phosphorylation at S387 and S360 consecutively. Additionally, cysteine and glycine-rich protein 3, which is a regulator of myogenesis and is involved in cardiac stress signalling, is phosphorylated by PKC/PRKCA (protein kinase C and its subunit alpha) [325]. Metabolism proteins included long-chain-fatty-acid--CoA ligase 1, which is involved in fatty acid metabolism, and succinyl-CoA ligase [ADP-forming] subunit beta, mitochondrial, which is involved in the TCA cycle and energy production. Both proteins were upregulated in phosphorylation in S230 and S176 consecutively in the ageing heart. Structural proteins included Reticulon-4 (involved in the formation and stabilisation of ER) and Dystonin (which integrates intermediate filaments with actin and microtubule cytoskeleton networks) [326]. Both proteins' phosphorylation was also upregulated in the ageing heart at S165 and S2148 consecutively.

Additional proteins that were upregulated in phosphorylation with ageing included heat shock protein HSP 90-beta and heat shock protein beta-6. Heat shock protein HSP 90-beta is a chaperone protein which is required for the function and regulation of other proteins [327]. Its phosphorylation at S255 (which is upregulated in the ageing heart) inhibits its interaction with AHR (aryl hydrocarbon; a client of HSP90 that promotes carcinogenesis) [328]. Also, heat shock protein beta-6 is a chaperone protein that is involved in regulating muscle function and

cardiac contractility [329]. Its over-expression may indicate cardioprotection from apoptosis [330]. Phosphorylation at S16 by PKA activates the protein, and this effect is increased in the ageing heart.

Finally, sodium channel protein type 5 subunit alpha was downregulated in phosphorylation at S460 in the ageing heart. This protein is involved in mediating the passage of sodium ions across the cell membrane and thus the action potential and is regulated by intracellular calcium levels [331]. No data are available in the literature on the phosphorylation of this protein at S460.

3.4.8 Ageing was Associated with Increased Size of Coronary Arteries and Their Lumen, and Decreased Artery Wall/Total Artery and Lumen Size Ratios

Ageing mice in this study had significantly larger arteries (total artery size and lumen size), and a lower artery wall/total artery and lumen size ratios, indicating a decrease in arterial wall thickness.

Generally, ageing is associated with increased artery wall thickness, specifically in the middle intima media layer. Most studies have been done on the carotid artery, but other central and peripheral arteries were investigated as well [332-336]. A possible reason for not observing this in the ageing mice in this study is that they are not considered aged (senescent).

With ageing, there is also an increase in the size of arteries, specifically the lumen [336]. Even though this increase in size was suggested to happen because of plaque formation, lumen size increased with ageing in the absence of plaque formation [337]. This increase in size was suggested to be an expansion in the artery due to loss of elastic fibres with ageing, and an adaptation to the stiffening of the vessels [338, 339].

3.4.9 Ageing was not Associated with a Change in Cardiac Fibrosis

Ageing mice in this study did not exhibit any difference in fibrous tissue percentage in the heart compared to their adult controls.

It has been reported in the literature that fibrosis is a characteristic of the aged heart and occurs due to the loss of myocytes, hypertrophy of the remaining myocytes, increased collagen content and deposition, increase in activity of TIMPs 1 and 4, and decrease in MMPs 1, 2, 3, and 14 (regulators of the fibrotic process) [340, 341]. A possible reason for fibrosis not occurring in our ageing hearts in this study is that these mice are not considered exactly aged (senescent). This is explained later in chapter 5 discussion (Ageing Does Not Alter Cardiac Vulnerability to Ischaemia/Reperfusion Injury), showing the mice used in this work are considered to be older adults rather than aged according to the Kaplan-Meier survival curve for C57Bl/6 mice.

3.4.10 Ageing was Associated with Increased Cardiac Capillary/Myocyte Ratio

Capillary/myocyte ratio increased significantly in the ageing heart.

The importance of measuring this lies in the fact that capillary/myocyte ratio is an important determinant for the myocyte oxygen supply [342]. It has been reported in the literature that capillary density is not affected by the normal physiological growth in the heart. However, with pathological hypertrophy the capillary proliferation mechanisms are not constant and this leads to capillary/myocyte mismatch [343, 344]. This defect in adaptive mechanisms is age-dependant as it is not seen in children where capillary angiogenesis is proportional to cardiac hypertrophy [345].

One possible reason why the ratio here increased in the ageing heart is that the capillary number remained constant, but myocyte numbers decreased (loss of myocytes with ageing), leading to a bigger capillary/myocyte ratio in a measured area.

3.4.11 Ageing was not Associated with a Change in Cardiomyocyte Diastolic Sarcomere Length

The importance of studying sarcomere length lies in the role of it in muscle function. Sarcomere length is indicated in the contractility force of the heart according to the Frank-Starling relationship which describes the relationship between the end-diastolic volume and cardiac

ejection volume, and explains that the responsiveness of myofilaments to activation by calcium depends on the sarcomere length (myofilament length dependent activation) [346].

The sarcomere in the ageing mice myocytes did not change in length compared to those of adult mice. This is consistent with what Nance et al. 2015 reported that cardiomyocyte sarcomere length in aged mice (24-28 months) was not different compared to adult mice (3-6 months) and only showed impaired lengthening in response to various filling pressures which could explain stiffening and cardiac dysfunction seen with ageing [47]. This was also proven in aged hamsters of different strains (Bio 14.6 and F1b Syrian hamsters) where sarcomere length in cardiomyocytes did not change with ageing [347]. On the other hand, a study in aged female Fischer 344 rats showed that cardiomyocyte sarcomere length decreased significantly between 6 and 18 months, but did not change between 18 and 22 months of age [348]. Similarly, cardiomyocyte sarcomere length in male Wistar rats was shown to decrease between the ages of 2 and 6-9 months, 2 and 24-25 months, but was not found to be different between 6-9 and 24-25 months of age [349]. These differences in sarcomere length change with ageing could be due to the differences in species as they seem to change in rats but not in mice or hamsters.

3.4.12 Ageing was Associated with Changes in Mitochondrial Morphometry but not Mitochondrial Distribution

Results from this work show that mitochondrial distribution (generally and within mitochondrial subpopulation) did not change in the ageing heart compared to the adult heart. This is consistent with what Schmucker and Sachs, 1985 reported where mitochondrial volume/myocyte in aged male Fischer 344 rats (6, 16, and 30 months of age) did not change [350]. Similarly, in aged Wistar rats (6, and 22-24 months of age), mitochondrial total volume did not change, however they appeared to increase in size with aging and thus decrease in numbers [351]. On the other hand, a study in aged C57BL/6J mice (9, 18, and 36 months of

age) showed that the total mitochondrial volume as well as numbers were decreased with ageing (at 36 months) in both heart and liver tissue [352]. Additionally, another study in C57BL/6 mice aged 2 and 11 months showed a decrease in total mitochondrial volume and numbers in aged mice in both skeletal and cardiac tissue [353]. It is possible that the difference seen in mitochondrial distribution in aged animals (36 months of age) in Tate and Harbener's study is due to their senescence. These animals were a lot older than the ones used in this study and that could indicate that these ultrastructural changes occur at an older age in mice. Authors of the second study also indicated that the ultrastructural changes they described often occur at an older age and stated the need for further investigation.

The second observation from our work on mitochondria in ageing was the change in mitochondrial morphometry, where they became smaller and more elongated (which indicates fusion of mitochondria, supported by the increased expression of mitochondrial fusion proteins Opa1 and Mfn2 in aged hearts) for all three subpopulations but only significantly in SSL and PN mitochondria.

Studies on morphometric changes of mitochondria with ageing have shown that there are some age-related changes including a decrease in size in a hamster model as well as human samples [354, 355]. The inner mitochondria membrane area in aged hamsters fell compared to the adult controls, and in human samples the overall density of mitochondria in cardiac tissue samples did not change with ageing while the numerical density increased (indicating a decrease in mitochondria size). In the mouse, studies looking at the effect of ageing on mitochondrial morphology mainly looked at disruption to cristae, and reported a loss of mitochondrial density and vacuolation occurring in the aged heart, as well as in liver tissue [352, 356].

3.4.13 Ageing was Associated with Increased Lipid Deposits (Lipid Droplets) in the Heart

Lipid droplets were significantly increased in the ageing heart compared to its adult control.

The importance of studying this arises from the role lipid droplets play, as they are dynamic cytosolic organelles that are composed of neutral lipids surrounded by a layer of phospholipids and surface proteins. They have many roles in lipid metabolism and energy homeostasis, metabolic gene expression, intracellular lipid and membrane trafficking, viral infection, and inflammatory responses [357].

The increase in lipid droplet count in these ageing hearts can be justified by the increase in lipid metabolism and storage evident by the upregulation of lipid metabolism proteins. Measuring the accumulation of lipids in the aged heart through gene expression of lipid metabolism and transport regulatory protein has been reported in the literature and was associated with heart dysfunction, however lipid droplets were not counted [358]. Additionally, the accumulation of lipid droplets are associated with heart disease in conditions characterised by hyperlipidaemia (which was not found in our ageing mice) [359, 360].

3.5   Summary and Conclusion

In conclusion, changes occurring with ageing in the mice used in this study (C57BL6/J) were increases in body weight, body fat, hypertrophy of the heart, and significant decrease in blood glucose levels.

The remodelling of the heart that was observed with ageing included changes in cardiac energy metabolites and AA content. Ageing hearts had higher levels of inosine, lower levels of hypoxanthine, and a decreased phosphorylation potential (seen in guanosine metabolites). This could be an indication of a decreased ability of the heart to produce energy as well as a deficiency in mitochondrial capacity. Additionally, ageing hearts had a significantly lower total AA pool reflected by lower levels of most of the AAs examined such as taurine, arginine, and alanine. As mentioned in the discussion, AAs play an important role as energy metabolites in certain conditions as well as aiding in the control of the ionic state of the heart, so a decrease

in their content could be an indicator of increased vulnerability of the ageing heart, but reports on the relation of some of these AAs to CVD are contradictory.

Age-related remodelling also included a change in the proteome and phospho-proteome profiles of the heart. The majority of proteins detected were all upregulated with ageing, as was their phosphorylation. Proteins were categorised into various groups chosen for their relation to I/R injury such as mitochondrial proteins, ionic transport proteins, apoptosis-related proteins, antioxidant proteins, and metabolism and transport proteins. Upregulation in mitochondrial proteins, ionic transport proteins, and lipid metabolism proteins could be a compensatory mechanism for the deficiency in mitochondrial function in the ageing heart and thus lipid utilisation, and ionic transport alterations. Antioxidant enzymes upregulation could be a compensatory mechanism for the increased ROS production associated with the ageing process. Upregulation in carbohydrate metabolism proteins and apoptosis-related proteins could possibly reflect normal ageing associated changes, such as the shift in metabolism and increased apoptosis. Expression of collagen proteins was also upregulated in the ageing heart, but this was not associated with increased collagen deposition (fibrosis) in the heart. Changes in phosphorylation of proteins included ionic transport, cardiac signalling and apoptosis, metabolism and energy production, and structural proteins, and were all upregulated in the ageing heart. Not much information is available on the specific phosphorylation sites detected, but from the changes seen, phosphorylation of heat shock protein beta-6 at Ser-16 could have a protective role in the aged heart.

Structural remodelling of the ageing heart included larger coronary arteries with larger lumen sizes, a lower arterial wall/total artery size and lumen size ratios, and an increase in capillary/myocyte ratio. Because the capillary/myocyte ratio is an important indicator of myocyte oxygen supply, an increase in this ratio could indicate a protection in the ageing heart and improvement in oxygen delivery. However, as mentioned in the discussion this increase

could be due to the fact that the larger myocytes in the ageing heart led to the appearance of a lower myocyte number in the area used for the counting (as the same area size was used in adult heart images), thus the ratio seemed to be increased in the ageing heart.

Finally, ultrastructural remodelling of the ageing heart included a change in mitochondrial morphometry, where mitochondria became smaller in size, and more elongated (indicating fusion of mitochondria), especially in PN and SSL mitochondria where these changes were significant in the ageing heart. Additionally, ageing hearts had significantly higher numbers of lipid droplets compared to their adult controls. No changes were seen in sarcomere length nor mitochondrial density (distribution). Figure 3.32 shows a diagram of this summary.
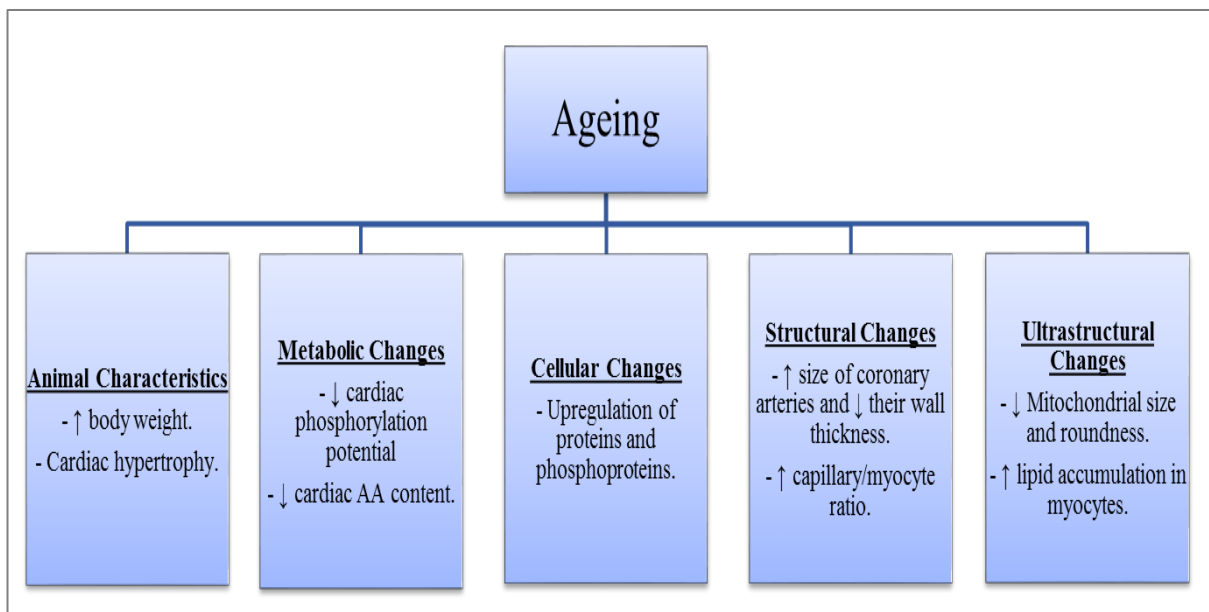
Figure 3.32: Remodelling with ageing.

4. Cardiac Remodelling with High-Fat Diet in the Ageing Heart

4.1 Introduction

4.1.1 High-Fat Diet and Cardiac Remodelling in Adulthood

Consuming HFDs have effects on cardiac remodelling. Studies have shown that HFDs are associated with obesity, metabolic changes such as hyperglycaemia, and morphological changes of the heart such as cardiomyocyte hypertrophy and interstitial fibrosis; which were maintained even after adjusting for the adiposity [196]. Additionally, HFD leads to increased ROS in the heart, impaired hypoxia inducible factor (HIF), a reduction in capillary density, cardiac hypertrophy, cardiac dysfunction, and reduced SIRT3 expression in the heart (a mitochondrial protein associated with increased human life span and metabolism) [208]. Other effects of HFD on cardiac remodelling include cellular apoptosis and mitochondrial swelling and damage, insulin resistance, metabolic syndrome, increased protein expression of c-Jun N-terminal kinase (JNK), activated protein 1 (AP-1), insulin receptor substrate 1 (IRS-1), caspase 3, and reduced Akt phosphorylation [204]. Additionally, upregulation of the expression of collagen I and III and transforming growth factor β1 (TGF-β1) were all reported with HFD [204]. Also, mice fed a HFD have shown to develop cardiomyocyte lipid droplets, hypertrophy of the heart, and an ineffective metabolic adaptation [210]. Another study using rats fed HFD showed that they developed cardiac dysfunction and LV fibrosis, with increased phosphorylation levels of Smad2 and the expression of fibrotic genes; such as connective tissue growth factor, collagen-1α1 (Col1α1), Col3α1, and Col4α1 [361]. Additional structural remodelling of the heart with HFD includes collagen deposits, intercellular spaces, disorganisation of cardiomyocytes, deposition of fat under the pericardium as well as around vessels and between cardiomyocytes, and a thicker vascular wall with reoriented nuclei [201]. The same previously mentioned study, which was done on rabbits, found ultrastructural remodelling of the heart with HFD manifested in a decrease of myofibrils that became degenerated, sarcomere disorganization, larger intracellular junctions, decreased mitochondria

distribution, damaged junctional complexes, and multiple vacuolization. The damage in the mitochondria resulted in swelling, elongation, with variations in size and cristae organisation. Short term HF feeding was also shown to have effects on cardiac remodelling, as it leads to hyperglycaemia, adipose tissue remodelling, increased apoptosis level, interstitial fibrosis, and LV dysfunction; which all worsened with increased duration of HFD exposure [362]. On the other hand, HFD was shown to reduce cardiac growth, left ventricular remodelling, contractile dysfunction, and alterations in gene expression (myosin heavy chain β) but only in the presence of hypertension [198].

4.1.2 High-Fat Diet and Cardiac Remodelling in Ageing

In addition to studying the effects of HFD on the heart, some researchers have compared this effect on young and aged hearts. HFDs effects on cardiac remodelling seem to be exacerbated by ageing. Young and aged (3 and 18 months) C57BL/6 mice were fed a normal diet, a low-fat diet, and a high fat diet for 16 weeks. Results of this study showed that the aged heart was less able to adapt to a high fatty acid load, and this led to more prominent structural alterations and accumulation of lipid intermediates in the cardiomyocytes [155]. Another study in aged rats with hypertensive disease looked at the effects of HFD on cardiac remodelling. 44 week old spontaneously hypertensive rates and Wistar Kyoto rats were given either ND or HFD for 27 weeks [215]. Results of this study showed that HFD aggravates hypertensive heart disease associated with ageing, worsened atrial and ventricular remodelling, and led to left ventricular systolic function impairment.

In this chapter, we studied the effects of HFD on the remodelling of ageing hearts, looking at metabolic, cellular (protein expression), and structural aspects that are related to I/R injury in order to understand whether or not this remodelling eventually affects the heart's vulnerability.

4.2 Methods

Several techniques have been used to obtain the results in this chapter. These techniques are described in detail in chapter 2, page 59 (Materials & Methods).

4.2.1 High Performance Liquid Chromatography

HPLC was used for analysis of cardiac ventricular tissue to measure cardiac energy metabolites and AA content in the heart. However, AA data was not be obtained as drying of the samples could not be done. Five samples for ageing ND and four for ageing HFD were used. Details on this are found in chapter 2 under this method's section.

4.2.2 Nuclear Magnetic Resonance Spectroscopy

NMR was used to analyse plasma samples for blood lipid and glucose profile. Four ageing ND and four ageing HFD samples were used. For details on this technique and analysis see chapter 2 under this method's section.

4.2.3 Liquid Chromatography Tandem Mass Spectrometry

LC-MS/MS was used to detect proteins and phosphoproteins levels in cardiac tissue. Five samples for each age group were sent for analysis (10plex). No pool sample was created for this run. For details on this technique and analysis see chapter 2 under this method's section.

4.2.4 Light Microscopy

Hearts from ageing mice fed ND or HFD (5 samples for each) were collected, fixed, processed, embedded, cut, and stained with four different stains (H&E, EVG, Masson's trichrome, and IHC-IB4) to examine cardiovascular structure and how it remodels with HFD. For details on techniques, imaging, and analysis see chapter 2 under this method's section.

4.2.5 Electron Microscopy

Hearts from ageing mice fed ND or HFD (4 samples for each) were collected, fixed, processed, embedded, cut, and stained to examine cardiac ultrastructure and how it remodels with HFD. For details on techniques, imaging, and analysis see chapter 2 under this method's section.

4.3   Results

4.3.1 Animal Characteristic Changes

4.3.1.1   Changes in Body and Heart Weights of Ageing Mice with High-Fat Diet

Table 4.1 shows the general characteristics of the mice. Ageing mice became obese and their weights increased significantly ($P < 0.001$) with HFD, with an approximate 68 % increase compared to mice fed a normal diet. Epididymal fat pads also showed a significant increase ($P < 0.001$) after HF feeding, with a 244 % increase from the ND group, with their percentage from total body weight also increasing significantly with HFD ($P < 0.001$).

Table 4.1: Body weight, body fat, and heart weights (wet and dry) in ageing mice with and without HFD. Data are presented as mean ± SEM. Data were analysed using the unpaired t-test. * = $P < 0.05$, ** = $P < 0.001$ vs. normal diet.

Measurement	ND (n=10)	HFD (n=5)
Body weight (gm)	32.74 ± 0.83	54.93 ± 0.9 **
Epididymal fat pads weight (gm)	0.91 ± 0.11	3.1 ± 0.13 **
Epididymal fat pads % of total body weight	2.73 ± 0.3	5.64 ± 0.2 **
Heart Wet Weight (gm)	0.19 ± 0.01	0.22 ± 0.01
Heart wet weight % of total body weight	0.59 ± 0.03	0.41 ± 0.03 *
Heart Dry Weight (gm)	0.04 ± 0.001	0.03 ± 0.001
Heart dry weight % of total body weight	0.11 ± 0.01	0.05 ± 0.002 **

Additionally, table 4.1 shows changes in heart wet and dry weights and their percentages from total body weight with HFD in ageing mice. Heart weights (wet and dry) did not change with HFD in ageing mice. However, their percentages from total body weight showed a significant difference between the two dietary groups only because total body weights were significantly different to start with.

4.3.1.2 Changes in Plasma Metabolome in Ageing Mice with High-Fat Diet

Several carbohydrate and lipid metabolites were measured in the plasma of animals from both dietary groups. Figure 4.1 shows samples of the NMR spectra for both groups. These metabolites were measured and expressed as area under the curve (AUC). Lipid metabolites increased with HFD in ageing mice plasma, with LDL and VLDL lipids increasing significantly ($P = 0.008$). Carbohydrate-related metabolites all decreased after HF feeding in ageing mice, with lactate, and glucose being significantly lower compared to the normal diet group ($P = 0.02$ for lactate, and $P = 0.005$ for glucose). Figure 4.2 shows the comparison of these metabolites between the two dietary groups expressed as area under the curve.
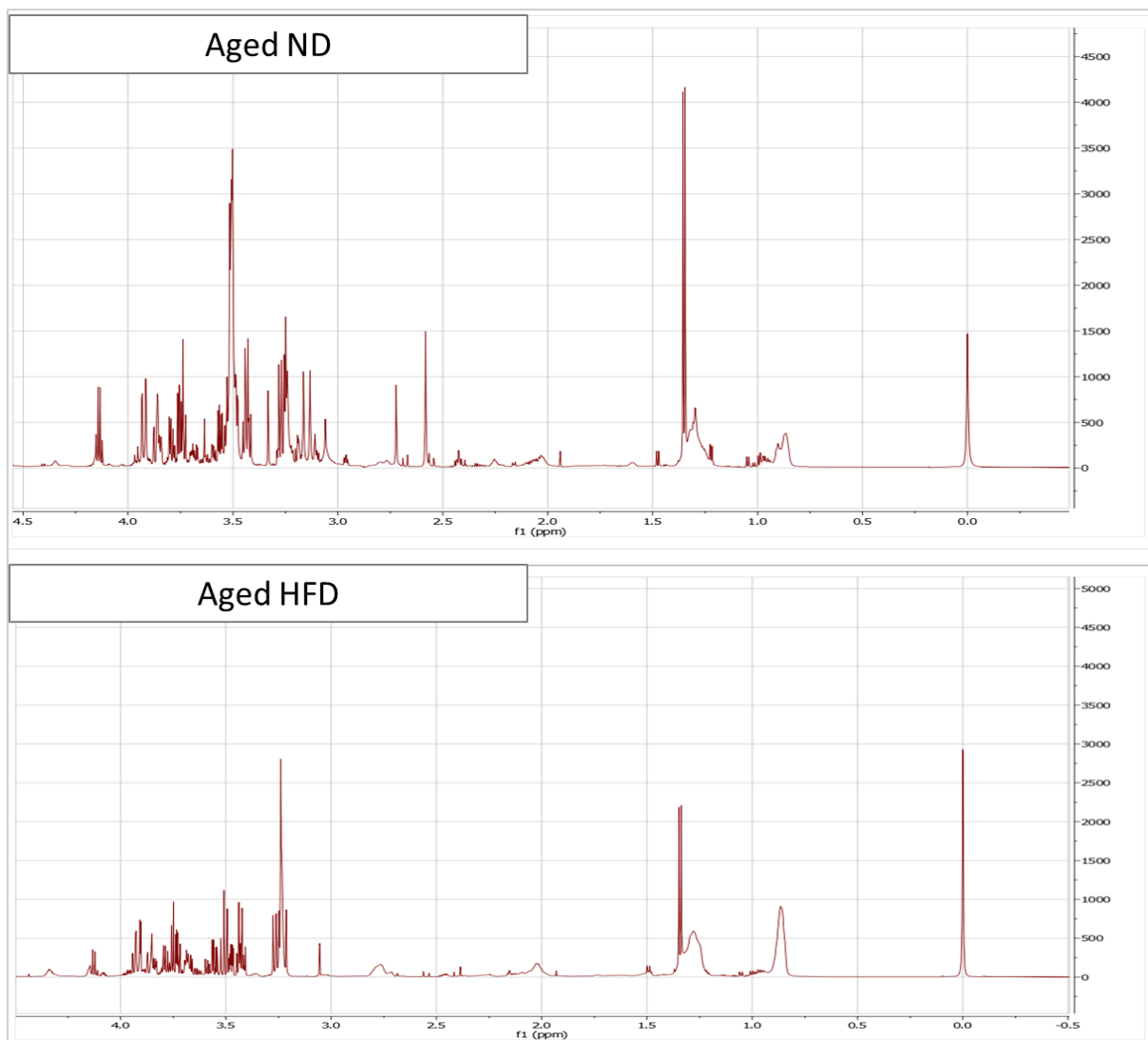
Figure 4.1: Samples of the NMR spectra for plasma of ageing mice with and without HFD.
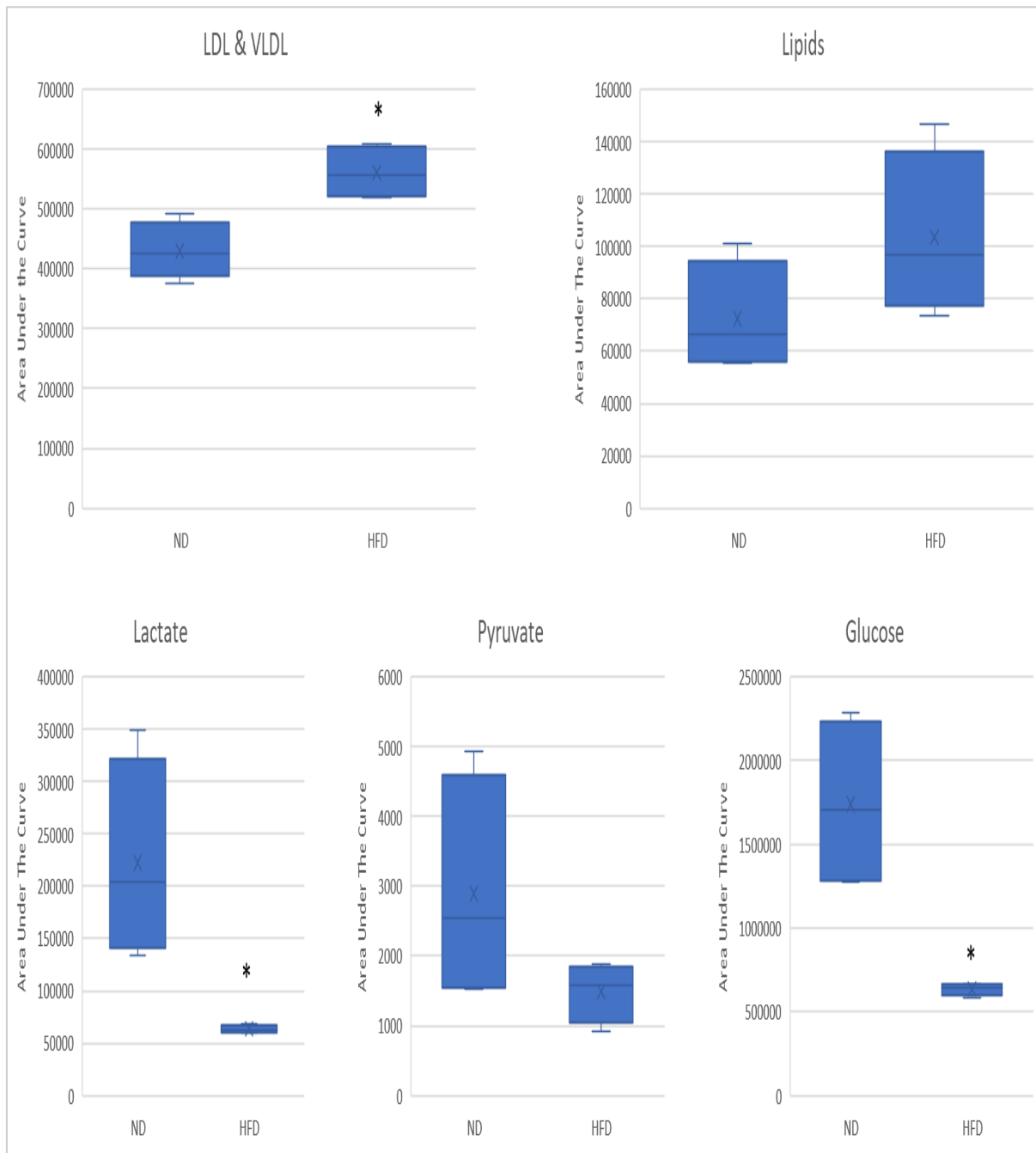
Figure 4.2: Plasma lipid and carbohydrate metabolites of ageing mice with and without HFD. Data are presented as box plots showing the minimum, 25th, 50th, 75th percentile, and maximum values of area under the peak for each metabolite. Data were analysed using the unpaired t-test. * = $P < 0.05$ vs. ND. N = 4 for each group.

4.3.2 Metabolic Changes

4.3.2.1   Changes in Cardiac Energy Metabolites in Ageing Hearts with High-Fat Diet

Various energy metabolites were measured in the heart tissue of both dietary groups as shown in table 4.2. The majority of these metabolites decreased in the aged heart after HFD, with only GTP and adenosine increasing. However, only 3 metabolites changed significantly. Adenosine di-phosphate (ADP), β-nicotinamide adenine dinucleotide (β-NAD), and inosine all decrease significantly after HFD.

Table 4.2: Cardiac energy metabolites in ageing hearts with and without HFD. Data are presented as mean ± SEM. Data were analysed using the unpaired t-test. * = $P < 0.05$. N = 5 and 4 for ND and HFD groups, respectively.

Metabolite	ND (µmole/gm of tissue)	HFD (µmole/gm of tissue)	*P*-Value
GTP	0.13 ± 0.01	0.15 ± 0.03	0.407
GDP	0.09 ± 0.01	0.09 ± 0.01	0.728
GMP	0.04 ± 0.002	0.03 ± 0.01	0.465
ATP	1.98 ± 0.33	1.39 ± 0.21	0.197
ADP	1.77 ± 0.15	0.94 ± 0.13	0.005 *
AMP	1.02 ± 0.25	0.74 ± 0.08	0.369
β-NAD	0.55 ± 0.07	0.32 ± 0.03	0.023 *
Inosine	0.27 ± 0.03	0.09 ± 0.014	0.001 *
Adenosine	0.10 ± 0.01	0.12 ± 0.03	0.543

Phosphorylation ratios (phosphorylation potential) for adenosine and guanosine energy metabolites were calculated alongside the energy charge of the heart before and after HFD. Phosphorylation potential mostly increased after HFD; however, this was not significant. Cardiac energy charge decreased after HFD in the aged heart, also not significantly. On the other hand, total adenosine metabolites (adenosine metabolite pool) were significantly decreased from 4.8 ± 0.3 µmole/gm in ND aged hearts to 3.1 ± 0.4 µmole/gm in HFD aged hearts ($P = 0.024$) (Figure 4.3).
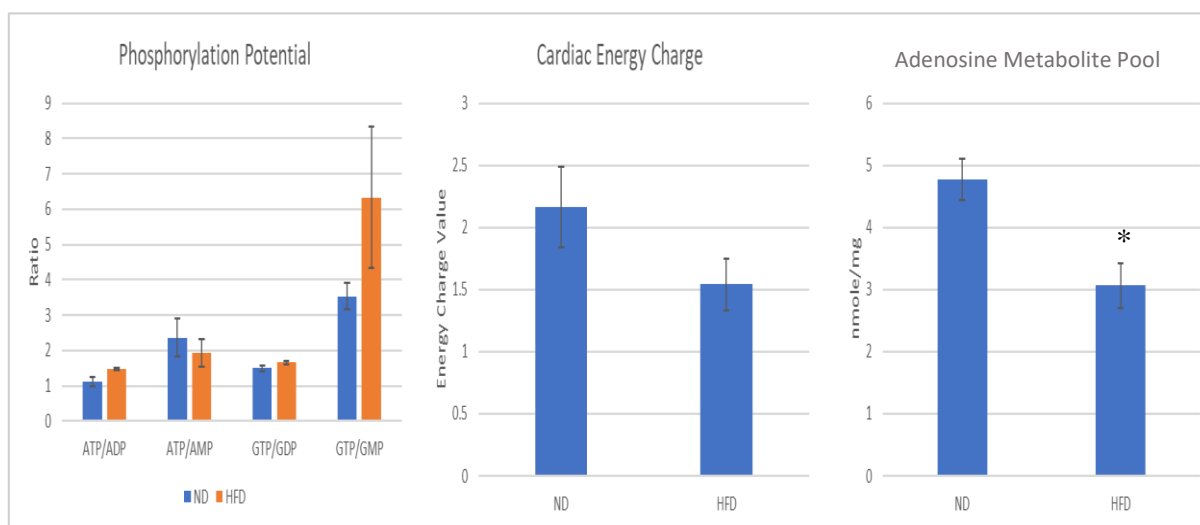
Figure 4.3: Phosphorylation potential, cardiac energy charge, and total adenosine metabolites in ageing hearts with and without HFD. Data are presented as mean ± SEM. Data were analysed using unpaired t-test. N = 5 and 4 for ND and HFD, respectively. * $P < 0.05$ vs. ND.

4.3.3 Cellular (Protein Expression) Changes

4.3.3.1 Changes in Proteome Profile in Ageing Heart with High-Fat Diet

A total of 4983 proteins were detected in the proteomics analysis and 1884 proteins changed significantly with HFD in the ageing mouse heart (figure 4.4). The majority of significant proteins (67 %) were downregulated with HFD, while the remaining 33 % (630 proteins) were upregulated. Specific fold changes were selected (FD < 0.8 and > 1.3) in order to avoid false positive results, and 762 proteins were within selected folds (385 were downregulated with HFD and 341 were upregulated), and these were further categorised using the PANTHER classification system according to molecular function and biological processes (figure 4.5). Similar to the classification seen with ageing compared to adult hearts, the majority of significant proteins that changed in the ageing heart with HFD fall under binding and catalytic

activity (based on molecular function) and cellular and metabolic processes (based on biological function).
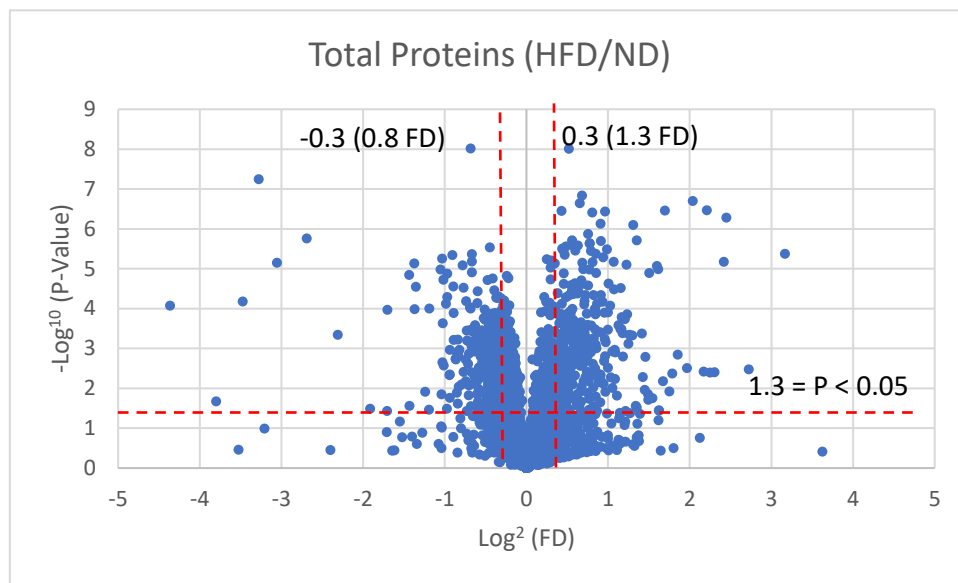
Figure 4.4: Volcano plot showing changes in proteins of HFD/ND in ageing mice hearts. X axis represents $\log^2$ of the fold difference (HFD/ND) and Y axis represents $-\log^{10}$ of the *P*-value. Proteins above the horizontal red line are significantly different between the two age groups. Proteins on the right of the Y axis are upregulated with HFD in the aged heart (with the ones on the right of the vertical red line having a FD > 1.3), and proteins on the left side of the Y axis are downregulated with HFD in the aged heart (with the ones on the left of the second vertical red line having a FD < 0.8). Data were analysed using the unpaired t-test. N= 5 for each group.
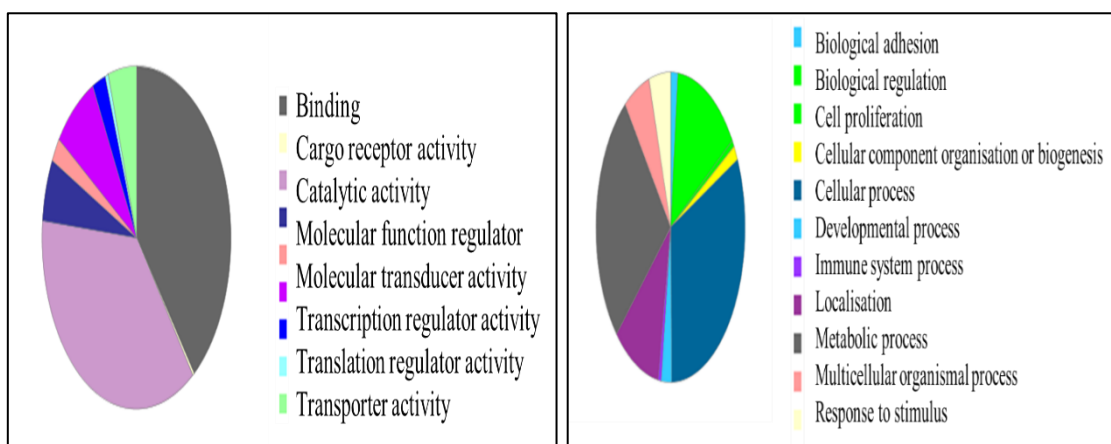
Figure 4.5: Classification of significantly different proteins within selected fold change (< 0.8 and > 1.3) between ND and HFD in ageing hearts using the PANTHER classification system. Proteins are classified according to molecular function and biological processes.

Proteins within selected fold change were further categorised into several groups including mitochondrial proteins, lipid and carbohydrate metabolism, ionic transport related proteins, antioxidant proteins, apoptosis related proteins, and structural (collagen) proteins.

4.3.3.1.1 Mitochondrial Proteins

60 significant mitochondrial proteins were within selected fold change, with only 8 being upregulated after HFD in the ageing heart and the remaining 52 were downregulated. These proteins were further categorised according to function into 6 groups, mitochondrial lipid metabolism, energy metabolism, AA metabolism and transport, ionic transport, structural, and mitochondrial transport proteins (figure 4.6).

Upregulated mitochondrial proteins after HFD in the ageing heart included the lipid metabolism proteins (NAD-dependent protein lipoamidase sirtuin-4, mitochondrial and Delta(3,5)-Delta(2,4)-dienoyl-CoA isomerase), the energy metabolism protein [Pyruvate dehydrogenase (acetyl-transferring)] kinase isozyme 4, the mitochondrial structural protein Coenzyme Q-binding protein COQ10 homolog B, the transport protein Uncoupling protein 3 (Mitochondrial, proton carrier), and the AA transport protein Mitochondrial basic amino acids transporter. (For proteins full name list see appendix 7.3).
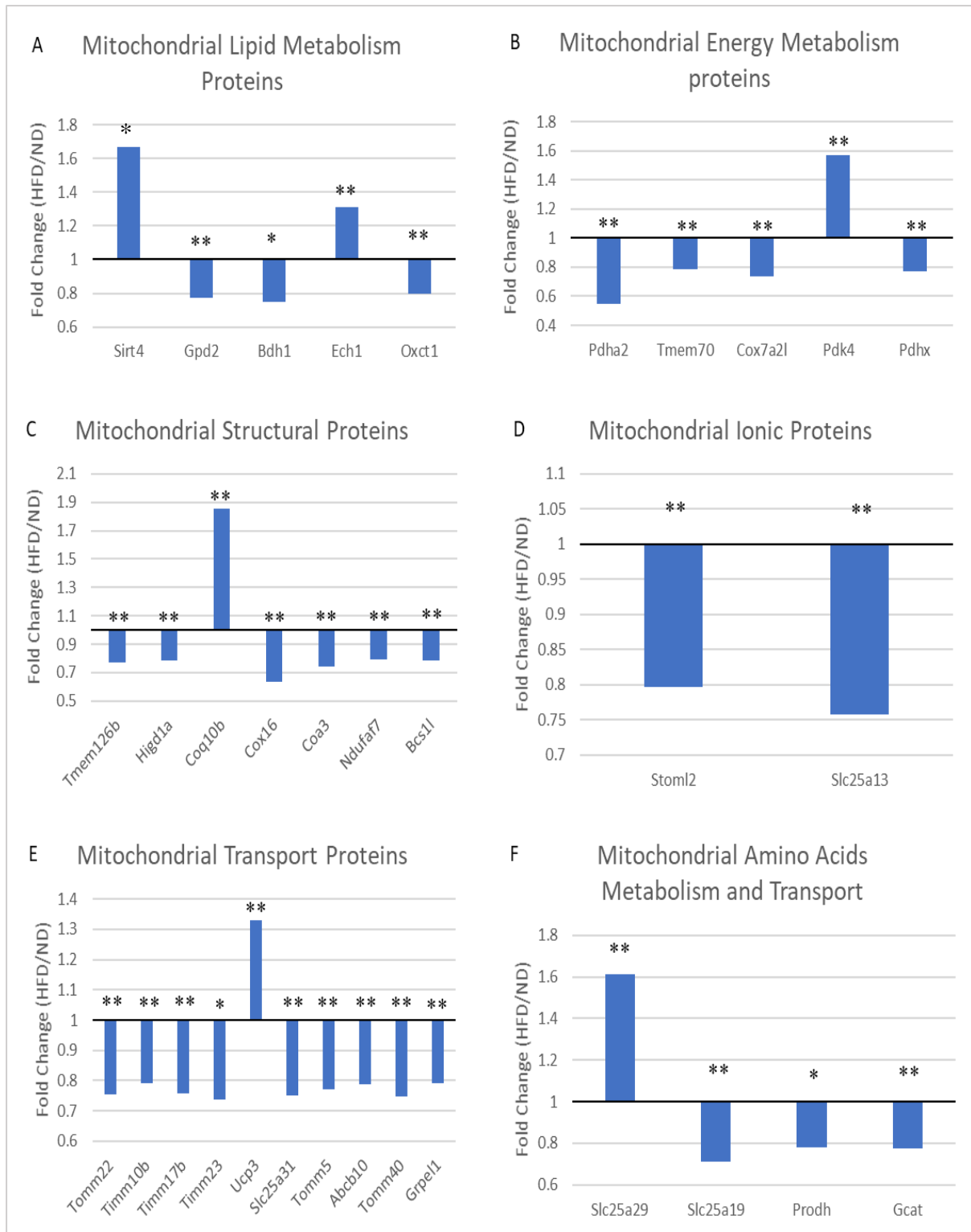
Figure 4.6: Significant mitochondrial proteins in ageing mice hearts with and without HFD. A) Mitochondrial lipid metabolism proteins. B) Mitochondrial energy metabolism proteins. C) Mitochondrial structural proteins. D) Mitochondrial ionic proteins. E) Mitochondrial transport proteins. F) Mitochondrial amino acid metabolism and transport proteins. Data are presented as fold change (HFD/ND). Data were analysed using the unpaired t-test. All proteins selected fall within a FD < 0.8 and > 1.3. * = P < 0.05, ** = P < 0.001. N = 5 for each group.

4.3.3.1.2   Ionic Transport-Related Proteins

Six ionic transport related proteins changed with HFD in the ageing heart, 3 were downregulated and 3 were upregulated. Upregulated proteins were Sodium channel subunit beta-4, Voltage-dependent L-type calcium channel subunit alpha-1D which mediates the entry of calcium ions into excitable cells, and Store-operated calcium entry-associated regulatory factor which protects the cell from increased cellular calcium levels. Downregulated proteins were Potassium voltage-gated channel subfamily KQT member 1 potassium channel, Sodium/potassium-transporting ATPase subunit alpha which is involved in the exchange of sodium and potassium ions across cell membrane creating a gradient across the membrane, and chloride channel protein. (Figure 4.7).
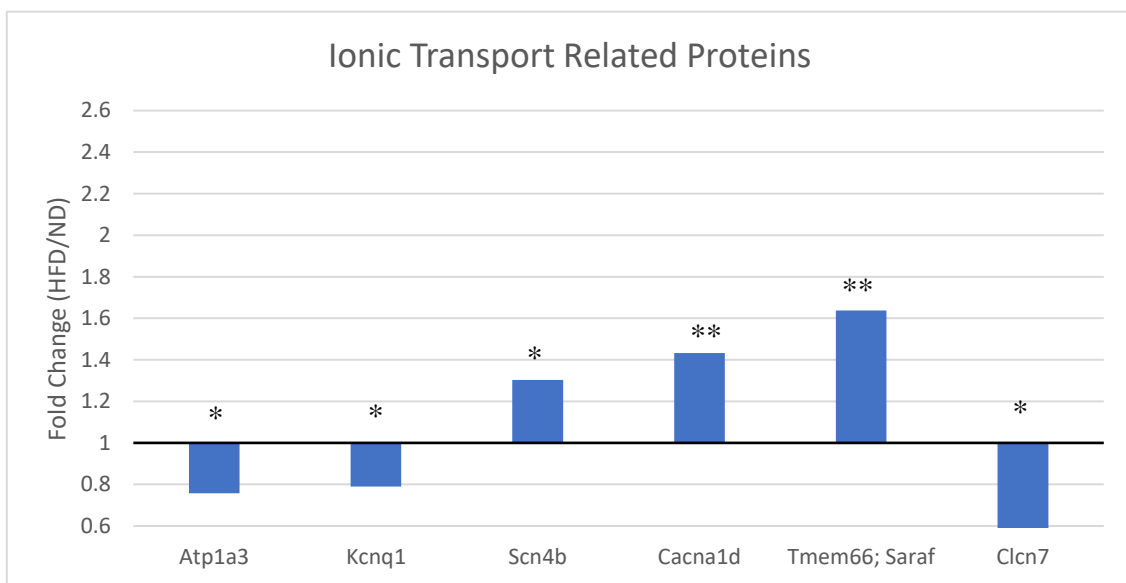
Figure 4.7 Significant ionic transport related proteins (calcium, sodium, chloride, and potassium) in ageing mice hearts with and without HFD. Data are presented as fold change (HFD/ND). Data were analysed using the unpaired t-test. All proteins selected fall within a FD < 0.8 and > 1.3. * = $P < 0.05$, ** = $P < 0.001$. N = 5 for each group.

4.3.3.1.3   Antioxidant Proteins

Antioxidant proteins changed significantly in expression in the ageing heart after HFD, with some being downregulated and others upregulated. Glutathione peroxidase 7 and Glutathione S-transferase omega-1 were both downregulated with HFD, while catalase and superoxide dismutase were upregulated (figure 4.8).
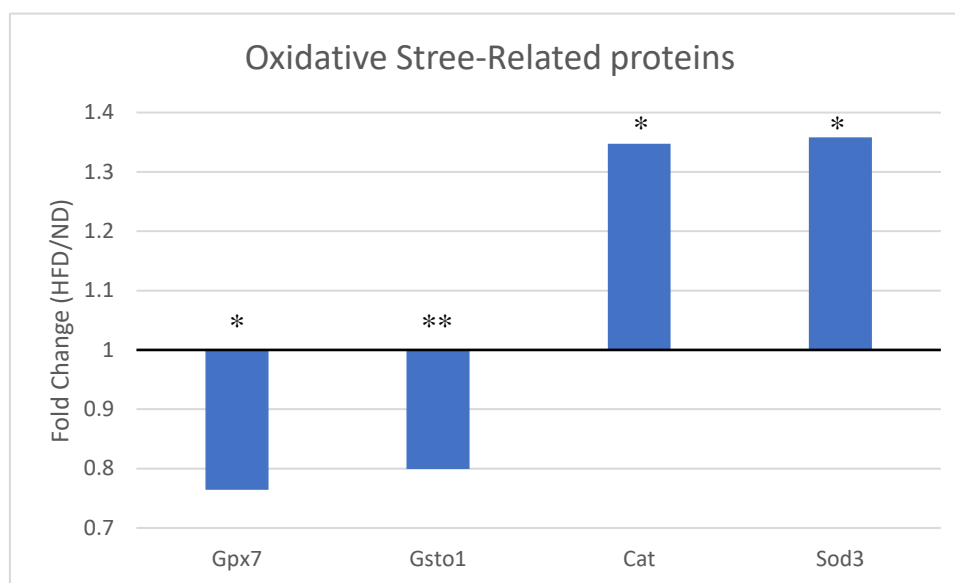
Figure 4.8: Significant antioxidant proteins in ageing mice hearts with and without HFD. Data are presented as fold change (HFD/ND). Data were analysed using the unpaired t-test. All proteins selected fall within a FD < 0.8 and > 1.3. * = $P < 0.05$, ** = $P < 0.001$. N = 5 for each group.

4.3.3.1.4   Apoptosis Related Proteins

Three apoptosis-related proteins increased in the ageing heart with HFD. BCL2-associated athanogene 3 is an anti-apoptotic protein that acts as a co-chaperone to HSP70 and HSC70. Bcl-2-associated transcription factor 1 is a pro-apoptotic protein that promotes death by repressing transcription. Finally, Cell division cycle and apoptosis regulator protein 1, which is a pro-apoptotic protein that also acts on p53 activation (figure 4.9).
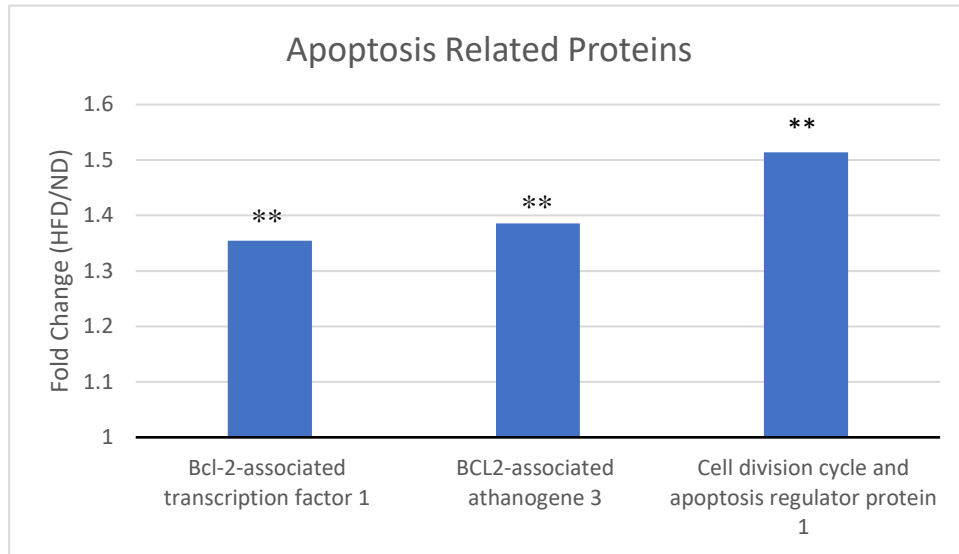
Figure 4.9: Significant apoptosis related proteins in ageing mice hearts with and without HFD. Data are presented as fold change (HFD/ND). Data were analysed using the unpaired t-test. All proteins selected fall within a FD < 0.8 and > 1.3. ** = $P < 0.001$. N = 5 for each group.

4.3.3.1.5   Structural (Collagen) Proteins

Various alpha chains (1, 2, and 3) of collagen type IV, VI, and XVIII were significantly upregulated with HFD in the ageing mouse heart (figure 4.10).
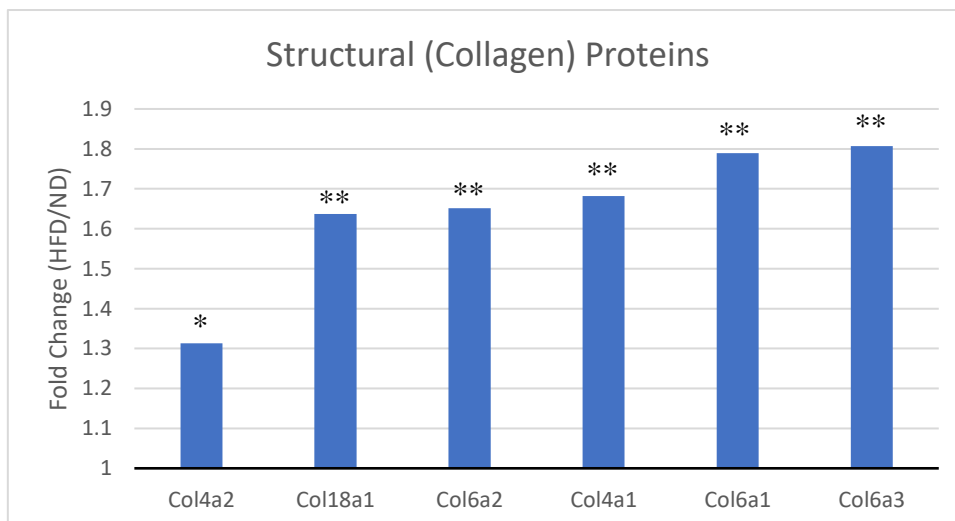
Figure 4.10: Significant structural (collagen) proteins in ageing mice hearts with and without HFD. Data are presented as fold change (HFD/ND). Data were analysed using the unpaired t-test. All proteins selected fall within a FD < 0.8 and > 1.3. * = $P < 0.05$, ** = $P < 0.001$. N = 5 for each group.

4.3.3.1.6   Lipid and Carbohydrate Metabolism and Transport Proteins

Carbohydrate and lipid metabolism and transport proteins also changed significantly with HFD in the ageing heart (figure 4.11). All carbohydrate-related proteins were downregulated after HFD, while lipid metabolism proteins were mostly upregulated. An exception was downregulation of lipid metabolism proteins Acyl-coenzyme A thioesterase 11, N-acyl-aromatic-L-amino acid amidohydrolase (carboxylate-forming), and Acyl-Coenzyme A binding domain containing 3, isoform CRA_b protein.
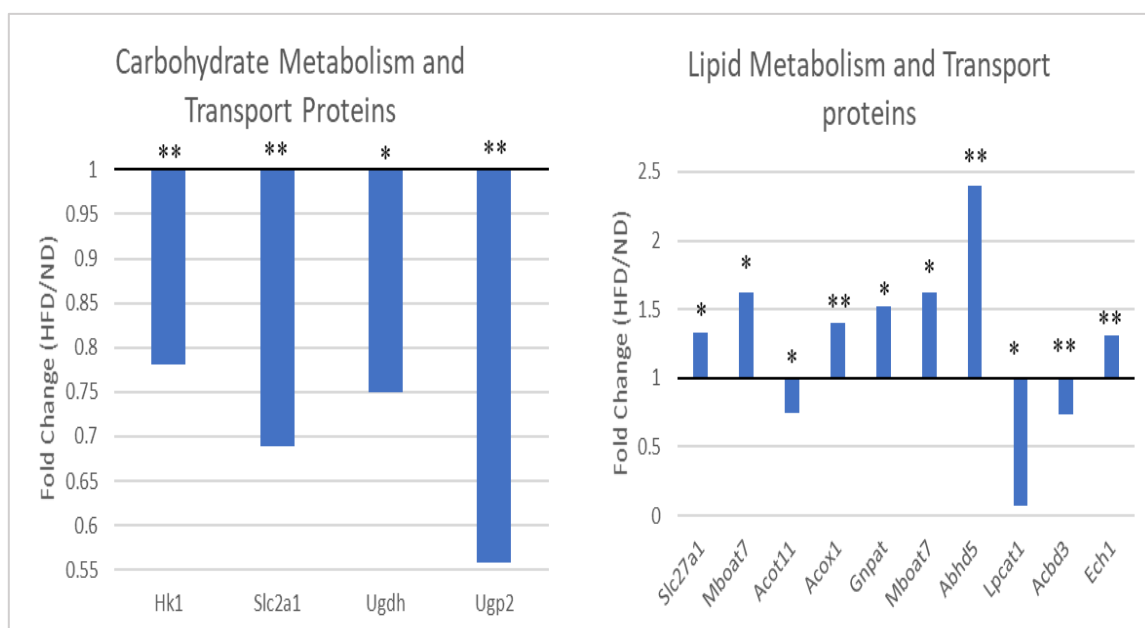
Figure 4.11: Significant lipid and carbohydrate metabolism and transport proteins in ageing mice hearts with and without HFD. Data are presented as fold change (HFD/ND). Data were analysed using the unpaired t-test. All proteins selected fall within a FD < 0.8 and > 1.3. * = $P < 0.05$, ** = $P < 0.001$. N = 5 for each group.

4.3.3.2 Changes in Phosphoproteome Profile in Ageing Hearts with High-Fat Diet

In the ageing mouse heart, 927 phosphorylated peptides were detected (figure 4.12), and 246 changed significantly after HFD. Of the significantly changed peptides, 151 were downregulated in phosphorylation after HFD and the remaining 95 were upregulated in phosphorylation. Significant peptides were categorised using the IPA software.
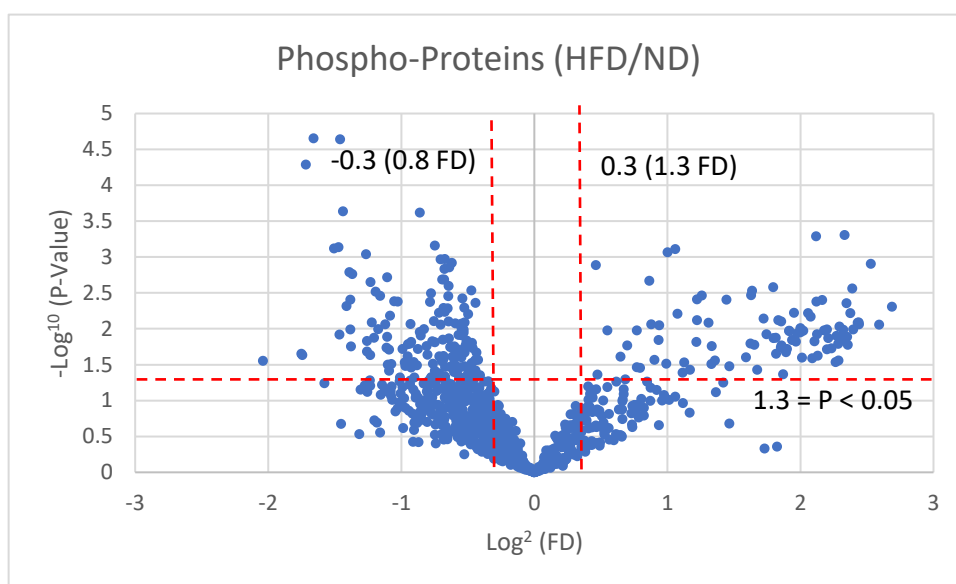
Figure 4.12: Volcano plot showing changes in phospho-proteins of HFD/ND in ageing mice hearts. X axis represents $\log^2$ of the FD (HFD/ND) and Y axis represents -$\log^{10}$ of the P-value. Phosphoproteins above the horizontal red line are significantly different between the two age groups. Phosphoproteins on the right of the Y axis are upregulated with HFD in the aged heart (with the ones on the right of the vertical red line having a FD > 1.3), and phosphoproteins on the left side of the Y axis are downregulated with HFD in the aged heart (with the ones on the left of the second vertical red line having a FD < 0.8). Data were analysed using the unpaired t-test. N= 5 for each diet group.

Over half of the significantly altered peptides detected in ageing hearts after HFD were downregulated in phosphorylation (61 %). Analysis using the IPA software categorised these peptides and the main groups of interest included ionic transport, cardiac signalling and apoptosis, carbohydrate metabolism, transport, enzymes, and structural proteins (table 4.3).

Table 4.3: Changes in phosphoproteins in the ageing mouse heart with HFD. Table shows protein description, accession number, altered phospho-site, fold change (HFD/ND), and *P*-value. Data were analysed using unpaired t-test. * = $P < 0.05$, ** = $P < 0.001$. N = 5 for each group.

Protein	Accession Number	Phospho-site	FD (HFD/ND)	*P*-Value
Downregulated phospho-proteins in aged heart with HFD				
Ionic transport				
ATPase, Ca++ transporting, cardiac muscle, slow twitch 2, isoform CRA_b (Fragment) GN=Atp2a2	Q5DTI2	S680	0.75	0.044 *
Ryanodine receptor 2 GN=Ryr2	E9Q401	S2367	0.85	0.0007 **
Cardiac signalling and apoptosis				
Heat shock protein HSP 90-beta GN=Hsp90ab1	P11499	S226 S255	0.56 0.64	0.007 * 0.032 *
Heat shock protein HSP 90-alpha GN=Hsp90aa1	Q3TKA2	S231 S263	0.29 0.36	0.023 * 0.012 *
Carbohydrate metabolism				
Glycogen [starch] synthase, muscle GN=Gys1	Q9Z1E4	S657	0.53	0.009 *
Transport proteins				
Syntaxin-4 GN=Stx4	P70452	S15	0.63	0.003 *
Structural proteins				
Microtubule-associated protein tau GN=Mapt	A2A5Y6	S712	0.36	0.0005 *
A kinase (PRKA) anchor protein (Gravin) 12 GN=Akap12	B2RRE0	S584	0.70	0.014 *
Intersectin-1 GN=Itsn1	E9Q0N0	S335	0.52	0.016 *
Caveolae-associated protein 1	O54724	S42	0.70	0.027 *

GN=Cavin1				
Alpha-1-syntrophin GN=Snta1	Q61234	S194 S195	0.62	0.048
Enzymes				
Protein phosphatase 1 regulatory subunit 7 GN=Ppp1r7	Q3UM45	S24 S27	0.51	0.033 *
Pyruvate dehydrogenase E1 component subunit alpha, somatic form, mitochondrial GN=Pdha1	P35486	S293	0.46	0.018 *
Upregulated phospho-proteins in aged heart with HFD				
Structural				
Actin-binding LIM protein 1 GN=Ablim1	E9QK41	S475	2.34	0.004 *

From the previous table, downregulated phosphorylated proteins in the ageing heart after HFD were divided into several groups including ionic transport, cardiac signalling and apoptosis, carbohydrate metabolism, transport, and enzymes. All these proteins were phosphorylated at serine sites, with some of them having more than one phosphorylated site that changed significantly with HFD. Even though 39 % of significantly changed phosphoproteins with HFD in the ageing heart were upregulated, the only upregulated protein that was identified and marked for importance was Actin-binding LIM protein 1; a structural protein involved in the bundling of actin filaments. Phosphorylation of this protein at S475 was upregulated with HFD in the ageing heart.

4.3.4 Structural Changes

4.3.4.1 Changes in Cardiomyocyte Structure in Ageing Hearts with High-Fat Diet

H&E staining is a basic stain used here only provide a comprehensive picture of the heart sections from both diet groups as shown in figure 4.13.
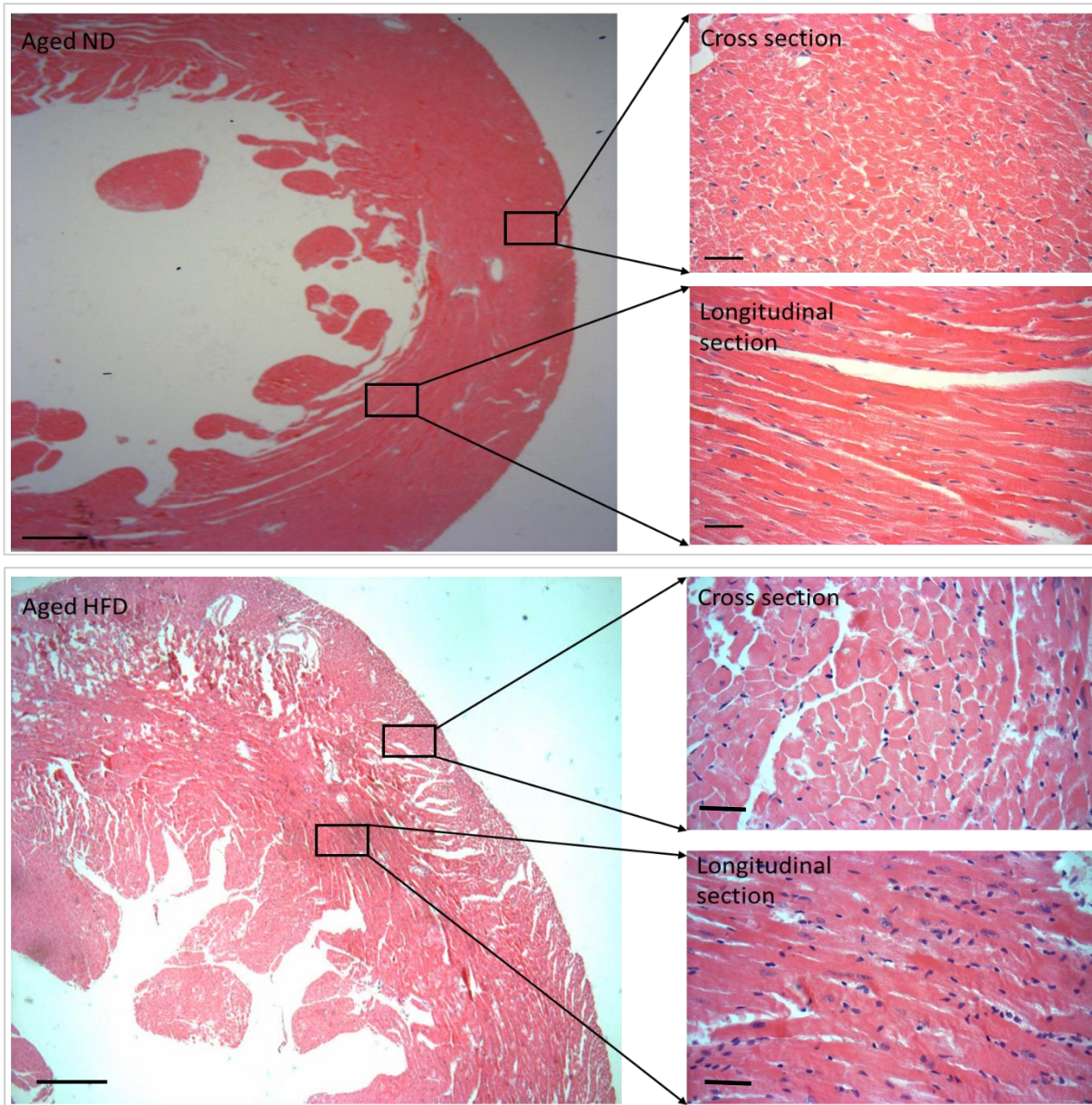
Figure 4.13: Haematoxylin and eosin staining of ageing mice heart sections with and without HFD. Images show the left ventricle (objective lens magnification x4), and longitudinal and cross-sectional areas from the LV (objective lens magnification x40). Dark blue-purple dots in the images represent the nuclei. Scale bar is 20 microns.

.

4.3.4.2 Changes in Coronary Arteries in Ageing Hearts with High-Fat Diet

EVG staining was used to highlight the arteries and show the elastin (stained in black) around them. Figure 4.14 shows representative images of large coronary arteries and some of the smaller arteries in both diet groups.

Using EVG stained sections, measurements of total artery size, artery lumen size, artery wall thickness, and artery wall/total artery size and lumen ratios were taken. Figures 4.15 and 4.16 show the comparison between the two groups.
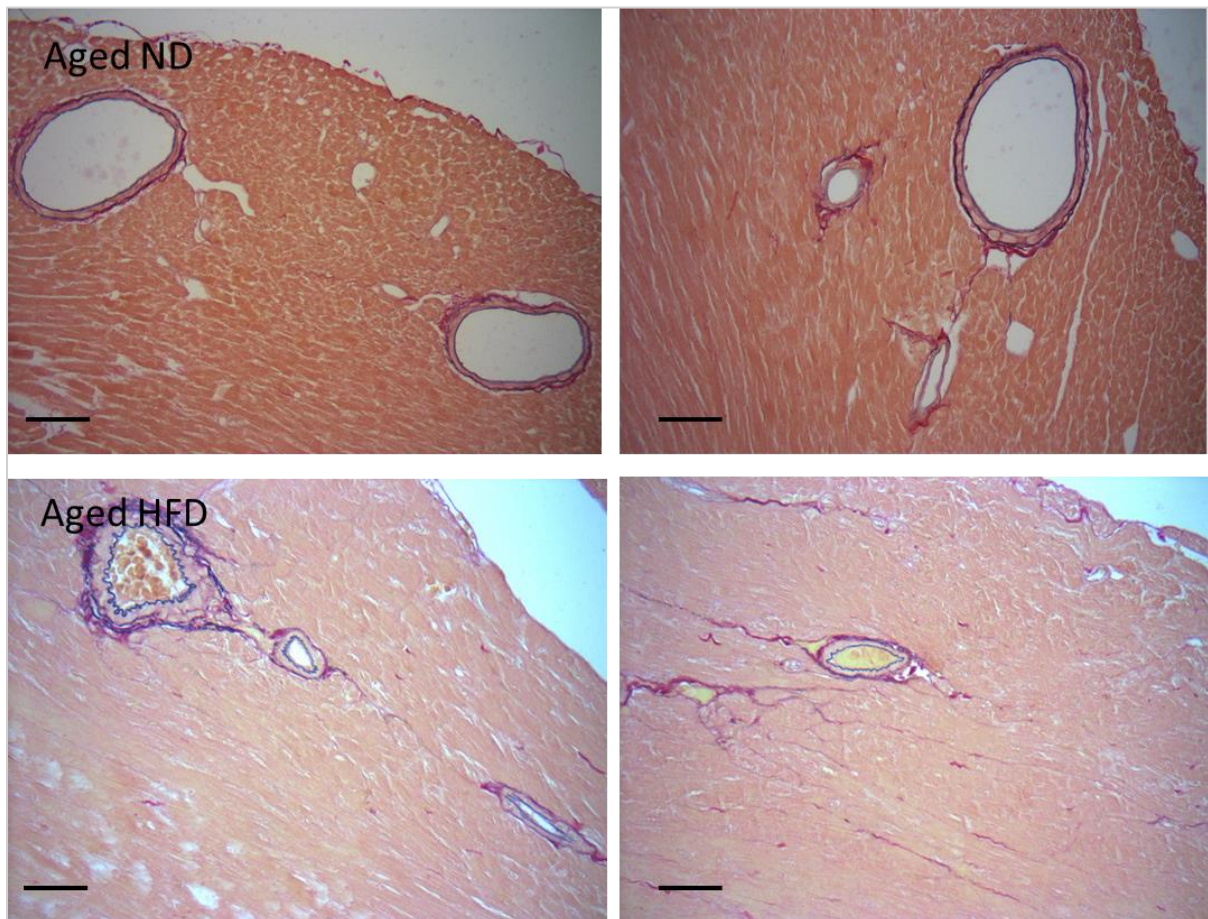
Figure 4.14: Verhoeff-van Gieson Staining of ageing mice heart sections with and without HFD. Images show different size arteries (objective lens magnification x20). Black colour around the arteries in the images represents elastic fibres. Yellow colour inside the artery shows atherosclerosis (lipid accumulation). Scale bar is 20 microns.

Arteries of various sizes in the stained sections have been measured for their total size and lumen size, and quartiles (minimum value, 25th, 50th, 75th, and maximum value) have been calculated (excluding the outlier values). These values for both diet group are presented in table 4.4. Total artery size and lumen size decreased significantly with HFD in the ageing heart ($P <$ 0.001) (figure 4.15).
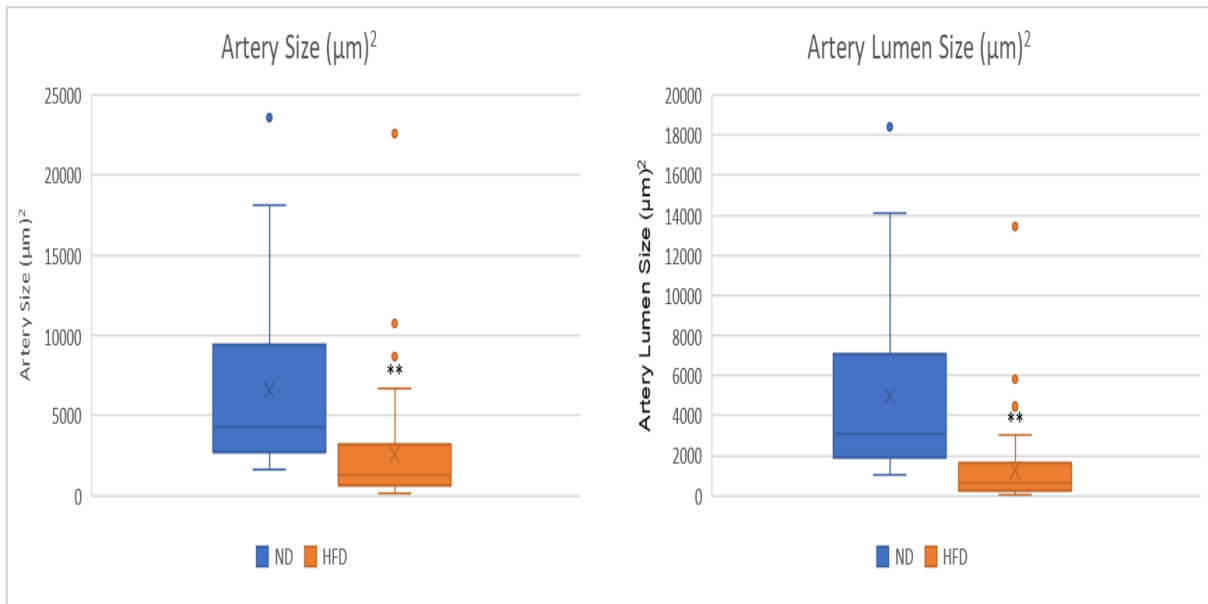
Figure 4.15: A) Total artery size (μm)^2 and B) Artery lumen size (μm)^2 in ageing mice hearts with and without HFD. Data are presented as quartiles showing the minimum value, 25th percentile, 50th percentile, 75th percentile, maximum value, and the outliers. Data were analysed using the unpaired t-test. ** = $P <$ 0.001 vs. ND. N= 5 for each group.

Quartile values shown in table 4.4 show the decrease in HFD group Compared to the ND group. Coronary arteries in ND ageing hearts seem to be about 3.6 folds larger (50th percentile) compared to HFD ageing hearts, with their lumen sizes also being 6.4 folds larger.

Table 4.4: Quartile values of total artery sizes and artery lumen size in ageing mice hearts with and without HFD. Values include the minimum value, 25th percentile, 50th percentile, 75th percentile, maximum value, and the outliers. N= 5 for each diet group.

Quartiles	Total Artery Size in HFD Hearts $(\mu m)^2$ N = 5	Total Artery Size in ND Hearts $(\mu m)^2$ N = 5	Artery Lumen Size in HFD Hearts $(\mu m)^2$ N = 5	Artery Lumen Size in ND Hearts $(\mu m)^2$ N = 5
Min Value	160	1650	48	1027
25 Percentile	644	2772	219	1995
50 Percentile	1145	4214	471	3026
75 Percentile	2612	8608	1491	6429
Max Value	6722	18096	3059	14074
Outlier	8705 10749 22603	23605	4456 5822 13448	18424

Arterial wall thickness measured from four different sides of the artery wall and averaging that measurement showed no significant difference between the two groups. However, wall thickness/total artery size was significantly increased in the HFD heart ($P < 0.001$) from an average of 0.28 ± 0.01 in ND hearts to an average of 0.56 ± 0.02 in HFD hearts (figure 4.16).
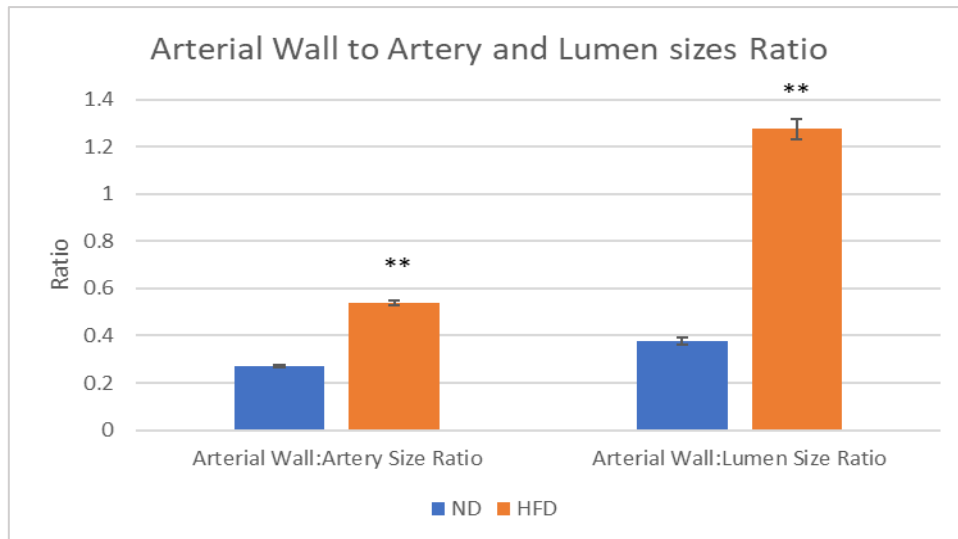
Figure 4.16: arterial wall to artery and lumen size ratios in ageing mice hearts with and without HFD. Data are presented as mean ± SEM. Data were analysed using the unpaired t-test. ** = $P < 0.001$ vs. ND. N= 5 for each group.

4.3.4.3 Changes in Fibrous Tissue in Ageing Hearts with High-Fat Diet

As mentioned earlier in the proteomics data (figure 4.10), collagen proteins expression increased significantly with HFD in ageing heart. This is also seen in the percentage of fibrous tissue in the myocyte calculated using Masson's trichrome stain for collagen fibres. Figure 4.17 shows that with HFD, the ageing heart had a significantly higher percentage of fibrous tissue ($P = 0.005$). Fibrosis increases from an average of 1.8 ± 0.3 % with ND to an average of 4.8 ± 0.7 % with HFD. Figure 4.18 shows examples of fibrous tissue, around the arteries and between myocytes, in ageing hearts with HFD.
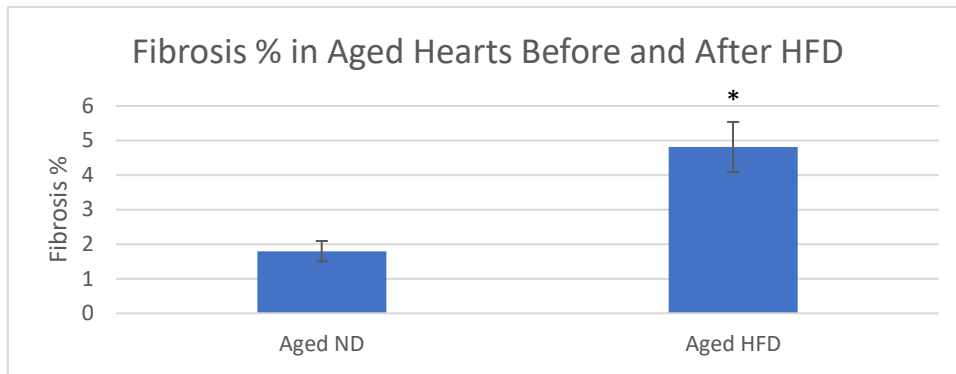
Figure 4.17: Fibrous tissue percentage in ageing mice hearts with and without HFD. Quantification was done using Masson's Trichrome stained heart sections. Data are presented as mean ± SEM. Data were analysed using the unpaired t-test. * $P < 0.05$ vs ND. N= 5 for each group.
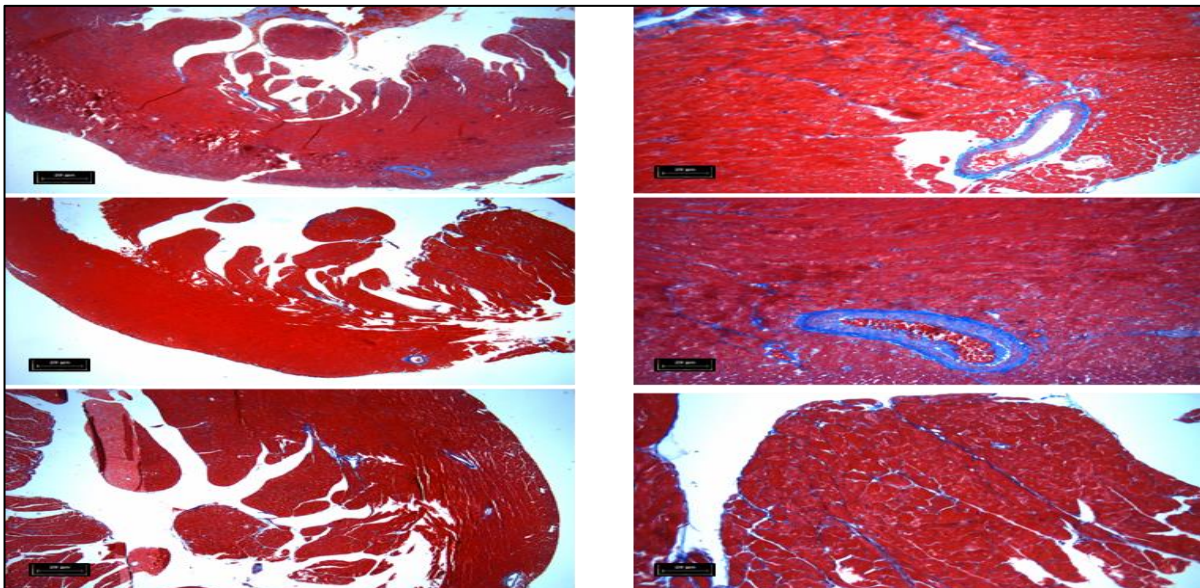
Figure 4.18: Examples of fibrous tissue (blue colour) in ageing hearts with HFD. Objective lens magnification x4 and x20. Scale bar is 20 microns.

4.3.4.4   Changes in Capillary/Myocyte Ratio in Ageing Heart with High-Fat Diet

Immunohistology staining Isolectin biotin 4 (IB4) was used to stain capillaries with a brown colour. Images taken from the left ventricle of the hearts were used to measure capillary/cardiomyocyte ratio, and this ratio was significantly decreased ($P = 0.03$) from an average of 2.3 ± 0.03 with ND to 2.1 ± 0.05 with HFD in ageing hearts (figure 4.19).
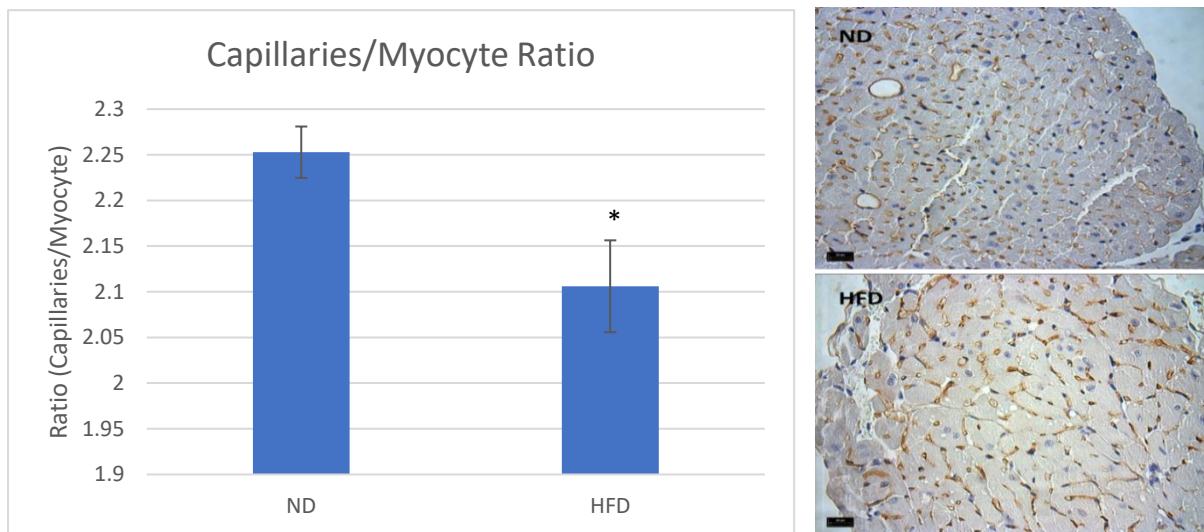
Figure 4.19: Capillary/myocyte ratio in ageing mice hearts with and without HFD. Quantification was done using Isolectin biotin 4 (IB4) stained heart sections. Data are presented as mean ± SEM. Data were analysed using the unpaired t-test. * = $P < 0.05$ vs. ND. N= 5 for each group. Images show an example of ND and HFD hearts. Objective lens magnification x40. Scale bar is 20 microns.

4.3.5 Ultra-structural Changes

4.3.5.1   Changes in Diastolic Sarcomere Length in Ageing Hearts with High-Fat Diet

Diastolic sarcomere length in ageing cardiomyocytes increased slightly but not significantly with HFD, from an average of 2.02 ± 0.1 μm in the ND hearts to an average of 2.3 ± 0.3 μm in the HFD hearts as seen in figure 4.20.
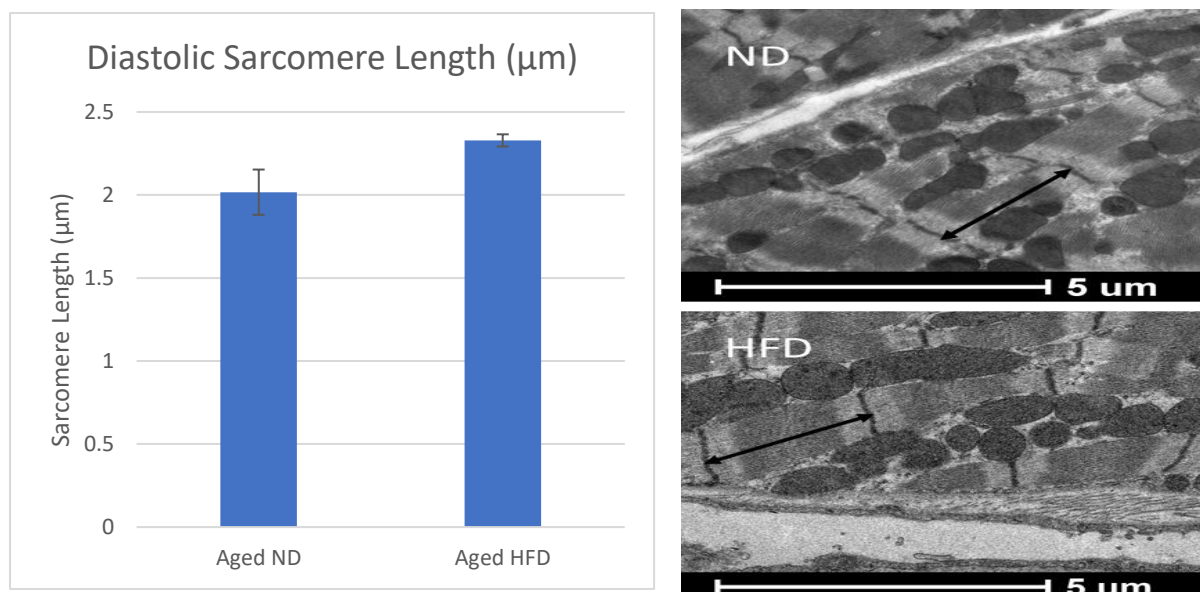
Figure 4.20: Diastolic sarcomere length in ageing mice hearts with and without HFD. A total of 200-300 sarcomeres were measured from 3-4 different areas in each heart. Data are presented as mean ± SEM. Data were analysed using the unpaired t-test. N= 4 for each group. Image on the right shows electron micrographs from aged ND heart (top) and aged HFD heart (bottom) with sarcomere length defined (black arrows).

4.3.5.2   Changes in Mitochondrial Sub-Population Distribution in Ageing Hearts with High-Fat Diet

The distribution or density of mitochondria and each of its subpopulations was measured in both groups. In the ND hearts, the total mitochondrial area was 32 % of the myocyte, with the IF comprising 25 % of total myocyte area, followed by the SSL mitochondria comprising 6 % of this area, and finally the PN mitochondria covering only 1 %. With HFD, the total mitochondrial area was increased to 35 % of the myocyte, with IF mitochondria comprising 2 3%, SSL 8 %, and PN 4 % of total myocyte area (figure 4.21).
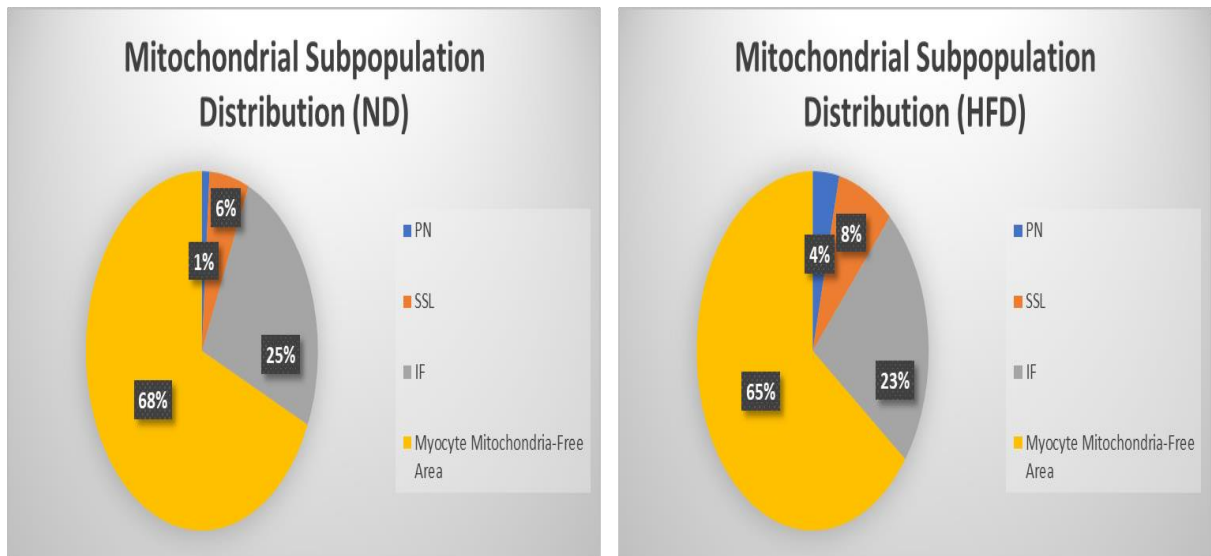
Figure 4.21: Mitochondrial sub-population distribution in ageing mice hearts with and without HFD. Figure shows the percentage of myocyte covered the percent of each mitochondrial sub-population in both groups. N= 4 for each group. 3-4 areas of each heart were used to measure the mitochondrial distribution.

Comparing these figures to understand the effects of HFD on the mitochondrial density in the ageing heart, no significant change was found between the percentage of myocyte area covered by total mitochondria. However, the percentage of each subpopulation of total mitochondrial area is significantly increased for PN and SSL mitochondria with HFD ($P = 0.01$ for PN, and $P = 0.029$ for SSL) (figure 4.22).
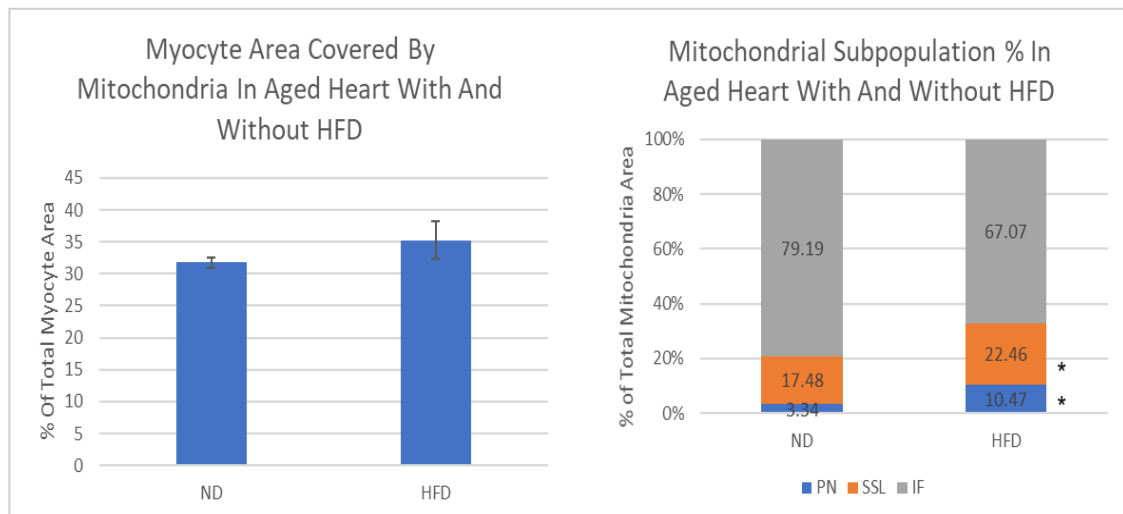
Figure 4.22: Mitochondrial % of total myocyte area and subpopulation % of total mitochondrial area in ageing hearts with and without HFD. Data are presented as mean ± SEM. Data were analysed using the unpaired t-test. * $P < 0.05$ vs. ND. N= 4 for both groups.

4.3.5.3   Changes in Mitochondrial Sub-Population Morphometry

Before comparing the mitochondrial subpopulation morphometry between the two groups, we compared the different subpopulations with one another within one group.

4.3.5.3.1 Mitochondrial Sub-Population Morphometry in Ageing Normal Diet Hearts

Mitochondrial morphometry in the ageing ND hearts has been described in detail in chapter 3 results under the section (Mitochondrial sub-population morphometry in ageing hearts).

4.3.5.3.2 Mitochondrial Sub-Population Morphometry in Ageing High-Fat Diet Hearts

When comparing the three subpopulations of mitochondria in the ageing HFD heart, the PN mitochondria appeared to be smaller in size and shorter in length and width, and they were more rounded in shape compared to the other two subpopulations (figure 4.23). However, the only significant differences were the length of PN mitochondria compared to IF mitochondria ($P = 0.005$) and their size compared to IF mitochondria ($P = 0.03$). PN mitochondria length averaged 0.91 ± 0.04 μm compared to 1.2 ± 0.03 μm for IF mitochondria. In size, PN mitochondria in ageing HFD hearts averaged 0.55 ± 0.05 μm^2 compared to 0.76 ± 0.04 μm^2 in IF mitochondria. Additionally, SSL mitochondria were significantly shorter in length averaging at 0.97 ± 0.05 μm compared to IF mitochondria ($P= 0.046$).
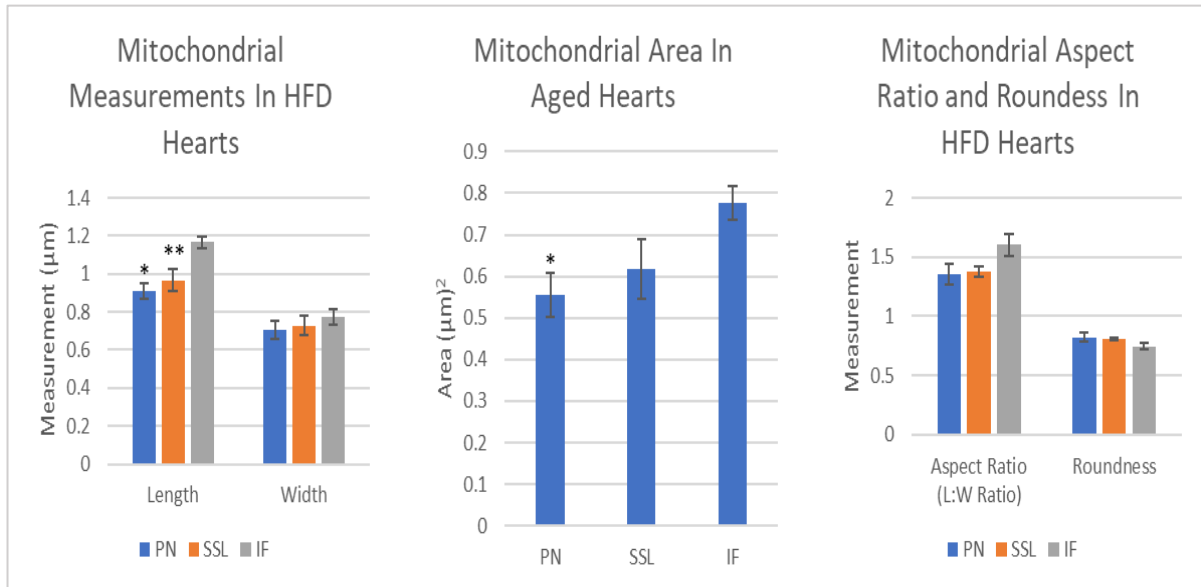
Figure 4.23: Mitochondrial sub-population morphometry in ageing hearts with HFD. A) Mitochondrial length and width. B) Mitochondrial size. C) Mitochondrial roundness and aspect (L/W) ratio. Data are presented as mean ± SEM. Data were analysed using one-way ANOVA followed by the Bonferroni and Games-Howell post-hoc tests. * = $P < 0.05$ vs. IF, ** = $P < 0.05$ vs IF mitochondria. N= 4. ≈ 100 mitochondria of each subpopulation were measured in each heart.

4.3.5.3.3 Changes in Mitochondrial Sub-Population Morphometry in Ageing Hearts with High-Fat Diet

I. *Perinuclear Mitochondria*

With HFD, PN mitochondria became significantly larger with an increase in both length and width and became more rounded in shape (figure 4.24). Length of PN mitochondria with HFD averaged 0.91 ± 0.04 μm compared to 0.67 ± 0.04 μm in ND ageing hearts ($P = 0.009$). Width of PN mitochondria increased to an average of 0.71 ± 0.04 μm in ageing HFD hearts compared to 0.42 ± 0.01 μm in ageing ND hearts ($P = 0.004$). PN mitochondrial size also increased to 0.55 ± 0.05 μm^2 in ageing HFD hearts compared to 0.25 ± 0.02 μm^2 in ageing ND hearts ($P = 0.006$). Finally, the aspect ratio and roundness of PN mitochondria did not change significantly with HFD in ageing hearts.
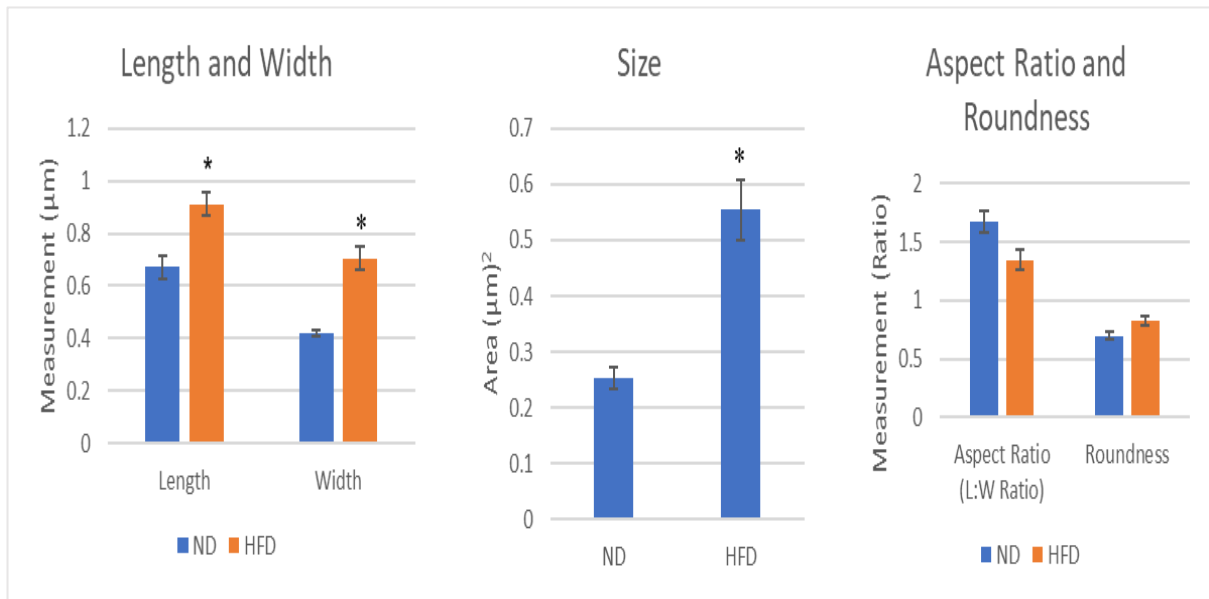
Figure 4.24: PN mitochondria morphometry in ageing hearts with and without HFD.
A) Mitochondrial length and width. B) Mitochondrial size. C) Mitochondrial roundness and aspect (L/W) ratio. Data are presented as mean ± SEM. Data were analysed using unpaired t-test. * = $P < 0.05$ vs. ND. N= 4 for each group. ≈ 100 mitochondria of each subpopulation were measured in each heart.

II. _Subsarcolemmal Mitochondria_

SSL mitochondria also changed with HFD in the ageing heart as they appeared to be larger (longer and wider) and became more rounded (figure 4.25). Significantly, SSL mitochondria in ageing hearts increased in width, size, and roundness with HFD. Average width of SSL mitochondria in the ageing heart increased from 0.51 ± 0.01 μm to 0.73 ± 0.05 μm with HFD ($P = 0.012$). The size of SSL mitochondria also increased in the ageing heart from an average of 0.37 ± 0.02 μm^2 to 0.63 ± 0.07 μm^2 with HFD ($P = 0.047$). Finally, the roundness of SSL mitochondria increased from 0.71 ± 0.03 to 0.8 ± 0.01 in ageing hearts with HFD compared to ND hearts ($P = 0.015$).
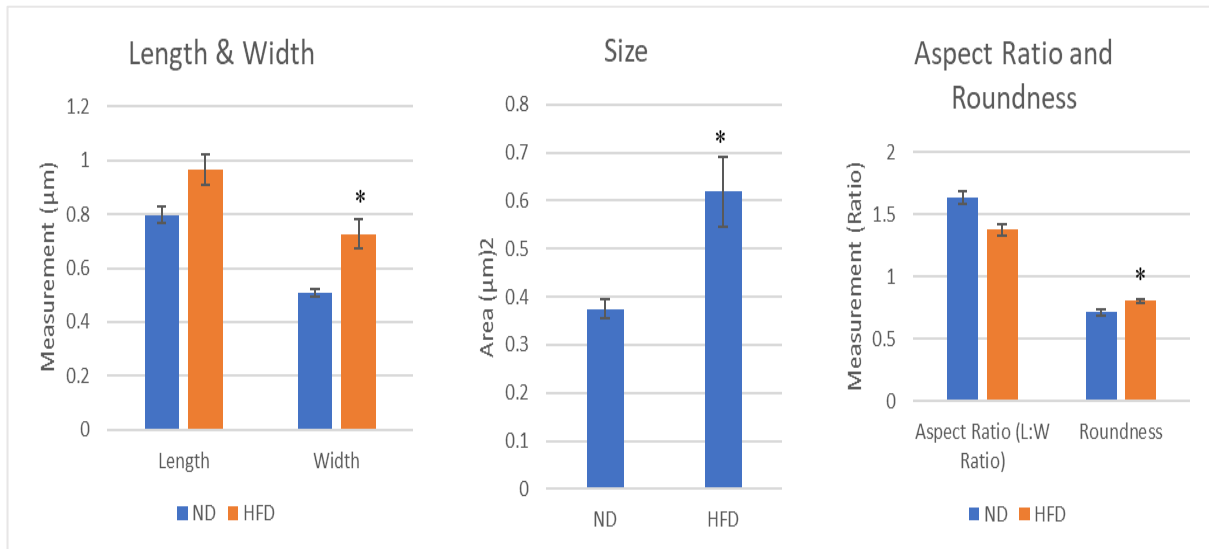
Figure 4.25: SSL mitochondria morphometry in ageing hearts with and without HFD. A) Mitochondrial length and width. B) Mitochondrial size. C) Mitochondrial roundness and aspect (L/W) ratio. Data are presented as mean ± SEM. Data were analysed using unpaired t-test. * = $P < 0.05$ vs. ND. N= 4 for each group. ≈ 100 mitochondria of each subpopulation were measured in each heart.

III.   *Interfibrillar Mitochondria*

For IF mitochondria, HFD in the ageing heart seemed to have an effect on mitochondrial dimensions (length, width, and size) but not shape (figure 4.26). IF mitochondria became significantly larger with increase in both length and width with HFD. Length of IF mitochondria increased significantly from an average of 0.9 ± 0.01 μm to 1.17 ± 0.03 μm in ageing hearts with HFD ($P = 0.001$). Additionally, the width of IF mitochondria also increased significantly from an average of 0.57 ± 0.002 μm to 0.77 ± 0.04 μm in ageing hearts after HFD ($P = 0.008$). The size of IF mitochondria in ageing HFD hearts increased to 0.78 ± 0.04 μm^2 from an average of   0.46 ± 0.004 μm^2 in ND ageing hearts ($P = 0.001$).
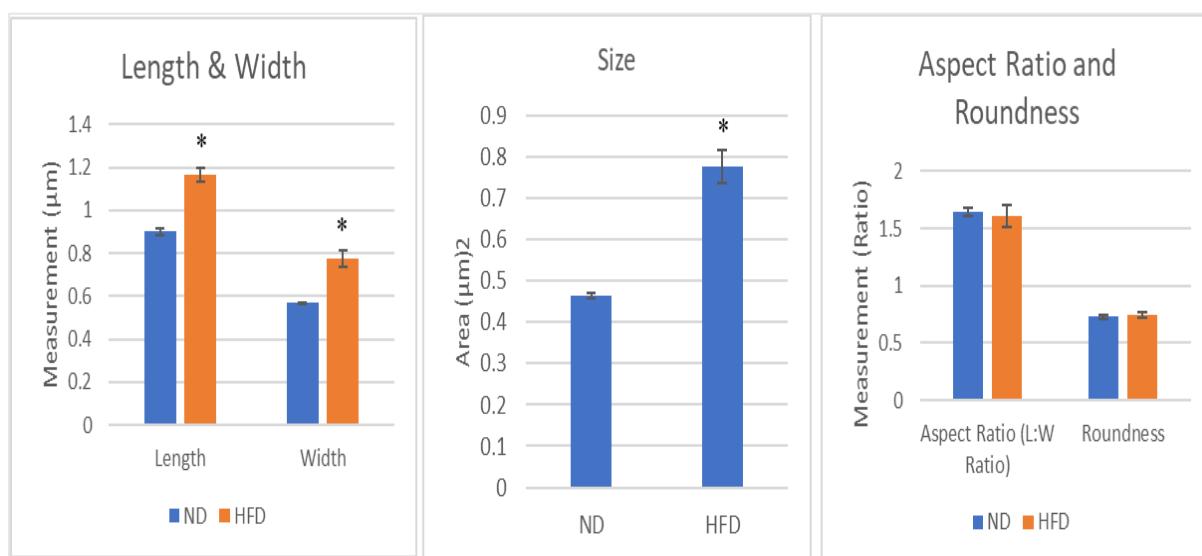
Figure 4.26: IF mitochondria morphometry in ageing hearts with and without HFD.
A) Mitochondrial length and width. B) Mitochondrial size. C) Mitochondrial roundness and aspect (L/W) ratio. Data are presented as mean ± SEM. Data were analysed using unpaired t-test. * = $P < 0.01$ vs. ND. N= 4. ≈ 100 mitochondria of each subpopulation were measured in each heart.

4.3.5.4　　Mitochondrial Fission and Fusion Proteins

With HFD, mitochondria seemed to become more rounded in the ageing heart (only significantly in the SSL mitochondria), and this indicate fission of mitochondria, which is supported by the significant decrease in mitochondrial fusion protein Opa1 in ageing HFD hearts (figure 4.27). Fusion protein Mfn2 was also downregulated with HFD, and Mfn1 was upregulated with HFD in the ageing heart, but none of these changes were significant. On the other hand, fission proteins Fis1 and Mff were also downregulated with HFD in the ageing heart; with Mff reduction being significant.
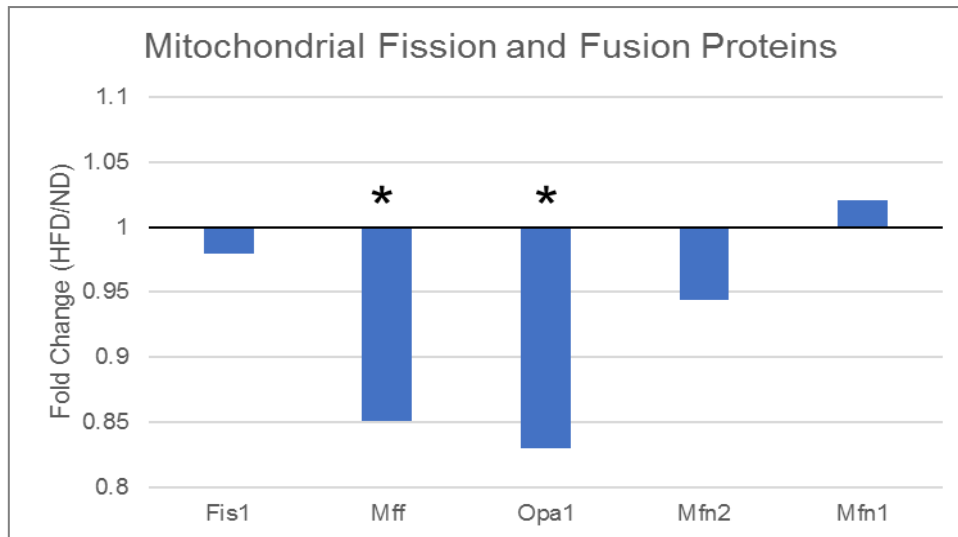
Figure 4.27: Mitochondrial fission and fusion proteins in ageing mice hearts with and without HFD. Data are expressed as fold change (HFD/ND). Data were analysed using the unpaired t-test. * = $P < 0.05$. n = 5 for each group.

4.3.5.5 Changes in Lipid Content (Lipid Droplet Count) in Ageing Hearts with High-Fat Diets

Lipid content (lipid droplet count) increased slightly in ageing hearts with HFD from an average of 0.05 ± 0.01 to an average of 0.06 ± 0.006 droplets/μm^2, but this change was not significant (figure 4.28).
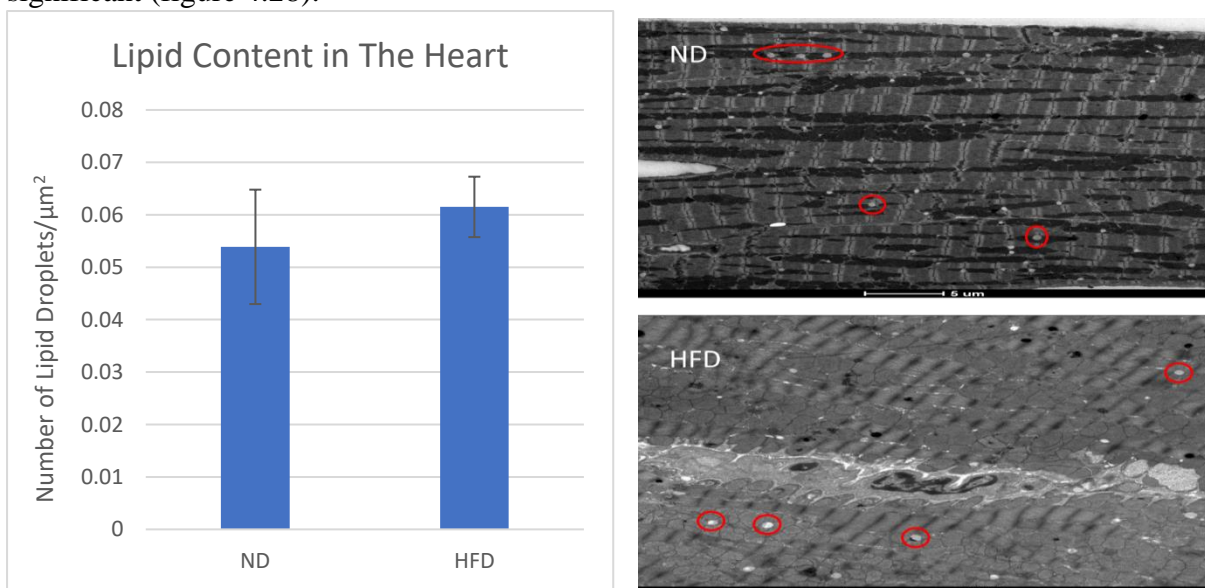
Figure 4.28: Lipid content (droplet count) in ageing hearts with and without HFD. Data are presented as mean ± SEM. Data were analysed using unpaired t-test. N= 4 for each group. 3-4 areas from each heart were used for counting number of lipid droplets.

4.4   Discussion

4.4.1 Key Findings

Unlike earlier work with young adults, feeding aging mice HFD was associated with marked obesity and significantly higher plasma VLDL and LDL levels, but lower glucose and lactate levels. HFD was also associated with atherosclerosis, smaller coronary arteries with smaller lumen sizes, and a higher artery wall/artery size and lumen size ratios. Additionally, HFD reduced capillary/myocyte ratio and increased fibrosis in ageing hearts.

Metabolic alterations in the ageing heart after HFD included reduced total energy rich phosphates, which was associated with altered mitochondrial morphometry in the ageing heart as they became larger in size and more rounded. Mitochondria also became more densely distributed (but only PN and SSL).

For protein expression, the majority of proteins that changed with HFD decreased. These included mitochondrial proteins and carbohydrate metabolism. Proteins that increased with HFD included structural (collagen) proteins, and proteins related to apoptosis and lipid metabolism. Some of the antioxidant enzymes (e.g. catalase and superoxide dismutase) increased while others (e.g. glutathione peroxidase 7) decreased with HFD. Similarly, ionic channel-related proteins changed significantly with some being upregulated whilst others were downregulated after HFD in the ageing heart. Phospho-proteins were also mainly downregulated with HFD in the ageing heart and they included ionic transport, cardiac signalling and apoptosis, carbohydrate metabolism, transport, structural proteins, and enzymes.

4.4.2 Ageing Mice Weights and Body Fat Increased Significantly with High-Fat Diet

Ageing mice had significant weight gain with a significant increase in body fat with HFD, and no change in heart weight.

An increase in body weight and fat percentage is commonly seen with HFDs that alter energy metabolism and cause various changes contributing to obesity, and this is seen in different animal species as well as humans [361, 363-366].

The energy content of the normal diet used here was 16.26 mJ/kg derived from 22 % protein, 13 % fat, and 65 % carbohydrates. The energy content of the HFD used was slightly higher (19.67 mJ/kg), derived from 45 % fat, 18 % carbohydrates, and 37 % proteins.

Even though food consumption was not measured for these animals, we cannot conclude that the weight gain in the HFD group was caused by increased intake. A study using the same diets was done previously by a colleague, and food consumption of the mice was not measured as well [367]. However, the HFD had a slightly higher energy content which could have contributed to the weight gain in mice. Additionally, a few studies on feeding behaviour in mice given HFD showed that switching from a normal diet to a palatable HFD changed feeding behaviours in mice and promotes hyperphagia, which could explain the obesity seen in our HFD mice [368, 369].

4.4.3 Ageing Mice had Significantly Higher Plasma Lipids, and Significantly Lower Glucose and Lactate Levels with High-Fat Diet

HFD mice had elevated plasma lipids with LDL and VLDL lipids significantly increasing, and low plasma carbohydrate metabolites, with glucose and lactate being significantly lower.

Generally, HFDs with high saturated fats (like the diet used in this study) are associated with increased LDL and VLDL lipids in the plasma, and increased glucose levels as insulin resistance develops [370-372]. Lower levels of fasting plasma glucose (though not significant)

with HFD were reported in both adult and aged mice [373]. Another study also showed insignificant decrease in plasma glucose levels, but only in adult mice and not aged ones [374]. Similarly, lactate measured by metabolomics is usually found to be elevated with obesity and /or HFD in mice, rats, and in human subjects [375-377]. One study reported significant decrease in urine lactate in obese Zucker rats, and explained it could have been caused by a small cohort number, which could possibly be the reason for the decrease in carbohydrate metabolites seen in our results [378].

4.4.4 High-Fat Diet Decreased Cardiac Energy Metabolites in Ageing Hearts

Three energy metabolites decreased after HFD in ageing hearts, ADP, β-NAD$^+$, and inosine. Cardiac energy charge and phosphorylation ratios did not change with HFD in the ageing heart. Normally in the heart elevated ADP levels are associated with heart failure [379]. The reason for this is, the energy reserve in the heart (phosphocreatine) is used to donate a phosphate to ADP to generate ATP via creatine kinase (CK), and elevated ADP levels indicate a reduction in the phosphorylation capacity. Our results show that both ATP and ADP levels are lower in the HFD group (even though ATP change was not significant), and this may be attributed to the decreased efficiency of the mitochondria and its phosphorylation capacity associated with both ageing (as mentioned previously) and HFD [380]. However, a difference in the reduction between ATP and ADP levels may also indicate improved phosphorylation with HFD in the ageing heart. This has been shown in livers of mice fed HFD where oxidative phosphorylation has increased in response to HF feeding, and also in liver of obese diabetic patients [381, 382]. Our phosphorylation results show an increase in the HFD group though it was not significant. NAD$^+$ has been studied in recent years for its role in combatting metabolic disturbances and mitochondrial dysfunction [383]. It has been shown to be reduced with ageing due to a reduction in its precursor nicotinamide mononucleotide (NMN) by increase in CD38 in mice

and humans, and this contributes to energy metabolic disturbances [384, 385]. NAD^+ is also reduced with HFD due to a reduction in its synthesising enzyme nicotinamide phosphoribosyltransferase (NAMPT) [383].

Inosine is a metabolite that is important for nucleotide synthesis through the salvage pathways especially during stress such as ischaemia, as well as inducing other cell-protective activities [386, 387]. As explained in the discussion of energy metabolites in chapter 3 (page 127), inosine is a by-product of ATP metabolism. Lower inosine levels in the HFD ageing heart might be merely due to its breakdown to hypoxanthine, but since hypoxanthine levels were not measured here, we cannot make this conclusion.

4.4.5 Majority of Cardiac Proteins were Downregulated with High-Fat Diet in Ageing

Ageing mice hearts' proteome profile changed with HFD compared to the ND controls. 4983 proteins were detected to be significantly different after HFD with the majority being downregulated and only 33 % were upregulated.

A number of studies investigating the effects of HFD on the proteome profile have been done examining different organs and in various species. A study in mice fed HFD showed alteration in 15 proteins related to structure, energy metabolism and citric acid cycle, and fatty acid oxidation [388]. Effects of HFD on protein expression of the heart was also studied in rats and showed an alteration in proteins involved in mitochondrial dynamics, where they were mainly downregulated with HFD [380]. The effects of HFD on the proteome was also studied in skeletal muscle in mice, liver, the hypothalamus, and visceral white adipose tissue, with a number of changes in proteins involved in metabolism (carbohydrate, tricarboxylic acid cycle, cellular amino acid and lipid metabolic processes), cytoskeleton and synaptic plasticity, stress response, and mitochondrial function [389-394].

Remodelling of the cardiac proteome profile after HFD was also studied in elderly mice [395]. The proteomic analysis revealed 417 proteins that have been altered with HFD in aged mice hearts, with most of the upregulated proteins being involved in oxidative phosphorylation, while downregulated proteins were mainly involved in cytoskeletal organisation.

It is important to note that the effects of HFD on the proteomic remodelling varies between strains [396]. C57Bl/6J and 129Sv mice were subjected to high fat feeding for the same period, and the proteomics analysis showed a domination of the peroxisomal β-oxidation proteins and lipogenesis proteins in both strains, respectively.

4.4.5.1   Mitochondrial Proteins were Mainly Downregulated in Ageing Hearts after High-Fat Diet

Mitochondrial proteins were mostly downregulated with HFD (87 %) in the ageing heart, with only 8 proteins being upregulated. This is consistent with other work in the literature as mitochondrial protein levels decrease with the decline in mitochondrial function seen with HFD [380]. The authors in this study reported a decline in most mitochondrial proteins in rat hearts involved in fatty acid oxidation, complex I and V, mitochondrial fusion, and energy metabolism.

4.4.5.2   High-Fat Diet Upregulated and Downregulated Ionic Transport-Related Proteins in Ageing Hearts

Six proteins changed with HFD in the ageing heart, 3 were downregulated and 3 were upregulated. Upregulated proteins were Sodium channel subunit beta-4, Voltage-dependent L-type calcium channel subunit alpha-1D which mediates the entry of calcium ions into excitable cells, and Store-operated calcium entry-associated regulatory factor which protects the cell from increased cellular calcium levels. Downregulated proteins were Potassium voltage-gated channel subfamily KQT member 1 potassium channel, Sodium/potassium-transporting ATPase subunit alpha which is involved in the exchange of sodium and potassium ions across

cell membrane creating a gradient to actively transport nutrients across the membrane, and chloride channel protein.

Ion channel proteins that have been indicated in models of HFD induced obesity are Potassium voltage-gated channel subfamily KQT member 1 potassium channel (KCNQ1), expression was increased but not protein levels in HF fed rats [397]. This specific protein was downregulated after HFD in our work, but animals used in the previously mentioned study were not aged. None of the other proteins were reported to be changed in expression or protein levels in models of HFD [398].

4.4.5.3 Antioxidant Enzymes Changed Significantly with High-Fat Diet in the Ageing Heart

HFD's effect on antioxidant proteins in the ageing mice hearts was not consistent, as some proteins were downregulated, and others were upregulated.

A study on the effect of HFD on serum antioxidant proteins in rats showed somewhat similar results, as catalase was upregulated and glutathione peroxidase was downregulated with HFD [399]. However, superoxide dismutase in the study was also downregulated contradictory to the upregulation seen in our results with HFD. Another study showed a reduction in all antioxidant enzymes after HF-feeding in the liver, heart, kidney, intestines, and aorta in rats [400]. Another study in mice fed HFD showed an elevation in glutathione peroxidase in adipose tissue but not in the liver after HF-feeding, with no change in superoxide dismutase level [401]. Additionally, another study on the effects of HFD on antioxidant enzymes in rat liver, heart, and kidney showed a significant reduction in both glutathione peroxidase and glutathione s-transferase (consistent with our findings), but no change in catalase except in the kidney where it was also reduced with HFD [402].

These conflicting findings may be attributed to the different samples/tissues used, and different methods/assays of measurements. Also, none of the studies referenced used ageing animals.

4.4.5.4 High-Fat Diet Upregulated Apoptosis Related Proteins in the Ageing Heart

Three apoptosis related proteins increased in the ageing heart with HFD. BCL2-associated athanogene 3 is an anti-apoptotic protein that acts as co-chaperone to HSP70 and HSC70. Bcl-2-associated transcription factor 1 is a pro-apoptotic protein that promotes death by repressing transcription. Cell division cycle and apoptosis regulator protein 1 is a pro-apoptotic protein that also acts on p53 activation.

As discussed earlier in the previous chapter, apoptosis increases with ageing in the heart (page 132). HFD has also been associated with increased pro-apoptotic proteins and reduced anti-apoptotic proteins in various species.

anti-apoptotic proteins such as BCL-2 with HFD [403-408].

The increased expression of the two pro-apoptotic proteins in our results can be justified as seen in the literature. The increased expression of the anti-apoptotic protein in our results on the other hand can be a compensatory mechanism for increased in pro-apoptotic proteins.

4.4.5.5 Structural (Collagen) Proteins were Upregulated with High-Fat Diet in the Ageing Heart

With HFD, different alpha chains (1, 2 and 3) of collagen 4, 6 and 18 were all upregulated in the ageing heart after HFD.

Data from the literature supports this effect of HFD on collagen expression. HFD increases cardiac fibrosis (perivascular and interstitial) [409]. Collagen protein expressions also tend to be upregulated in HFD. In Sprague–Dawley (SD) rats fed a normal or HFD for 24 weeks, hearts from the HFD group had significantly increased fibrosis and increased expression of collagen 1, 2, 3 and 4, in addition to an increase in connective tissue growth factor [361]. Additionally, in C57BL/6 mice fed a HFD for 20 weeks, collagen deposition and expression of type 1 and 3 were increased compared to ND fed mice [410].

4.4.5.6 Carbohydrates Metabolism Proteins were Downregulated with High-Fat Diet in the Ageing Heart, While Lipid Metabolism Proteins were Mainly Upregulated

Carbohydrate metabolism and transport proteins were downregulated with HFD in the ageing heart, while the majority of lipid metabolism and transport proteins were upregulated.

HFD usually leads to dyslipidaemia and insulin resistance, and this leads to decreased glucose uptake and increased lipid uptake for metabolism, which may explain the alterations seen in metabolism protein levels. This is consistent with other studies where HFD caused a suppression in glucose uptake and metabolism protein expression, and an adaptive elevation in FA uptake and metabolism proteins [199, 411].

Another study in mice also showed that carbohydrate uptake and metabolism protein GLUT4 (which is already downregulated in ageing) and hexokinase II were downregulated with HFD [210]. FA enzyme acetyl-CoA carboxylase (which regulates CPT I by malonyl-CoA as mentioned in the introduction) was upregulated in HFD hearts indicating a shift towards decreasing FA uptake due to the heart being saturated with FAs. The increase in FA metabolism enzymes in our work (even though FA metabolism decreases in the aged heart), can be a compensation of the heart to the increased amounts of FFAs in the plasma to increase uptake and metabolism.

4.4.6 High-Fat Diet Downregulated the Majority of Phospho-proteins in Ageing Hearts

As with the changes in proteome profile, the majority of phospho-proteins in the ageing heart were also downregulated with HFD. The effects of HFD on protein phosphorylation has been studied. A few studies reported these effects on mouse brain tissue, white adipose tissue, and liver [412-414]. However, no data was found on cardiac protein phosphorylation with HFD.

Pospho-proteins were categorised into ionic transport, cardiac signalling and apoptosis, carbohydrate metabolism, transport, structural proteins, and enzymes. The only upregulated

phospho-protein was a structural protein (Actin-binding LIM protein 1), which is involved in the bundling of actin filaments, and phosphorylation at S475 of this protein was upregulated with HFD. There is no data in the literature on the phosphorylation at this specific site.

For the downregulated phospho-proteins, calcium channel protein ryanodine receptor 2; which mediates the release of calcium from the sarcoplasmic reticulum into the cytoplasm, controlling cardiac contraction, was downregulated in phosphorylation at S2367 with HFD [415]. There is no information on the relevance of phosphorylation on this specific site. However, Phosphorylation on S2807 and S2813 increases the open probability of this channel; which is increased in heart failure [416, 417]. Additionally, phosphorylation at S2030 enhances the response to luminal calcium [416].

SERCA2A is another important proteins that is involved in the regulation of contraction and relaxation, as it translocate calcium from the cytosol back to the SR using ATP [418]. HFD reduced phosphorylation at S680 in the ageing heart, but no data in the literature were found on this specific site.

Pyruvate dehydrogenase E1 component subunit alpha, somatic form, mitochondrial is an enzyme that links the glycolytic pathway to TCA cycle as it catalyses the conversion of pyruvate into acetyl-CoA [419]. Phosphorylation at S293 inactivates the enzyme, and this was reduced in the ageing heart after HFD indicating increased activity of the enzyme and utilisation of glucose for oxidation. Another protein involved in carbohydrate metabolism is glycogen synthase which is involved in glycogen biosynthesis. Its phosphorylation at S657 was decreased after HFD, and this phosphorylation is required for inhibitory phosphorylation at S641, S645, S649 and S653. Heat shock protein 90 beta is another protein downregulated in phosphorylation at S226 and S255 with HFD in the ageing heart. This is amolecular chaperone involved in cell survival. Phosphorylation at the two sites mentioned inhibits AHR interaction (AHR is a client of HSP90 and promotes carcinogenesis). Heat shock protein HSP 90-alpha is

another chaperone protein involved in survival signalling. Its phosphorylation at S231 and S263 decreased with HFD in the ageing heart, but there is no data in the literature on these phosphorylation sites.

Several structural proteins have also been downregulated in their phosphorylation by HFD in the ageing heart. Microtubule-associated protein tau is a protein responsible for the integrity and stability of microtubules. Its phosphorylation at numerous serine and threonine sites leads to its detachment from microtubules and their disassembly. Phosphorylation in the ageing heart at S712 was downregulated, indicating more structural stability in these hearts with HFD. Finally, caveolae associated protein 1 plays a role in the formation and organisation of caveolae [420]. Its phosphorylation at S42 was downregulated with HFD in the ageing heart, but no information is available in the literature on this phosphorylation site.

4.4.7 High-Fat Diet Decreased Sizes of Coronary Arteries and their Lumen, and Increased Artery Wall/Artery Size and Lumen Size Ratios in Ageing Hearts

Coronary arteries in the ageing heart became smaller with HFD (total artery size and lumen size), and the wall/total artery size and lumen size ratios increased significantly indicating a thicker artery wall.

The effect of HFD on the vasculature has been studied and showed endothelial dysfunction with HFD-induced obesity [421]. When it comes to the morphometry of the vessels, HFD increased the wall thickness (specifically the media) of the thoracic aorta in rats after 18 weeks of feeding, with a decrease in the lumen diameter [422]. This suggests that the artery size did not change but the wall became thicker. Another study in mice showed a significant increase in the tunica adventitia/tunica media ratio after 8 weeks of HFD [423]. In pigs fed HFD for 16 weeks, there were no differences in the coronary artery sizes or wall thickness compared to the control group [424]. Comparing small resistance arteries from abdominal subcutaneous tissue, obese subjects had significant increased wall (media) thickness, smaller lumen diameter (not

significant) and significantly larger cross-sectional area compared to lean controls [425]. The authors suggested the growth in artery wall is secondary to vascular smooth muscle cell growth that is related to obesity-associated factors such as the release of norepinephrine, adipocytokines, tumour necrosis factor-α, and leptin.

4.4.8 High-Fat Diet Increased Fibrosis in Ageing Hearts

Aged hearts had significantly increased fibrosis (interstitial and perivascular) with HFD compared to the ND group.

As discussed previously in the collagen proteins section (page 190), HFD is associated with cardiac fibrosis. Increased inflammation and oxidative stress associated with HFD contributes to the fibrosis in the heart, alongside other factors such as metabolic dysregulation [426]. However cardiac fibrosis has been reported in experimental models of HFD with the absence of metabolic dysregulation and hypertension [427].

4.4.9 High-Fat Diet Reduced Capillary/Myocyte Ratio in Ageing Heart

As mentioned previously, capillary/myocyte ratio is an important determinant for myocyte oxygen supply [342]. In our work, HFD reduced this ratio significantly in the ageing heart.

Findings in the literature were contradictory. In a study in mice fed HFD, capillary/myocyte ratio was not affected in the skeletal muscle of the soleus [428]. Another study found that HFD lead to increased capillary density in the quadriceps femoris muscle in mice suggesting improved capillary angiogenesis with HFD [429]. However, in the heart, a study in mice fed HFD for 17 weeks showed no change in capillary/myocyte ratio compared to the control group [430]. Another study in mice showed that HFD decreased levels of hypoxia inducible factor 1α and 2α in the heart, through increased ROS production, which in turn was associated with a decreased capillary/myocyte ratio (as seen in our results) [208].. Additionally, reduced capillary density was also observed in human heart in association with obesity [431].

HIF signalling is important for angiogenesis and an impairment in this pathway results in a decrease in the angiogenesis capacity. From our proteomics data, HIF protein was significantly downregulated in the ageing heart after HFD, which might support the impairment in angiogenesis capacity of these hearts and justifies the lower capillary/myocyte ratio found in our results.

4.4.10 High-Fat Diet did not Change Sarcomere Length in Ageing Hearts

Sarcomere length did not change with HFD in the ageing heart compared to ND.

Not many studies looked at the effects of HFD on sarcomere length, but in one study HFD was reported to be associated with a decrease in sarcomere length [432]. However, this study used adult mice and not aged ones, which could be the reason for the difference in findings.

As described previously, sarcomere length is indicated in the contractility force of the heart. A decrease in sarcomere length is associated with lower calcium responsiveness and a weaker contraction force. This is not indicated in HFD hearts in this study.

4.4.11 Mitochondria Became Larger in Size, More Rounded, and More Densely Distributed in Ageing Hearts after High-Fat Diet

Ageing hearts from mice fed HFD had an increased total myocyte area covered by mitochondria. Though this increase was not significant overall, it was significantly increased for two of the three subpopulations of mitochondria (PN and SSL) but not for IF mitochondria. Additionally, mitochondria in ageing hearts after HFD became larger in size (significantly for all three subpopulations) and rounder (significant for SSL mitochondria). Fusion proteins (Opa1 and Mfn2) were downregulated after HFD, which supports the fact that the mitochondria became more rounded in shape rather than being elongated (fused). There are not many studies that examined the effects of HFD on cardiac mitochondrial morphometry, and none were done in the ageing heart.

One study in rats fed HFD showed a decrease in mitochondrial density and size compared to controls [221]. Another study in mice fed HFD reported the mitochondria becoming smaller in size and decreased in density, with fusion protein Opa1 decreasing (as seen in our results) but Mfn2 increased, and Mfn1 did not change [236]. A possible reason for the difference found in our results is the age, as none of the studies mentioned were done using aged animals.

4.4.12 High-Fat Diet did not Increase Lipid Deposits in the Ageing Heart

There was no change in lipid droplet count with HFD in the ageing heart. However, there was a large scatter in the data (count) of the lipid droplets/area^2 of the ND hearts, and when the outliers were excluded from the analysis HFD hearts showed a significant increase in lipid content compared to their ND controls. Using a larger sample size might be needed for further investigation.

Additionally, HFD hearts also had significantly higher levels of perilipin proteins (Plin2 and Plin5) but lower levels of (Plin3) (this was taken from the proteomics data but was not used in the results section). Pirilipin is a protein involved in lipogenesis and lipolysis, and it protects the TAG in lipid droplets from lipolysis, which increases storage. This supports increased lipid storage (droplet count) in HFD hearts.

4.5   Summary and Conclusion

To summarise the findings in this chapter, ageing mice fed HFD had significant increases in body weight and body fat percentage (epididymal fat pads), but no change in heart weight. The obesity observed in these animals is a normal response to high-fat feeding. With the obesity, certain metabolic parameters also changed significantly in the HFD group including increased levels of plasma lipids (with LDL and VLDL increasing significantly). Unexpectedly, carbohydrate metabolites in the serum were decreased in the HFD group (glucose and lactate significantly). Even though this is not a normal response seen in HFD models in the literature,

it has been reported in a few studies (but was not significant) and could also be caused by the small sample number.

Regarding the remodelling of the heart in the HFD group, alteration in cardiac energy metabolites, proteome and phospho-proteome profile, and structural and ultrastructural changes have been demonstrated. Ageing hearts with HFD had significantly lower levels of ADP, β-NAD, and inosine. ADP reduction might indicate a deficiency in mitochondrial energy production, as ATP levels were also lower than those seen in the ND ageing hearts (not significantly). However, the difference in the reduction between ATP and ADP in HFD hearts compared to ND hearts might also indicate improved phosphorylation, which has been reported in the literature with HFD. The reduction in β-NAD is normal as it is reduced with ageing due to a reduction in its precursor nicotinamide mononucleotide (NMN) in mice and humans, which contributes to energy metabolic disturbances, and also NAD$^+$ is reduced with HFD due to a reduction in its synthesising enzyme nicotinamide phosphoribosyltransferase as mentioned earlier in the discussion section.

The proteome profile showed a significant change in ageing heart after HFD with the majority of proteins being downregulated and 33 % were upregulated. Looking at proteins of the groups that we chose in relation to I/R, there was a downregulation in mitochondrial proteins which could indicate mitochondrial insufficiency. Some changes in ionic transport proteins were also observed, which could indicate a disturbance in ionic transport caused by HFD. Additionally, there was a change in antioxidant enzymes with some being upregulated such as catalase, and some being downregulated such as glutathione peroxidase 7. Apoptotic proteins were mainly upregulated which might support the increased apoptosis induced by HFD. Similarly, collagen proteins were also upregulated, and ageing hearts had significantly higher levels of fibrosis after HFD. Finally, carbohydrate metabolism proteins were downregulated while lipid metabolism proteins were mainly upregulated, which could be a response to the high-fat

feeding to increase metabolism of the excess fat provided. Because the data we have from the proteomics shows the expression of proteins rather than their activity, we cannot conclude what the changes reflect. Similarly, the phospho-proteome profile was altered with HFD in the ageing heart with the majority of proteins being downregulated. These proteins were categorised into ionic transport, cardiac signalling and apoptosis, carbohydrate metabolism, transport, structural proteins, and enzymes. Not many of the proteins had information available in the literature on the specific phosphorylation sites detected. Pyruvate dehydrogenase E1 component subunit alpha, somatic form, mitochondrial, which links the glycolytic pathway to TCA cycle, was downregulated in phosphorylation in the ageing heart after HFD at S293, which inactivates the enzymes, indicating increased activity of the enzyme and utilisation of glucose for oxidation. Glycogen synthase; which is involved in glycogen biosynthesis, was downregulated in phosphorylation at S657 after HFD, and this phosphorylation is required for inhibitory phosphorylation at S641, S645, S649, and S653. Heat shock protein 90 beta is another protein downregulated in phosphorylation at S226 and S255 with HFD in the ageing heart which inhibits AHR interaction. Finally, microtubule-associated protein tau which is responsible for the integrity and stability of microtubules, was downregulated in phosphorylation at S712 after HFD, which indicates more structural stability in these hearts as its phosphorylation at numerous serine and threonine sites leads to its detachment from microtubules and their disassembly.

Structural changes in the ageing heart after HFD included a decrease in coronary artery sizes with increased arterial wall/total artery size and lumen size ratios (thicker walls). This has been reported in the literature in different muscles and various species. In addition, ageing hearts from the HFD group had significantly higher fibrosis (interstitial and perivascular), and a lower capillary/myocyte ratio; both of which could increase the vulnerability of the heart.

Finally, HFD also changed the ultrastructure of the ageing heart mainly in the mitochondria, which became larger in size, more rounded, and more densely distributed (specially PN and SSL mitochondria). Lipid droplet count did not show a difference after HFD but that could be due to the small sample size and the large scatter found in the data, which when removed we saw a significant increase after HFD compared to ND. Figure 4.28 shows a diagram for this summary.
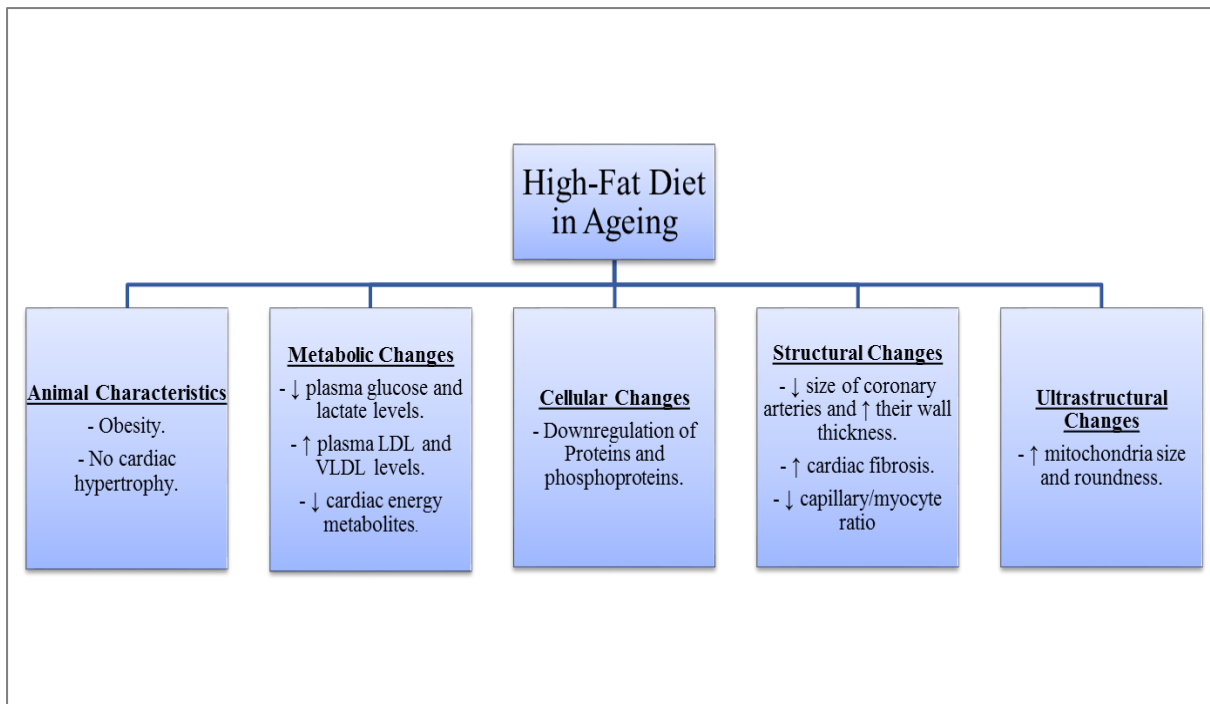
Figure 4.28: Remodelling with HFD in ageing.

5. Cardiac Vulnerability to Ischaemia/Reperfusion Injury with Ageing and with High-Fat Diet

5.1 Introduction

Cardiac vulnerability to I/R injury with ageing and with HFD in ageing have been discussed in the introduction (chapter 1, pages 48 and 55).

5.1.1 Cardiac Vulnerability to Ischaemia/Reperfusion Injury with Ageing

Mostly, reports on I/R injury in the aged heart support increased vulnerability of the heart and decreased ischaemic tolerance. Several *in vivo* and *ex vivo* experiments in mice and rats reported similar findings and associated this increased vulnerability with ageing to various factors including a decrease in oxidative phosphorylation as well as a decrease in complexes III and IV activity of the mitochondria, increased apoptosis, accumulation of intracellular sodium at the end of ischaemia, disturbances in calcium homeostasis, decrease in coronary circulation and collateral flow, and changes in AMPK-SIRT1 signalling pathways [174, 176-179, 186]. However, some studies showed contradictory findings and reported no change in cardiac vulnerability to I/R injury in both animal models (mice) and humans [183-185].

5.1.2 Cardiac Vulnerability to Ischaemia/Reperfusion Injury with High-Fat Diet

Similar to ageing, HFD effects on cardiac vulnerability and tolerance to I/R injury are contradictory. Even though obesity (which is induced by HFD in most cases) is a risk factor for cardiac disease and failure, it has been associated with lower mortality risk as well (the obesity paradox) [224]. HFD has been shown to be protective of the heart against I/R injury when consumed acutely prior to ischaemia, and also for longer periods of time [225-230]. The cardioprotective effects of the HFD were associated with various reasons including an increase in autophagy and reduction in apoptosis, a decrease in transcriptional factor of activated mitochondria (Tfam), delaying the normalisation of pH during the start of reperfusion, and insulin resistance and elevated insulin levels which activate the RISK pathways [64].

In contrast to the previous studies, HFD (including acute feeding for 2 weeks) has been associated with increased vulnerability to I/R in rats, mice, and Guinea pigs [231-233, 235-238]. Decreased tolerance to I/R was associated with a decrease in total and phosphorylated Akt, GSK-3β, eNOS expression, overexpression of NOD-like receptor pyrin domain containing 3 (Nlrp3) inflammasome, reduction in hypoxia inducible factor 2α and components of the pro-survival signalling pathway (RISK), increased inflammatory markers (tumor necrosis factor-α (TNF-α) and interleukin-6 (IL-6)) after reperfusion, and increased levels of plasma triglycerides and lipotoxicity [234].

Few studies have explored the combined effects of HFD and ageing on the vulnerability of the heart and results still show conflicting findings. One study in female mice reported that ageing has a positive effect on ischaemic tolerance, but this was lost with 6 months of HF feeding [239]. Another study in Wistar rats reported that HFD induced obesity did not affect the hearts vulnerability to regional ischaemia with ageing, but it improved it in young hearts [240].

5.2 Materials & Methods

Vulnerability of the hearts to I/R injury was measured using the Langendorff perfusion system (See Materials & Methods, page 82). Briefly, hearts were excised from freshly sacrificed mice, cannulated and perfused with Krebs-Henseleit buffer at 37° C for a stabilisation period of 20 mins. Pressure was stabilised and flow rate was monitored throughout the experiment to determine functional recovery of the hearts. Global ischaemia was then started for 35 mins, followed by an hour of reperfusion. Heart effluent was collected at various time points during the experiment to measure the degree of injury through CK release, and the heart was stained at the end of reperfusion with TTC to measure infarction percent. Figure 5.1 shows a diagram of the experimental protocol.

Figure 5.1: Diagram Showing the Perfusion Protocol.

5.3 Results

5.3.1 Vulnerability to Ischaemia/Reperfusion in the Ageing Heart

To determine the heart's vulnerability to I/R, three measurements/parameters were considered: flow rate (to determine functional recovery), CK release from the heart, alongside infarcted tissue percentage of the heart (to determine degree of injury).

5.3.1.1 Flow Rate and Functional Recovery

Adult hearts had a starting pre-ischaemic average flow rate of 2.5 ± 0.2 ml/min, which then decreased to 1.5 ± 0.1 ml/min in the first min of reperfusion (40 % decrease) and this was significant ($P = 0.005$). Flow rate increased gradually until 10 mins of reperfusion, then started to drop again until it reached 1.6 ± 0.1 ml/min at the end (60 mins) of reperfusion (36 % decrease compared to the starting flow rate) and this was also significant ($P < 0.001$). Flow rate in the adult heart was significantly lower at all time points of reperfusion compared to the starting pre-ischaemic flow rate. Comparison of flow rates in adult and ageing hearts are shown in figure 5.2.

Ageing hearts had a higher starting flow rate averaging at 3.6 ± 0.5 ml/min. Flow rate then dropped after ischaemia to an average of 2.9 ± 0.5 ml/min during the first min of reperfusion (19 % decrease). Following a similar pattern of flow rate change seen in adult hearts, flow rate in the ageing hearts also increased gradually but only until 5 mins of reperfusion before it started to decline again to reach an average of 2.5 ± 0.4 ml/min at 60 mins of reperfusion (31 % decrease). Decrease in flow rate in ageing hearts was only significantly different from the pre-ischaemic starting point at 30 mins of reperfusion ($P = 0.018$) and 60 mins of reperfusion ($P = 0.023$).
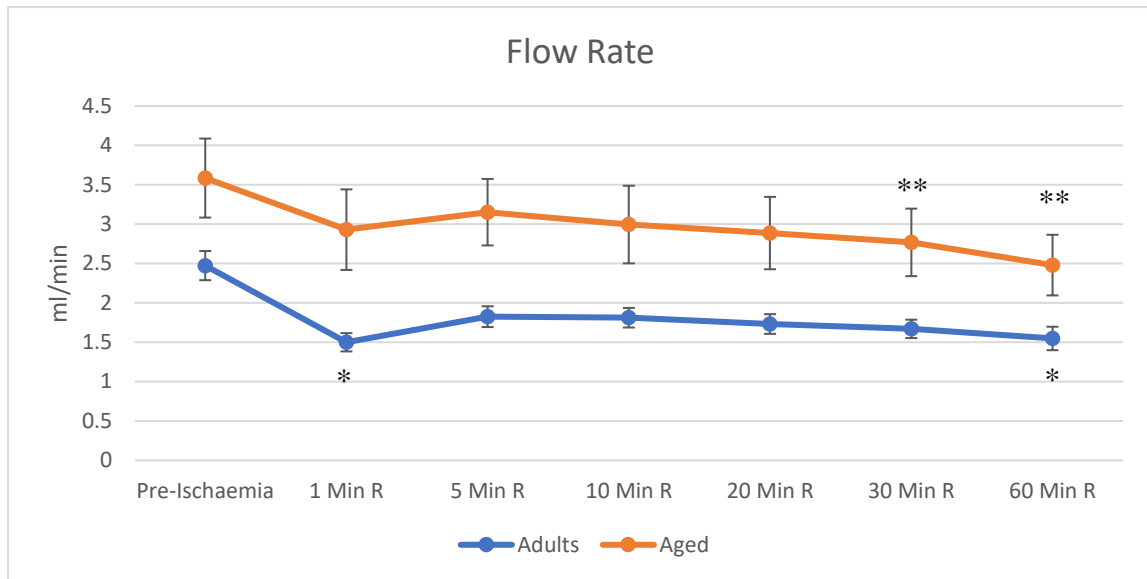
Figure 5.2: Flow rate in adult and ageing hearts. Data are presented as mean ± SEM. Data were analysed using repeated measures ANOVA. * = $P < 0.05$ vs. pre-ischaemia in the adult group, ** = $P < 0.05$ vs. pre-ischaemia in the ageing group. N = 6 for each age group.

To compare the functional recovery between both groups, we compare the percentage of change in flow rate during reperfusion. Figure 5.3 shows the flow rate as a percentage of the starting pre-ischaemic rate in both adult and aged hearts. The adult hearts seemed to have lower functional recovery as they had a larger decrease in flow rate during reperfusion than the ageing hearts compared to the pre-ischaemic flow rate within each group. Functional recovery was only significantly different at 1 min of reperfusion ($P = 0.046$), where ageing hearts had a recovery of 81 % compared to 61 % in adults, and at 5 mins of reperfusion ($P = 0.048$), where ageing hearts had 89 % recovery compared to 74 % in adults.
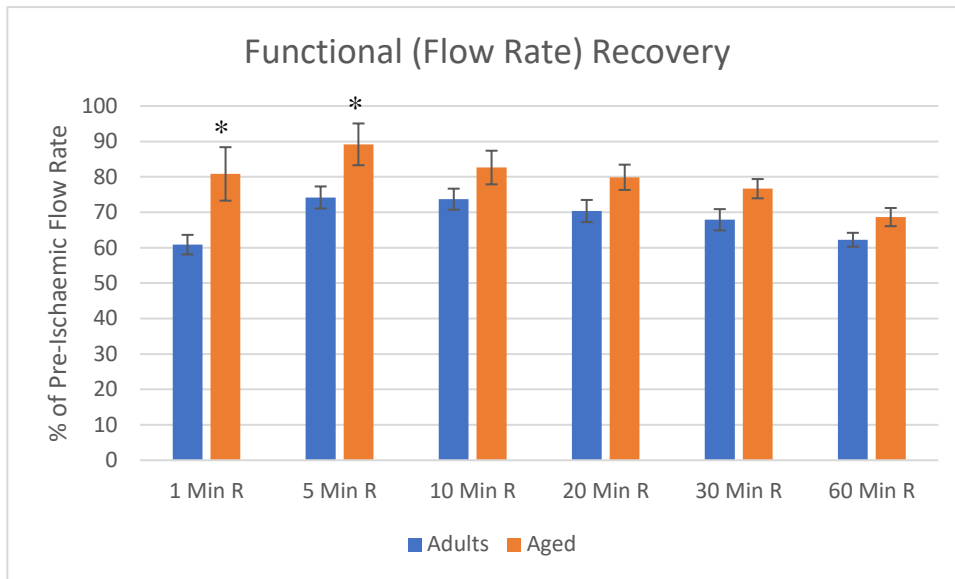
Figure 5.3: Flow rate % change from pre-ischaemic value in adult and ageing hearts. Data are presented as mean ± SEM. Data were analysed using unpaired t-test. * = *P* < 0.5 vs. adult. N = 6 for each age

5.3.1.2   Creatine Kinase Release

CK measured in heart effluent collected during different time points during the experiment was used as a marker of injury. Figure 5.4 shows CK release for adult and ageing hearts corrected for both heart weights and flow rates of each age group. The amount of CK released from the
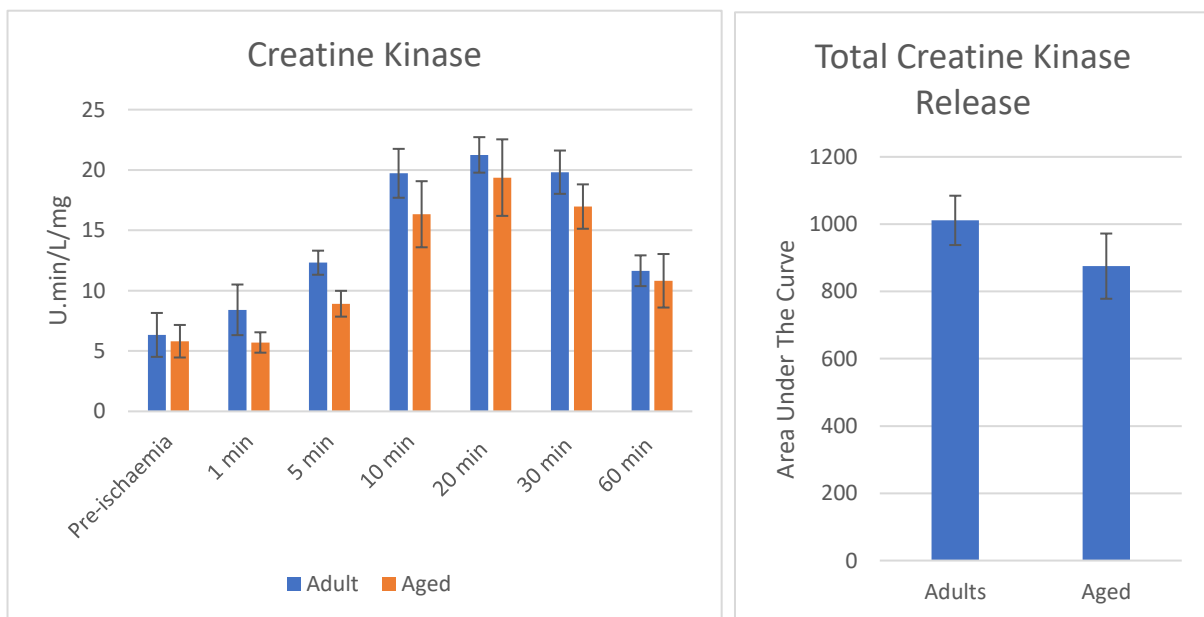
Figure 5.4: Creatine kinase release in adult and ageing hearts (corrected for heart weight and flow rate). Data are presented as mean ± SEM. Data were analysed using unpaired t-test. N = 6 for each age group.

heart follows a similar pattern in both age groups where it increases until reaching a peak at 20 mins of reperfusion and then starts to decrease. Increased CK release was not statistically significant at any time point during reperfusion compared to the pre-ischaemic point within each group, nor was it statistically different between the two groups. Additionally, comparing total CK release (by calculating area under the curve) was lower but not significantly in the ageing hearts compared to adults.

5.3.1.3   Infarct Size

Infarct size was measured and calculated as a percentage of total heart. When looking at the infarction, there were white areas (complete infarction), and pink areas (a mixture of viable and infarcted cells). Areas were compared separately and then together to compare injury between age groups (figure 5.5). The white and pink areas were both smaller in the ageing heart but not significantly. When added together, total infarcted area was significantly larger in the adult heart averaging at 76.04 ± 3.1 % compared to 59.8 ± 4.7 % in the ageing hearts (P = 0.02).
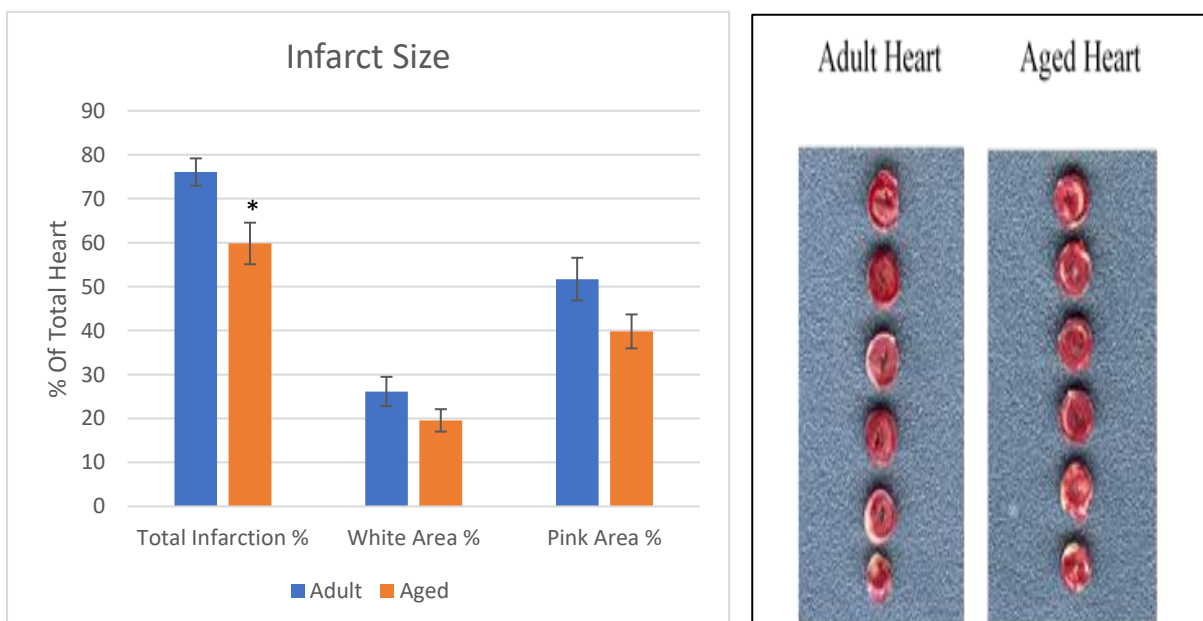
Figure 5.5: Infarct size in adult and ageing hearts demonstrated by area and as a total. Data are presented as mean ± SEM. Data were analysed using unpaired t-test. * = $P < 0.05$. N = 6 for each age group.

5.3.2 Vulnerability to Ischaemia/Reperfusion in the Ageing Heart with High-Fat Diet

5.3.2.1 Flow Rate and Functional Recovery

Ageing ND hearts had a starting flow rate averaging at 3.6 ± 0.5 ml/min. Flow rate dropped after ischaemia to an average of 2.9 ± 0.5 ml/min during the first min of reperfusion (19 % decrease). After that, it increased gradually but only until 5 mins of reperfusion before it started to decline again to reach an average of 2.5 ± 0.4 ml/min at 60 mins of reperfusion (31 % decrease). Decrease in flow rate in ageing hearts was only significantly different from the pre-ischaemic starting point at 30 mins of reperfusion ($P = 0.018$) and 60 mins of reperfusion ($P = 0.023$) (figure 5.6).

Ageing HFD hearts had a lower starting flow rate average at 2.9 ± 0.5 ml/min, which then decreased to 2.5 ± 0.3 ml/min in the first min of reperfusion (14 % decrease). Flow rate increased gradually between 1 and 5 mins of reperfusion then started to drop again until 20 mins of reperfusion where it plateaued at an average of 2.6 ± 0.3 ml/min until the end (60 mins) of reperfusion (10 % decrease compared to the starting flow rate). There were no significant differences in flow rates during any time point of reperfusion compared to the pre-ischaemic rate.
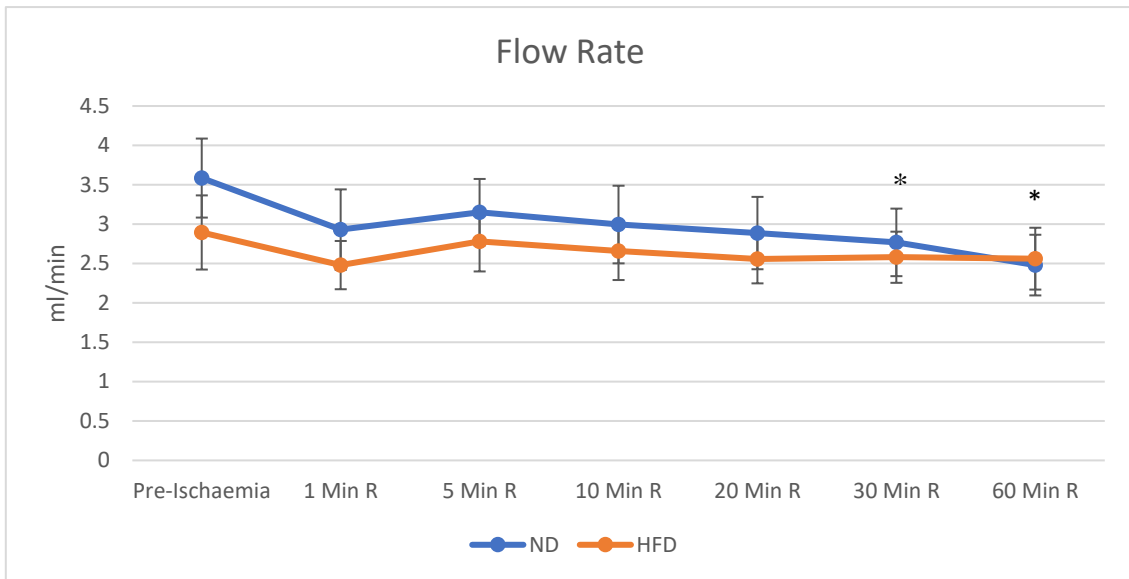
Figure 5.6: Flow rate in ageing hearts with and without HFD. Data are presented as mean ± SEM. Data were analysed using repeated measures ANOVA. * = $P < 0.5$ vs. pre-ischaemic value within the group. N = 6 ND and 5 HFD.

Even though ageing hearts had a lower flow rate after HFD, the decrease was not found to be significant at any time point during the experiment. When comparing the recovery of hearts after ischaemia, we found that HFD hearts had better recovery, but this was only significant at 30 mins of reperfusion (91 %) compared to ND hearts (77 %) ($P = 0.019$) (Figure 5.7).
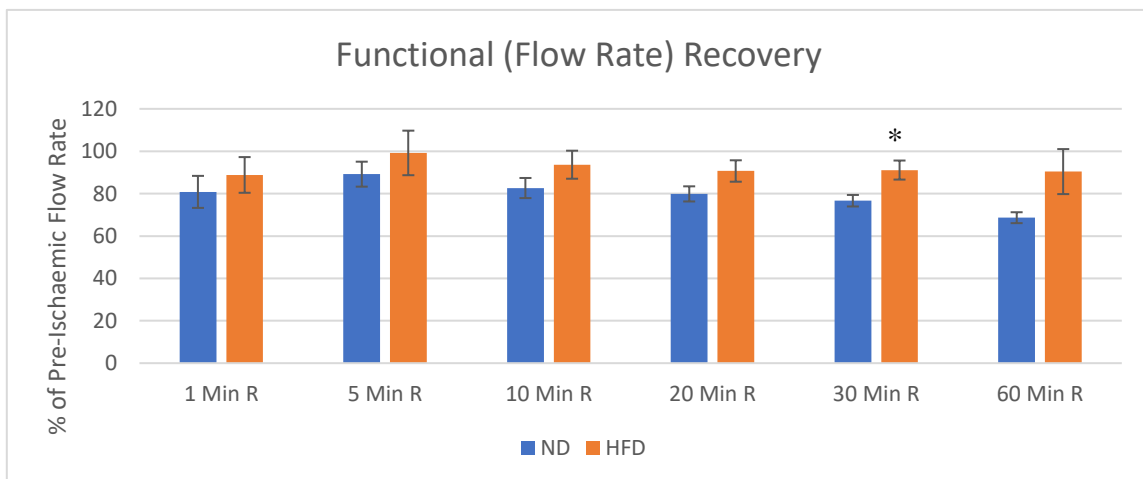
Figure 5.7: Flow rate % change from pre-ischaemic value in ageing hearts with and without HFD. Data are presented as mean ± SEM. Data were analysed using unpaired t-test. * = $P < 0.5$ vs. ND. N = 6 ND and 5 HFD.

5.3.2.2 Creatine Kinase Release

CK release from ageing hearts fed ND or HFD similarly increased during reperfusion until 20 mins and 30 mins of reperfusion for ND and HFD respectively, before decreasing at the end of reperfusion. As mentioned earlier, the ND hearts did not have a significant increase at any time point of reperfusion compared to the pre-ischaemic CK amount. However, HFD hearts had higher increase in CK release compared to pre-ischaemia, and this was found to be significant at 1 min of reperfusion (3.5 ± 0.3 u.min/L/mg, $P = 0.025$), 5 mins of reperfusion (7.8 ± 0.6 U.min/L/mg, $P = 0.01$), and at 20 mins of reperfusion (26.2 ± 4.6 U.min/L/mg, $P = 0.038$) compared to the pre-ischaemic CK release (1.1 ± 0.1 U.min/L/mg) (Figure 5.8). Comparing CK release between hearts in both groups, there were no significant differences between them at any time point of reperfusion, nor was there a significant difference in total CK release (AUC). However, pre-ischaemic CK release was significantly lower in the HFD group ($P = 0.032$), which explains the significance reported in CK released from HFD hearts during reperfusion in comparison to the pre-ischaemic point that was absent in the ND group. A higher CK release in the ND group indicates injury before ischaemia which could possibly be due to errors during heart cannulation.
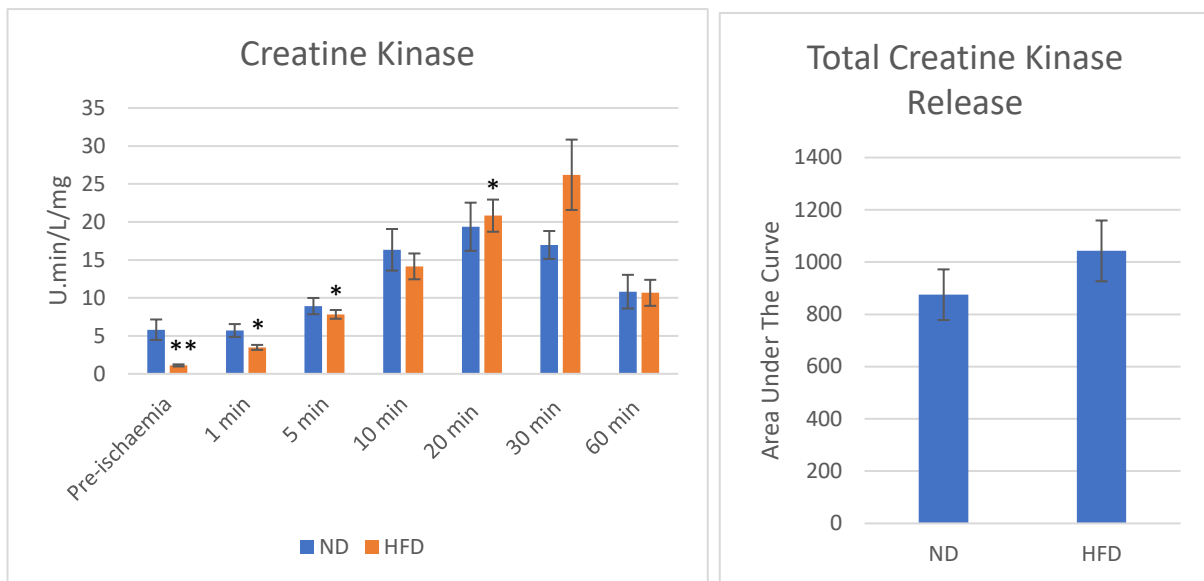
Figure 5.8: Creatine kinase release in ageing hearts with and without HFD (corrected for weight and flow rate). Data are presented as mean ± SEM. Data were analysed using unpaired t-test. * = $P < 0.05$ vs. pre-ischaemic value within the group, ** = $P < 0.05$ vs. ND. N = 6 ND and 5 HFD.

5.3.2.3   Infarct Size

Infarct size measured in HFD hearts showed larger white infarct area, and larger total infarct area, but none of these differences were significant (figure 5.9).
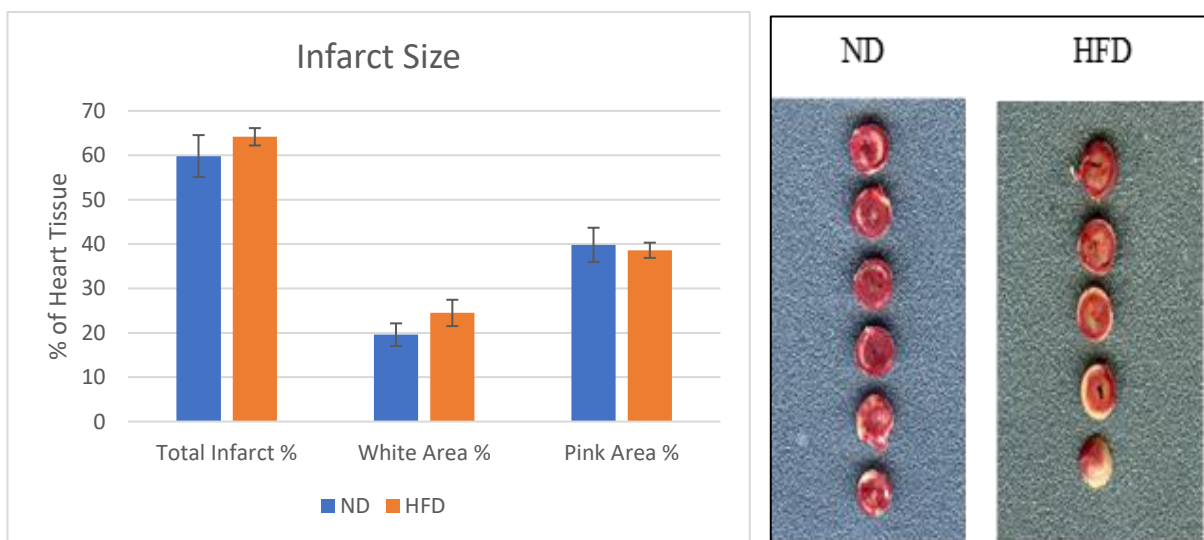
Figure 5.9: Infarct size in adult and ageing hearts demonstrated by area and as a total. Data are presented as mean ± SEM. Data were analysed using unpaired t-test. N = 6 ND and 5 HFD.

5.4 Discussion

5.4.1 Key Findings

Ageing does not alter vulnerability of the heart to I/R injury, nor does HFD in the ageing heart affect cardiac vulnerability to I/R.

5.4.2 Ageing Does Not Alter Cardiac Vulnerability to Ischaemia/Reperfusion Injury

In our work, ageing hearts seemed to have better tolerance to I/R injury compared to adult mice hearts, as seen by better functional recovery specially during the early stages of reperfusion (1 and 5 mins), a lower CK release from the heart (though not significantly different), and a lower total infarct size. However, if we analyse each parameter closely, we see no actual change with ageing.

Findings in the literature on vulnerability of the ageing heart to I/R injury have been contradictory (as mentioned in the introduction part of this chapter) where some studies showed an increased vulnerability of the heart to I/R injury with ageing and others showed no change [174, 176-179, 183-186].

If we rely on enzyme release and infarction size for measuring the tolerance to I/R and how it changed in the ageing heart, it might be concluded that the tolerance does not change. Total CK release was slightly (but not significantly) lower in the ageing heart and this is reported in another study (for LDH release) (figure 3.10) [2]. As seen in the figure, total LDH release from
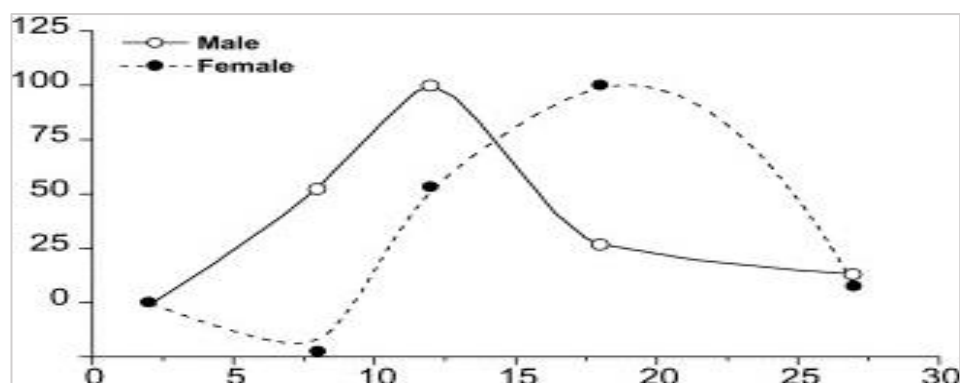
Figure 5.10: LDH release from the heart following ischaemia in different age groups of C57Bl/6 male and female mice. [2]

the heart during reperfusion peaked at middle aged mice (12 months) and started to decline afterwards in aged and senescent hearts to a point similar to that seen in young adults (2 months). Mice used in our work fall between the two aged groups used in the study.

Regarding infarct size of the heart, the significant difference found in our data is in total infarct size (this includes the white infarcted area and pink area which contains some viable tissue). If we use the white area only then we see no difference in the ageing hearts compared to adult hearts, and this is what most authors used in the studies mentioned in the introduction of this chapter when reporting infarct size.

Finally, looking at functional recovery (flow rate) which reflects vascular dysfunction, we see an improvement in the ageing heart recovery compared to adult hearts at certain time points of reperfusion. This is considered a valuable measurement as vascular dysfunction has been linked to worsened cardiovascular outcomes and it correlates with contractile dysfunction [2]. However, if we compare end of reperfusion recovery with pre-ischaemic flow rate in each age group, we see that they both have a significant decrease in FR by the end of reperfusion indicating vascular dysfunction in both age groups.

An important point to consider here is the age used (80 weeks) and where that falls in the C57Bl/6 mice frailty index. Figure 3.11 demonstrates the survival curves (Kaplan–Meier) for a colony of aged C57BL/6 mice at Dalhousie University, which shows mortality at different time points of aging [1]. This index shows that our ageing mice are not classified as aged but rather as older adults and have 100% survival. These mice start to show signs of frailty and a de crease in survival rate at an older age and are considered aged at around 122 weeks.
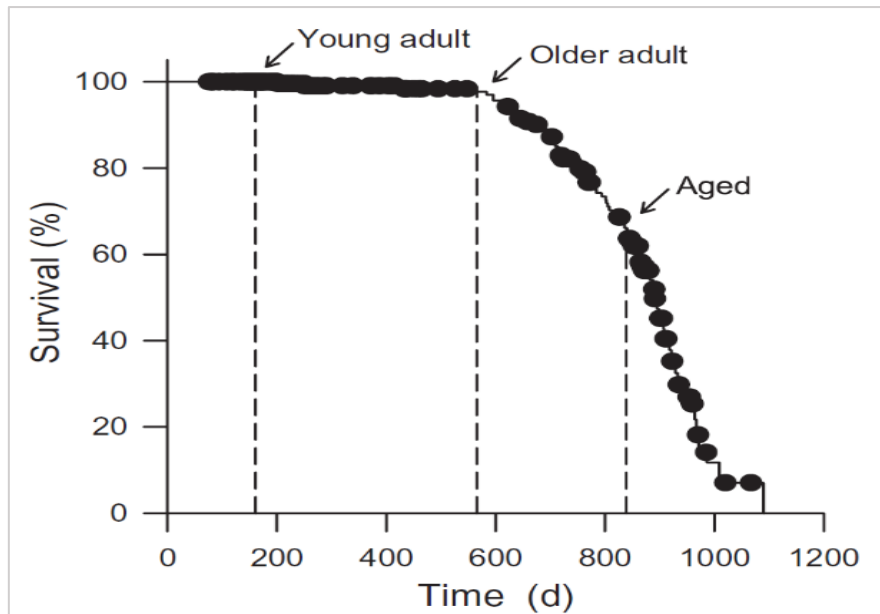
Figure 5.11: Kaplan–Meier curve showing survival and mortality in C57BL/6 mice [1]

5.4.3 High-Fat Diet Does Not Alter Cardiac Vulnerability to Ischaemia/Reperfusion in the Ageing Heart

In this work, ageing mice hearts seemed to have lower flow rate, higher CK release, and higher infarction rate after HFD. However, none of these changes were significant. The only significant difference between the two diet groups was the improved functional recovery (flow rate) at 30 mins of reperfusion in the HFD group.

As mentioned earlier in the introduction part of this chapter, HFD has been associated with increased tolerance to I/R as well as increased vulnerability in other contradictive studies. In aged animals however, HFD either had no effect on cardiac tolerance to I/R or decreased it [239, 240]. Additionally, obesity (which has been observed in our HFD animals), has also been associated with improved cardiac outcomes after I/R [225, 226].

Whether or not we can conclude an improvement in tolerance to I/R from our findings based on an improvement in functional recovery in the HFD group at a single time point of reperfusion cannot be concluded. Also, comparing end of reperfusion flow rate to pre-

ischaemic flow rate within each diet group shows a significant decrease (dysfunction) in the ageing heart, which was diminished after HFD. But the flow rate in the HFD group was lower to start with indicating a compromised heart.

5.5   Summary and Conclusion

Remodelling of the heart with ageing did not affect its vulnerability to I/R injury. Even though there was a significantly higher improvement seen in flow rate (functional recovery) in the ageing heart compared to the adult heart at 1 min and 5 mins of reperfusion, both age groups had a significantly lower flow rate at the end of reperfusion compared to their pre-ischaemic point. Similarly, HFD and its effects on remodelling the ageing heart did not change the hearts' tolerance to I/R injury. Even though there was an improvement in functional recovery of the HFD heart compared to the ND heart at 30 mins of reperfusion, and the change from pre-ischaemic flow rate to end of reperfusion flow rate was not significantly different in the HFD hearts (compared to the significant fall in flow rate from pre-ischaemia to end of reperfusion in the ND heart), HFD hearts had a lower flow rate than their ND controls to begin with.

6. Summary and Conclusion, Limitations, and Future Directions

6.1 Summary and Conclusion

Ageing is associated with metabolic, cellular, and structural cardiac remodelling. Figure 6.1 summarises the age-associated alterations in the heart from our findings.
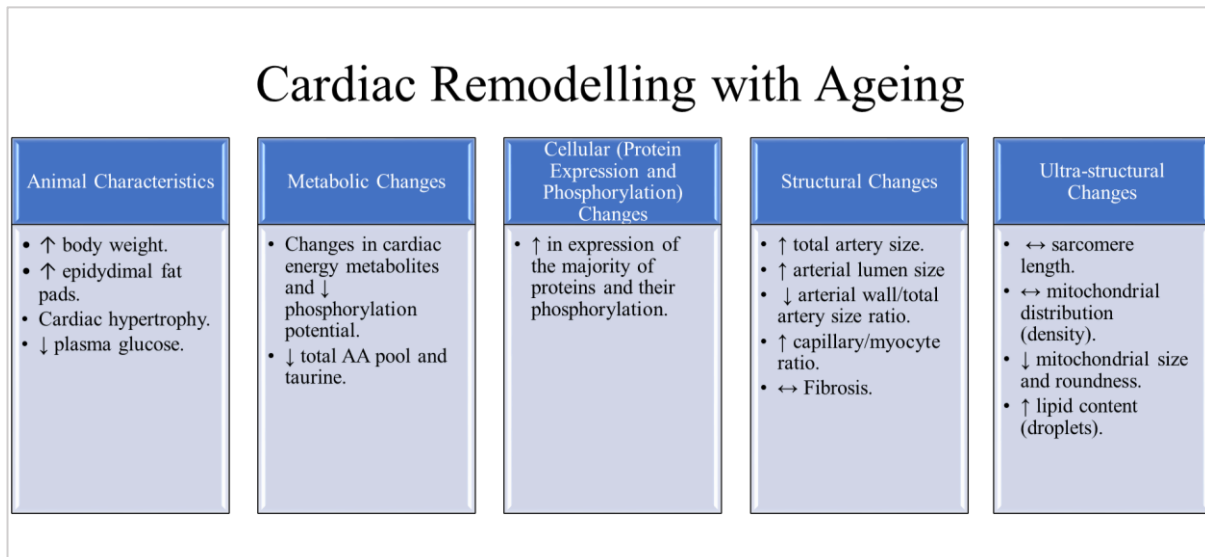
Figure 6.1: Remodelling of the ageing heart.

Ageing animals had an increase in body weight, body fat, hypertrophy of the heart, and significant decrease in blood glucose levels (figure 6.1).

The remodelling of the heart was studied in terms of four different aspects: metabolic changes, cellular changes (protein expression), structural and ultrastructural changes. Ageing hearts had changes in cardiac energy metabolites including higher levels of inosine, lower levels of hypoxanthine, a decreased phosphorylation potential (seen in guanosine metabolites), and a significant decrease in total AAs pool as well as the non-protein AA taurine.

Cellular (protein and phospho-protein expression) changes in the ageing heart mainly showed an upregulation in expression. Proteins including mitochondrial, ionic transport, apoptotic, antioxidants, structural (collagen), and lipid and carbohydrate metabolism were all upregulated in expression with ageing. Similarly, phospho-proteins showed an increased expression

especially ionic transport, cardiac signalling and apoptosis, metabolism and energy production, and structural proteins.

Lastly, structural remodelling of the ageing heart included larger coronary arteries with larger lumen sizes, a lower arterial wall/total artery size and lumen size ratios, and an increase in capillary/myocyte ratio, with no significant changes in fibrosis. Ultrastructural changes of the ageing heart included a change in mitochondrial morphometry, where mitochondria became smaller in size, and more elongated, increased lipid content (lipid droplets) of the heart, with no changes in sarcomere length or mitochondrial density (distribution).

Regarding the effects of HFD on the remodelling of the ageing heart, mice fed HFD had significant increases in body weight and body fat percentage (epididymal fat pads), but no change in heart weight. With the obesity, certain metabolic parameters also changed significantly in the HFD group including increased levels of plasma lipids (LDL and VLDL), and decreased plasma glucose and lactate.

The effects of HFD on cardiac remodelling included alteration in cardiac energy metabolites, with a decrease in total adenine metabolite pool. Additionally, the proteome and phospho-proteome profile changed with most proteins being downregulated even in phosphorylation after HFD. Downregulated proteins included mitochondrial and carbohydrate metabolism proteins. Other protein categories such as structural (collagen), apoptotic, and lipid metabolism were mostly upregulated after high fat feeding. Some protein groups showed changes in both directions (with some upregulating after HFD and others downregulating). These included antioxidant enzymes and ionic transport related proteins. Phospho-proteins were categorised into ionic transport, cardiac signalling and apoptosis, carbohydrate metabolism, transport, structural proteins, and enzymes, and were mainly all downregulated after HFD in the ageing heart.

Structural changes in the ageing heart after HFD included a decrease in coronary artery sizes and lumen sizes, with increased arterial wall/total artery size and lumen size ratios (thicker walls). In addition, ageing hearts from the HFD group had significantly higher fibrosis (interstitial and perivascular), and a lower capillary/myocyte ratio. Changes in the ultrastructure of the ageing heart after HFD were mainly in the mitochondria, which became larger in size, more rounded, and more densely distributed (specially PN and SSL mitochondria). Lipid content (lipid droplets) did not change nor did the sarcomere length in the myocytes. Figure 6.2 summarises all these changes.
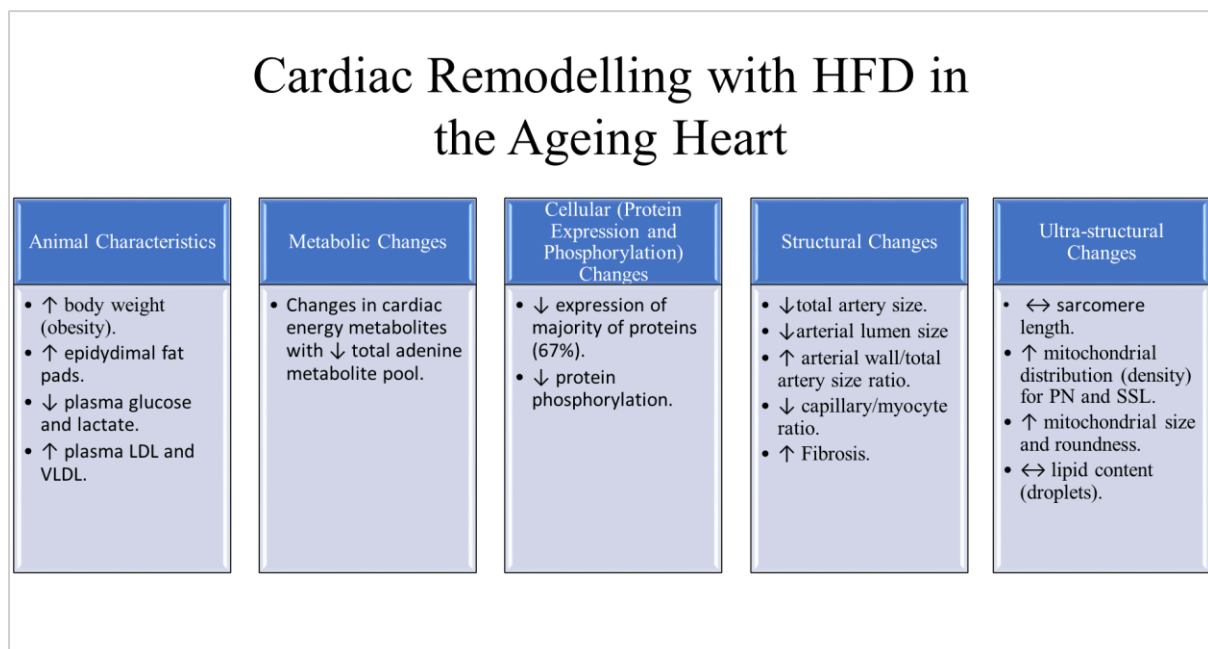
Figure 6.2: Remodelling of the ageing heart after HFD.

Despite the effects of ageing and HFD on cardiac remodelling, neither seemed to affect the heart's vulnerability to I/R injury. Ageing hearts seemed to have better functional recovery compared to their adult controls (seen by improved flow rate during reperfusion), but as explained earlier in chapter 5 discussion, both age groups had a significantly lower flow rate at the end of reperfusion compared to their pre-ischaemic points. This indicates similar vascular

dysfunction in both age groups after ischaemia. Similarly, hearts from ageing animals fed HFD seemed to have improved flow rate (functional recovery) during reperfusion, and no significant fall in their FR at the end of reperfusion compared to pre-ischaemic flow. However, these hearts had a starting lower flow rate compared to their ND controls indicating dysfunction after HFD.

6.2 Limitations

6.2.1 Animals

Using ageing mice in this work created a challenge in the sense that mice were hard to obtain at 80 weeks old from the suppliers, so often we had to purchase them at a much younger age and keep them in the university facility until they reached the age required, which caused a lot of delays in the work schedule plus additional expenses. Additionally, it was not feasible to get more mice when needed (extra sample numbers or a fault in an experiment) leading to having limited numbers for comparisons which may affects results due to a scatter in the analysis.

6.2.2 HPLC

For the HPLC samples, the first samples (adult vs. ageing) were run together for cardiac energy metabolites and then for AAs. For the HFD ageing samples, they were done separately (when the animals were ready for use) and by that period the SAVANT (AS160 Automatic Speed Vac) used for drying the samples in preparation for AA measurements, was not working. There was no alternative equipment to use so the HFD hearts were not measured for AA content.

6.2.3 NMR

Some of the issues encountered in NMR sample analysis included the collection of blood samples. As the blood was collected from the thoracic cavity after harvesting the heart, this led to a small amount of blood collected and inability to obtain it from all mice.

When analysing the data, references were used to determine the peaks of each metabolite measured. However, because peaks were slightly different in shape and shifted in the samples,

this made specifying where each metabolite occurred difficult at times, and possibly measurements were not completely accurate.

6.2.4 Light Microscopy

One major issue when using histological samples for analysis was the quality of the samples, which depends on processing, cutting, staining, and mounting the slides. Additionally, the method used in image analysis, which relies on choosing 3-4 areas from the section randomly to analyse them, may not be a true representation of what is being measured.

Using EVG staining to measure the morphometry of coronary arteries, certain samples had major arteries that could not be measured (due to the cutting of the tissue, arteries did not appear cross-sectional and were elongated), so they had to be excluded from the analysis.

For measuring fibrosis in the heart using Masson's Trichrome staining, the threshold of the image was altered using the software ImageJ to detect fibrous tissue (represented by blue colour), in certain images if the blue shade was extremely lighter or darker it could have been excluded from the analysis.

6.2.5 Electron Microscopy

One of the main limitations found during analysis of electron micrographs was the quality of sections and how they are oriented (during cutting). A lot of the samples used had been cut cross-sectionally, so finding areas that can be used for the required analysis was difficult. This made distinguishing mitochondrial subtype (for calculating distribution) and measuring mitochondrial morphometry difficult at times and possibly not very accurate.

6.2.6 Langendorff Perfusion

The major issue found in Langendorff experiments was measuring the infarct size of the hearts. Sections of the heart had clearly distinguished white areas (which many authors use for calculating infarction of the heart), and the viable part of the heart (stained in red) had a mix of shades of pink and brick-red areas. So, when measuring infarction, the brick-red area was

determined to be the absolute viable tissue, the white area was the infarcted tissue, and the pink area was measured separately as it represents a mix of dead and viable tissue. All three areas were presented in the data individually, and the white area was mostly used to determine the differences in infarct size between groups. However, this means that the actual percentage of infarction is not determined precisely as some infarcted tissue was not included.

6.3 Future Directions

Investigating cardiac remodelling in the C57BL/6J mouse model at 80 weeks old showed some changes that are associated with ageing (e.g. cardiac hypertrophy) while other expected changes (e.g. cardiac fibrosis) were not found. This indicates that the age used is possibly not the right one to use in age related studies. As seen earlier in the frailty index for C57BL/6 mice, the age we used in this study (and used in many studies related to ageing) is considered to be older adults. Mice are considered to be aged around 122 weeks old. Comparing the frailty index of mice to that of humans (after normalising age), they were found to be similar (figure 6.3) [1].
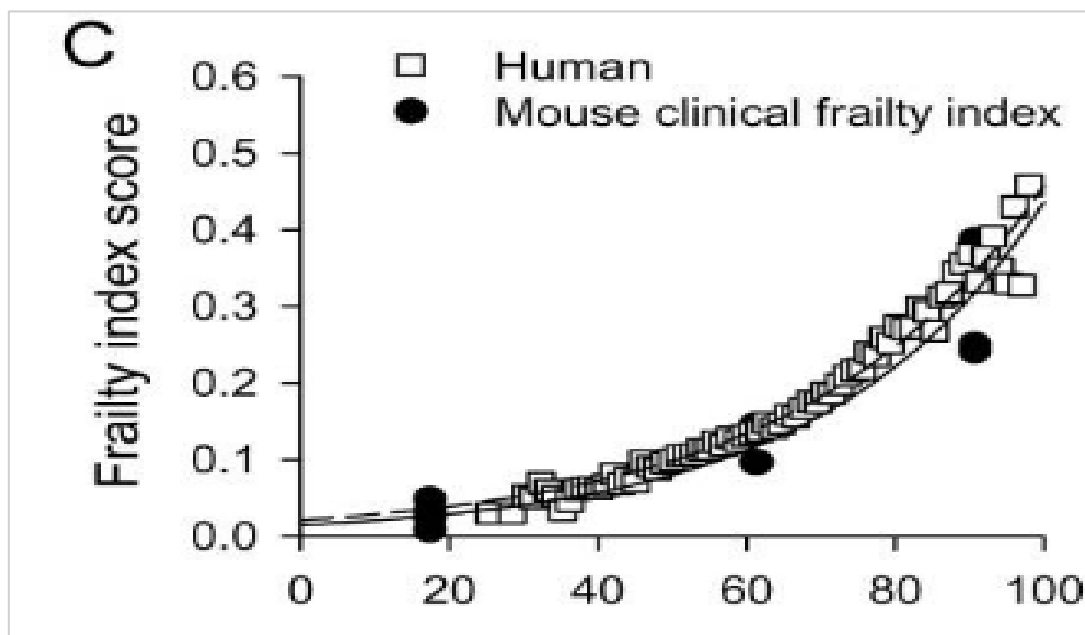
Figure 6.3: Clinical frailty index in human and mouse normalised for age.

For this reason, it would be interesting to study the remodelling and vulnerability of the heart to I/R injury using older animals. The downside to that is these older animals can be very costly and their survival decreases. Additionally, females of the same strain can be used for the purpose of investigating gender-related differences in cardiac remodelling and tolerance to I/R injury.

Regarding using HFD and studying its effects in the heart, work from a previous colleague used the same diet that was used in this work in a different age group (adult mice) [236]. Unlike ageing hearts used here, adult hearts with HFD became more vulnerable and had increased injury after I/R. Proteomics data from both age group were compared to look at changes in protein expression patterns (increase or decrease) with HFD, with some proteins showing change in opposite directions between the two age groups. It would perhaps be interesting to investigate the causes behind the change in cardiac tolerance to I/R after HFD in the ageing compared to the adult heart.

7. Appendices

7.1 Normal Chow Diet and High-Fat Diet Detailed Constituents

7.1.1 Normal Chow Diet

Calculated Analysis:

PROXIMATE ANALYSIS		Total		AMINO ACIDS		Total	Supp**
Moisture	%	10.00		Arginine	%	1.26	
Crude Oil	%	4.75		Lysine	%	1.02	0.1
Crude Protein	%	19.11		Methionine	%	0.43	0.15
Crude Fibre	%	3.85		Cystine	%	0.35	
Ash	%	6.97		Tryptophan	%	0.25	
NFE	%	55.32		Histidine	%	0.48	
				Threonine	%	0.71	
CARBOHYDRATE, FIBRE AND NON STARCH POLYSACCHARIDES (NSP)				Isoleucine		0.83	
Pectin	%	1.37		Leucine	%	1.34	
Hemicellulose	%	8.76		Phenylanine	%	0.96	
Cellulose	%	3.95		Valine	%	0.93	
Lignin	%	1.06		Tyrosine	%	0.61	
Starch	%	35.41		Glycine	%	0.81	
Sucrose	%	4.64		Aspartic acid	%	1.70	
				Glutamic acid	%	3.96	
ENERGY				Proline		1.33	
				Serine	%	0.97	
Gross Energy	MJ/kg	16.26					
Metabolisable Energy	MJ/kg	12.23					
Atwater Fuel Energy*	kcal/g	3.40		Alanine	%	0.80	

*Atwater Fuel Energy (kcal/g) = [(Crude Oil% x 9) + (Crude Protein% x 4) + (NFE% x 4)]/100
(1 MJ=239.23 kcal)

FATTY ACIDS		Total		MINERALS AND TRACE ELEMENTS		Total	Supp**
SATURATED FATTY ACIDS				Ca	%	1.01	0.73
				Total P	%	0.64	0.19
				Phytate P	%	0.24	
				Available P	%	0.40	0.19
				Na	%	0.32	0.27
C12:0 Lauric	%	0.02		Cl	%	0.49	0.43
C14:0 Myristic	%	0.06		K	%	0.88	
C16:0 Palmitic	%	0.54		Mg	%	0.20	0.01
				Fe	mg/kg	280	180
C18:0 Stearic	%	0.13		Cu	mg/kg	22	12
				Mn	mg/kg	145	99
				Zn	mg/kg	178	144
MONO-UNSATURATED FATTY ACIDS				Co	mg/kg	67	
C14:1 Myristoleic	%	0.00		I	mg/kg	2275	2154
C16:1 Palmitoleic	%	0.01		Se	mg/kg	310	150
C18:1 ω9 Oleic	%	1.06					
				VITAMINS			
				VIT A	IU/kg	31151	29955
				VIT D3	IU/kg	1527	1500
POLY UNSATURATED FATTY ACIDS				VIT E	IU/kg	96	80
C18:2 ω6 Linoleic	%	2.27		VIT B1 Thiamine	mg/kg	336	331
C18:3 ω3 Linolenic	%	0.28		VIT B2 Riboflavin	mg/kg	14	12
				VIT B6 Pyrodoxine	mg/kg	48	45
C20:4 ω6 Arachidonic	%	0.11		VIT B12 Cyanocobalamine	mg/kg	153	150
C22:5 ω3 Clupanodonic	%	0.00		VIT K Menadione	mg/kg	10	10
				Folic Acid	mg/kg	11	10
				Nicotinic Acid	mg/kg	129	78
				Pantothenic Acid	mg/kg	41	27
				Choline	mg/kg	1337	300
				Inositol	mg/kg	2297	245
				Biotin	mg/kg	543	280

**SUPP = Supplemented sources of amino acids, vitamins and minerals from manufactured and mined sources.

Ingredients (in descending order of inclusion):
Wheat, Dehulled Extracted Toasted Soya, Wheatfeed, Barley, Dehulled Cooked Soya, Soya Oil, Calcium Carbonate, Dicalcium Phosphate, Salt (NaCl), Silicon Dioxide, DL-Methionine, Choline Chloride, Ferrous Sulphate, Inositol, Magnesium Oxide, Zinc Oxide, L-Lysine, Manganese Oxide, Vitamin E (Tocopherol) Supplement, Vitamin B12 (Cyanocobalamin) Supplement, Vitamin B1 (Thiamine), Nicotinic Acid, Vitamin A (Retinol) Supplement, Copper Sulphate, Calcium-D-Pantothenate, Vitamin B6 (Pyridoxine), Vitamin K3 (Menedione), Selenium 1% Supplement, Vitamin B2 (Riboflamine), Biotin-Supplement, Folic Acid, Calcium Iodate, Vitamin D3 (Cholecalciferol) Supplement.

7.1.2   High-Fat Diet

CALCULATED ANALYSIS:

		FRESH	10% H2O			FRESH	10% H2O
TOTAL	%	100.00	100.00	TAURINE	%	0.00	0.00
MOISTURE	%	7.46	10.00	GLYCINE	%	0.83	0.81
CRUDE OIL	%	22.27	21.66	ASPARTIC ACID	%	1.09	1.06
CRUDE PROTEIN	%	19.87	19.32	GLUTAMIC ACID	%	3.34	3.25
CRUDE FIBRE	%	3.91	3.80	PROLINE	%	1.40	1.36
ASH	%	5.24	5.10	SERINE	%	0.79	0.77
NFE	%	41.02	39.89	HYD. PROLINE	%	0.01	0.01
PECTIN	%	0.46	0.45	HYD. LYSINE	%	0.00	0.00
HEMICELLULOSE	%	3.17	3.08	ALANINE	%	0.57	0.55
CELLULOSE	%	4.85	4.72	Ca	%	0.66	0.64
LIGNIN	%	0.43	0.42	P TOTAL	%	0.57	0.55
STARCH	%	34.74	33.79	P PHYTATE	%	0.05	0.05
SUGAR	%	1.24	1.21	P AVAILABLE	%	0.52	0.51
SDS GROSS ENERGY	MJ/kg	19.67	19.13	Na	%	0.23	0.22
SDS DIGESTIBLE ENERGY	MJ/kg	17.66	17.18	Cl	%	0.38	0.37
SDS METABOLISABLE ENERGY	MJ/kg	16.54	16.09	K	%	0.65	0.63
AFE ENERGY	MJ/kg	18.56	18.05	Mg	%	0.17	0.17
C14 1 MYRISTOLEIC	%	0.03	0.03	Fe	mg/kg	107.84	104.88
C16 1 PALMITOLEIC	%	0.11	0.11	Cu	mg/kg	15.32	14.90
C18 1 W9 OLEIC	%	6.69	6.51	Mn	mg/kg	61.83	60.13
C18 2 W6 LINOLEIC	%	1.95	1.90	Zn	mg/kg	53.72	52.25
C18 3 W3 LINOLENIC	%	0.11	0.11	Co	µg/kg	537.57	522.81
C20 4 W6 ARICHIDONIC	%	0.03	0.03	I	µg/kg	12.74	12.39
C22 5 W3 CLUPANODONIC	%	0.00	0.00	Se	µg/kg	45.28	44.04
C12:0 LAURIC	%	0.03	0.03	F	mg/kg	4.67	4.54
C14:0 MYRISTIC	%	0.37	0.36	VITAMIN A	iu/kg	6575.48	6395.00
C16:0 PALMITIC	%	4.56	4.43	VITAMIN D3	iu/kg	8050.00	7829.05
C18:0 STEARIC	%	2.04	1.98	VITAMIN E	iu/kg	56.95	55.39
ARGININE	%	0.71	0.69	VITAMIN B1 THIAMINE	mg/kg	6.52	6.34
LYSINE	%	1.16	1.13	VITAMIN B2 RIBOFLAVIN	mg/kg	4.64	4.51
METHIONINE	%	0.48	0.47	VITAMIN B6 PYRIDOXIN	mg/kg	5.82	5.66
CYSTINE	%	0.09	0.09	VITAMIN B12 CYANOCOBALAMINE	µg/kg	5.45	5.30
TRYPTOPHAN	%	0.18	0.18	VITAMIN C ASCORBIC ACID	mg/kg	7.97	7.75
HISTIDINE	%	0.48	0.47	VITAMIN K	mg/kg	4.91	4.78
				MENEDIONE			
THREONINE	%	0.70	0.68	FOLIC ACID	mg/kg	0.15	0.15
ISOLEUCINE	%	0.97	0.94	NICOTINIC ACID	mg/kg	21.44	20.85
LEUCINE	%	1.60	1.56	PANTOTHENIC ACID	mg/kg	13.30	12.93
PHENYLALANINE	%	0.85	0.83	CHOLINE	mg/kg	278.07	270.44
VALINE	%	1.17	1.14	INOSITOL	mg/kg	908.50	883.56
TYROSINE	%	0.83	0.81	BIOTIN	µg/kg	56.35	54.80

INGREDIENTS:

NAME
LARD
CORN STARCH
CASEIN
MAIZE
WHEAT
WHEATFEED
VITAMINS, MINERALS, AMINO ACIDS AND TRACE ELEMENTS
CELLULOSE
CHOLESTEROL

7.2 Protein Description List (Adult Vs. Ageing)

Gene	Protein Name
Lipid metabolism and transport proteins	
Hacd2	Very-long-chain (3R)-3-hydroxyacyl-CoA dehydratase 2
Plpp1	Lipid phosphate phosphohydrolase 1
Gltp	Glycolipid transfer protein
Slc25a20	Solute carrier family 25 (Mitochondrial carnitine/acylcarnitine translocase), member 20
Echdc2	Enoyl-CoA hydratase domain-containing protein 2, mitochondrial
Acox1	Peroxisomal acyl-coenzyme A oxidase 1
Acad11	Acyl-CoA dehydrogenase family member 11
Acox3	Peroxisomal acyl-coenzyme A oxidase 3
Acsl6	Long-chain acyl-CoA synthetase
Acsm5	Acyl-coenzyme A synthetase ACSM5, mitochondrial
Carbohydrate metabolism and transport proteins	
Eno2	Gamma-enolase
Slc2a1	Solute carrier family 2, facilitated glucose transporter member 1
Gyg1	Glycogenin-1
Naglt1c	Sodium-dependent glucose transporter 1C
Gys1	Glycogen [starch] synthase, muscle
Ugdh	UDP-glucose 6-dehydrogenase
Ugp2	UTP--glucose-1-phosphate uridylyltransferase
Ionic transport-related proteins	
Camk2b	Calcium/calmodulin-dependent protein kinase II, beta, isoform CRA_b
Slc8a1	Sodium/calcium exchanger 1
Scn2b	Sodium channel subunit beta-2
Scn4b	Sodium channel subunit beta-4
Naglt1c	Sodium-dependent glucose transporter 1C
Slc4a4	Electrogenic sodium bicarbonate cotransporter NBCe1 variant D
Kcna7	Voltage-gated potassium channel Kv1.7 (Fragment)
Kcnj13	Inward rectifier potassium channel 13
Mitochondrial proteins: Lipid metabolism	

Acsm5	Acyl-coenzyme A synthetase ACSM5, mitochondrial
Bdh1	D-beta-hydroxybutyrate dehydrogenase, mitochondrial
Echdc2	Enoyl-CoA hydratase domain-containing protein 2, mitochondrial
Hmgcs2	Hydroxymethylglutaryl-CoA synthase, mitochondrial
Slc25a20	Solute carrier family 25 (Mitochondrial carnitine/acylcarnitine translocase), member 20
Cyp27a1	Sterol 26-hydroxylase, mitochondrial
Mitochondrial proteins: Energy production	
Atp5i	ATP synthase subunit e, mitochondrial
Ckmt1	Creatine kinase U-type, mitochondrial
Uqcrh	Cytochrome b-c1 complex subunit 6, mitochondrial
Idh2	Isocitrate dehydrogenase [NADP], mitochondrial
L2hgdh	L-2-hydroxyglutarate dehydrogenase, mitochondrial
Suclg2	Succinyl-CoA ligase [GDP-forming] subunit beta, mitochondrial
Mitochondrial proteins: Amino acids metabolism	
Abat	4-aminobutyrate aminotransferase, mitochondrial
Lactb	Serine beta-lactamase-like protein LACTB, mitochondrial
Tmlhe	Trimethyllysine dioxygenase, mitochondrial
Mitochondrial proteins: Mitochondrial transport	
Grpel2	GrpE protein homolog 2, mitochondrial
Slc25a10	Mitochondrial dicarboxylate carrier
Timm17a	Mitochondrial import inner membrane translocase subunit Tim17-A (Fragment)
Tomm6	Mitochondrial import receptor subunit TOM6 homolog

7.3 Protein Description List (Ageing Normal Diet Vs. Ageing High-Fat Diet)

7.3.1 Mitochondrial Proteins

Gene	Protein Name
Mitochondrial Lipid Metabolism Proteins	
Sirt4	NAD-dependent protein lipoamidase sirtuin-4, mitochondrial
Gpd2	Glycerol-3-phosphate dehydrogenase, mitochondrial
Bdh1	D-beta-hydroxybutyrate dehydrogenase, mitochondrial
Ech1	Delta(3,5)-Delta(2,4)-dienoyl-CoA isomerase, mitochondrial
Oxct1	Succinyl-CoA:3-ketoacid coenzyme A transferase 1, mitochondrial
Mitochondrial Energy Metabolism Proteins	
Pdha2	Pyruvate dehydrogenase E1 component subunit alpha, testis-specific form, mitochondrial
Tmem70	Transmembrane protein 70, mitochondrial
Cox7a2l	Cytochrome c oxidase subunit 7A-related protein, mitochondrial
Pdk4	[Pyruvate dehydrogenase (acetyl-transferring)] kinase isozyme 4, mitochondrial
Pdhx	Pyruvate dehydrogenase protein X component, mitochondrial
Mitochondrial Structural Proteins	
Tmem126b	Complex I assembly factor TMEM126B, mitochondrial
Higd1a	HIG1 domain family member 1A, mitochondrial
Coq10b	Coenzyme Q-binding protein COQ10 homolog B, mitochondrial
Cox16	Cytochrome c oxidase assembly protein COX16 homolog, mitochondrial
Coa3	Cytochrome c oxidase assembly factor 3 homolog, mitochondrial
Ndufaf7	Protein arginine methyltransferase NDUFAF7, mitochondrial
Bcs1l	Mitochondrial chaperone BCS1
Mitochondrial Ionic-Related Proteins	
Stoml2	Stomatin-like protein 2, mitochondrial
Slc25a13	Calcium-binding mitochondrial carrier protein Aralar2
Mitochondrial Transport Proteins	
Tomm22	Mitochondrial import receptor subunit TOM22 homolog
Timm10b	Mitochondrial import inner membrane translocase subunit Tim10 B

Timm17b	Mitochondrial import inner membrane translocase subunit TIM17
Timm23	Mitochondrial import inner membrane translocase subunit TIM23
Ucp3	Uncoupling protein 3 (Mitochondrial, proton carrier)
Slc25a31	Solute carrier family 25 (Mitochondrial carrier adenine nucleotide translocator), member 31
Tomm5	Mitochondrial import receptor subunit TOM5 homolog
Abcb10	ATP-binding cassette sub-family B member 10, mitochondrial
Tomm40	Mitochondrial import receptor subunit TOM40 homolog
Grpel1	GrpE protein homolog 1, mitochondrial
Mitochondrial AA Metabolism and Transport Proteins	
Slc25a29	Mitochondrial basic amino acids transporter
Slc25a19	Solute carrier family 25 (Mitochondrial thiamine pyrophosphate carrier), member 19
Prodh	Proline dehydrogenase 1, mitochondrial
Gcat	2-amino-3-ketobutyrate coenzyme A ligase, mitochondrial

7.3.2   Ionic Transport-Related Proteins

Protein Gene	Protein Name
Atp1a3	Sodium/potassium-transporting ATPase subunit alpha
Slc25a13	Calcium-binding mitochondrial carrier protein Aralar2
Tmco1	Calcium load-activated calcium channel (Fragment)
Kcnq1	Potassium voltage-gated channel subfamily KQT member 1
Camk2a	Calcium/calmodulin-dependent protein kinase type II subunit alpha
Scn4b	Sodium channel subunit beta-4
Cacna1d	Voltage-dependent L-type calcium channel subunit alpha-1D
Tmem66; Saraf	Store-operated calcium entry-associated regulatory factor
Slc38a3	Sodium-coupled neutral amino acid transporter 3
Clic5	Chloride intracellular channel protein 5 OS=Mus musculus GN=Clic5 PE=1 SV=1
Clcn7	Chloride channel protein OS=Mus musculus GN=Clcn7 PE=1 SV=1

7.3.3   Antioxidant Proteins

Protein Gene	Protein Name
Gpx7	Glutathione peroxidase 7
Gsto1	Glutathione S-transferase omega-1
Cat	Catalase
Sod3	Superoxide dismutase [Cu-Zn]

7.3.4   Collagen (Structural) Proteins

Protein Gene	Protein Name
Col4a2	Collagen alpha-2(IV) chain
Col18a1	Collagen alpha-1(XVIII) chain
Col6a2	Collagen alpha-2(VI) chain
Col4a1	Collagen alpha-1(IV) chain
Col6a1	Collagen alpha-1(VI) chain
Col6a3	Collagen, type VI, alpha 3

7.3.5   Lipid and Carbohydrate Metabolism and Transport Proteins

Protein Gene	Protein Name
Lipid Proteins	
Slc27a1	Long-chain fatty acid transport protein 1
Mboat7	Lysophospholipid acyltransferase 7
Acot11	Acyl-coenzyme A thioesterase 11
Acox1	Peroxisomal acyl-coenzyme A oxidase 1
Gnpat	Dihydroxyacetone phosphate acyltransferase
Mboat7	Lysophospholipid acyltransferase 7
Abhd5	1-acylglycerol-3-phosphate O-acyltransferase ABHD5
Lpcat1	Lysophosphatidylcholine acyltransferase 1
Acbd3	Acyl-Coenzyme A binding domain containing 3, isoform CRA_b
Ech1	Delta(3,5)-Delta(2,4)-dienoyl-CoA isomerase, mitochondrial

Carbohydrate Proteins	
Hk1	Hexokinase-1
Slc2a1	Solute carrier family 2, facilitated glucose transporter member 1
Ugdh	UDP-glucose 6-dehydrogenase
Ugp2	UTP--glucose-1-phosphate uridylyltransferase

8. References

1. Whitehead, J.C., et al., *A clinical frailty index in aging mice: comparisons with frailty index data in humans.* The journals of gerontology. Series A, Biological sciences and medical sciences, 2014. **69**(6): p. 621-632.

2. Willems, L., et al., *Age-related changes in ischemic tolerance in male and female mouse hearts.* J Mol Cell Cardiol, 2005. **38**(2): p. 245-56.

3. Correa, T., S. M Jakob, and J. Takala, *Mitochondrial Function in Sepsis.* Critical Care Horizons, 2015. **1**: p. 31.

4. Fares, E. and S.E. Howlett, *Effect of age on cardiac excitation–contraction coupling.* 2010. **37**(1): p. 1-7.

5. Stanley, W.C., F.A. Recchia, and G.D. Lopaschuk, *Myocardial Substrate Metabolism in the Normal and Failing Heart.* 2005. **85**(3): p. 1093-1129.

6. Bers, D.M., *Cardiac excitation–contraction coupling.* Nature, 2002. **415**(6868): p. 198-205.

7. Neri, M., et al., *Ischemia/Reperfusion Injury following Acute Myocardial Infarction: A Critical Issue for Clinicians and Forensic Pathologists %J Mediators of Inflammation.* 2017. **2017**: p. 14.

8. North, B.J. and D.A. Sinclair, *The intersection between aging and cardiovascular disease.* Circulation Research, 2012. **110**(8): p. 1097-1108.

9. Walker, C.A. and F.G. Spinale, *The structure and function of the cardiac myocyte: A review of fundamental concepts.* The Journal of Thoracic and Cardiovascular Surgery, 1999. **118**(2): p. 375-382.

10. Wijeyesekera, A., et al., *Metabotyping of Long-Lived Mice using 1H NMR Spectroscopy.* Journal of Proteome Research, 2012. **11**(4): p. 2224-2235.

11. Chen, J.-Q., T.R. Brown, and J. Russo, *Regulation of energy metabolism pathways by estrogens and estrogenic chemicals and potential implications in obesity associated with increased exposure to endocrine disruptors.* Biochimica et Biophysica Acta (BBA) - Molecular Cell Research, 2009. **1793**(7): p. 1128-1143.

12. Strait, J.B. and E.G. Lakatta, *Aging-associated cardiovascular changes and their relationship to heart failure.* Heart Fail Clin, 2012. **8**(1): p. 143-64.

13. Hausenloy, D.J. and D.M. Yellon, *Myocardial ischemia-reperfusion injury: a neglected therapeutic target.* The Journal of clinical investigation, 2013. **123**(1): p. 92-100.

14. Jennings, R.B., et al., *Total ischemia in dog hearts, in vitro. 1. Comparison of high energy phosphate production, utilization, and depletion, and of adenine nucleotide catabolism in total ischemia in vitro vs. severe ischemia in vivo.* Circ Res, 1981. **49**(4): p. 892-900.

15. Doenst, T., T.D. Nguyen, and E.D. Abel, *Cardiac Metabolism in Heart Failure.* 2013. **113**(6): p. 709-724.

16. Dampney, R.A.L., *Central neural control of the cardiovascular system: current perspectives.* 2016. **40**(3): p. 283-296.

17. Pugsley, M.K. and R. Tabrizchi, *The vascular system: An overview of structure and function.* Journal of Pharmacological and Toxicological Methods, 2000. **44**(2): p. 333-340.

18. Lesnefsky, E.J., Q. Chen, and C.L. Hoppel, *Mitochondrial Metabolism in Aging Heart.* Circ Res, 2016. **118**(10): p. 1593-611.

19. Suga, H., *Ventricular energetics.* 1990. **70**(2): p. 247-277.

20. Lopaschuk, G.D., et al., *Myocardial fatty acid metabolism in health and disease.* Physiol Rev, 2010. **90**(1): p. 207-58.

21. Beer, M., et al., *Absolute concentrations of high-energy phosphate metabolites in normal, hypertrophied, and failing human myocardium measured noninvasively with (31)P-SLOOP magnetic resonance spectroscopy.* J Am Coll Cardiol, 2002. **40**(7): p. 1267-74.

22. Aerni-Flessner, L., et al., *GLUT4, GLUT1, and GLUT8 are the dominant GLUT transcripts expressed in the murine left ventricle.* Cardiovasc Diabetol, 2012. **11**: p. 63.

23. Abel, E.D., *Glucose transport in the heart.* Front Biosci, 2004. **9**: p. 201-15.

24. Entman, M.L., et al., *Association of glycogenolysis with cardiac sarcoplasmic reticulum: II. Effect of glycogen depletion, deoxycholate solubilization and cardiac ischemia: evidence for a phorphorylase kinase membrane complex.* J Mol Cell Cardiol, 1977. **9**(7): p. 515-28.

25. Kusuoka, H. and E. Marban, *Mechanism of the diastolic dysfunction induced by glycolytic inhibition. Does adenosine triphosphate derived from glycolysis play a favored role in cellular Ca2+ homeostasis in ferret myocardium?* The Journal of Clinical Investigation, 1994. **93**(3): p. 1216-1223.

26. Fillmore, N., J. Mori, and G.D. Lopaschuk, *Mitochondrial fatty acid oxidation alterations in heart failure, ischaemic heart disease and diabetic cardiomyopathy.* Br J Pharmacol, 2014. **171**(8): p. 2080-90.

27. Huang, B., et al., *Regulation of pyruvate dehydrogenase kinase expression by peroxisome proliferator-activated receptor-alpha ligands, glucocorticoids, and insulin.* Diabetes, 2002. **51**(2): p. 276-83.

28. Wu, P., J.M. Peters, and R.A. Harris, *Adaptive increase in pyruvate dehydrogenase kinase 4 during starvation is mediated by peroxisome proliferator-activated receptor alpha.* Biochem Biophys Res Commun, 2001. **287**(2): p. 391-6.

29. McCormack, J.G. and R.M. Denton, *Influence of calcium ions on mammalian intramitochondrial dehydrogenases.* Methods Enzymol, 1989. **174**: p. 95-118.

30. McCormack, J.G. and R.M. Denton, *Role of Ca2+ ions in the regulation of intramitochondrial metabolism in rat heart. Evidence from studies with isolated mitochondria that adrenaline activates the pyruvate dehydrogenase and 2-oxoglutarate dehydrogenase complexes by increasing the intramitochondrial concentration of Ca2+.* Biochem J, 1984. **218**(1): p. 235-47.

31. McCormack, J.G., A.P. Halestrap, and R.M. Denton, *Role of calcium ions in regulation of mammalian intramitochondrial metabolism.* 1990. **70**(2): p. 391-425.

32. van der Vusse, G.J., M. van Bilsen, and J.F.C. Glatz, *Cardiac fatty acid uptake and transport in health and disease.* Cardiovascular Research, 2000. **45**(2): p. 279-293.

33. Glatz, J.F.C., J.J.F.P. Luiken, and A.J.J.o.M.N. Bonen, *Involvement of membrane-associated proteins in the acute regulation of cellular fatty acid uptake.* 2001. **16**(2): p. 123-132.

34. Schaffer, J.E., *Fatty acid transport: the roads taken.* 2002. **282**(2): p. E239-E246.

35. Kintaka, T., et al., *CD36 Genotype and Long-Chain Fatty Acid Uptake in the Heart.* Circulation Journal, 2002. **66**(9): p. 819-825.

36. Lopaschuk, G.D., et al., *Myocardial Fatty Acid Metabolism in Health and Disease.* 2010. **90**(1): p. 207-258.

37. Lopaschuk, G.D., et al., *Regulation of fatty acid oxidation in the mammalian heart in health and disease.* Biochimica et Biophysica Acta (BBA) - Lipids and Lipid Metabolism, 1994. **1213**(3): p. 263-276.

38. Saddik, M. and G.D. Lopaschuk, *Myocardial triglyceride turnover and contribution to energy substrate utilization in isolated working rat hearts.* J Biol Chem, 1991. **266**(13): p. 8162-70.

39. Saddik, M. and G.D. Lopaschuk, *Myocardial triglyceride turnover during reperfusion of isolated rat hearts subjected to a transient period of global ischemia.* J Biol Chem, 1992. **267**(6): p. 3825-31.

40. McGarry, J.D., et al., *Observations on the affinity for carnitine, and malonyl-CoA sensitivity, of carnitine palmitoyltransferase I in animal and human tissues. Demonstration of the presence of malonyl-CoA in non-hepatic tissues of the rat.* 1983. **214**(1): p. 21-28.

41. Zammit, V.A., F. Fraser, and C.G. Orstorphine, *Regulation of mitochondrial outer-membrane carnitine palmitoyltransferase (CPT I): Role of membrane-topology.* Advances in Enzyme Regulation, 1997. **37**: p. 295-317.

42.   Zhou, L., et al., *Metabolic response to an acute jump in cardiac workload: effects on malonyl-CoA, mechanical efficiency, and fatty acid oxidation.* 2008. **294**(2): p. H954-H960.

43.   Avogaro, A., et al., *Myocardial metabolism in insulin-deficient diabetic humans without coronary artery disease.* 1990. **258**(4): p. E606-E618.

44.   Goodwin, G.W. and H. Taegtmeyer, *Regulation of fatty acid oxidation of the heart by MCD and ACC during contractile stimulation.* 1999. **277**(4): p. E772-E777.

45.   Saddik, M., et al., *Acetyl-CoA carboxylase regulation of fatty acid oxidation in the heart.* J Biol Chem, 1993. **268**(34): p. 25836-45.

46.   MUOIO, D.M., et al., *AMP-activated kinase reciprocally regulates triacylglycerol synthesis and fatty acid oxidation in liver and muscle: evidence that sn-glycerol-3-phosphate acyltransferase is a novel target.* 1999. **338**(3): p. 783-791.

47.   Nance, M.E., et al., *Attenuated sarcomere lengthening of the aged murine left ventricle observed using two-photon fluorescence microscopy.* American journal of physiology. Heart and circulatory physiology, 2015. **309**(5): p. H918-H925.

48.   Dyck, J.R.B., et al., *Malonyl Coenzyme A Decarboxylase Inhibition Protects the Ischemic Heart by Inhibiting Fatty Acid Oxidation and Stimulating Glucose Oxidation.* 2004. **94**(9): p. e78-e84.

49.   Kornberg, H.L., *The regulation of anaplerotic enzymes in E. coli.* Bull Soc Chim Biol (Paris), 1967. **49**(11): p. 1479-90.

50.   Des Rosiers, C., et al., *Cardiac anaplerosis in health and disease: food for thought.* Cardiovascular Research, 2011. **90**(2): p. 210-219.

51.   Russell, R.R., 3rd and H. Taegtmeyer, *Changes in citric acid cycle flux and anaplerosis antedate the functional decline in isolated rat hearts utilizing acetoacetate.* The Journal of Clinical Investigation, 1991. **87**(2): p. 384-390.

52.   Murphy, Michael P., *How mitochondria produce reactive oxygen species.* 2009. **417**(1): p. 1-13.

53.   Bing, R.J., et al., *Metabolism of the human heart: II. Studies on fat, ketone and amino acid metabolism.* The American Journal of Medicine, 1954. **16**(4): p. 504-515.

54.   Stanley, W.C., et al., *β-Hydroxybutyrate inhibits myocardial fatty acid oxidation in vivo independent of changes in malonyl-CoA content.* 2003. **285**(4): p. H1626-H1631.

55.   Ungar, I., et al., *Studies on myocardial metabolism: IV. Myocardial metabolism in diabetes.* The American Journal of Medicine, 1955. **18**(3): p. 385-396.

56.   Forsey, R.G.P., K. Reid, and J.T. Brosnan, *Competition between fatty acids and carbohydrate or ketone bodies as metabolic fuels for the isolated perfused heart.* Canadian Journal of Physiology and Pharmacology, 1987. **65**(3): p. 401-406.

57.   Lei, M., et al., *Characterisation of the transient outward K+ current in rabbit sinoatrial node cells.* Cardiovascular Research, 2000. **46**(3): p. 433-441.

58.   Cooper, G., *Cardiocyte Cytoskeleton in Hypertrophied Myocardium.* Heart Failure Reviews, 2000. **5**(3): p. 187-201.

59.   Huxley, H. and J. Hanson, *Changes in the Cross-Striations of Muscle during Contraction and Stretch and their Structural Interpretation.* Nature, 1954. **173**(4412): p. 973-976.

60.   Eisenberg, E. and W.W. Kielley, *Troponin-tropomyosin complex. Column chromatographic separation and activity of the three, active troponin components with and without tropomyosin present.* J Biol Chem, 1974. **249**(15): p. 4742-8.

61.   Eisner, D.A., et al., *Calcium and Excitation-Contraction Coupling in the Heart.* 2017. **121**(2): p. 181-195.

62.   Jayasinghe, I.D., M.B. Cannell, and C. Soeller, *Organization of Ryanodine Receptors, Transverse Tubules, and Sodium-Calcium Exchanger in Rat Myocytes.* Biophysical Journal, 2009. **97**(10): p. 2664-2673.

63.   Periasamy, M., P. Bhupathy, and G.J. Babu, *Regulation of sarcoplasmic reticulum Ca2+ ATPase pump expression and its relevance to cardiac muscle physiology and pathology.* Cardiovascular Research, 2007. **77**(2): p. 265-273.

64. Hausenloy, D.J. and D.M. Yellon, *Reperfusion injury salvage kinase signalling: taking a RISK for cardioprotection.* Heart Fail Rev, 2007. **12**(3-4): p. 217-34.

65. Krug, A., R. Du Mesnil de, and G. Korb, *Blood supply of the myocardium after temporary coronary occlusion.* Circ Res, 1966. **19**(1): p. 57-62.

66. Ito, H., et al., *Clinical implications of the 'no reflow' phenomenon. A predictor of complications and left ventricular remodeling in reperfused anterior wall myocardial infarction.* Circulation, 1996. **93**(2): p. 223-8.

67. Wu, K.C., et al., *Prognostic significance of microvascular obstruction by magnetic resonance imaging in patients with acute myocardial infarction.* Circulation, 1998. **97**(8): p. 765-72.

68. Ito, H., *No-reflow phenomenon and prognosis in patients with acute myocardial infarction.* Nat Clin Pract Cardiovasc Med, 2006. **3**(9): p. 499-506.

69. Kleinbongard, P., et al., *Vasoconstrictor potential of coronary aspirate from patients undergoing stenting of saphenous vein aortocoronary bypass grafts and its pharmacological attenuation.* Circ Res, 2011. **108**(3): p. 344-52.

70. Lemasters, J.J., et al., *The pH paradox in ischemia-reperfusion injury to cardiac myocytes.* Exs, 1996. **76**: p. 99-114.

71. Qian, T., et al., *Mitochondrial permeability transition in pH-dependent reperfusion injury to rat hepatocytes.* Am J Physiol, 1997. **273**(6): p. C1783-92.

72. Miyamae, M., et al., *Attenuation of postischemic reperfusion injury is related to prevention of [Ca2+]m overload in rat hearts.* 1996. **271**(5): p. H2145-H2153.

73. GOLL, D.E., et al., *The Calpain System.* 2003. **83**(3): p. 731-801.

74. Letavernier, E., et al., *The role of calpains in myocardial remodelling and heart failure.* Cardiovascular Research, 2012. **96**(1): p. 38-45.

75. Moldoveanu, T., et al., *A Ca2+ Switch Aligns the Active Site of Calpain.* Cell, 2002. **108**(5): p. 649-660.

76. Hernando, V., et al., *Calpain translocation and activation as pharmacological targets during myocardial ischemia/reperfusion.* Journal of Molecular and Cellular Cardiology, 2010. **49**(2): p. 271-279.

77. Jánossy, J., et al., *Calpain as a multi-site regulator of cell cycle.* Biochemical Pharmacology, 2004. **67**(8): p. 1513-1521.

78. Barta, J., et al., *Calpain-1-sensitive myofibrillar proteins of the human myocardium.* Molecular and Cellular Biochemistry, 2005. **278**(1): p. 1-8.

79. Wu, C.Y.C., et al., *Calpain‐Dependent Cleavage of Junctophilin‐2 and T‐Tubule Remodeling in a Mouse Model of Reversible Heart Failure.* 2014. **3**(3): p. e000527.

80. Murphy, R.M., et al., *Ca2+-dependent proteolysis of junctophilin-1 and junctophilin-2 in skeletal and cardiac muscle.* 2013. **591**(3): p. 719-729.

81. Sachse, F.B., et al., *Subcellular Structures and Function of Myocytes Impaired During Heart Failure Are Restored by Cardiac Resynchronization Therapy.* 2012. **110**(4): p. 588-597.

82. Balijepalli, R.C. and T.J. Kamp, *Cardiomyocyte transverse tubule loss leads the way to heart failure.* 2011. **7**(1): p. 39-42.

83. Portbury, A.L., M.S. Willis, and C. Patterson, *Tearin' up my heart: proteolysis in the cardiac sarcomere.* J Biol Chem, 2011. **286**(12): p. 9929-34.

84. Haworth, R.A. and D.R. Hunter, *The Ca2+-induced membrane transition in mitochondria. II. Nature of the Ca2+ trigger site.* Arch Biochem Biophys, 1979. **195**(2): p. 460-7.

85. Crompton, M., A. Costi, and L. Hayat, *Evidence for the presence of a reversible Ca²⁺-dependent pore activated by oxidative stress in heart mitochondria.* 1987. **245**(3): p. 915-918.

86. Griffiths, E.J. and A.P. Halestrap, *Mitochondrial non-specific pores remain closed during cardiac ischaemia, but open upon reperfusion.* 1995. **307**(1): p. 93-98.

87. Qian, T., et al., *Mitochondrial permeability transition in pH-dependent reperfusion injury to rat hepatocytes.* 1997. **273**(6): p. C1783-C1792.

88. Suleiman, M.S., A.P. Halestrap, and E.J. Griffiths, *Mitochondria: a target for myocardial protection.* Pharmacology & Therapeutics, 2001. **89**(1): p. 29-46.

89. Kroemer, G., B. Dallaporta, and M. Resche-Rigon, *THE MITOCHONDRIAL DEATH/LIFE REGULATOR IN APOPTOSIS AND NECROSIS.* 1998. **60**(1): p. 619-642.

90. Gottlieb, R.A., et al., *Reperfusion injury induces apoptosis in rabbit cardiomyocytes.* The Journal of Clinical Investigation, 1994. **94**(4): p. 1621-1628.

91. Scarabelli, T.M., et al., *Quantitative assessment of cardiac myocyte apoptosis in tissue sections using the fluorescence-based tunel technique enhanced with counterstains.* Journal of Immunological Methods, 1999. **228**(1): p. 23-28.

92. Zhao, Z.-Q., et al., *Reperfusion induces myocardial apoptotic cell death.* Cardiovascular Research, 2000. **45**(3): p. 651-660.

93. Eaton, P. and H. Clements-Jewery, *Peroxynitrite: in vivo cardioprotectant or arrhythmogen?* Br J Pharmacol, 2008. **155**(7): p. 972-3.

94. Zimmerman, J.J., *Defining the role of oxyradicals in the pathogenesis of sepsis.* Crit Care Med, 1995. **23**(4): p. 616-7.

95. Brandes, R.P. and J. Kreuzer, *Vascular NADPH oxidases: molecular mechanisms of activation.* Cardiovasc Res, 2005. **65**(1): p. 16-27.

96. Braunersreuther, V., et al., *Role of NADPH oxidase isoforms NOX1, NOX2 and NOX4 in myocardial ischemia/reperfusion injury.* Journal of Molecular and Cellular Cardiology, 2013. **64**: p. 99-107.

97. Wang, X., et al., *A superoxide anion biosensor based on direct electron transfer of superoxide dismutase on sodium alginate sol-gel film and its application to monitoring of living cells.* Anal Chim Acta, 2012. **717**: p. 61-6.

98. González-Montero, J., et al., *Myocardial reperfusion injury and oxidative stress: Therapeutic opportunities.* World journal of cardiology, 2018. **10**(9): p. 74-86.

99. Vasquez-Vivar, J., et al., *Superoxide generation by endothelial nitric oxide synthase: the influence of cofactors.* Proc Natl Acad Sci U S A, 1998. **95**(16): p. 9220-5.

100. Schulz, E., et al., *Nitric oxide, tetrahydrobiopterin, oxidative stress, and endothelial dysfunction in hypertension.* Antioxid Redox Signal, 2008. **10**(6): p. 1115-26.

101. Hayward, R., et al., *Recombinant soluble P-selectin glycoprotein ligand-1 protects against myocardial ischemic reperfusion injury in cats.* Cardiovasc Res, 1999. **41**(1): p. 65-76.

102. Zhao, Z.Q., et al., *Monoclonal antibody to ICAM-1 preserves postischemic blood flow and reduces infarct size after ischemia-reperfusion in rabbit.* J Leukoc Biol, 1997. **62**(3): p. 292-300.

103. Vakeva, A.P., et al., *Myocardial infarction and apoptosis after myocardial ischemia and reperfusion: role of the terminal complement components and inhibition by anti-C5 therapy.* Circulation, 1998. **97**(22): p. 2259-67.

104. Granger, C.B., et al., *Pexelizumab, an anti-C5 complement antibody, as adjunctive therapy to primary percutaneous coronary intervention in acute myocardial infarction: the COMplement inhibition in Myocardial infarction treated with Angioplasty (COMMA) trial.* Circulation, 2003. **108**(10): p. 1184-90.

105. Armstrong, P.W., et al., *Pexelizumab for acute ST-elevation myocardial infarction in patients undergoing primary percutaneous coronary intervention: a randomized controlled trial.* Jama, 2007. **297**(1): p. 43-51.

106. Heidenreich, P.A., et al., *Forecasting the future of cardiovascular disease in the United States: A policy statement from the American Heart Association.* Circulation, 2011. **123**(8): p. 933-944.

107. Kuller, L.H., et al., *Subclinical Cardiovascular Disease and Death, Dementia, and Coronary Heart Disease in Patients 80+ Years.* Journal of the American College of Cardiology, 2016. **67**(9): p. 1013-1022.

108. Newman, A.B., et al., *Coronary Artery Calcium, Carotid Artery Wall Thickness, and Cardiovascular Disease Outcomes in Adults 70 to 99 Years Old.* The American Journal of Cardiology, 2008. **101**(2): p. 186-192.

109. Camici, G.G., et al., *Molecular mechanism of endothelial and vascular aging: implications for cardiovascular disease.* European Heart Journal, 2015. **36**(48): p. 3392-3403.

110. Gerstenblith, G., et al., *Echocardiographic assessment of a normal adult aging population.* Circulation, 1977. **56**(2): p. 273-8.

111. Olivetti, G., et al., *Cardiomyopathy of the aging human heart. Myocyte loss and reactive cellular hypertrophy.* Circ Res, 1991. **68**(6): p. 1560-8.

112. Hees, P.S., et al., *Left ventricular remodeling with age in normal men versus women: novel insights using three-dimensional magnetic resonance imaging.* Am J Cardiol, 2002. **90**(11): p. 1231-6.

113. Lakatta, E.G., M. Wang, and S.S. Najjar, *Arterial aging and subclinical arterial disease are fundamentally intertwined at macroscopic and molecular levels.* Med Clin North Am, 2009. **93**(3): p. 583-604, Table of Contents.

114. Ungvari, Z., et al., *Mechanisms of vascular aging: new perspectives.* J Gerontol A Biol Sci Med Sci, 2010. **65**(10): p. 1028-41.

115. Zieman, S.J., V. Melenovsky, and D.A. Kass, *Mechanisms, pathophysiology, and therapy of arterial stiffness.* Arterioscler Thromb Vasc Biol, 2005. **25**(5): p. 932-43.

116. Lakatta, E.G. and D. Levy, *Arterial and cardiac aging: major shareholders in cardiovascular disease enterprises: Part I: aging arteries: a "set up" for vascular disease.* Circulation, 2003. **107**(1): p. 139-46.

117. Tschudi, M.R., et al., *Effect of age on kinetics of nitric oxide release in rat aorta and pulmonary artery.* J Clin Invest, 1996. **98**(4): p. 899-905.

118. Cernadas, M.R., et al., *Expression of constitutive and inducible nitric oxide synthases in the vascular wall of young and aging rats.* Circ Res, 1998. **83**(3): p. 279-86.

119. Schulman, S.P., et al., *Age-related decline in left ventricular filling at rest and exercise.* Am J Physiol, 1992. **263**(6 Pt 2): p. H1932-8.

120. Kates, A.M., et al., *Impact of aging on substrate metabolism by the human heart.* 2003. **41**(2): p. 293-299.

121. Hall, J.L., et al., *Exercise training does not compensate for age-related decrease in myocardial GLUT-4 content.* 1994. **76**(1): p. 328-332.

122. Moreau, R., et al., *Age-related compensatory activation of pyruvate dehydrogenase complex in rat heart.* Biochem Biophys Res Commun, 2004. **325**(1): p. 48-58.

123. McMillin, J.B., et al., *Mitochondrial metabolism and substrate competition in the aging Fischer rat heart.* Cardiovasc Res, 1993. **27**(12): p. 2222-8.

124. Iemitsu, M., et al., *Aging-induced decrease in the PPAR-α level in hearts is improved by exercise training.* 2002. **283**(5): p. H1750-H1760.

125. Gao, X., D.G. Jakovljevic, and D.A. Beard, *Cardiac Metabolic Limitations Contribute to Diminished Performance of the Heart in Aging.* 2019: p. 560649.

126. Nathania, M., et al., *Impact of age on the association between cardiac high-energy phosphate metabolism and cardiac power in women.* 2018. **104**(2): p. 111-118.

127. Beadle, R.M., et al., *Improvement in Cardiac Energetics by Perhexiline in Heart Failure Due to Dilated Cardiomyopathy.* JACC: Heart Failure, 2015. **3**(3): p. 202-211.

128. Spoladore, R., et al., *Beneficial effects of beta-blockers on left ventricular function and cellular energy reserve in patients with heart failure.* 2013. **27**(4): p. 455-464.

129. Fragasso, G., et al., *Effects of metabolic modulation by trimetazidine on left ventricular function and phosphocreatine/adenosine triphosphate ratio in patients with heart failure.* European Heart Journal, 2006. **27**(8): p. 942-948.

130. Lakatta, E.G. and S.J. Sollott, *Perspectives on mammalian cardiovascular aging: humans to molecules.* Comp Biochem Physiol A Mol Integr Physiol, 2002. **132**(4): p. 699-721.

131. Buttrick, P., et al., *Effect of aging and hypertension on myosin biochemistry and gene expression in the rat heart.* 1991. **68**(3): p. 645-652.
132. Lim, C.C., et al., *Impaired lusitropy-frequency in the aging mouse: role of Ca2+-handling proteins and effects of isoproterenol.* 1999. **277**(5): p. H2083-H2090.
133. Assayag, P., et al., *Effects of sustained low-flow ischemia on myocardial function and calcium-regulating proteins in adult and senescent rat hearts.* Cardiovasc Res, 1998. **38**(1): p. 169-80.
134. Nicholl, P.A. and S.E. Howlett, *Sarcoplasmic Reticulum Calcium Release Channels in Ventricles of Older Adult Hamsters.* Canadian Journal on Aging / La Revue canadienne du vieillissement, 2006. **25**(1): p. 107-113.
135. Xu, A. and N. Narayanan, *Effects of aging on sarcoplasmic reticulum Ca2+-cycling proteins and their phosphorylation in rat myocardium.* 1998. **275**(6): p. H2087-H2094.
136. Froehlich, J.P., et al., *Studies of sarcoplasmic reticulum function and contraction duration in young adult and aged rat myocardium.* Journal of Molecular and Cellular Cardiology, 1978. **10**(5): p. 427-438.
137. Orchard, C.H. and E.G. Lakatta, *Intracellular calcium transients and developed tension in rat heart muscle. A mechanism for the negative interval-strength relationship.* 1985. **86**(5): p. 637-651.
138. Heyliger, C.E., A.R. Prakash, and J.H.J.A. McNeill, *Alterations in membrane Na+-Ca2+ exchange in the aging myocardium.* 1988. **11**(1): p. 1-6.
139. Abete, P., et al., *The Role of Aging on the Control of Contractile Force by Na+-Ca2+ Exchange in Rat Papillary Muscle.* The Journals of Gerontology: Series A, 1996. **51A**(5): p. M251-M259.
140. Mace, L.C., et al., *Influence of age and run training on cardiac Na+/Ca2+ exchange.* 2003. **95**(5): p. 1994-2003.
141. Fannin, S.W., et al., *Aging selectively decreases oxidative capacity in rat heart interfibrillar mitochondria.* Arch Biochem Biophys, 1999. **372**(2): p. 399-407.
142. Riva, A., et al., *Structural differences in two biochemically defined populations of cardiac mitochondria.* Am J Physiol Heart Circ Physiol, 2005. **289**(2): p. H868-72.
143. Riva, A., et al., *Structure of cristae in cardiac mitochondria of aged rat.* Mech Ageing Dev, 2006. **127**(12): p. 917-21.
144. El'darov, C.M., et al., *Morphometric examination of mitochondrial ultrastructure in aging cardiomyocytes.* 2015. **80**(5): p. 604-609.
145. Hollander, J.M., D. Thapa, and D.L. Shepherd, *Physiological and structural differences in spatially distinct subpopulations of cardiac mitochondria: influence of cardiac pathologies.* 2014. **307**(1): p. H1-H14.
146. Hoppel, C.L., et al., *Hamster cardiomyopathy. A defect in oxidative phosphorylation in the cardiac interfibrillar mitochondria.* J Biol Chem, 1982. **257**(3): p. 1540-8.
147. Boengler, K., et al., *Mitochondria and ageing: role in heart, skeletal muscle and adipose tissue.* Journal of cachexia, sarcopenia and muscle, 2017. **8**(3): p. 349-369.
148. Lesnefsky, E.J., et al., *Aging decreases electron transport complex III activity in heart interfibrillar mitochondria by alteration of the cytochrome c binding site.* J Mol Cell Cardiol, 2001. **33**(1): p. 37-47.
149. Takasawa, M., et al., *Age-associated damage in mitochondrial function in rat hearts.* Exp Gerontol, 1993. **28**(3): p. 269-80.
150. Escobales, N., et al., *Mitochondria-targeted ROS scavenger improves post-ischemic recovery of cardiac function and attenuates mitochondrial abnormalities in aged rats.* J Mol Cell Cardiol, 2014. **77**: p. 136-46.
151. Suh, J.H., S.H. Heath, and T.M. Hagen, *Two subpopulations of mitochondria in the aging rat heart display heterogenous levels of oxidative stress.* Free Radic Biol Med, 2003. **35**(9): p. 1064-72.

152. Preston, C.C., et al., *Aging-induced alterations in gene transcripts and functional activity of mitochondrial oxidative phosphorylation complexes in the heart.* Mech Ageing Dev, 2008. **129**(6): p. 304-12.

153. Moreno-Ulloa, A., et al., *Recovery of Indicators of Mitochondrial Biogenesis, Oxidative Stress, and Aging With (-)-Epicatechin in Senile Mice.* J Gerontol A Biol Sci Med Sci, 2015. **70**(11): p. 1370-8.

154. Niemann, B., et al., *Obesity induces signs of premature cardiac aging in younger patients: the role of mitochondria.* J Am Coll Cardiol, 2011. **57**(5): p. 577-85.

155. Aurich, A.C., et al., *Age-dependent effects of high fat-diet on murine left ventricles: role of palmitate.* Basic Res Cardiol, 2013. **108**(5): p. 369.

156. Paradies, G., et al., *Functional role of cardiolipin in mitochondrial bioenergetics.* Biochim Biophys Acta, 2014. **1837**(4): p. 408-17.

157. Fujioka, H., et al., *Decreased cytochrome c oxidase subunit VIIa in aged rat heart mitochondria: immunocytochemistry.* Anat Rec (Hoboken), 2011. **294**(11): p. 1825-33.

158. Mejia, E.M., L.K. Cole, and G.M. Hatch, *Cardiolipin metabolism and the role it plays in heart failure and mitochondrial supercomplex formation.* Cardiovasc Hematol Disord Drug Targets, 2014. **14**(2): p. 98-106.

159. Barja, G., *Mitochondrial oxygen radical generation and leak: sites of production in states 4 and 3, organ specificity, and relation to aging and longevity.* J Bioenerg Biomembr, 1999. **31**(4): p. 347-66.

160. Pinton, P., et al., *Protein kinase C beta and prolyl isomerase 1 regulate mitochondrial effects of the life-span determinant p66Shc.* Science, 2007. **315**(5812): p. 659-63.

161. Duicu, O.M., et al., *Ageing-induced decrease in cardiac mitochondrial function in healthy rats.* Can J Physiol Pharmacol, 2013. **91**(8): p. 593-600.

162. Petrosillo, G., et al., *Mitochondrial complex I dysfunction in rat heart with aging: critical role of reactive oxygen species and cardiolipin.* Free Radic Biol Med, 2009. **46**(1): p. 88-94.

163. Hansford, R.G., B.A. Hogue, and V. Mildaziene, *Dependence of H2O2 formation by rat heart mitochondria on substrate availability and donor age.* J Bioenerg Biomembr, 1997. **29**(1): p. 89-95.

164. Gredilla, R., et al., *Caloric restriction decreases mitochondrial free radical generation at complex I and lowers oxidative damage to mitochondrial DNA in the rat heart.* Faseb j, 2001. **15**(9): p. 1589-91.

165. Judge, S., et al., *Age-associated increases in oxidative stress and antioxidant enzyme activities in cardiac interfibrillar mitochondria: implications for the mitochondrial theory of aging.* Faseb j, 2005. **19**(3): p. 419-21.

166. Saura, J., J.G. Richards, and N. Mahy, *Differential age-related changes of MAO-A and MAO-B in mouse brain and peripheral organs.* Neurobiol Aging, 1994. **15**(4): p. 399-408.

167. Ljubicic, V., K.J. Menzies, and D.A. Hood, *Mitochondrial dysfunction is associated with a pro-apoptotic cellular environment in senescent cardiac muscle.* Mech Ageing Dev, 2010. **131**(2): p. 79-88.

168. Dai, D.F., et al., *Overexpression of catalase targeted to mitochondria attenuates murine cardiac aging.* Circulation, 2009. **119**(21): p. 2789-97.

169. Jang, Y.C., et al., *Overexpression of Mn superoxide dismutase does not increase life span in mice.* J Gerontol A Biol Sci Med Sci, 2009. **64**(11): p. 1114-25.

170. Van Remmen, H., et al., *Life-long reduction in MnSOD activity results in increased DNA damage and higher incidence of cancer but does not accelerate aging.* Physiol Genomics, 2003. **16**(1): p. 29-37.

171. Boengler, K., G. Heusch, and R. Schulz, *Mitochondria in postconditioning.* Antioxid Redox Signal, 2011. **14**(5): p. 863-80.

172. Dorn, G.W., 2nd, *Mitochondrial dynamics in heart disease.* Biochim Biophys Acta, 2013. **1833**(1): p. 233-41.

173. Liu, L., et al., *Age-associated differences in the inhibition of mitochondrial permeability transition pore opening by cyclosporine A.* Acta Anaesthesiol Scand, 2011. **55**(5): p. 622-30.

174. Lesnefsky, E.J. and C.L. Hoppel, *Ischemia–reperfusion injury in the aged heart: role of mitochondria.* Archives of Biochemistry and Biophysics, 2003. **420**(2): p. 287-297.

175. Lesnefsky, E.J., et al., *Aging increases ischemia-reperfusion injury in the isolated, buffer-perfused heart.* J Lab Clin Med, 1994. **124**(6): p. 843-51.

176. Liu, P., et al., *Age-related difference in myocardial function and inflammation in a rat model of myocardial ischemia–reperfusion.* Cardiovascular Research, 2002. **56**(3): p. 443-453.

177. Tani, M., et al., *Decrease in Ischemic Tolerance with Aging in Isolated Perfused Fischer 344 Rat Hearts: Relation to Increases in Intracellular Na+After Ischemia.* Journal of Molecular and Cellular Cardiology, 1997. **29**(11): p. 3081-3089.

178. Frolkis, V.V., et al., *Age-Dependent Effects of Ischemia and Reperfusion on Cardiac Function and Ca2+ Transport in Myocardium.* Gerontology, 1991. **37**(5): p. 233-239.

179. Azhar, G., et al., *Ischemia-reperfusion in the adult mouse heart: Influence of age☆11Both authors contributed equally to this work.* Experimental Gerontology, 1999. **34**(5): p. 699-714.

180. Willems, L., et al., *Age-related changes in ischemic tolerance in male and female mouse hearts.* Journal of Molecular and Cellular Cardiology, 2005. **38**(2): p. 245-256.

181. Quan, N., et al., *Sestrin2 prevents age-related intolerance to ischemia and reperfusion injury by modulating substrate metabolism.* 2017. **31**(9): p. 4153-4167.

182. Porter, G.A., et al., *SIRT3 deficiency exacerbates ischemia-reperfusion injury: implication for aged hearts.* 2014. **306**(12): p. H1602-H1609.

183. Boengler, K., et al., *Loss of ischemic preconditioning's cardioprotection in aged mouse hearts is associated with reduced gap junctional and mitochondrial levels of connexin 43.* 2007. **292**(4): p. H1764-H1769.

184. Mariani, J., et al., *Tolerance to ischemia and hypoxia is reduced in aged human myocardium.* The Journal of Thoracic and Cardiovascular Surgery, 2000. **120**(4): p. 660-667.

185. Loubani, M., S. Ghosh, and M. Galiñanes, *The aging human myocardium: tolerance to ischemia and responsiveness to ischemic preconditioning.* The Journal of Thoracic and Cardiovascular Surgery, 2003. **126**(1): p. 143-147.

186. GUO, Z., T. ROUSSELLE, and J. LI, *Caloric Restriction Increases the Resistance of Aged Heart to Myocardial Ischemia/Reperfusion Injury.* 2018. **67**(Supplement 1): p. 153-OR.

187. Whittington, H.J., et al., *Protective Effect of Creatine Elevation against Ischaemia Reperfusion Injury Is Retained in the Presence of Co-Morbidities and during Cardioplegia.* PLOS ONE, 2016. **11**(1): p. e0146429.

188. Golay, A. and E. Bobbioni, *The role of dietary fat in obesity.* Int J Obes Relat Metab Disord, 1997. **21 Suppl 3**: p. S2-11.

189. Marshall, J.A. and D.H. Bessesen, *Dietary Fat and the Development of Type 2 Diabetes.* Diabetes Care, 2002. **25**(3): p. 620-622.

190. La Vecchia, C., *Cancers associated with high-fat diets.* J Natl Cancer Inst Monogr, 1992(12): p. 79-85.

191. Willett, W.C., *Dietary fats and coronary heart disease.* Journal of Internal Medicine, 2012. **272**(1): p. 13-24.

192. Hu, F.B. and W.C. Willett, *Optimal diets for prevention of coronary heart disease.* JAMA, 2002. **288**(20): p. 2569-2578.

193. Teodoro, J.S., et al., *High-fat and obesogenic diets: current and future strategies to fight obesity and diabetes.* Genes Nutr, 2014. **9**(4): p. 406.

194. Schreyer, S.A., D.L. Wilson, and R.C. LeBoeuf, *C57BL/6 mice fed high fat diets as models for diabetes-accelerated atherosclerosis.* Atherosclerosis, 1998. **136**(1): p. 17-24.

195. Nascimento, T.B., et al., *Vascular alterations in high-fat diet-obese rats: role of endothelial L-arginine/NO pathway.* Arq Bras Cardiol, 2011. **97**(1): p. 40-5.

196.	Martins, F., et al., *High-fat Diet Promotes Cardiac Remodeling in an Experimental Model of Obesity.* Arquivos brasileiros de cardiologia, 2015. **105**(5): p. 479-486.

197.	Oliveira Junior, S.A., et al., *Extensive impact of saturated fatty acids on metabolic and cardiovascular profile in rats with diet-induced obesity: a canonical analysis.* Cardiovascular diabetology, 2013. **12**: p. 65-65.

198.	Okere, I.C., et al., *Low carbohydrate/high-fat diet attenuates cardiac hypertrophy, remodeling, and altered gene expression in hypertension.* Hypertension, 2006. **48**(6): p. 1116-23.

199.	Calligaris, S.D., et al., *Mice long-term high-fat diet feeding recapitulates human cardiovascular alterations: an animal model to study the early phases of diabetic cardiomyopathy.* PloS one, 2013. **8**(4): p. e60931-e60931.

200.	Zarzoso, M., et al., *Ventricular remodelling in rabbits with sustained high-fat diet.* Acta Physiol (Oxf), 2014. **211**(1): p. 36-47.

201.	Sibouakaz, D., et al., *Biochemical and Ultrastructural Cardiac Changes Induced by High-Fat Diet in Female and Male Prepubertal Rabbits.* Anal Cell Pathol (Amst), 2018. **2018**: p. 6430696.

202.	Raher, M.J., et al., *A short duration of high-fat diet induces insulin resistance and predisposes to adverse left ventricular remodeling after pressure overload.* American Journal of Physiology-Heart and Circulatory Physiology, 2008. **295**(6): p. H2495-H2502.

203.	Silva, D.C., et al., *Influence of term of exposure to high-fat diet-induced obesity on myocardial collagen type I and III.* Arq Bras Cardiol, 2014. **102**(2): p. 157-63.

204.	Li, C., et al., *Aldehyde Dehydrogenase-2 Attenuates Myocardial Remodeling and Contractile Dysfunction Induced by a High-Fat Diet.* Cellular Physiology and Biochemistry, 2018. **48**(5): p. 1843-1853.

205.	Lima-Leopoldo, A.P., et al., *Obesity induces upregulation of genes involved in myocardial Ca2+ handling.* Braz J Med Biol Res, 2008. **41**(7): p. 615-20.

206.	Freire, P.P., et al., *Obesity does not lead to imbalance between myocardial phospholamban phosphorylation and dephosphorylation.* Arq Bras Cardiol, 2014. **103**(1): p. 41-50.

207.	Lima-Leopoldo, A.P., et al., *Myocardial dysfunction and abnormalities in intracellular calcium handling in obese rats.* Arq Bras Cardiol, 2011. **97**(3): p. 232-40.

208.	Zeng, H., et al., *High-fat diet induces cardiac remodelling and dysfunction: assessment of the role played by SIRT3 loss.* Journal of cellular and molecular medicine, 2015. **19**(8): p. 1847-1856.

209.	Li, H., et al., *Mediation of exogenous hydrogen sulfide in recovery of ischemic post-conditioning-induced cardioprotection via down-regulating oxidative stress and up-regulating PI3K/Akt/GSK-3beta pathway in isolated aging rat hearts.* Cell Biosci, 2015. **5**: p. 11.

210.	Roberts, N.W., et al., *Successful metabolic adaptations leading to the prevention of high fat diet-induced murine cardiac remodeling.* Cardiovascular Diabetology, 2015. **14**(1): p. 127.

211.	Duda, M.K., et al., *Low-Carbohydrate/High-Fat Diet Attenuates Pressure Overload–Induced Ventricular Remodeling and Dysfunction.* Journal of Cardiac Failure. **14**(4): p. 327-335.

212.	Hu, N. and Y. Zhang, *TLR4 knockout attenuated high fat diet-induced cardiac dysfunction via NF-kappaB/JNK-dependent activation of autophagy.* Biochim Biophys Acta, 2017. **1863**(8): p. 2001-2011.

213.	Birse, R.T., et al., *High-fat-diet-induced obesity and heart dysfunction are regulated by the TOR pathway in Drosophila.* Cell Metab, 2010. **12**(5): p. 533-44.

214.	Ouwens, D.M., et al., *Cardiac dysfunction induced by high-fat diet is associated with altered myocardial insulin signalling in rats.* Diabetologia, 2005. **48**(6): p. 1229-1237.

215.	Shiou, Y.-L., et al., *High fat diet aggravates atrial and ventricular remodeling of hypertensive heart disease in aging rats.* Journal of the Formosan Medical Association, 2017.

216.	Cole, M.A., et al., *A high fat diet increases mitochondrial fatty acid oxidation and uncoupling to decrease efficiency in rat heart.* Basic Research in Cardiology, 2011. **106**(3): p. 447-457.

217. Putti, R., et al., *Skeletal Muscle Mitochondrial Bioenergetics and Morphology in High Fat Diet Induced Obesity and Insulin Resistance: Focus on Dietary Fat Source.* 2016. **6**(426).

218. Jørgensen, W., et al., *Your mitochondria are what you eat: a high-fat or a high-sucrose diet eliminates metabolic flexibility in isolated mitochondria from rat skeletal muscle.* 2017. **5**(6): p. e13207.

219. Hoeks, J., et al., *Mitochondrial function, content and ROS production in rat skeletal muscle: Effect of high-fat feeding.* 2008. **582**(4): p. 510-516.

220. Hoeks, J., et al., *High Fat Diet-Induced Changes in Mouse Muscle Mitochondrial Phospholipids Do Not Impair Mitochondrial Respiration Despite Insulin Resistance.* PLOS ONE, 2011. **6**(11): p. e27274.

221. Chen, D., et al., *A high-fat diet impairs mitochondrial biogenesis, mitochondrial dynamics, and the respiratory chain complex in rat myocardial tissues.* Journal of cellular biochemistry, 2018. **119**(11): p. 9602-9602.

222. Emelyanova, L., et al., *High calories but not fat content of lard-based diet contribute to impaired mitochondrial oxidative phosphorylation in C57BL/6J mice heart.* PLOS ONE, 2019. **14**(7): p. e0217045.

223. Cormier, R.P.J., et al., *Dynamic mitochondrial responses to a high-fat diet in Drosophila melanogaster.* Scientific Reports, 2019. **9**(1): p. 4531.

224. Curtis, J.P., et al., *The Obesity Paradox: Body Mass Index and Outcomes in Patients With Heart Failure.* Archives of Internal Medicine, 2005. **165**(1): p. 55-61.

225. Poncelas, M., et al., *Obesity induced by high fat diet attenuates postinfarct myocardial remodeling and dysfunction in adult B6D2F1 mice.* Journal of Molecular and Cellular Cardiology, 2015. **84**: p. 154-161.

226. Inserte, J., et al., *High-fat diet improves tolerance to myocardial ischemia by delaying normalization of intracellular PH at reperfusion.* Journal of Molecular and Cellular Cardiology, 2019. **133**: p. 164-173.

227. Haar, L., et al., *Acute consumption of a high-fat diet prior to ischemia-reperfusion results in cardioprotection through NF-κB-dependent regulation of autophagic pathways.* 2014. **307**(12): p. H1705-H1713.

228. Salie, R., B. Huisamen, and A. Lochner, *High carbohydrate and high fat diets protect the heart against ischaemia/reperfusion injury.* Cardiovascular diabetology, 2014. **13**: p. 109-109.

229. Li, Y., et al., *HIGH FAT DIET EXACERBATES AND ENDURANCE EXERCISE AMELIORATES MYOCARDIAL ISCHEMIA REPERFUSION INJURY IN MICE.* 2011. **57**(14 Supplement): p. E968.

230. Lochner, A., et al., *Abstract 14724: Mitophagy in Ischemia/Reperfusion: Effects of High Fat Diet and Melatonin.* 2016. **134**(suppl_1): p. A14724-A14724.

231. Wensley, I., et al., *Myocardial structure, function and ischaemic tolerance in a rodent model of obesity with insulin resistance.* 2013. **98**(11): p. 1552-1564.

232. Mastrocola, R., et al., *Maladaptive Modulations of NLRP3 Inflammasome and Cardioprotective Pathways Are Involved in Diet-Induced Exacerbation of Myocardial Ischemia/Reperfusion Injury in Mice %J Oxidative Medicine and Cellular Longevity.* 2016. **2016**: p. 12.

233. Dasagrandhi, D., et al., *Ischemia/reperfusion injury in male guinea pigs: An efficient model to investigate myocardial damage in cardiovascular complications.* Biomedicine & Pharmacotherapy, 2018. **99**: p. 469-479.

234. Mozaffari, M.S. and S.W. Schaffer, *Myocardial Ischemic-reperfusion Injury in a Rat Model of Metabolic Syndrome.* 2008. **16**(10): p. 2253-2258.

235. Pongkan, W., et al., *Vildagliptin reduces cardiac ischemic-reperfusion injury in obese orchiectomized rats.* 2016. **231**(1): p. 81.

236. Littlejohns, B., et al., *Hearts from Mice Fed a Non-Obesogenic High-Fat Diet Exhibit Changes in Their Oxidative State, Calcium and Mitochondria in Parallel with Increased Susceptibility to Reperfusion Injury.* PLOS ONE, 2014. **9**(6): p. e100579.

237. Liu, J., et al., *High-fat, low-carbohydrate diet promotes arrhythmic death and increases myocardial ischemia-reperfusion injury in rats.* American Journal of Physiology-Heart and Circulatory Physiology, 2014. **307**(4): p. H598-H608.

238. Liu, J., et al., *Impact of high-fat, low-carbohydrate diet on myocardial substrate oxidation, insulin sensitivity, and cardiac function after ischemia-reperfusion.* American Journal of Physiology-Heart and Circulatory Physiology, 2016. **311**(1): p. H1-H10.

239. Slamova, K., et al., *Adverse effects of AMP-activated protein kinase alpha2-subunit deletion and high-fat diet on heart function and ischemic tolerance in aged female mice.* Physiol Res, 2016. **65**(1): p. 33-42.

240. Webster, I., et al., *Myocardial susceptibility to ischaemia/reperfusion in obesity: a re-evaluation of the effects of age.* BMC Physiol, 2017. **17**(1): p. 3.

241. Soininen, P., et al., *High-throughput serum NMR metabonomics for cost-effective holistic studies on systemic metabolism.* Analyst, 2009. **134**(9): p. 1781-1785.

242. Watkins, D.W., et al., *Construction and in vivo assembly of a catalytically proficient and hyperthermostable de novo enzyme.* Nature Communications, 2017. **8**(1): p. 358.

243. Hyyti, O.M., et al., *Aging impairs myocardial fatty acid and ketone oxidation and modifies cardiac functional and metabolic responses to insulin in mice.* Am J Physiol Heart Circ Physiol, 2010. **299**(3): p. H868-75.

244. Martineau, L.C., S.G. Chadan, and W.S. Parkhouse, *Age-associated alterations in cardiac and skeletal muscle glucose transporters, insulin and IGF-1 receptors, and PI3-kinase protein contents in the C57BL/6 mouse.* Mech Ageing Dev, 1999. **106**(3): p. 217-32.

245. Bratic, A., *The role of mitochondria in aging.* 2013. **123**(3): p. 951-7.

246. Hewitson, T.D., et al., *Relaxin and castration in male mice protect from, but testosterone exacerbates, age-related cardiac and renal fibrosis, whereas estrogens are an independent determinant of organ size.* Endocrinology, 2012. **153**(1): p. 188-99.

247. Cui, H., Y. Kong, and H. Zhang, *Oxidative Stress, Mitochondrial Dysfunction, and Aging.* Journal of Signal Transduction, 2012. **2012**: p. 13.

248. Chakravarti, B. and D.N. Chakravarti, *Oxidative Modification of Proteins: Age-Related Changes.* Gerontology, 2007. **53**(3): p. 128-139.

249. Harman, D., *Aging: a theory based on free radical and radiation chemistry.* 1955.

250. Martínez-Cisuelo, V., et al., *Rapamycin reverses age-related increases in mitochondrial ROS production at complex I, oxidative stress, accumulation of mtDNA fragments inside nuclear DNA, and lipofuscin level, and increases autophagy, in the liver of middle-aged mice.* Experimental Gerontology, 2016. **83**: p. 130-138.

251. Cristol, J.P., et al., *Impairment of antioxidant defense mechanisms in elderly women without increase in oxidative stress markers: "A weak equilibrium".* Lipids, 1999. **34**(1): p. S289-S289.

252. Vertechy, M., et al., *Antioxidant enzyme activities in heart and skeletal muscle of rats of different ages.* Exp Gerontol, 1989. **24**(3): p. 211-8.

253. Espinoza, S.E., et al., *Glutathione peroxidase enzyme activity in aging.* J Gerontol A Biol Sci Med Sci, 2008. **63**(5): p. 505-9.

254. Hall, D.M., et al., *Aging lowers steady-state antioxidant enzyme and stress protein expression in primary hepatocytes.* J Gerontol A Biol Sci Med Sci, 2001. **56**(6): p. B259-67.

255. Lessard-Beaudoin, M., et al., *Characterization of age-associated changes in peripheral organ and brain region weights in C57BL/6 mice.* Experimental Gerontology, 2015. **63**: p. 27-34.

256. CAMERON, T.P., et al., *History, Survival, and Growth Patterns of B6C3F1 Mice and F344 Rats in the National Cancer Institute Carcinogenesis Testing Program.* Toxicological Sciences, 1985. **5**(3): p. 526-538.

257. Cao, J., et al., *Expression of RANKL and OPG Correlates With Age-Related Bone Loss in Male C57BL/6 Mice.* 2003. **18**(2): p. 270-277.

258. Fahlström, A., Q. Yu, and B. Ulfhake, *Behavioral changes in aging female C57BL/6 mice.* Neurobiology of Aging, 2011. **32**(10): p. 1868-1880.

259. Glatt, V., et al., *Age-Related Changes in Trabecular Architecture Differ in Female and Male C57BL/6J Mice.* 2007. **22**(8): p. 1197-1207.

260. Marino, D.J., *Age-Specific Absolute and Relative Organ Weight Distributions For B6C3F1 Mice.* Journal of Toxicology and Environmental Health, Part A, 2012. **75**(2): p. 76-99.

261. Mancuso, P. and B. Bouchard, *The Impact of Aging on Adipose Function and Adipokine Synthesis.* Frontiers in endocrinology, 2019. **10**: p. 137-137.

262. Krishna, K.B., et al., *Similar degrees of obesity induced by diet or aging cause strikingly different immunologic and metabolic outcomes.* Physiological reports, 2016. **4**(6): p. e12708.

263. Lipman, R.D. and J.A. Grinker, *Weight gain by middle-aged mice: dietary modification does not result in loss.* Growth Dev Aging, 1996. **60**(2): p. 61-70.

264. Leiter, E.H., et al., *Aging and glucose homeostasis in C57BL/6J male mice.* Faseb j, 1988. **2**(12): p. 2807-11.

265. Gregg, T., et al., *Pancreatic β-Cells From Mice Offset Age-Associated Mitochondrial Deficiency With Reduced K_{ATP} Channel Activity.* 2016. **65**(9): p. 2700-2710.

266. J P Manfredi, a. and E.W. Holmes, *Purine Salvage Pathways in Myocardium.* 1985. **47**(1): p. 691-705.

267. Murray, A.W., D.C. Elliott, and M.R. Atkinson, *Nucleotide biosynthesis from preformed purines in mammalian cells: regulatory mechanisms and biological significance.* Prog Nucleic Acid Res Mol Biol, 1970. **10**: p. 87-119.

268. Finelli, C., et al., *Incorporation of [14C]hypoxanthine into cardiac adenine nucleotides: effect of aging and post-ischemic reperfusion.* Biochim Biophys Acta, 1993. **1180**(3): p. 262-6.

269. Martín-Fernández, B. and R. Gredilla, *Mitochondria and oxidative stress in heart aging.* Age (Dordrecht, Netherlands), 2016. **38**(4): p. 225-238.

270. Lewis, M., et al., *Cardiac taurine and principal amino acids in right and left ventricles of patients with either aortic valve stenosis or coronary artery disease: the importance of diabetes and gender.* Springerplus, 2014. **3**: p. 523.

271. Grajeda-Iglesias, C. and M. Aviram, *Specific Amino Acids Affect Cardiovascular Diseases and Atherogenesis via Protection against Macrophage Foam Cell Formation: Review Article.* Rambam Maimonides Med J, 2018. **9**(3).

272. Modi, P., et al., *Changes in myocardial free amino acids during pediatric cardiac surgery: a randomised controlled trial of three cardioplegic techniques.* Eur J Cardiothorac Surg, 2006. **30**(1): p. 41-8.

273. Giuseppe, M., et al., *The Role of Amino Acids in the Modulation of Cardiac Metabolism During Ischemia and Heart Failure.* Current Pharmaceutical Design, 2008. **14**(25): p. 2592-2604.

274. Schaffer, S.W., et al., *Physiological roles of taurine in heart and muscle.* J Biomed Sci, 2010. **17 Suppl 1**: p. S2.

275. Yang, A.N., et al., *High-methionine diets accelerate atherosclerosis by HHcy-mediated FABP4 gene demethylation pathway via DNMT1 in ApoE(-/-) mice.* FEBS Lett, 2015. **589**(24 Pt B): p. 3998-4009.

276. Shah, S.H., et al., *Association of a peripheral blood metabolic profile with coronary artery disease and risk of subsequent cardiovascular events.* Circ Cardiovasc Genet, 2010. **3**(2): p. 207-14.

277. Wurtz, P., et al., *High-throughput quantification of circulating metabolites improves prediction of subclinical atherosclerosis.* Eur Heart J, 2012. **33**(18): p. 2307-16.

278. Chernyavskiy, I., et al., *Atherogenesis: hyperhomocysteinemia interactions with LDL, macrophage function, paraoxonase 1, and exercise.* Ann N Y Acad Sci, 2016. **1363**: p. 138-54.

279. Paynter, N.P., et al., *Metabolic Predictors of Incident Coronary Heart Disease in Women.* Circulation, 2018. **137**(8): p. 841-853.

280. Deveaux, A., et al., *l-Arginine Supplementation Alleviates Postprandial Endothelial Dysfunction When Baseline Fasting Plasma Arginine Concentration Is Low: A Randomized Controlled Trial*

in Healthy Overweight Adults with Cardiometabolic Risk Factors. J Nutr, 2016. **146**(7): p. 1330-40.

281. Bahls, M., et al., *L-Arginine and SDMA Serum Concentrations Are Associated with Subclinical Atherosclerosis in the Study of Health in Pomerania (SHIP).* PLoS One, 2015. **10**(6): p. e0131293.

282. Lancaster, T.S., et al., *Quantitative proteomic analysis reveals novel mitochondrial targets of estrogen deficiency in the aged female rat heart.* 2012. **44**(20): p. 957-969.

283. Tanaka, T., et al., *Plasma proteomic signature of age in healthy humans.* Aging cell, 2018. **17**(5): p. e12799-e12799.

284. Nishtala, K., et al., *Proteomic analyses of age related changes in A.BY/SnJ mouse hearts.* Proteome science, 2013. **11**: p. 29.

285. Dai, D.-F., *GLOBAL PROTEOMICS REMODELING OF CARDIAC AGING AND PRESSURE-OVERLOAD INDUCED HEART FAILURE IS ATTENUATED BY SUPPRESSION RF TARGET OF RAPAMYCIN.* 2014. **63**(12 Supplement): p. A2149.

286. Chakravarti, B., et al., *Proteomic profiling of aging in the mouse heart: Altered expression of mitochondrial proteins.* Archives of Biochemistry and Biophysics, 2008. **474**(1): p. 22-31.

287. Vitorica, J., et al., *Comparison between developmental and senescent changes in enzyme activities linked to energy metabolism in rat heart.* Mechanisms of Ageing and Development, 1981. **16**(2): p. 105-116.

288. Savitha, S., et al., *Efficacy of levo carnitine and alpha lipoic acid in ameliorating the decline in mitochondrial enzymes during aging.* Clinical Nutrition, 2005. **24**(5): p. 794-800.

289. Yan, L., et al., *Gender-specific proteomic alterations in glycolytic and mitochondrial pathways in aging monkey hearts.* Journal of Molecular and Cellular Cardiology, 2004. **37**(5): p. 921-929.

290. Toro, L., et al., *Aging, ion channel expression, and vascular function.* Vascular Pharmacology, 2002. **38**(1): p. 73-80.

291. Climent, B., et al., *Underlying mechanisms preserving coronary basal tone and NO-mediated relaxation in obesity: Involvement of beta1 subunit-mediated upregulation of BKCa channels.* Atherosclerosis, 2017. **263**: p. 227-236.

292. Molina-Navarro, M.M., et al., *Differential Gene Expression of Cardiac Ion Channels in Human Dilated Cardiomyopathy.* PLOS ONE, 2013. **8**(12): p. e79792.

293. Strickland, M., et al., *Relationships Between Ion Channels, Mitochondrial Functions and Inflammation in Human Aging.* 2019. **10**(158).

294. Sohal, R.S., L.A. Arnold, and B.H. Sohal, *Age-related changes in antioxidant enzymes and prooxidant generation in tissues of the rat with special reference to parameters in two insect species.* Free Radic Biol Med, 1990. **9**(6): p. 495-500.

295. Baek, M.-K., et al., *Age-Related Changes in Antioxidative Enzyme Capacity in Tongue of Fischer 344 Rats.* Clinical and experimental otorhinolaryngology, 2016. **9**(4): p. 352-357.

296. Boldyrev, A.A., et al., *Antioxidant systems in tissues of senescence accelerated mice.* Biochemistry (Mosc), 2001. **66**(10): p. 1157-63.

297. Siqueira, I.R., et al., *Total antioxidant capacity is impaired in different structures from aged rat brain.* Int J Dev Neurosci, 2005. **23**(8): p. 663-71.

298. Ehrenbrink, G., et al., *Antioxidant enzymes activities and protein damage in rat brain of both sexes.* Exp Gerontol, 2006. **41**(4): p. 368-71.

299. Gomes, P., et al., *Aging increases oxidative stress and renal expression of oxidant and antioxidant enzymes that are associated with an increased trend in systolic blood pressure.* Oxidative medicine and cellular longevity, 2009. **2**(3): p. 138-145.

300. Lambertucci, R.H., et al., *Effects of aerobic exercise training on antioxidant enzyme activities and mRNA levels in soleus muscle from young and aged rats.* Mech Ageing Dev, 2007. **128**(3): p. 267-75.

301. Kajstura, J., et al., *Necrotic and apoptotic myocyte cell death in the aging heart of Fischer 344 rats.* Am J Physiol, 1996. **271**(3 Pt 2): p. H1215-28.

302. Liu, L., et al., *Bcl-2 and Bax expression in adult rat hearts after coronary occlusion: age-associated differences.* Am J Physiol, 1998. **275**(1): p. R315-22.

303. Kwak, H.B., W. Song, and J.M. Lawler, *Exercise training attenuates age-induced elevation in Bax/Bcl-2 ratio, apoptosis, and remodeling in the rat heart.* Faseb j, 2006. **20**(6): p. 791-3.

304. Song, W., H.B. Kwak, and J.M. Lawler, *Exercise training attenuates age-induced changes in apoptotic signaling in rat skeletal muscle.* Antioxid Redox Signal, 2006. **8**(3-4): p. 517-28.

305. Nitahara, J.A., et al., *Intracellular calcium, DNase activity and myocyte apoptosis in aging Fischer 344 rats.* J Mol Cell Cardiol, 1998. **30**(3): p. 519-35.

306. Higami, Y. and I. Shimokawa, *Apoptosis in the aging process.* Cell Tissue Res, 2000. **301**(1): p. 125-32.

307. Xiao, Z.Q., et al., *Aging is associated with increased proliferation and decreased apoptosis in the colonic mucosa.* Mech Ageing Dev, 2001. **122**(15): p. 1849-64.

308. Zhang, Y., E. Chong, and B. Herman, *Age-associated increases in the activity of multiple caspases in Fisher 344 rat organs.* Exp Gerontol, 2002. **37**(6): p. 777-89.

309. Suh, Y., et al., *Aging alters the apoptotic response to genotoxic stress.* Nat Med, 2002. **8**(1): p. 3-4.

310. Annoni, G., et al., *Age-dependent expression of fibrosis-related genes and collagen deposition in the rat myocardium.* Mech Ageing Dev, 1998. **101**(1-2): p. 57-72.

311. Thomas, D.P., et al., *Collagen gene expression in rat left ventricle: interactive effect of age and exercise training.* J Appl Physiol (1985), 2000. **89**(4): p. 1462-8.

312. Besse, S., et al., *Nonsynchronous changes in myocardial collagen mRNA and protein during aging: effect of DOCA-salt hypertension.* Am J Physiol, 1994. **267**(6 Pt 2): p. H2237-44.

313. Horn, M.A. and A.W. Trafford, *Aging and the cardiac collagen matrix: Novel mediators of fibrotic remodelling.* Journal of molecular and cellular cardiology, 2016. **93**: p. 175-185.

314. Mays, P.K., et al., *Age-related changes in collagen synthesis and degradation in rat tissues. Importance of degradation of newly synthesized collagen in regulating collagen production.* Biochem J, 1991. **276 (Pt 2)**: p. 307-13.

315. Chiao, Y.A., et al., *Matrix metalloproteinase-9 deletion attenuates myocardial fibrosis and diastolic dysfunction in ageing mice.* Cardiovasc Res, 2012. **96**(3): p. 444-55.

316. Boluyt, M.O., et al., *Alterations in cardiac gene expression during the transition from stable hypertrophy to heart failure. Marked upregulation of genes encoding extracellular matrix components.* Circ Res, 1994. **75**(1): p. 23-32.

317. Querejeta, R., et al., *Increased collagen type I synthesis in patients with heart failure of hypertensive origin: relation to myocardial fibrosis.* Circulation, 2004. **110**(10): p. 1263-8.

318. Kurokawa, T., N. Ozaki, and S. Ishibashi, *Difference between senescence-accelerated prone and resistant mice in response to insulin in the heart.* Mech Ageing Dev, 1998. **102**(1): p. 25-32.

319. Ozaki, N., et al., *Early changes in the expression of GLUT4 protein in the heart of senescence-accelerated mouse.* Mech Ageing Dev, 1996. **88**(3): p. 149-58.

320. Ji, L.L., D. Dillon, and E. Wu, *Myocardial aging: antioxidant enzyme systems and related biochemical properties.* Am J Physiol, 1991. **261**(2 Pt 2): p. R386-92.

321. Kates, A.M., et al., *Impact of aging on substrate metabolism by the human heart.* J Am Coll Cardiol, 2003. **41**(2): p. 293-9.

322. Janero, D.R., D. Hreniuk, and H.M. Sharif, *Hydroperoxide-induced oxidative stress impairs heart muscle cell carbohydrate metabolism.* Am J Physiol, 1994. **266**(1 Pt 1): p. C179-88.

323. Kim, I. and C.O. Lee, *Cloning of the mouse cardiac Na(+)-Ca2+ exchanger and functional expression in Xenopus oocytes.* Ann N Y Acad Sci, 1996. **779**: p. 126-8.

324. Fan, G.C., et al., *Regulation of myocardial function by histidine-rich, calcium-binding protein.* Am J Physiol Heart Circ Physiol, 2004. **287**(4): p. H1705-11.

325. Arber, S., G. Halder, and P. Caroni, *Muscle LIM protein, a novel essential regulator of myogenesis, promotes myogenic differentiation.* Cell, 1994. **79**(2): p. 221-31.

326. Liu, J.J., et al., *Retrolinkin, a membrane protein, plays an important role in retrograde axonal transport.* Proc Natl Acad Sci U S A, 2007. **104**(7): p. 2223-8.

327. Didelot, C., et al., *Interaction of heat-shock protein 90 beta isoform (HSP90 beta) with cellular inhibitor of apoptosis 1 (c-IAP1) is required for cell differentiation.* Cell Death Differ, 2008. **15**(5): p. 859-66.

328. Ogiso, H., et al., *Phosphorylation analysis of 90 kDa heat shock protein within the cytosolic arylhydrocarbon receptor complex.* Biochemistry, 2004. **43**(49): p. 15510-9.

329. Bukach, O.V., et al., *Some properties of human small heat shock protein Hsp20 (HspB6).* Eur J Biochem, 2004. **271**(2): p. 291-302.

330. Sin, Y.Y. and G.S. Baillie, *Heat shock protein 20 (HSP20) is a novel substrate for protein kinase D1 (PKD1).* Cell Biochem Funct, 2015. **33**(7): p. 421-6.

331. Zimmer, T., et al., *Mouse heart Na+ channels: primary structure and function of two isoforms and alternatively spliced variants.* Am J Physiol Heart Circ Physiol, 2002. **282**(3): p. H1007-17.

332. Homma, S., et al., *Carotid Plaque and Intima-Media Thickness Assessed by B-Mode Ultrasonography in Subjects Ranging From Young Adults to Centenarians.* 2001. **32**(4): p. 830-835.

333. Tanaka, H., et al., *Carotid Artery Wall Hypertrophy With Age Is Related to Local Systolic Blood Pressure in Healthy Men.* 2001. **21**(1): p. 82-87.

334. van den Munckhof, I., et al., *Impact of age and sex on carotid and peripheral arterial wall thickness in humans.* Acta Physiol (Oxf), 2012. **206**(4): p. 220-8.

335. Dinenno, F.A., et al., *Age-associated arterial wall thickening is related to elevations in sympathetic activity in healthy humans.* 2000. **278**(4): p. H1205-H1210.

336. Green, D.J., et al., *Impact of age, sex and exercise on brachial and popliteal artery remodelling in humans.* Atherosclerosis, 2010. **210**(2): p. 525-530.

337. Eigenbrodt, M.L., et al., *Common carotid arterial interadventitial distance (diameter) as an indicator of the damaging effects of age and atherosclerosis, a cross-sectional study of the Atherosclerosis Risk in Community Cohort Limited Access Data (ARICLAD), 1987–89.* Cardiovascular Ultrasound, 2006. **4**(1): p. 1.

338. Heijden-Spek, J.J.v.d., et al., *Effect of Age on Brachial Artery Wall Properties Differs From the Aorta and Is Gender Dependent.* 2000. **35**(2): p. 637-642.

339. Schmidt-Trucksäss, A., et al., *Structural, Functional, and Hemodynamic Changes of the Common Carotid Artery With Age in Male Subjects.* 1999. **19**(4): p. 1091-1097.

340. Vigetti, D., et al., *Matrix metalloproteinase 2 and tissue inhibitors of metalloproteinases regulate human aortic smooth muscle cell migration during in vitro aging.* 2006. **20**(8): p. 1118-1130.

341. Wang, M., et al., *Matrix Metalloproteinases Promote Arterial Remodeling in Aging, Hypertension, and Atherosclerosis.* 2015. **65**(4): p. 698-703.

342. AMANN, K., et al., *Endothelin A Receptor Blockade Prevents Capillary/Myocyte Mismatch in the Heart of Uremic Animals.* 2000. **11**(9): p. 1702-1711.

343. Anversa, P., R. Ricci, and G. Olivetti, *Quantitative structural analysis of the myocardium during physiologic growth and induced cardiac hypertrophy: a review.* J Am Coll Cardiol, 1986. **7**(5): p. 1140-9.

344. Anversa, P., et al., *Morphometric analysis of coronary capillaries during physiologic myocardial growth and induced cardiac hypertrophy: a review.* Int J Microcirc Clin Exp, 1989. **8**(4): p. 353-63.

345. Rakusan, K., et al., *Morphometry of human coronary capillaries during normal growth and the effect of age in left ventricular pressure-overload hypertrophy.* 1992. **86**(1): p. 38-46.

346. de Tombe, P.P., et al., *Myofilament length dependent activation.* Journal of molecular and cellular cardiology, 2010. **48**(5): p. 851-858.

347. Gilloteaux, J., et al., *Cardiomyocyte aging and hypertrophy: atrial and ventricular changes in normal and myopathic Syrian hamsters.* J Submicrosc Cytol Pathol, 1990. **22**(2): p. 249-64.

348. Campbell, S.G., et al., *Altered ventricular torsion and transmural patterns of myocyte relaxation precede heart failure in aging F344 rats.* Am J Physiol Heart Circ Physiol, 2013. **305**(5): p. H676-86.

349. Fraticelli, A., et al., *Morphological and contractile characteristics of rat cardiac myocytes from maturation to senescence.* Am J Physiol, 1989. **257**(1 Pt 2): p. H259-65.

350. Schmucker, D.L. and H.G. Sachs, *Age-dependent alterations in rat ventricular myocardium: a quantitative analysis.* Mech Ageing Dev, 1985. **31**(1): p. 89-101.

351. Mozet, C., et al., *Cardioprotective effect of EGb 761 on myocardial ultrastructure of young and old rat heart and antioxidant status during acute hypoxia.* Aging Clin Exp Res, 2009. **21**(1): p. 14-21.

352. Tate, E.L. and G.H. Herbener, *A morphometric study of the density of mitochondrial cristae in heart and liver of aging mice.* J Gerontol, 1976. **31**(2): p. 129-34.

353. Corsetti, G., et al., *Morphometric Changes Induced by Amino Acid Supplementation in Skeletal and Cardiac Muscles of Old Mice.* The American Journal of Cardiology, 2008. **101**(11, Supplement): p. S26-S34.

354. Sachs, H.G., J.A. Colgan, and M.L. Lazarus, *Ultrastructure of the aging myocardium: a morphometric approach.* Am J Anat, 1977. **150**(1): p. 63-71.

355. Fleischer, M., et al., *[Ultrastructural morphometric analysis of normally loaded human myocardial left ventricles from young and old patients (author's transl)].* Virchows Arch A Pathol Anat Histol, 1978. **380**(2): p. 123-33.

356. Dai, D.F. and P.S. Rabinovitch, *Cardiac aging in mice and humans: the role of mitochondrial oxidative stress.* Trends Cardiovasc Med, 2009. **19**(7): p. 213-20.

357. Goldberg, I.J., et al., *Deciphering the Role of Lipid Droplets in Cardiovascular Disease.* 2018. **138**(3): p. 305-315.

358. Christoffersen, C., et al., *Cardiac lipid accumulation associated with diastolic dysfunction in obese mice.* Endocrinology, 2003. **144**(8): p. 3483-90.

359. SHARMA, S., et al., *Intramyocardial lipid accumulation in the failing human heart resembles the lipotoxic rat heart.* 2004. **18**(14): p. 1692-1700.

360. Liu, L., et al., *DGAT1 expression increases heart triglyceride content but ameliorates lipotoxicity.* J Biol Chem, 2009. **284**(52): p. 36312-23.

361. Zou, T., et al., *MicroRNA-410-5p exacerbates high-fat diet-induced cardiac remodeling in mice in an endocrine fashion.* Scientific Reports, 2018. **8**(1): p. 8780.

362. Ternacle, J., et al., *Short-term high-fat diet compromises myocardial function: a radial strain rate imaging study.* European Heart Journal - Cardiovascular Imaging, 2017. **18**(11): p. 1283-1291.

363. Lee, M.R., et al., *Anti-obesity effect in high-fat-diet-induced obese C57BL/6 mice: Study of a novel extract from mulberry (Morus alba) leaves fermented with Cordyceps militaris.* Experimental and therapeutic medicine, 2019. **17**(3): p. 2185-2193.

364. Zarzoso, M., et al., *Ventricular remodelling in rabbits with sustained high-fat diet.* Acta Physiologica, 2014. **211**(1): p. 36-47.

365. Soares, A.F., J.M.N. Duarte, and R. Gruetter, *Increased hepatic fatty acid polyunsaturation precedes ectopic lipid deposition in the liver in adaptation to high-fat diets in mice.* Magnetic Resonance Materials in Physics, Biology and Medicine, 2018. **31**(2): p. 341-354.

366. Lizarbe, B., et al., *High-fat diet consumption alters energy metabolism in the mouse hypothalamus.* International Journal of Obesity, 2019. **43**(6): p. 1295-1304.

367. Littlejohns, B., P. Pasdois, and S. Duggan, *Hearts from mice fed a non-obesogenic high-fat diet exhibit changes in their oxidative state, calcium and mitochondria in parallel with increased susceptibility to reperfusion injury.* PLoS One, 2014. **9**: p. e100579.

368. Bake, T., et al., *Large, binge-type meals of high fat diet change feeding behaviour and entrain food anticipatory activity in mice.* Appetite, 2014. **77**(100): p. 60-71.

369. Bake, T., et al., *Arcuate nucleus homeostatic systems are not altered immediately prior to the scheduled consumption of large, binge-type meals of palatable solid or liquid diet in rats and Mice.* J Neuroendocrinol, 2013. **25**(4): p. 357-71.

370. Du, J., et al., *Betaine Supplementation Enhances Lipid Metabolism and Improves Insulin Resistance in Mice Fed a High-Fat Diet.* Nutrients, 2018. **10**(2): p. 131.

371. Ding, S.Y., et al., *Pioglitazone can ameliorate insulin resistance in low-dose streptozotocin and high sucrose-fat diet induced obese rats.* Acta Pharmacol Sin, 2005. **26**(5): p. 575-80.

372. Luo, J., et al., *Nongenetic mouse models of non-insulin-dependent diabetes mellitus.* Metabolism, 1998. **47**(6): p. 663-8.

373. Kesby, J.P., et al., *Spatial Cognition in Adult and Aged Mice Exposed to High-Fat Diet.* PloS one, 2015. **10**(10): p. e0140034-e0140034.

374. Liu, C.-Y., et al., *Metabolic Damage Presents Differently in Young and Early-Aged C57BL/6 Mice Fed a High-Fat Diet.* International Journal of Gerontology, 2016. **10**(2): p. 105-111.

375. Serkova, N.J., et al., *Metabolic profiling of livers and blood from obese Zucker rats.* J Hepatol, 2006. **44**(5): p. 956-62.

376. Newgard, C.B., et al., *A branched-chain amino acid-related metabolic signature that differentiates obese and lean humans and contributes to insulin resistance.* Cell Metab, 2009. **9**(4): p. 311-26.

377. Duggan, G.E., et al., *Differentiating short- and long-term effects of diet in the obese mouse using (1) H-nuclear magnetic resonance metabolomics.* Diabetes Obes Metab, 2011. **13**(9): p. 859-62.

378. Zhao, L.C., et al., *A metabonomic comparison of urinary changes in Zucker and GK rats.* J Biomed Biotechnol, 2010. **2010**: p. 431894.

379. Sequeira, V., et al., *Synergistic role of ADP and Ca(2+) in diastolic myocardial stiffness.* The Journal of physiology, 2015. **593**(17): p. 3899-3916.

380. Chen, D., et al., *A high-fat diet impairs mitochondrial biogenesis, mitochondrial dynamics, and the respiratory chain complex in rat myocardial tissues.* J Cell Biochem, 2018. **119**(11): p. 9602.

381. Poussin, C., et al., *Oxidative phosphorylation flexibility in the liver of mice resistant to high-fat diet-induced hepatic steatosis.* Diabetes, 2011. **60**(9): p. 2216-2224.

382. Takamura, T., et al., *Obesity upregulates genes involved in oxidative phosphorylation in livers of diabetic patients.* Obesity (Silver Spring), 2008. **16**(12): p. 2601-9.

383. Yoshino, J., et al., *Nicotinamide mononucleotide, a key NAD(+) intermediate, treats the pathophysiology of diet- and age-induced diabetes in mice.* Cell Metab, 2011. **14**(4): p. 528-36.

384. Zhu, X.H., et al., *In vivo NAD assay reveals the intracellular NAD contents and redox state in healthy human brain and their age dependences.* Proc Natl Acad Sci U S A, 2015. **112**(9): p. 2876-81.

385. Camacho-Pereira, J., et al., *CD38 Dictates Age-Related NAD Decline and Mitochondrial Dysfunction through an SIRT3-Dependent Mechanism.* Cell Metab, 2016. **23**(6): p. 1127-1139.

386. Giannecchini, M., et al., *Uptake and utilization of nucleosides for energy repletion.* The International Journal of Biochemistry & Cell Biology, 2005. **37**(4): p. 797-808.

387. Connolly, M.W., et al., *Inosine enhances salvage of reperfused myocardium.* Curr Surg, 1985. **42**(6): p. 469-71.

388. Cruz-Topete, D., et al., *Proteomic changes in the heart of diet-induced pre-diabetic mice.* J Proteomics, 2011. **74**(5): p. 716-27.

389. Dasari, S., et al., *Remodeling of skeletal muscle mitochondrial proteome with high-fat diet involves greater changes to β-oxidation than electron transfer proteins in mice.* 2018. **315**(4): p. E425-E434.

390. Nesteruk, M., et al., *Mitochondrial-related proteomic changes during obesity and fasting in mice are greater in the liver than skeletal muscles.* 2014. **14**(1): p. 245-259.

391. Kleinert, M., et al., *Quantitative proteomic characterization of cellular pathways associated with altered insulin sensitivity in skeletal muscle following high-fat diet feeding and exercise training.* Scientific Reports, 2018. **8**(1): p. 10723.

392. McLean, F.H., et al., *A high-fat diet induces rapid changes in the mouse hypothalamic proteome.* Nutrition & Metabolism, 2019. **16**(1): p. 26.

393. Benard, O., et al., *Impact of high-fat diet on the proteome of mouse liver.* The Journal of Nutritional Biochemistry, 2016. **31**: p. 10-19.

394. Andrade, J.M.O., et al., *Proteomic white adipose tissue analysis of obese mice fed with a high-fat diet and treated with oral angiotensin-(1–7).* Peptides, 2014. **60**: p. 56-62.

395. Hung, C.-L., et al., *Membrane Proteomics of Impaired Energetics and Cytoskeletal Disorganization in Elderly Diet-Induced Diabetic Mice.* Journal of Proteome Research, 2017. **16**(10): p. 3504-3513.

396. Sabidó, E., et al., *Targeted proteomics reveals strain-specific changes in the mouse insulin and central metabolic pathways after a sustained high-fat diet.* 2013. **9**(1): p. 681.

397. Ashrafi, R., et al., *Altered Left Ventricular Ion Channel Transcriptome in a High-Fat-Fed Rat Model of Obesity: Insight into Obesity-Induced Arrhythmogenesis.* Journal of obesity, 2016. **2016**: p. 7127898-7127898.

398. Aromolaran, A.S. and M. Boutjdir, *Cardiac Ion Channel Regulation in Obesity and the Metabolic Syndrome: Relevance to Long QT Syndrome and Atrial Fibrillation.* Frontiers in physiology, 2017. **8**: p. 431-431.

399. Chung, A.P.Y.S., et al., *Geraniin Protects High-Fat Diet-Induced Oxidative Stress in Sprague Dawley Rats.* Frontiers in nutrition, 2018. **5**: p. 17-17.

400. Vijayakumar, R.S., D. Surya, and N. Nalini, *Antioxidant efficacy of black pepper (Piper nigrum L.) and piperine in rats with high fat diet induced oxidative stress.* Redox Report, 2004. **9**(2): p. 105-110.

401. Matsuzawa-Nagata, N., et al., *Increased oxidative stress precedes the onset of high-fat diet–induced insulin resistance and obesity.* Metabolism, 2008. **57**(8): p. 1071-1077.

402. Noeman, S.A., H.E. Hamooda, and A.A. Baalash, *Biochemical study of oxidative stress markers in the liver, kidney and heart of high fat diet induced obesity in rats.* Diabetology & metabolic syndrome, 2011. **3**(1): p. 17-17.

403. Ballal, K., et al., *Obesogenic high fat western diet induces oxidative stress and apoptosis in rat heart.* Molecular and cellular biochemistry, 2010. **344**(1-2): p. 221-230.

404. Lin, Y.Y., et al., *Anti-apoptotic and Pro-survival Effects of Food Restriction on High-Fat Diet-Induced Obese Hearts.* Cardiovasc Toxicol, 2017. **17**(2): p. 163-174.

405. Sahraoui, A., et al., *Myocardial Structural and Biological Anomalies Induced by High Fat Diet in Psammomys obesus Gerbils.* PLoS One, 2016. **11**(2): p. e0148117.

406. Cheng, Y.-C., et al., *Garlic oil attenuates the cardiac apoptosis in hamster-fed with hypercholesterol diet.* Food Chemistry, 2013. **136**(3): p. 1296-1302.

407. Zhu, X.-Y., et al., *Redox-sensitive myocardial remodeling and dysfunction in swine diet-induced experimental hypercholesterolemia.* Atherosclerosis, 2007. **193**(1): p. 62-69.

408. Perales, S., et al., *Effect of Oxysterol-Induced Apoptosis of Vascular Smooth Muscle Cells on Experimental Hypercholesterolemia %J Journal of Biomedicine and Biotechnology.* 2009. **2009**: p. 8.

409. Watanabe, S., et al., *A High-Fat and High-Cholesterol Diet Induces Cardiac Fibrosis, Vascular Endothelial, and Left Ventricular Diastolic Dysfunction in SHRSP5/Dmcr Rats.* Journal of atherosclerosis and thrombosis, 2018. **25**(5): p. 439-453.

410. Li, S., et al., *Disruption of calpain reduces lipotoxicity-induced cardiac injury by preventing endoplasmic reticulum stress.* Biochimica et biophysica acta, 2016. **1862**(11): p. 2023-2033.

411. Finck, B.N., et al., *The cardiac phenotype induced by PPARalpha overexpression mimics that caused by diabetes mellitus.* J Clin Invest, 2002. **109**(1): p. 121-30.

412. Siino, V., et al., *Impact of diet-induced obesity on the mouse brain phosphoproteome.* J Nutr Biochem, 2018. **58**: p. 102-109.

413. Alli Shaik, A., et al., *Phosphoprotein network analysis of white adipose tissues unveils deregulated pathways in response to high-fat diet.* Scientific Reports, 2016. **6**: p. 25844.

414. Dittmann, A., et al., *High-fat diet in a mouse insulin-resistant model induces widespread rewiring of the phosphotyrosine signaling network.* 2019. **15**(8): p. e8849.

415. Takeshima, H., et al., *Embryonic lethality and abnormal cardiac myocytes in mice lacking ryanodine receptor type 2.* The EMBO journal, 1998. **17**(12): p. 3309-3316.

416. Xiao, B., et al., *Functional consequence of protein kinase A-dependent phosphorylation of the cardiac ryanodine receptor: sensitization of store overload-induced Ca2+ release.* J Biol Chem, 2007. **282**(41): p. 30256-64.

417. van Oort, R.J., et al., *Ryanodine receptor phosphorylation by calcium/calmodulin-dependent protein kinase II promotes life-threatening ventricular arrhythmias in mice with heart failure.* Circulation, 2010. **122**(25): p. 2669-79.

418. Swift, F., et al., *Extreme sarcoplasmic reticulum volume loss and compensatory T-tubule remodeling after Serca2 knockout.* Proc Natl Acad Sci U S A, 2012. **109**(10): p. 3997-4001.

419. Srinivasan, M., et al., *ss-Cell-specific pyruvate dehydrogenase deficiency impairs glucose-stimulated insulin secretion.* Am J Physiol Endocrinol Metab, 2010. **299**(6): p. E910-7.

420. Hill, M.M., et al., *PTRF-Cavin, a conserved cytoplasmic protein required for caveola formation and function.* Cell, 2008. **132**(1): p. 113-24.

421. Costa, R.R., et al., *High fat diet induces central obesity, insulin resistance and microvascular dysfunction in hamsters.* Microvasc Res, 2011. **82**(3): p. 416-22.

422. Oishi, J.C., et al., *Endothelial Dysfunction and Inflammation Precedes Elevations in Blood Pressure Induced by a High-Fat Diet.* Arquivos brasileiros de cardiologia, 2018. **110**(6): p. 558-567.

423. Santana, A.B.C., et al., *Effect of high-fat diet upon inflammatory markers and aortic stiffening in mice.* BioMed research international, 2014. **2014**: p. 914102-914102.

424. Reifenberger, M.S., et al., *Perivascular fat alters reactivity of coronary artery: effects of diet and exercise.* Medicine and science in sports and exercise, 2007. **39**(12): p. 2125-2134.

425. Grassi, G., et al., *Structural and functional alterations of subcutaneous small resistance arteries in severe human obesity.* Obesity (Silver Spring), 2010. **18**(1): p. 92-8.

426. Kong, P., et al., *The pathogenesis of cardiac fibrosis.* 2014. **71**(4): p. 549-574.

427. Li, S.-J., et al., *The high-fat diet induces myocardial fibrosis in the metabolically healthy obese minipigs—The role of ER stress and oxidative stress.* Clinical Nutrition, 2017. **36**(3): p. 760-767.

428. Motta, V. and C. Mandarim-de-Lacerda, *Efectos Beneficiosos del Ejercicio Físico (Cinta) sobre la Masa Corporal y Relación Capilares/Miocito del Músculo Esquelético en Ratones C57BL/6 Alimentados con una Dieta Alta en Grasas.* International Journal of Morphology, 2012. **30**: p. 205-210.

429. Silvennoinen, M., et al., *High-fat feeding induces angiogenesis in skeletal muscle and activates angiogenic pathways in capillaries.* 2013. **16**(2): p. 297-307.

430. Naresh, N.K., et al., *Cardiovascular magnetic resonance detects the progression of impaired myocardial perfusion reserve and increased left-ventricular mass in mice fed a high-fat diet.* 2016. **18**(1): p. 53.

431. Campbell, D.J., et al., *Obesity is associated with lower coronary microvascular density.* PLoS One, 2013. **8**(11): p. e81798.

432. Jeong, E.M., et al., *Role of Mitochondrial Oxidative Stress in Glucose Tolerance, Insulin Resistance, and Cardiac Diastolic Dysfunction.* 2016. **5**(5): p. e003046.

433. Richard E. Klabunde, 2008, Cardiovascular Physiology, <www.cvphysiology.com>